

# **CHARACTERISATION OF SUPPRESSOR OF CYTOKINE SIGNALING 1 REGULATION OF TYPE I INTERFERON SIGNALING**

Submitted for the full requirements  
of the degree of Doctor of Philosophy

Rebecca Piganis  
Bachelor of Biomedical Science (Honours)

Centre for Innate Immunity and Infectious Diseases  
Monash Institute of Medical Research  
Monash University

2013

**Notice 1**

Under the Copyright Act 1968, this thesis must be used only under the normal conditions of scholarly fair dealing. In particular no results or conclusions should be extracted from it, nor should it be copied or closely paraphrased in whole or in part without the written consent of the author. Proper written acknowledgement should be made for any assistance obtained from this thesis.

# TABLE OF CONTENTS

TABLE OF CONTENTS .....	ii
ABSTRACT .....	vii
GENERAL DECLARATION.....	ix
ACKNOWLEDGEMENTS .....	x
LIST OF FIGURES.....	xi
LIST OF TABLES .....	xiv
ABBREVIATIONS .....	xvi
CHAPTER 1 .....	1
LITERATURE REVIEW.....	1
INTERFERON SIGNALING AND ITS REGULATION BY SOCS1 .....	1
1.1 Introduction.....	1
1.2 The Interferons .....	1
1.3 Production of the Type I IFNs.....	2
1.3.1 Transcriptional Activation of Type I IFN Production .....	2
1.3.2 Toll Like Receptors and Type I IFN Induction .....	4
1.3.3 Cytosolic Receptors and Type I IFN Induction .....	6
1.4 Type I IFN Signaling.....	8
1.4.1 The IFN Alpha Receptor (IFNAR) .....	8
1.4.2 Janus Tyrosine Kinases (JAKs).....	12
1.4.3 Signal Transducers and Activators of Transcription .....	14
1.4.4 STAT Independent Type I IFN Signaling.....	21
1.5 Summary of IFN Signaling Mechanism .....	22

1.6 Type I IFN Functions .....	23
1.6.1 Antiviral Functions.....	23
1.6.2 Immunomodulatory Functions.....	25
1.7 Clinical Applications of the Type I IFNs .....	28
1.7.1 Treatment of Viral Infections .....	28
1.7.2 Treatment of cancer.....	29
1.7.3 Autoimmune Disease .....	30
1.7.4 Side Effects of type I IFN treatment .....	30
1.8 Regulation of Type I IFN Signaling.....	31
1.9 Suppressors of Cytokine Signaling (SOCS).....	33
1.9.1 SOCS Structure .....	33
1.9.2 SOCS1 Expression .....	34
1.9.3 SOCS1 Inhibition of Interferon Signaling.....	35
1.9.4 Mechanisms of SOCS1 inhibition.....	37
1.9.5 SOCS1 and Immune Cell Development .....	38
1.10 Summary .....	39
CHAPTER 2 .....	40
METHODS .....	40
2.1 Mouse Models .....	40
2.2 Detection of STAT1, STAT3 and STAT5 phosphorylation in immune cell populations by Phosphoflow Cytometry.....	40
2.2.1 Collection and isolation of thymic and splenic immune cells .....	40
2.2.2 Collection and Isolation of Peripheral Blood Mononuclear Cells (PBMCs).....	41
2.2.3 Cell Stimulation .....	41

2.2.4 Cell Fixing and Permeabilisation.....	41
2.2.5 Anti-body staining .....	42
2.2.6 Data Collection and Analysis .....	42
2.3 Western Blot Analysis of total STAT1, STAT3 and STAT5 protein expression.....	35
2.3.1 Preparation of Cell Lysates.....	43
2.3.2 Lowry Protein Assay .....	43
2.3.3 SDS-Polyacrylamide Gel Electrophoresis (SDS-PAGE) .....	43
2.3.4 Protein Transfer to Nitrocellulose Membrane .....	43
2.3.5 Immunoblotting.....	44
2.4 Microarray .....	45
2.4.2 IFN Treatment .....	45
2.4.3 Organ Collection.....	45
2.4.4 RNA isolation from Whole Thymus .....	45
2.4.5 RNA clean up .....	46
2.4.6 RNA Quality Control .....	46
2.4.7 Reverse Transcription of RNA to cDNA .....	46
2.4.8 GAPDH PCR.....	46
2.4.9 Quantitative Real Time PCR (qRT-PCR) .....	47
2.5.10 Microarray Procedure .....	47
2.5.11 Data Analysis .....	50
CHAPTER 3 .....	53
DECLARATION.....	53
PUBLICATION: SUPPRESSOR OF CYTOKINE SIGNALING (SOCS) 1 INHIBITS TYPE I INTERFERON (IFN) SIGNALING VIA THE INTERFERON RECEPTOR (IFNAR1)-ASSOCIATED TYROSINE KINASE TYK2.....	55

CHAPTER 4 .....	63
CHARACTERISATION OF IFN $\alpha$ INDUCTION OF STAT PHOSPHORYLATION IN IMMUNE CELL POPULATIONS AND ITS REGULATION BY SOCS1 .....	63
4.1 Basal MFI of pSTAT1, pSTAT3 and pSTAT5 in thymic CD4/CD8 T-cell subsets .....	54
4.2 Dose Response to IFN $\alpha$ – Thymic CD4/CD8 T-cell Subsets .....	67
4.3 Time Course – Thymic CD4/CD8 T-cell subsets.....	68
4.3.1 Time course of STAT1 phosphorylation in the thymus .....	68
4.3.2 Time course of STAT3 phosphorylation in the thymus .....	68
4.3.3 Time course of STAT5 phosphorylation in the thymus .....	69
4.3.4 Summary and Discussion – IFN $\alpha$ induced STAT phosphorylation in thymocytes .....	69
4.4 Basal MFI of pSTAT1, pSTAT3 and pSTAT5 in PBMC CD4/CD8 T-cell subsets .....	72
4.5.1 Time course of STAT1 phosphorylation in the blood .....	73
4.5.2 Time course of STAT3 phosphorylation in the blood .....	74
4.5.3 Time course of STAT5 phosphorylation in the blood .....	75
4.5.4 Thymic CD4/CD8 T-cells vs Periphery CD4/CD8 T-cells.....	75
4.5.5 Summary and Discussion – IFN $\alpha$ induced STAT phosphorylation in peripheral immune cells .....	76
4.6 SOCS1 effect on IFN $\alpha$ induced STAT phosphorylation .....	77
4.6.1 STAT1 phosphorylation .....	76
4.6.2 STAT3 phosphorylation .....	79
4.6.3 STAT5 phosphorylation .....	80
4.6.4 Summary and Discussion.....	80
4.7 Total STAT1, STAT3 and STAT5 expression levels in the thymus of <i>Socs1<sup>-/-</sup>Ifn<math>\gamma</math><sup>-/-</sup></i> and <i>Socs1<sup>+/+</sup>Ifn<math>\gamma</math><sup>-/-</sup></i> mice.....	81
4.8 Summary .....	82

CHAPTER 5 .....	83
IFN $\alpha$ AND SOCS1 REGULATION OF GENE EXPRESSION IN THE THYMUS .....	83
5.1 Time Course of IFN $\alpha$ stimulation in the Thymus of Wild Type C57BL/6 mice .....	84
5.2 Thymic IFN $\alpha$ regulated genes and the Interferome .....	89
5.3 Basal Differences in Gene Expression between <i>Socs1<sup>-/-</sup>Ifn<math>\gamma</math><sup>-/-</sup></i> and <i>Socs1<sup>+/+</sup>Ifn<math>\gamma</math><sup>-/-</sup></i> mice .....	92
5.3.1 Basal Cluster 1 .....	93
5.3.2 Basal Cluster 2 .....	95
5.3.3 Basal Cluster 3 .....	96
5.4 SOCS1 regulation of IFN Stimulated Genes .....	97
CHAPTER 6 .....	103
DISCUSSION .....	103
REFERENCES .....	112
APPENDICES I: SOLUTIONS .....	- 1 -
APPENDICES II: PRIMERS for PCR and RT-PCR .....	- 3 -
APPENDICES III: GENE LISTS .....	- 4 -
A. IFN $\alpha$ regulated probes within the thymus of wt mice .....	- 4 -
B. Thymic IFN $\alpha$ regulated genes absent from the Interferome .....	- 17 -
C. Probes basally different between <i>Socs1<sup>+/+</sup>Ifn<math>\gamma</math><sup>-/-</sup></i> and <i>Socs1<sup>-/-</sup>Ifn<math>\gamma</math><sup>-/-</sup></i> mice .....	- 20 -
D. IFN $\alpha$ regulated probes within the thymus of <i>Socs1<sup>+/+</sup>Ifn<math>\gamma</math><sup>-/-</sup></i> mice .....	- 46 -
E. IFN $\alpha$ regulated probes within the thymus of <i>Socs1<sup>-/-</sup>Ifn<math>\gamma</math><sup>-/-</sup></i> mice .....	- 56 -

## ABSTRACT

Type I Interferons (IFNs) are critical players in host innate and adaptive immunity. IFN signaling is tightly controlled to ensure an appropriate immune response is generated, as an imbalance could result in uncontrolled inflammation or inadequate responses to infection. It is therefore important to understand the signaling events activated in the cell following type I IFN stimulation and how signaling is regulated. SOCS1 is a negative regulator of type I IFN signaling, acting in a negative feedback loop. This thesis details the mechanism of SOCS1 regulation of type I IFN signaling as well as the consequences of this regulation in terms of its effect on IFN $\alpha$  induced STAT activation and the resultant transcriptional response.

Results in this thesis demonstrate that SOCS1 inhibits type I IFN signaling through an interaction with the type I IFN receptor (IFNAR1) associated kinase, TYK2. SOCS1 associates via its SH2 domain with conserved phospho-tyrosines 1054 and 1055 of TYK2 as well with the kinase inhibitor region (KIR). TYK2 is preferentially Lys-63 polyubiquitinated and this activation reaction is inhibited by SOCS1. The consequent effect of SOCS1 inhibition of TYK2 not only results in a reduced IFN response due to inhibition of TYK2 kinase mediated STAT signaling, but also negatively impacts IFNAR1 surface expression which is stabilised by TYK2.

The STAT family of transcription factors are major mediators of the type I IFN response. This thesis demonstrates STAT activation by the type I IFNs occurs in a cell-type specific manner. STAT1 is up-regulated by type I IFN in a broad range of immune cell types including thymic and peripheral T-cells, B-cells and macrophages whereas activation of STAT3 and STAT5 is more confined to the thymic T-cells. Type I IFN stimulation of thymic cells results in rapid phosphorylation of STAT1, STAT3 and STAT5 and the resultant transcriptional response results in the up-regulation of an array of genes involved in innate defence. The promoter regions of these genes are enriched in ISGF3, STAT1, STAT3 and STAT5 binding elements.

Results of this thesis demonstrate that the downstream consequence of SOCS1 action is to suppress IFN induced STAT activation and subsequent gene induction. We found SOCS1 selectively regulates STAT phosphorylation in response to IFN $\alpha$ . The activation profile of STAT1 and STAT3 is altered by SOCS1, whereas STAT5 is independent of this regulation. Using microarray expression profiling, we identified subsets of IFN stimulated genes regulated by SOCS1. Promoter analysis of these gene sets identifies transcription factor enrichment of numerous ISGF3, STAT1 and STAT3 binding sites but not STAT5. These results support a model whereby SOCS1 negative regulation of type I IFN signaling

selectively modulates the activation profile of STAT1 and STAT3 and consequent gene induction.

These studies have mapped specific pathways of IFN regulation from the receptor component to transcription factor activation and interferon regulated gene induction. I demonstrate that SOCS1 selectively interacts with the IFNAR1 associated kinase, TYK2 and regulates the signaling of a subset of IFN activated STATs and IFN/STAT regulated genes. These findings therefore enhance our understanding of type I IFN signaling and its regulation by SOCS1 and provide the foundation for future therapies to select for specific type I IFN signaling pathways.

## GENERAL DECLARATION

In accordance with Monash University Doctorate Regulation 17 Doctor of Philosophy and Research Master's regulations the following declarations are made:

I hereby declare that this thesis contains no material which has been accepted for the award of any other degree or diploma at any university or equivalent institution and that, to the best of my knowledge and belief, this thesis contains no material previously published or written by another person, except where due reference is made in the text of the thesis.

This thesis includes one original paper published in peer reviewed journals and no unpublished publications. The core theme of the thesis is the characterisation of suppressor of cytokine signaling 1 regulation of type I Interferon signaling. The ideas, development and writing up of all the papers in the thesis were the principal responsibility of myself, the candidate, working within the Centre for Innate Immunity and Infectious Diseases under the supervision of Prof. Paul Hertzog.

The inclusion of co-authors reflects the fact that the work came from active collaboration between researchers and acknowledges input into team-based research.

In the case of chapter 3, my contribution to the work involved the following:

Thesis chapter	Publication title	Publication status*	Nature and extent of candidate's contribution
3	Suppressor of cytokine signaling (SOCS) 1 inhibits type I interferon (IFN) signaling via the interferon alpha receptor (IFNAR1)-associated tyrosine kinase Tyk2.  J Biol Chem 286(39): 33811-33818.	Published	I performed all laboratory experiments with exception of flow cytometry analysis of IFNAR1 surface levels and cloning of TYK2/mutant expression constructs. I was responsible for writing the publication.

I have renumbered sections of submitted or published papers in order to generate a consistent presentation within the thesis.

Signed:



Date:

13/5/13

## **ACKNOWLEDGEMENTS**

There are many people who I am grateful to for their guidance and support throughout my PhD.

I would like to thank my supervisors Paul Hertzog and Nicky de Weerd. Thank you Paul for providing me with many opportunities to develop as a scientist whilst studying in your lab and thank you Nicky for starting me off in the lab and for your guidance throughout my PhD.

To everyone at the Centre for Innate Immunity and Infectious Diseases thank you for all the support, advice and knowledge you have given me throughout the years. I have learnt so much during my time here as I have been surrounded by many talented scientists. I would especially like to thank Bernadette Scott, Tali Lang, Claire Greenhill, Brett Verstak, Jodee Gould, Niamh Mangan, Ashley Mansell, Dale Carey, Sam Forster and Michelle Tate who have taught me, helped me or read my thesis. I would also like to thank everyone at CIID for creating a great environment in which to undertake a PhD and for all the fun times we have had unwinding after a busy week in the lab.

Lastly, I would like to thank my friends and family for all their love and support over the years. I couldn't have done it without you.

## LIST OF FIGURES

<b>Figure 1.1</b>	Pathways leading to the transcriptional activation of the type I IFNs	ff2
<b>Figure 1.2</b>	The type I IFN JAK/STAT pathway	ff8
<b>Figure 1.3</b>	Structure of hu-IFNAR1 and mu-Ifnar1	ff9
<b>Figure 1.4</b>	Structure of hu-IFNAR2 (long form) and mu-Ifnar2c	ff10
<b>Figure 1.5</b>	Structure of the JAK kinases	ff12
<b>Figure 1.6</b>	Structure of the STAT family of transcription factors	ff14
<b>Figure 1.7</b>	JAK/STAT independent pathways activated by the type I IFNs	ff21
<b>Figure 1.8</b>	Structure of SOCS1 and SOCS3	ff34
<b>Figure 2.1</b>	Flow chart of the microarray procedure	ff45
<b>Figure 2.2</b>	Flow chart of the initial steps in microarray analysis using Genespring GX	ff50
<b>Figure 2.3</b>	Flow chart of analysis for the identification of genes regulated following 3 and 6 hours IFN $\alpha$ treatment, administered intraperitoneally, in the thymus of wt C57BL/6 mice	ff51
<b>Figure 2.4</b>	Flow chart of analysis for the identification of genes differentially expressed within <i>Socs1<sup>+/+</sup>Ifn<math>\gamma</math><sup>-/-</sup></i> vs <i>Socs1<sup>-/-</sup>Ifn<math>\gamma</math><sup>-/-</sup></i> mice.	ff51
<b>Figure 2.5</b>	Flow chart of analysis for the identification of genes regulated following 3 and 6 hours IFN $\alpha$ treatment, administered intraperitoneally, in the thymus of <i>Socs1<sup>+/+</sup>Ifn<math>\gamma</math><sup>-/-</sup></i> C57BL/6 mice	ff51
<b>Figure 2.6</b>	Flow chart of analysis for the identification of genes regulated following 3 and 6 hours IFN $\alpha$ treatment, administered intraperitoneally, in the thymus of <i>Socs1<sup>-/-</sup>Ifn<math>\gamma</math><sup>-/-</sup></i> C57BL/6 mice	ff51
<b>Figure 2.7</b>	Flow chart of analysis for the identification of SOCS1/IFN regulated genes	ff51
<b>Figure 4.1</b>	Gating of thymic CD4/CD8 T-cell populations	ff65
<b>Figure 4.2</b>	Gating of PBMC CD4, CD8, B220 and MAC1 cell populations	ff65
<b>Figure 4.3</b>	Gating of splenic CD4, CD8 and MAC1 cell populations	ff65
<b>Figure 4.4</b>	Methods of phosphoflow cytometry analysis	ff65
<b>Figure 4.5</b>	Basal STAT1, STAT3 and STAT5 phosphorylation levels in thymic CD4/CD8 T-cell subsets	ff66
<b>Figure 4.6</b>	Dose response of IFN $\alpha$ on STAT1, STAT3 and STAT5 phosphorylation in thymic CD4/CD8 T-cell subsets	ff67

<b>Figure 4.7</b>	Time course of IFN $\alpha$ induced STAT1 phosphorylation in thymic CD4/CD8 T-cell subsets	ff68
<b>Figure 4.8</b>	Time course of IFN $\alpha$ induced STAT3 phosphorylation in thymic CD4/CD8 T-cell subsets	ff68
<b>Figure 4.9</b>	Time course of IFN $\alpha$ induced STAT5 phosphorylation in thymic CD4/CD8 T-cell subsets	ff69
<b>Figure 4.10</b>	Basal STAT1, STAT3 and STAT5 phosphorylation levels in PBMC CD4/CD8 T-cell subsets, B220 positive or MAC1 positive cells	ff73
<b>Figure 4.11</b>	Time course IFN $\alpha$ induced STAT1 phosphorylation in PBMC CD4/CD8 T-cell subsets, B220 positive or MAC1 positive cells	ff73
<b>Figure 4.12</b>	Time course IFN $\alpha$ induced STAT3 phosphorylation in PBMC CD4/CD8 T-cell subsets, B220 positive or MAC1 positive cells	ff74
<b>Figure 4.13</b>	Time course of IFN $\alpha$ induced STAT5 phosphorylation in PBMC CD4/CD8 T-cell subsets, B220 positive or MAC1 positive cells	ff75
<b>Figure 4.14</b>	Thymic and peripheral T-cell STAT1, STAT3 and STAT5 phosphorylation in response to 15 minutes IFN $\alpha$ stimulation	ff75
<b>Figure 4.15</b>	Basal STAT1, STAT3 and, STAT5 phosphorylation levels in thymic CD4/CD8 T-cell subsets from <i>Socs1<sup>-/-</sup>Ifn<math>\gamma</math><sup>-/-</sup></i> and <i>Socs1<sup>+/+</sup>Ifn<math>\gamma</math><sup>-/-</sup></i> mice	ff77
<b>Figure 4.16</b>	Time course of IFN $\alpha$ induced STAT1 phosphorylation in thymic CD4/CD8 T-cell subsets from <i>Socs1<sup>-/-</sup>Ifn<math>\gamma</math><sup>-/-</sup></i> and <i>Socs1<sup>+/+</sup>Ifn<math>\gamma</math><sup>-/-</sup></i> mice	ff78
<b>Figure 4.17</b>	Time course of IFN $\alpha$ induced STAT1 phosphorylation in splenic CD4/CD8 T-cell subsets and splenic B-cells from <i>Socs1<sup>-/-</sup>Ifn<math>\gamma</math><sup>-/-</sup></i> and <i>Socs1<sup>+/+</sup>Ifn<math>\gamma</math><sup>-/-</sup></i> mice	ff78
<b>Figure 4.18</b>	Time course of IFN $\alpha$ induced STAT1 phosphorylation in splenic macrophages and BMMs	ff78
<b>Figure 4.19</b>	Time course of IFN $\alpha$ induced STAT3 phosphorylation in thymic CD4/CD8 T-cell subsets from <i>Socs1<sup>-/-</sup>Ifn<math>\gamma</math><sup>-/-</sup></i> and <i>Socs1<sup>+/+</sup>Ifn<math>\gamma</math><sup>-/-</sup></i> mice	ff79
<b>Figure 4.20</b>	Time course of IFN $\alpha$ induced STAT5 phosphorylation in thymic CD4/CD8 T-cell subsets from <i>Socs1<sup>-/-</sup>Ifn<math>\gamma</math><sup>-/-</sup></i> and <i>Socs1<sup>+/+</sup>Ifn<math>\gamma</math><sup>-/-</sup></i> mice	ff80
<b>Figure 4.21</b>	Total STAT1, STAT3 and STAT5 levels in the thymus of <i>Socs1<sup>-/-</sup>Ifn<math>\gamma</math><sup>-/-</sup></i> and <i>Socs1<sup>+/+</sup>Ifn<math>\gamma</math><sup>-/-</sup></i> mice following IFN $\alpha$ stimulation	ff81
<b>Figure 5.1</b>	Heatmap of IFN $\alpha$ regulated probes in the thymus of wt mice	ff85
<b>Figure 5.2</b>	qRT-PCR validation of microarray data	ff85
<b>Figure 5.3</b>	Venn diagram of IFN $\alpha$ up-regulated probes and probes within the Interferome	ff89

<b>Figure 5.4</b>	Heatmap of basal gene expression in the thymus of <i>Socs1<sup>-/-</sup>Ifnγ<sup>-/-</sup></i> , <i>Socs1<sup>+/+</sup>Ifnγ<sup>-/-</sup></i> and wt mice	ff92
<b>Figure 5.5</b>	Scatter plots of probe cluster found differentially expressed in the thymus of <i>Socs1<sup>+/+</sup>Ifnγ<sup>-/-</sup></i> and <i>Socs1<sup>-/-</sup>Ifnγ<sup>-/-</sup></i> mice	ff92
<b>Figure 5.6</b>	Venn diagram of basal SOCS1 negatively regulated (Basal Cluster 1) and IFNα regulated (IFNα regulated in WT mice) probes	ff94
<b>Figure 5.7</b>	Heatmap of IFNα regulated probes in <i>Socs1<sup>+/+</sup>Ifnγ<sup>-/-</sup></i> mice	ff97
<b>Figure 5.8</b>	Heatmap of IFNα regulated probes in <i>Socs1<sup>-/-</sup>Ifnγ<sup>-/-</sup></i> mice	ff97
<b>Figure 5.9</b>	Venn Diagram of probes found via two-way anova analysis of 3 and 6 hours IFNα stimulations in the thymus of <i>Socs1<sup>-/-</sup>Ifnγ<sup>-/-</sup></i> and <i>Socs1<sup>+/+</sup>Ifnγ<sup>-/-</sup></i> mice	ff99
<b>Figure 5.10</b>	Heatmap of genes that interact over IFNα and SOCS1 regulation	ff99
<b>Figure 5.11</b>	Clusters of co-regulated probes that interact over IFNα and SOCS1 regulation	ff100
<b>Figure 5.12</b>	Expression profile and list of genes within Interaction Cluster 1	ff100
<b>Figure 5.13</b>	qRT-PCR validation of microarray data	ff100
<b>Figure 5.14</b>	Venn diagram of probes found via two-way anova analysis of 3 hour and 6 hour IFNα stimulations in the thymus of <i>Socs1<sup>-/-</sup>Ifnγ<sup>-/-</sup></i> and <i>Socs1<sup>+/+</sup>Ifnγ<sup>-/-</sup></i> mice	ff101

## LIST OF TABLES

<b>Table 2.1</b>	List of antibodies used for flow cytometry	ff42
<b>Table 5.1</b>	DAVID functional annotation clustering of genes up-regulated in the thymus of wt mice 3 and 6 hours post IFN $\alpha$	ff86
<b>Table 5.2</b>	List of genes annotated with the GOTERM; GTPase activity or GTP binding, found up-regulated in wt mice 3 and 6 hours post IFN $\alpha$ .	ff86
<b>Table 5.3</b>	List of genes annotated with the GOTERM; Transferase activity, found up-regulated in wt mice 3 and 6 hours post IFN $\alpha$	ff86
<b>Table 5.4</b>	List of genes annotated with the GOTERM; Defence Response, found up-regulated in wt mice 3 and 6 hours post IFN $\alpha$	ff86
<b>Table 5.5</b>	Over-represented IRF, STAT and NF- $\kappa$ B transcription factor binding elements within the promoters of genes up-regulated in the thymus of wt mice 3 and 6 hours post IFN $\alpha$	ff88
<b>Table 5.6</b>	Over-represented transcription factor elements within IFN $\alpha$ up-regulated genes in the thymus of WT mice	ff88
<b>Table 5.7</b>	DAVID functional annotation clustering of the genes up-regulated in the thymus of wt mice 3 and 6 hours post IFN $\alpha$ that are <i>not</i> present within the Interferome	ff90
<b>Table 5.8</b>	DAVID functional annotation clustering of the genes up-regulated in the thymus of wt mice 3 and 6 hours post IFN $\alpha$ that are present within the Interferome	ff90
<b>Table 5.9</b>	Over-represented IRF, STAT and NF- $\kappa$ B transcription factor binding elements within the promoters of genes up-regulated in the thymus of wt mice 3 and 6 hours post IFN $\alpha$ and that were not present within the Interferome	ff91
<b>Table 5.10</b>	Over-represented IRF, STAT and NF- $\kappa$ B transcription factor binding elements within the promoters of genes up-regulated in the thymus of wt mice 3 and 6 hours post IFN $\alpha$ and that were present within the Interferome	ff91
<b>Table 5.11</b>	DAVID functional annotation of genes from Basal Cluster 1	ff93
<b>Table 5.12</b>	Clover promoter analysis of Basal Cluster 1 displaying A) Over-represented IRF, STAT and NF- $\kappa$ B binding elements, B) Over-represented “non-STAT, IRF or NF- $\kappa$ B” binding elements	ff93

<b>Table 5.13</b>	Gene list of Basal SOCS1 negatively regulated (Basal Cluster 1) and IFN $\alpha$ regulated (IFN $\alpha$ regulated in WT mice) genes with associated Ensemble gene transcript IDs	ff94
<b>Table 5.14</b>	DAVID functional annotation of basal SOCS1 negatively regulated (Basal Cluster 1) and IFN $\alpha$ regulated (IFN $\alpha$ regulated in WT mice) genes	ff94
<b>Table 5.15</b>	Clover promoter enrichment analysis of genes that are Basal SOCS1 negatively regulated (Basal Cluster 1) and IFN $\alpha$ regulated (IFN $\alpha$ regulated in WT mice) genes	ff94
<b>Table 5.16</b>	DAVID functional annotation of genes from Basal Cluster 2	ff95
<b>Table 5.17</b>	Clover promoter analysis of Basal Cluster 2 displaying A) Under-represented IRF, STAT and NF- $\kappa$ B binding elements, B) Over-represented “non-STAT, IRF or NF- $\kappa$ B” binding elements and C) Under-represented “non-STAT, IRF or NF- $\kappa$ B” binding elements	ff95
<b>Table 5.18</b>	DAVID functional annotation of genes from Basal Cluster 3	ff96
<b>Table 5.19</b>	Clover promoter analysis of Basal Cluster 3 displaying A) Over-represented IRF, STAT and NF- $\kappa$ B binding elements, B) Over-represented “non-STAT, IRF or NF- $\kappa$ B” binding elements and C) Under-represented “non-STAT, IRF or NF- $\kappa$ B” binding elements	ff96
<b>Table 5.20</b>	DAVID functional annotation clustering of genes up-regulated in the thymus of <i>Socs1</i> <sup>+/+</sup> <i>Ifn<math>\gamma</math></i> <sup>-/-</sup> mice with 3 and 6 hour IFN $\alpha$ stimulations	ff98
<b>Table 5.21</b>	DAVID functional annotation clustering of genes up-regulated in the thymus of <i>Socs1</i> <sup>-/-</sup> <i>Ifn<math>\gamma</math></i> <sup>-/-</sup> mice 3 and 6 hours post IFN $\alpha$	ff98
<b>Table 5.22</b>	DAVID functional annotation of genes that interact over IFN $\alpha$ and Socs1 regulation	ff99
<b>Table 5.23</b>	Over-represented STAT, IRF and NF- $\kappa$ B binding elements within the promoters of genes that interaction over IFN $\alpha$ and SOCS1 regulation	ff99
<b>Table 5.24</b>	DAVID functional annotation of genes from Interaction Cluster 1	ff100
<b>Table 5.25</b>	Over-represented STAT, IRF and NF- $\kappa$ B binding elements within the promoters of genes within Interaction Cluster 1	ff100
<b>Table 5.26</b>	DAVID Functional Annotation clustering of genes found regulated by IFN $\alpha$ yet not by Socs1 (Time – Interaction)	ff101
<b>Table 5.27</b>	Promoter Enrichment of genes found regulated by IFN $\alpha$ yet not by Socs1 (Time minus Interaction)	ff101

## ABBREVIATIONS

AP-1	Activator protein-1
ATP	Adenosine triphosphate
BMM	Bone marrow-derived macrophages
CARD	Caspase activation and recruitment domain
CBP	CREB-binding protein
cDNA	Complimentary DNA
Cmpk2	Cytidine monophosphate (UMP-CMP) kinase 2
CpG	2' -deoxyribo(cytidine-phosphate-guanosine)
CREB	cAMP responsive element binding
DC	Dendritic cell
Dhx58	DEXH (Asp-Glu-X-His) box polypeptide 58
DNA	Deoxyribonucleic acid
dsRNA	Double stranded RNA
EAR2	Nuclear receptor subfamil 2
ES	Enrichment score
Ets	Erythroblastosis virus E26 oncogene homolog
GAPDH	Glyceraldehyde phosphate dehydrogenase
GTP	Guanosine triphosphate
HAT	Histone acetyltransferase
HMG	High-mobility group
IFN	Interferon
IFNAR1	IFN alpha receptor 1
IFNAR2	IFN alpha receptor 2

IL	Interleukin
IRF	Interferon regulated factor
ISG	Interferon-stimulated gene
ISG15	Interferon stimulated gene 15kDa
ISGF3	Interferon-stimulated gene factor 3
ISRE	Interferon stimulated response element
IU	International units
I $\kappa$ B	Inhibitors of $\kappa$ B
JAK	Janus kinase
Lck	Lymphocyte-specific protein tyrosine kinase
LMCV	Lymphocytic chorimeningitis
LPS	Lipopolysaccharide
MDA5	Melanoma Differentiation-Associated protein 5
MFI	Mean Flourescence Intensity
Mx	Myxovirus (influenza virus) resistance
MyD88	Myeloid differentiation protein 88
NF- $\kappa$ B	Nuclear factor of kappa light chain gene enhancer in B-
OAS	Oligoadenylate synthetase
PAMP	Pathogen associated molecular pattern
PARP	Poly(ADP-ribose) polymerase
PBMC	Peripheral blood mononuclear cells
PBS	Phosphate buffered saline
PCR	Polymerase chain reaction
pDC	Plasmacytoid dendritic cell
PI3K	Phosphatidylinositol-3 kinase

PRD	Positive regulatory domain
PU.1	Purine-rich 1
PUR1	Purine-rich element binding protein 1
RA	Rheumatoid arthritis
RIG-I	Retinoic acid-inducible gene 1
RNA	Ribonucleic acid
RNAseL	Ribonuclease L
RSAD2	Radical S-adenosyl methionine domain containing 2
RT	Reverse transcriptase
RT-PCR	Real-time polymerase chain reaction
SDS	Sodium dodecyl sulphate
SLE	Systemic lupus erythematosus
SOCS	Suppressor of cytokine signaling
ssRNA	Single stranded RNA
STAT	Signal transducer and activator of transcription
SVK	Spleen tyrosine kinase
TF	Transcription factor
TLR	Toll like receptor
TRAF	TNF receptor-associated factor
TRAM	TRIF-related adaptor molecule
TRIF	TIR domain containing adaptor inducing IFN $\beta$
TRIM	Tripartite motif
TRP4	Transient receptor potential cation channel, subfamily
TYK2	Tyrosine kinase 2
USP18	Ubiquitin specific peptidase
VSV	Vesicular stomatitis virus

**CHAPTER 1**  
**LITERATURE REVIEW**  
**INTERFERON SIGNALING AND ITS REGULATION BY SOCS1**

**1.1 Introduction**

The IFNs were first discovered approximately 50 years ago due to their potent antiviral activity (Nagano and Kojima 1954; Isaacs and Lindenmann 1957). Since then, the critical importance of type I IFNs in controlling innate and adaptive immune responses has emerged and there are many examples of their use in clinical settings for the treatment of viral infections, cancers and some autoimmune diseases. The mechanism of type I IFN signaling, however, is complex and not yet fully understood. This review aims to highlight the current understanding of type I IFN signaling pathways and their functions, as well as investigate the negative regulation of type I IFN signaling via the potent inhibitor, suppressor of cytokine signaling (SOCS)1.

**1.2 The Interferons**

The interferons are a family of cytokines that elicit multifaceted effects in host innate and adaptive immunity. Produced in response to a number of stimuli, in particular viral infection, they exhibit antiviral, antiproliferative and immunomodulatory properties.

There are three types of IFNs: type I, type II and type III IFNs. The type I IFN family is extensive, consisting of multiple IFN $\alpha$  subtypes, IFN $\beta$ , IFN $\omega$ , IFN $\epsilon$  and IFN $\kappa$ , IFN $\delta$ , IFN $\tau$  and limitin (Hardy, Owczarek et al. 2004). The type II IFN family consists solely of IFN $\gamma$  and the type III interferon family consists of IFN $\lambda$ 1, IFN $\lambda$ 2 and IFN $\lambda$ 3 (Kotenko, Gallagher et al. 2003; Sheppard, Kindsvogel et al. 2003).

Human type I IFNs consist of 13 IFN $\alpha$ 's as well as IFN $\beta$ , IFN $\omega$ , IFN $\epsilon$  and IFN $\kappa$ . IFN $\delta$ , IFN $\tau$  and limitin are only found in pigs/cattle, ruminants and mice respectively (Hardy, Owczarek et al. 2004). The type I IFN genes are clustered on human chromosome 9p21 and in mouse they are clustered in a region of conserved synteny on chromosome 4 (Hardy, Owczarek et al. 2004). Phylogenetic analysis reveals three

main subfamilies of type I IFNs in mammals, IFN $\alpha$ , IFN $\beta$  and IFN $\omega$ . IFN $\beta$  appears as an out-group. Clustering based on amino acids identifies greater intra-species rather than interspecies similarities among the type I IFN subtypes (Hardy, Owczarek et al. 2004).

Although, by definition, all type I IFNs signal through the same receptor, they have a range of different functions and biological activities. Most studies performed with type I IFNs use IFN $\alpha$  subtypes and IFN $\beta$ . These are therefore extensively characterised and the main focus of this literature review.

### **1.3 Production of the Type I IFNs**

All nucleated cell types can produce type I IFN upon pathogenic infection via the detection of pathogen associated molecular patterns. Plasmacytoid dendritic cells, however, are specialised IFN producing cells that can produce large amounts of IFN (Liu 2005).

There are a number of complementary systems for pathogen detection leading to type I IFN production. These include the transmembrane toll-like receptors (TLR's) that localise at the plasma membrane or within intracellular vesicles, and cytosolic receptors including the RIG-I like helicases, DNA sensors such as STING and the DEAD/H-box helicases, the NOD-like receptors and C-type lectins (Dostert, Meylan et al. 2008; Takeuchi and Akira 2010; Sancho and Reis e Sousa 2012). The induction of type I IFNs in response to these pathogen detectors occurs in a cell-type specific and pathogen specific manner (Kato, Sato et al. 2005). Pathogen detection via these receptors leads to downstream signaling events resulting in the activation of transcription factors which regulate IFN production. Figure 1.1 shows the general signaling pathways from TLRs and the RIG-I like receptors following pathogen detection and the subsequent expression of type I IFNs.

#### **1.3.1 Transcriptional Activation of Type I IFN Production**

The promoter regions of the type I IFNs contain a number of regulatory *cis* elements. The IFN $\beta$  gene contains the positive regulatory domains (PRDs) I, II, III and IV while the promoter regions of the IFN $\alpha$  genes contain PRDI-like and PRDIII-like elements (Kim and Maniatis 1997; Honda, Takaoka et al. 2006). These elements bind transcription factors such as IRFs, NF- $\kappa$ B (for IFN $\beta$  only) and AP-1 along with the high-

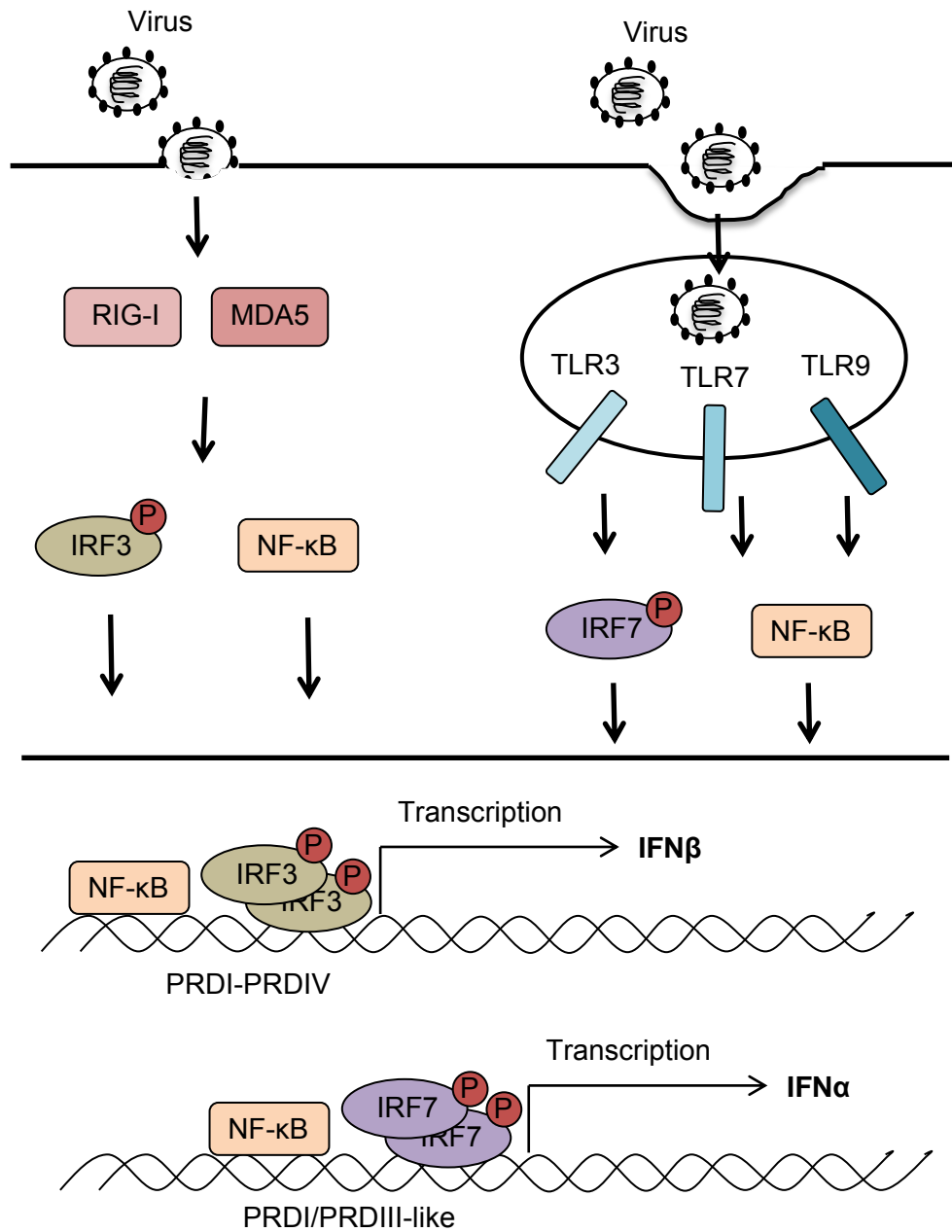


**Figure 1.1. Pathways leading to the transcriptional activation of the type I IFNs.** Type I IFN expression is activated in response to TLR mediated or cytosolic receptor mediated detection of pathogen associated molecular patterns. Activation of these pathways leads to transcription factor expression and activation of IRF factors and NFκB, resulting in type I IFN production.

mobility group protein HMG-I(Y) to form the “enhanceosome” complex (Kim and Maniatis 1997). For IFN $\beta$  gene expression, the enhanceosome recruits the histone acetyl transferase (HAT), called GCN5, which acetylates the nucleosomes blocking the TATA box and the transcription start site (Agalioti, Lomvardas et al. 2000). GCN5 then dissociates and the CBP-PolIII holoenzyme complex is recruited by the enhanceosome. Next the SWI/SNF complex is recruited by CBP and is stabilised by the acetylated histones. SWI/SNF remodels the nucleosomes allowing the transcription factor II D (TFIID) complex access to the promoter to drive gene expression (Agalioti, Lomvardas et al. 2000).

IRF3 and IRF7 are critical regulators of type I IFN production (Sakaguchi, Negishi et al. 2003; Honda, Yanai et al. 2005). They are members of a family of nine transcription factors (IRF1-9) which contain a conserved N-terminal DNA binding domain consisting of five tryptophan repeats (Mamane, Heylbroeck et al. 1999). Through this domain they bind specific DNA motifs within the promoter regions of responsive genes. IRF3 is constitutively expressed in many cell types and exists in the cytoplasm in an inactive state. In response to viral infection, it is activated via phosphorylation resulting in dimerisation and translocation to the nucleus (Sato, Tanaka et al. 1998). IRF3 binds to PRDI and PRDIII located within the IFN $\beta$  promoter and interacts with CBP to mediate IFN $\beta$  gene expression (Sato, Tanaka et al. 1998). In contrast, IRF3 has little effect on IFN $\alpha$  gene induction (Sato, Hata et al. 1998; Sato, Tanaka et al. 1998). Instead the IFN $\alpha$ 's are expressed as a result of IRF7 activation. IRF7 is expressed at low levels in most cell types but is strongly induced by type I IFN signaling through Interferon-stimulated gene factor 3 (ISGF3) (Sato, Hata et al. 1998). IRF7 also exists in an inactive state in the cytoplasm and upon viral infection undergoes phosphorylation, dimerisation and translocation into the nucleus. It can bind to the PRDI and PRDIII-like domains in the IFN $\alpha$  promoter regions inducing the expression of IFN $\alpha$  subtypes as well to the IFN $\beta$  promoter to induce IFN $\beta$  expression (Sato, Hata et al. 1998). The regulated expression of IRF7 by type I IFN signaling through ISGF3 creates a two phase expression of type I IFNs; IRF3 initially induces IFN $\beta$  which then acts in a positive feedback loop to induce IRF7, resulting in a subsequent second phase of IFN $\alpha$ 's expression (Sato, Tanaka et al. 1998). IRF7 also has a short half-life which may be a means to prevent overproduction of IFN (Honda, Takaoka et al. 2006).

Unlike other cell types, plasmacytoid dendritic cells (pDCs) are specialised IFN producing cells (Liu 2005). They constitutively express high levels of IRF7 and are thus primed to respond rapidly to viral infection (Honda, Yanai et al. 2005). This results in the rapid production of large amounts of IFN $\alpha$  and IFN $\beta$ . Within 24 hours of viral stimulation, pDCs produce 100 -1000 times the amount of IFN produced by any other cell type. pDCs have an important role in adaptive immune responses via the regulation of T-cells and B-cells thus linking innate and adaptive immunity (Liu 2005). In addition to pDCs, the constitutive expression of IRF7 may also occur in other cell types such as mammary epithelium where it has critical immune-regulatory effects (Bidwell, Slaney et al. 2012).

NF- $\kappa$ B and AP-1 are transcription factors that are also activated by viral infection and involved in the regulation of type I IFN production. They bind to PRDII and PRDIV elements within the promoter region of the IFN $\beta$  gene only (Kim and Maniatis 1997). Activation of NF- $\kappa$ B is central to TLR signaling, regulating a multitude of anti-pathogenic genes. NF- $\kappa$ B is maintained in the cytoplasm in the un-induced state through an interaction with I $\kappa$ B proteins. Activation of the IKK complex induces phosphorylation of the I $\kappa$ B proteins and their consequent ubiquitination and degradation. This releases NF- $\kappa$ B allowing translocation into the nucleus and activation of gene transcription (Carmody and Chen 2007).

### **1.3.2 Toll Like Receptors and Type I IFN Induction**

Toll-like receptors (TLRs) are key pathogen recognition receptors involved in innate immunity. They are transmembrane receptor proteins expressed at the cell surface and within endosomes. They recognise pathogen associated molecular patterns (PAMPs) from a wide range of microorganisms resulting in the activation of downstream signaling pathways and an innate immune response (Uematsu and Akira 2007). There are 13 mammalian TLRs. They contain a cytoplasmic Toll/IL-1 receptor (TIR) domain that is highly similar to the cytoplasmic domain of IL-1R and is required for activation of signaling events. The extracellular domains of TLRs contain leucine rich repeats and are responsible for PAMP recognition. Each TLR recognises specific PAMPs and activates its own intrinsic pathways to induce a specific biological response. A subset of TLRs induce type I IFN production in response to both viral and bacterial pathogen recognition. These include TLR3, TLR4, TLR7, TLR8 and TLR9 (Uematsu and Akira 2007). TLRs signal through their TIR domain by recruiting other TIR domain-containing

adaptor proteins in a homotypic interaction. These adaptor proteins include MyD88, MAL, TRIF and TRAM. TLR stimulation results in activation of the MyD88-dependent or the TRIF-dependent signaling pathways. All TLRs, except TLR3 activate the MyD88-dependent pathway whereas only TLR3 and TLR4 activate the TRIF-dependent pathway (Uematsu and Akira 2007).

TLR3 recognises viral dsRNAs from dsRNA and ssRNA viruses as well as a synthetic analogue of dsRNA, poly(I:C) (Choe, Kelker et al. 2005; Akira, Uematsu et al. 2006). Ligand stimulation of TLR3 results in activation of IRF3 and NF- $\kappa$ B via the TRIF signaling pathway (Yamamoto, Sato et al. 2003). TLR4, located on the cell surface plasma membrane, recognises lipopolysaccharide (LPS) from Gram negative bacterial cell walls as well as a number of viral proteins (Poltorak, He et al. 1998; Hoshino, Takeuchi et al. 1999; Akira, Uematsu et al. 2006). Once TLR4 activates the MyD88-dependent signaling pathway at the cell surface it is then internalised in an endosome and recruits TRAM and TRIF to activate the TRIF-dependent signaling pathway. This results in NF- $\kappa$ B and IRF3 activation which translocate to the nucleus and drive the transcription of IFN $\beta$  (Kawai, Adachi et al. 1999; Fitzgerald, Rowe et al. 2003; Hertzog, O'Neill et al. 2003; Hoebe, Janssen et al. 2003; Yamamoto, Sato et al. 2003). TLR4 induced IFN $\beta$  production is dependent on IRF3 rather than IRF7 activation. This is evident as IFN $\beta$  production in response to LPS in *Irf3*<sup>-/-</sup> mice is abolished whereas there is little effect on IFN $\beta$  production in *Irf7*<sup>-/-</sup> mice (Honda, Takaoka et al. 2006).

pDCs, the specialised IFN producing cells, express high levels of TLR7 and TLR9 and are thus primed to respond rapidly to pathogen. TLR9 recognises CpG DNA (CpG DNA motifs are found in the genomes of DNA viruses) and TLR7 recognises guanosine or uridine rich ssRNA from a number of viruses. Type I IFN production via TLR7 and TLR9 in pDCs is dependent on MyD88 and results in the activation of IRF7. This occurs through a direct interaction of MyD88 with IRF7 via its death domain while TRAF6 activates IRF7 through its ubiquitin E3 ligase activity (Hemmi, Kaisho et al. 2003; Honda, Yanai et al. 2004; Kawai, Sato et al. 2004). Other signaling events have also been linked to the activation of IRF7 in pDCs. IRAK1, IRAK4 and IKK $\alpha$  have been shown to be important for IRF7 activation suggesting that the IRAK1, IRAK4 and IKK $\alpha$  pathway may also be involved in full IRF7 phosphorylation (Uematsu and Akira 2007). The exact mechanisms of IRF7 activation need to be further elucidated to get a clearer picture of the pathways involved.

IRF1 is also activated by TLR signaling via a direct interaction with MyD88. This pathway appears more important in myeloid DCs rather than pDCs. IRF1 is strongly induced by IFN $\gamma$  and IFN $\beta$  induction is increased in DCs in an IRF1 dependent fashion following pre-treatment with IFN $\gamma$  (Negishi, Fujita et al. 2006).

In addition to the TLRs, the C-type Lectins are another family of plasma membrane receptors that recognise PAMPs (Zelensky and Gready 2005). The cytoplasmic domains of the C-type lectins contain Immunoreceptor Tyrosine based Activation Motifs (ITAMs) which signal via the recruitment of Syk kinases, MAP kinases, NFAT and NF $\kappa$ B pathways leading to the modulation of cytokine production (Zelensky and Gready 2005). In the context of type I IFN expression, the C-type lectin, CLEC4C, has been shown to inhibit TLR-9 induced type I IFN production in pDCs through activation of Syk kinases (Dzionic, Sohma et al. 2001). An increase in CLEC4C antigen expression by peripheral blood leukocytes following infection is thought to help control excessive IFN production activated by pDCs in pathological tissue (Riboldi, Daniele et al. 2011). Furthermore, the expression of CLEC4C antigen on tumour cells is thought to be a mechanism to evade type I IFN responses (Riboldi, Daniele et al. 2011).

### 1.3.3 Cytosolic Receptors and Type I IFN Induction

Host mechanisms have also developed for the detection of cytosolic pathogens and associated antigens. These include the RIG-I like helicases, the NOD-like receptors and other sensors such as STING.

Viral replication can result in the production of intracellular dsRNA. RNA helicase retinoic acid inducible gene (RIG-I) and its homologue melanoma-differentiation-associated gene 5 (MDA5) are essential cytosolic proteins involved in intracellular dsRNA recognition leading to the production of type I IFNs (Yoneyama, Kikuchi et al. 2004; Kato, Takeuchi et al. 2006). They serve complementary roles both *in vivo* and *in vitro* in dsRNA detection. *In vitro* RIG-I and MDA5 detect different types of dsRNA; RIG-I detects *in vitro* transcribed dsRNAs whereas MDA5 detects poly(I:C) (Kato, Takeuchi et al. 2006). RIG-I and MDA5 also have differential roles in the recognition of RNA viruses (Kato, Takeuchi et al. 2006). *Rig-I*<sup>-/-</sup> mice are unable to produce type I IFN in response to negative-sense ssRNA viruses including Newcastle Disease virus (NDV), Sendai virus (SeV), Vesicular Stomatitis virus (VSV) and influenza as well as positive sense ssRNA viruses such as Japanese encephalitis virus whereas MDA5 is dispensable for type I IFN production in response to these viruses (Kato, Sato et al.

2005; Kato, Takeuchi et al. 2006). In contrast, *Mda5*<sup>-/-</sup> mice are unable to produce type I IFN in response to positive-sense ssRNA viruses such as Encephalomyocarditis virus (EMCV), Theiler's virus and Mengo virus (Kato, Takeuchi et al. 2006).

RIG-I and MDA5 are similar in overall structure containing two N-terminal caspase recruitment domains (CARD) and a C-terminal DEcD/H box RNA helicase domain. The DEcD/H box helicase domain is a characteristic motif of many RNA binding proteins. It recognises, binds to, and unwinds dsRNA via ATP hydrolysis. This causes a conformational change within RIG-I and MDA5 allowing the N-terminal CARD domains to interact with the N-terminal CARD domain of the IFN $\beta$  promoter stimulator 1 (IPS-1, also known as MAVS, Cardif and VISA) which is localised to the outer mitochondrial membrane via a C-terminal hydrophobic transmembrane region (Yoneyama, Kikuchi et al. 2004; Kawai, Takahashi et al. 2005) (Kumar, Kawai et al. 2006). The interaction of RIG-I and IPS-1 is facilitated by the E3 ubiquitin ligase, TRIM25. IPS-1 and TRAF3 also directly interact; this is via a TRAF-interaction motif (TIM) within IPS-1 and the TRAF domain of TRAF3 (Saha, Pietras et al. 2006). TRAF3 is involved in the activation of TANK binding kinase (TBK1), the essential serine-threonine kinase for the phosphorylation and activation of IRF3 and IRF7 (Oganesyan, Saha et al. 2006). IPS-1 has also been shown to interact with TRAF6, FADD and RIP1, most likely involved with the activation of NF- $\kappa$ B (Kawai, Takahashi et al. 2005; Xu, Wang et al. 2005). These signaling pathways ultimately result in activation of the transcription factors IRF3, IRF7 and NF- $\kappa$ B consequently leading to type IFN production. IRF3 and IRF7 are both critical to IFN production in the cytosolic pathway however the conventional two-step model of IFN production does not occur. In the cytosolic pathway, in addition to a role in later phase IFN production, IRF7 expression is critical in early phase type I IFN production. In the absence of IRF7 during the early phase, the contribution of IRF3 is minor. It is hypothesised that an IRF7 homodimer or an IRF3/IRF7 heterodimer rather than an IRF3 homodimer may be necessary for IFN production in the cytosolic pathway (Honda, Takaoka et al. 2006).

In addition to cytosolic RNA sensors, there are also a number of cytosolic DNA sensors such as STING and the DEAD/H-box helicases which recognise DNA viruses and drive type I IFN production. STING which recognises dsDNA is localised to the ER. Activation of STING results in its translocation to other subcellular organelles, an association with TBK and subsequent activation of IRF3 and IFN $\beta$  production (Ishikawa and Barber 2008). The DEAD/H-box helicases, DHX36 and DHX9 sense CpG DNA

motifs and interact with MyD88 leading to activation of NF- $\kappa$ B or IRF7 activation of IFN $\alpha$  transcription (Kim, Pazhoor et al. 2010).

Other cytosolic receptors involved in pathogen recognition include the NOD-Like receptors (NLRs). Members of the NLR family recognise a range of pathogen antigens including viral RNA, bacterial cell wall peptidoglycans and bacterial associated toxins as well as non-microbial stimuli such as uric acid crystals, amyloid plaques, ATP and cholesterol (Inohara and Nunez 2003; Dostert, Meylan et al. 2008). NLRs contain a C-terminal ligand recognition domain, a central oligomerisation and binding domain (Nod) and an N-terminal interaction domain such as CARD, Pypin or Baculovirus inhibitor of apoptosis protein repeat (BIR). Ligand binding results in aggregation of NLRs through their central domain and protein interactions through their N-terminal domains to drive inflammation. NOD1 and NOD2 which contain N-terminal CARD domains recruit signaling adaptors leading to activation of NF- $\kappa$ B and the MAP kinase pathways (Inohara and Nunez 2003). NLRs containing BIR or Pypin domains primarily signal through recruitment of ASC resulting in activation of Caspase 1 which cleaves IL1, IL18 and IL33 to their mature forms (Dostert, Meylan et al. 2008). Interestingly, the NLRP3-ASC-Caspase 1 pathway, while activating IL-1 does not appear to induce expression of the type I IFNs, a notable distinction from most of the other pathogen recognition pathways.

## **1.4 Type I IFN Signaling**

The type I IFNs signal through a common receptor, the IFN alpha-receptor, IFNAR. As demonstrated in Figure 1.2, the primary signaling pathway activated by the type I IFNs is the JAK/STAT signaling pathway resulting in formation of the transcription factor ISGF3 (composed of STAT1 STAT2 and IRF9) as well as other STAT homodimers and heterodimers, which regulate transcription of interferon stimulated genes (ISGs). Below is a detailed review of the signaling events leading to the activation of the JAK/STAT pathway from the receptor to STAT mediated expression of ISGs.

### **1.4.1 The IFN Alpha Receptor (IFNAR)**

All type I IFNs signal through the IFN $\alpha$ -receptor, IFNAR, composed of two transmembrane glycoproteins belonging to the class II helical cytokine receptor (hCR)

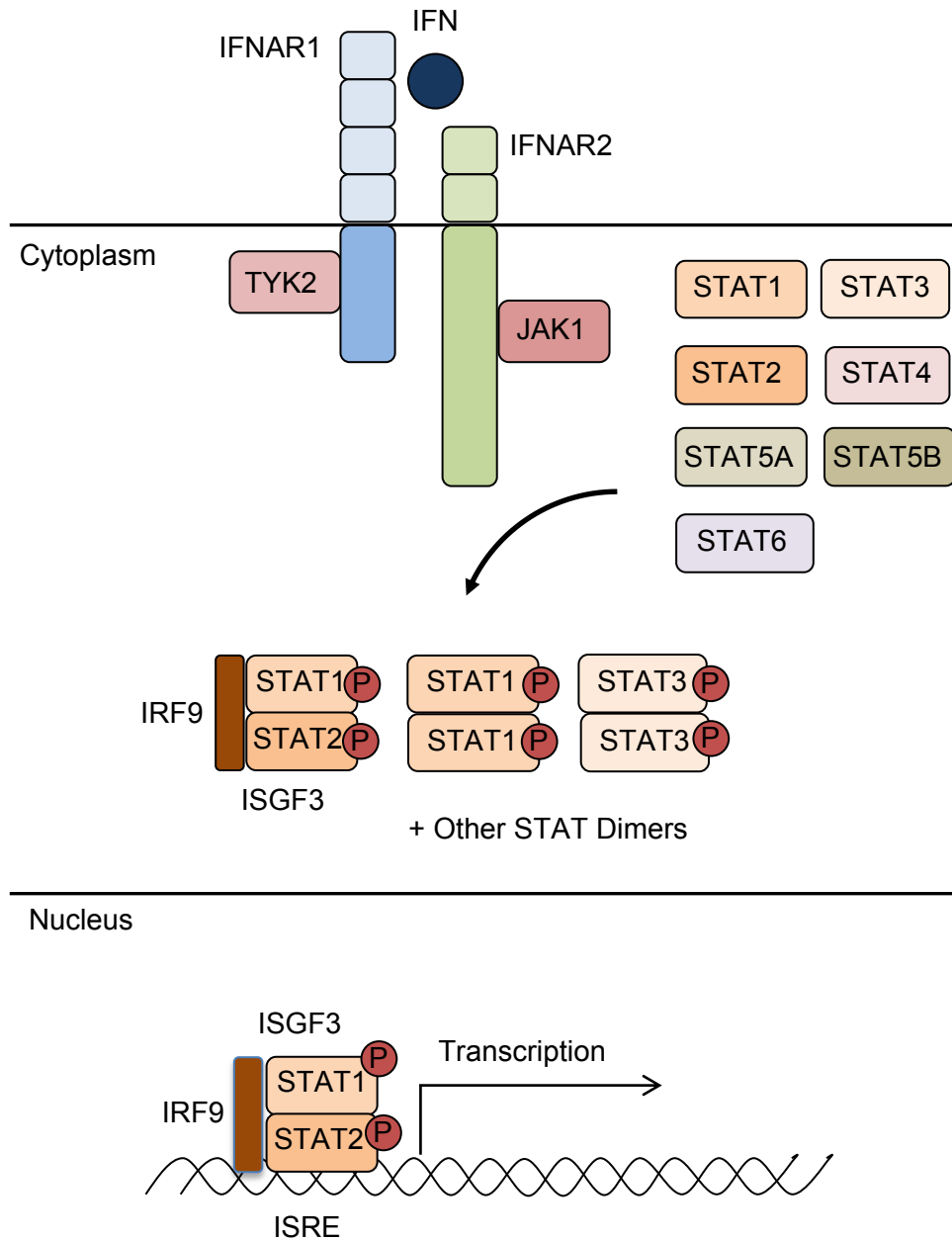


**Figure 1.2. The Type I IFN JAK/STAT pathway.** Type I IFN binding to IFNAR results in cross-activation of the intracellular associated kinases, Tyk2 and Jak1. These in turn phosphorylate intracellular tyrosine residues of IFNAR1 and IFNAR2. STATs are recruited to the receptor via the interaction of their SH2 domain with phosphorylated receptor tyrosines. Recruited STATs are phosphorylated via the receptor associated kinases resulting in STAT dimerisation and translocation to the nucleus to regulate gene expression. All STAT family members can be activated by the type I IFNs resulting in various combinations of STAT dimers which bind distinct DNA elements to regulate transcription. The complex ISGF3, composed of STAT1, STAT2 and IRF9, is highly activated by type I IFNs and binds ISRE sites within the promoters of ISGs.

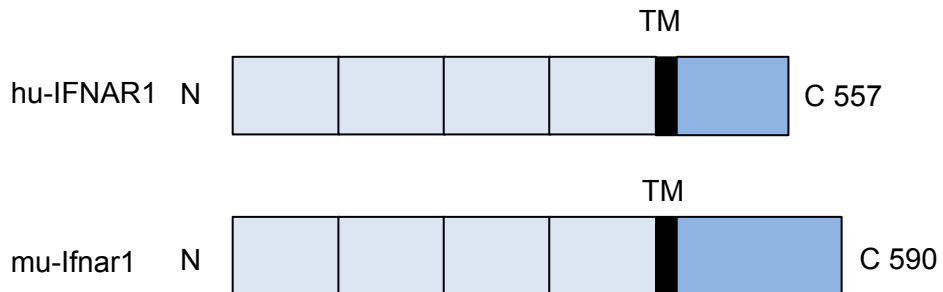
family (Kim, Cohen et al. 1997; Krause and Pestka 2005). The two receptor subunits IFNAR1 and IFNAR2 are expressed in almost every cell type (Kim, Cohen et al. 1997). Many cells are therefore able to respond to IFN stimulation. The genes encoding IFNAR1 and IFNAR2 are located on human chromosome 21q22.1 in a cytokine receptor gene cluster.

Both receptor subunits are required for type I IFN signaling (Domanski, Witte et al. 1995). A two-step mechanism of IFN binding to IFNAR occurs by which IFN initially docks onto the high affinity receptor subunit IFNAR2 to form an IFN-IFNAR2 complex which then binds IFNAR1 (Cohen, Novick et al. 1995). IFN binding to the receptor is species specific as mu-Ifn cannot bind hu-IFNAR and vice versa (Constantinescu, Croze et al. 1994).

Hu-IFNAR1 and mu-Ifnar1 were first cloned in 1990 and 1992, respectively (Uze, Lutfalla et al. 1990; Uze, Lutfalla et al. 1992). Figure 1.3 shows the structure of hu-IFNAR1 and mu-Ifnar1. Hu-IFNAR1 is a glycoprotein of 557 amino acids. It consists of a 27 amino acid leader sequence, a large extracellular domain of 409 amino acids, a single transmembrane domain of 21 amino acids and an intracellular domain of 100 amino acids (Uze, Lutfalla et al. 1990). Mu-Ifnar1 is a 590 amino acid protein with 46% amino acid homology with hu-IFNAR1. It contains a leader sequence of 26 amino acids, a large extracellular domain of 403 amino acids, a single transmembrane domain of 20 amino acids and a 141 amino acid intracellular domain (Uze, Lutfalla et al. 1992).

The extracellular domain of IFNAR1 consists of four subdomains (SD1-SD4) each containing a fibronectin (FBN-like) domain. The subdomains SD1-SD3 are involved in ligand binding (SD1-SD3) as well as binding membrane glycosphingolipids (SD1) (Ghislain, Lingwood et al. 1994; Cajean-Feroldi, Nosal et al. 2004; Chill, Quadt et al. 2004; Lamken, Lata et al. 2004; Strunk, Gregor et al. 2008). SD4 is required for inducing a conformation change in IFNAR1 following ligand binding which is essential for signal activation (Strunk, Gregor et al. 2008). The intracellular domain of IFNAR1 is constitutively associated with the Janus Tyrosine Kinase, TYK2 (Colamonici, Uyttendaele et al. 1994; Gutterman 1994). The TYK2 binding site on hu-IFNAR1 has been mapped to residues 481 - 511 (Yan, Krishnan et al. 1996). The recruitment of SH2 domain-containing signaling molecules (such as STATs) to the receptor requires phosphorylated tyrosine residues. The intracellular domain of human and murine IFNAR1 contains four tyrosine residues (hu-IFNAR1; Tyr466, Tyr481, Tyr527 and

### Full Length IFNAR1



### Intracellular Domain

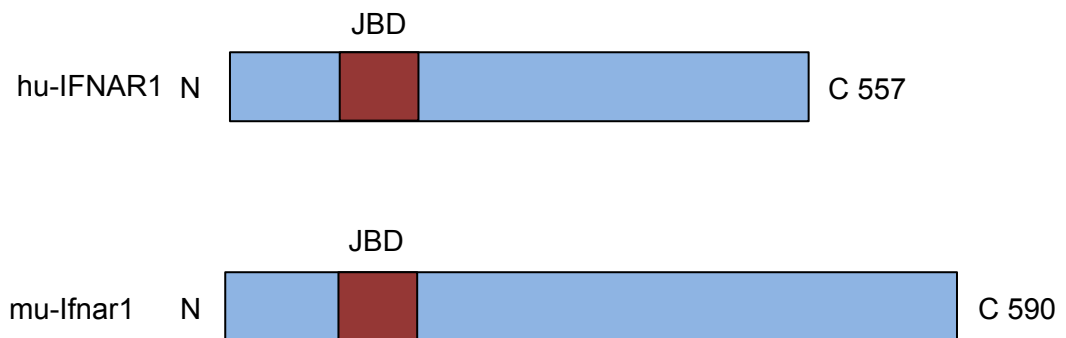


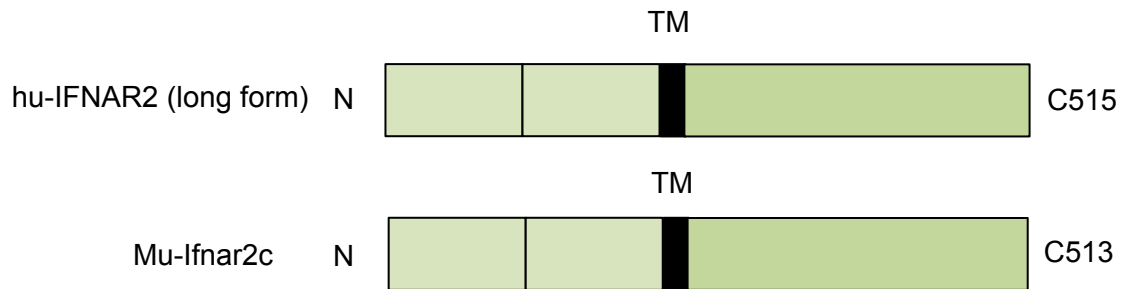
**Figure 1.3: Structure of hu-IFNAR1 and mu-Ifnar1.** hu-IFNAR1 and mu-Ifnar1 consist of four extracellular subdomains (SD1 – SD4) involved in ligand binding and ternary complex formation, a transmembrane domain (TM) and an intracellular domain containing a JAK binding domain (JBD) and four tyrosine phosphorylation sites.

Tyr538, mu-Ifnar1; Tyr455, Tyr518, Tyr529 and Tyr576). The two most C-terminal tyrosine residues of hu-IFNAR1, Tyr527 and Tyr538, are conserved in mouse and correspond to Tyr518 and Tyr529 of mu-Ifnar1. A negative regulatory region of IFNAR1 has been mapped to 16 residues surrounding the two conserved tyrosines, as deletion of this region resulted in increased sensitivity to IFN (Gibbs, Takahashi et al. 1996; Basu, Yang et al. 1998).

The importance of IFNAR1 is evident in the phenotype of *Ifnar1*<sup>-/-</sup> mice (Muller, Steinhoff et al. 1994; Hwang, Hertzog et al. 1995). IFNAR1 is vital for mediating the antiviral activities of type I IFNs and *Ifnar1*<sup>-/-</sup> mice are extremely susceptible to viral infection (Hwang, Hertzog et al. 1995). Compared to wild type mice, *Ifnar1*<sup>-/-</sup> mice die rapidly after SFV and EMCV infection with extremely high viral titres detected in multiple organs. The induction of antiviral IFN stimulated genes such as 2'-5'OAS were undetectable in *Ifnar1*<sup>-/-</sup> cells following treatment with IFN. Abnormalities of hemopoietic cells are also seen in the *Ifnar1*<sup>-/-</sup> mice (Hwang, Hertzog et al. 1995). Elevated levels of myeloid lineage cells are detected in the peripheral blood and bone marrow. In addition, bone marrow macrophages from *Ifnar1*<sup>-/-</sup> mice are functionally abnormal showing reduced antiproliferative and antiviral effects and aberrant responses to CSF-1 (Hwang, Hertzog et al. 1995). Interestingly there were no differences observed in the levels of peripheral blood CD4 or CD8 T-cell populations in *Ifnar1*<sup>-/-</sup> compared to wild type mice (Hwang, Hertzog et al. 1995).

There are three forms of hu-IFNAR2: a soluble form (hu-IFNAR2a) and two transmembrane forms (short; IFNAR2b and long; IFNAR2c). The soluble and short transmembrane forms of hu-IFNAR2 were identified and cloned in 1994 and the long transmembrane form in 1995 (Novick, Cohen et al. 1994; Domanski, Witte et al. 1995; Lutfalla, Holland et al. 1995). Three forms of mu-Ifnar2 have also been cloned including two soluble forms, mu-Ifnar2a and mu-Ifnar2a' and one transmembrane form, Mu-Ifnar2c (Kim, Cohen et al. 1997; Owczarek, Hwang et al. 1997). Figure 1.4 shows the structure of long hu-IFNAR2 and mu-IFNAR2c. There has also been *in vitro* evidence for the generation of a soluble IFNAR2 by cleavage of transmembrane IFNAR2 by intramembrane proteases (Saleh, Fang et al. 2004). Long transmembrane hu-IFNAR2 is 515 amino acids, short transmembrane hu-IFNAR2 is 331 amino acids and soluble hu-IFNAR2 is 239 amino acids in length. The transmembrane forms share the same 26 amino acid leader sequence and an extracellular region of 217 amino acids. The 239 amino acid soluble form of IFNAR2 consists of the leader sequence and extracellular

### Full Length



### Intracellular Domain



**Figure 1.4: Structure of hu-IFNAR2 (long form) and mu-Ifnar2c.** hu-IFNAR2 (long form) and mu-Ifnar2c consist of two extracellular subdomains involved in ligand binding, a transmembrane domain (TM) and an intracellular domain containing a JAK binding domain (JBD) and seven (human) or six (mouse) tyrosine phosphorylation sites.

region up to amino acid 237 with an additional two amino acids at its C-terminal end (Novick, Cohen et al. 1994). Short and long transmembrane forms diverge at amino acid 280, which is just distal to the 21 amino acid transmembrane region. Long hu-IFNAR2 has an intracellular region of 251 amino acids and short IFNAR2 has an intracellular region of 67 amino acids (Novick, Cohen et al. 1994; Lutfalla, Holland et al. 1995). The structure of mu-Ifnar2c includes a 27 amino acid leader sequence, an extracellular region of 215 amino acids, a transmembrane region of 21 amino acids and an intracellular region of 250 amino acids (Kim, Cohen et al. 1997; Owczarek, Hwang et al. 1997). The two soluble forms of mu-Ifnar2, mu-Ifnar2a and mu-Ifnar2a', contain all but the last six C-terminal amino acid residues of the extracellular domain of mu-Ifnar2c. Each variant has an additional 12 (mu-Ifnar2a) and 11 (mu-Ifnar2a') unique amino acid residues at their C-terminus. Long transmembrane forms of murine and human IFNAR2 share 49% structural identity.

Only the long form of IFNAR2, when expressed with IFNAR1, can activate the JAK-STAT signaling pathway in response to type I IFN (Lutfalla, Holland et al. 1995). The short IFNAR2 form does not contain the full JAK1 binding motif and although it can bind IFN, is unable to activate IFN induced pathways. It has been reported to have a dominant negative role following IFN $\alpha$  stimulation, inhibiting the signaling pathways activated by the long form (Pfeffer, Basu et al. 1997; Gazzola, Cordani et al. 2005). For example, when expressed with IFNAR1, the short form of IFNAR2 reduces the IFN-induced antiviral, antiproliferative and ISRE-dependent gel shift binding activity conferred by IFNAR1 alone (Pfeffer, Basu et al. 1997). The soluble forms of IFNAR2 have been found to have both agonistic and antagonistic effects *in vitro* (Hardy, Owczarek et al. 2001). In L929 cells, recombinant mu-Ifnar2a competitively inhibited IFN $\alpha$  and IFN $\beta$  in reporter assays as well as the anti-viral and anti-proliferative effects of IFN. In contrast, in primary thymocytes from *Ifnar2<sup>-/-</sup>* mice, recombinant mu-Ifnar2a was able to form a complex with IFN $\alpha$  or IFN $\beta$  and mu-Ifnar1 and transmit an anti-proliferative signal (Hardy, Owczarek et al. 2001). *In vivo*, soluble Ifnar2 has been found to potentiate IFN signaling; transgenic mice overexpressing soluble Ifnar2 are more susceptible to LPS- and IFN $\beta$ - induced septic shock (Samarajiwa et al, unpublished data). Soluble Ifnar2 may therefore be involved in trans-signaling events (similar to sIL6R) (de Weerd, Samarajiwa et al. 2007; Waetzig and Rose-John 2012). Low concentrations of soluble Ifnar2 have also found to increase the stability of IFN $\beta$

and may therefore potentiate signaling by reducing the clearance and increasing the half-life of IFN $\beta$  *in vivo* (McKenna, Vergilis et al. 2004).

The remainder of this section of the review will focus on signaling events mediated by the long transmembrane form of IFNAR2 rather than the short forms. The intracellular domain of IFNAR2 is constitutively associated with the JAK tyrosine kinase, JAK1 (Domanski, Fish et al. 1997). The JAK1 binding region of hu-IFNAR2 maps to amino acids 300-346 (Domanski, Fish et al. 1997). The intracellular region of hu-IFNAR2 contains two clusters of tyrosines, a proximal cluster (Tyr269, Tyr306, Tyr316, Tyr318, and Tyr377) and a distal cluster (Tyr411 and Tyr512). The intracellular region of mu-Ifnar2c contains Tyr268, Tyr315, Tyr317, Tyr355, Tyr398 and Tyr 510.

IFNAR2 is also essential for IFN signaling as demonstrated in *Ifnar2*<sup>-/-</sup> mice. These mice are highly susceptible to viral and bacterial infections and have abnormal thymic T-cell development (Hertzog et al, unpublished data).

#### **1.4.2 Janus Tyrosine Kinases (JAKs)**

The Janus Tyrosine Kinases (JAKs) are a family of non-receptor protein tyrosine kinases that include JAK1, JAK2, JAK3 and TYK2. Figure 1.5 shows the general structure of the JAK kinases. These kinases are 115 – 135 kDa and consist of seven JH regions. C-terminal JH1 is a pseudo-kinase domain, JH2 is an adjacent kinase domain and JH3-JH7 are involved in protein interactions. TYK2 and JAK1 are intracellularly associated with IFNAR1 and IFNAR2 respectively and upon IFN binding, TYK2 and JAK1 are thought to be trans-phosphorylated and activated resulting in phosphorylation of the receptor subunits (Muller, Briscoe et al. 1993; Barbieri, Velazquez et al. 1994; Constantinescu, Croze et al. 1994).

##### **1.4.2.1 TYK2**

The intracellular domain of IFNAR1 is constitutively associated with the Janus Tyrosine Kinase, TYK2 (Colamonici, Uyttendaele et al. 1994; Gutterman 1994). TYK2 was first linked to type I IFN signaling by chemical mutagenesis of a 2fTGH cell line resulting in a mutant cell line (Mutant 11,1) unresponsive to IFN $\alpha$  and only partially sensitive to IFN $\beta$  (Velazquez, Fellous et al. 1992). Transfection of a cosmid containing the TYK2 gene into the mutant cells reverted the cell phenotype back to that of wild type 2fTGH cells (Velazquez, Fellous et al. 1992). The TYK2 binding site on IFNAR1 has been

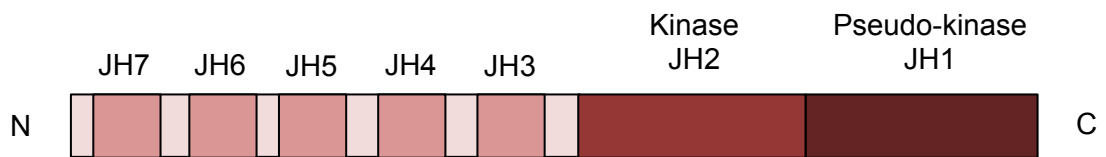


**Figure 1.5 Structure of the JAK kinases.** JAK kinases consist of seven Janus Homology regions (JH1 – JH7). C-terminal JH1 is a pseudo-kinase domain, JH2 is a kinase domain and JH3 – JH7 are involved in protein interactions.

mapped to residues 481 - 511 of hu-IFNAR1 with most of the conserved residues within this region required for binding (Yan, Krishnan et al. 1996). The mutation of critical residues within this site results in reduced TYK2, STAT1 and STAT2 phosphorylation in response to IFN $\alpha$  (Yan, Krishnan et al. 1996).

TYK2 has also been linked to the stabilisation of IFNAR1 at the plasma membrane (Gauzzi, Barbieri et al. 1997; Ragimbeau, Dondi et al. 2003). In cells lacking TYK2, IFNAR1 is only weakly expressed at the cell surface and is instead found localised in a perinuclear endosomal compartment (Ragimbeau, Dondi et al. 2003). Increased expression of TYK2 results in increased localisation of IFNAR1 to the cell surface and reduced degradation of IFNAR1 due, in part, to reduced endocytosis (Ragimbeau, Dondi et al. 2003).

TYK2 deficient mice show no overt developmental deficiencies however contain defects in IL-12 induced T-cell functions (Shimoda, Kato et al. 2000). Although un-responsive to low doses of IFN $\alpha$ , *Tyk2*<sup>-/-</sup> embryonic fibroblasts (EFs) are still sensitive to high doses of IFN $\alpha$  as assessed by phosphorylation of STAT1, STAT2 and the induction of MHC class-1 (Shimoda, Kato et al. 2000). These mice also respond normally to IL-6 and IL-10 which both activate TYK2 *in vitro*. In addition, the level of expression of IFNAR1 on the cell surface membrane was similar to that of wild type mice, which contradicts previous findings that TYK2 stabilises IFNAR1 at the plasma membrane (Shimoda, Kato et al. 2000). These findings were somewhat surprising as a larger defect in type I IFN signaling was expected. The JAKs are quite similar in structure and perhaps in the absence of TYK2 another JAK is able to bind IFNAR1 or other cytokine receptors (such as receptors of IL-6 and IL-10) and mediate IFN signaling.

#### **1.4.2.2 JAK1**

The intracellular domain of IFNAR2 is constitutively associated with the Janus Tyrosine Kinase, JAK1 (Domanski, Fish et al. 1997). Similarly to TYK2, JAK1 was first linked to type I IFN signaling via mutagenesis of a 2fTGH cell line resulting in a mutant cell line (U4A) unresponsive to IFN $\alpha$ . Transfection of JAK1 back into the mutant cell line resulted in restoration of the type I IFN response (Muller, Briscoe et al. 1993). The JAK1 binding region on IFNAR2 comprises amino acids 300-346. This is distinct from the Box 1 motif (amino acids 287-295) of IFNAR2, which is important for the binding of other cytokine receptors to JAK kinases (Domanski, Witte et al. 1995).

Disruption of the JAK1 gene in mice show that it is essential for type I and II IFN signaling as well as for many other cytokine signaling pathways, including those involving class II cytokine receptors and those that utilise the gp130 receptor subunit and  $\gamma_c$  subunit (Rodig, Meraz et al. 1998). JAK1 null mice die perinatally and weigh 40% less than their wild type littermates. Although no gross abnormalities are found in most organs, the thymus is significantly reduced in size, containing a severely reduced number of thymocytes, possibly due to a lack of IL-7 signaling (Rodig, Meraz et al. 1998). Fibroblasts and macrophages from JAK1 null embryos are unresponsive to IFN $\alpha$  and IFN $\gamma$ , demonstrating the importance of JAK1 in type I and II IFN signaling (Rodig, Meraz et al. 1998).

#### **1.4.2.3 JAK Activation and Function**

TYK2 and JAK1 are rapidly phosphorylated and activated in response to IFN $\alpha$  (Muller, Briscoe et al. 1993; Barbieri, Velazquez et al. 1994; Colamonici, Yan et al. 1994; Constantinescu, Croze et al. 1994; Plataniias, Uddin et al. 1994). This is likely via cross-phosphorylation. In mutant U4A cells lacking JAK1, TYK2 fails to be phosphorylated in response to IFN. Conversely, JAK1 fails to be phosphorylated in mutant U1D cells lacking TYK2 (Muller, Briscoe et al. 1993). TYK2 is phosphorylated on amino acids Tyr1054 and Tyr1055, located within its kinase domain (Gauzzi, Velazquez et al. 1996). Activated TYK2 and JAK1 are then likely to phosphorylate IFNAR. Phosphorylation of the JAKs and IFNAR subunits follows similar kinetics peaking within 1 - 5 minutes and reducing by 60 minutes (Constantinescu, Croze et al. 1994; Plataniias, Uddin et al. 1994). Phosphorylated receptor chains and JAK kinases then recruit and activate signaling molecules (such as STATs) to elicit the type I IFN response.

#### **1.4.3 Signal Transducers and Activators of Transcription**

STATs are a family of transcription factors activated in response to cytokine signaling. Figure 1.6 shows the general structure of the STAT proteins. They are between 750 and 800 amino acids in length and contain an SH2 domain that mediates binding to other proteins, a carboxyl-terminal tyrosine phosphorylation site, a DNA binding site between amino acids 400 and 500 and an N-terminal portion that mediates cooperative binding to multiple DNA sites (Akira 1999). There are 7 STAT family members: STAT1, STAT2, STAT3, STAT4, STAT5a, STAT5b and STAT6. Type I IFNs can activate all STAT family members (van Boxel-Dezaire, Rani et al. 2006). The mechanism however is complex and occurs in a cell type and specific manner (as discussed below).

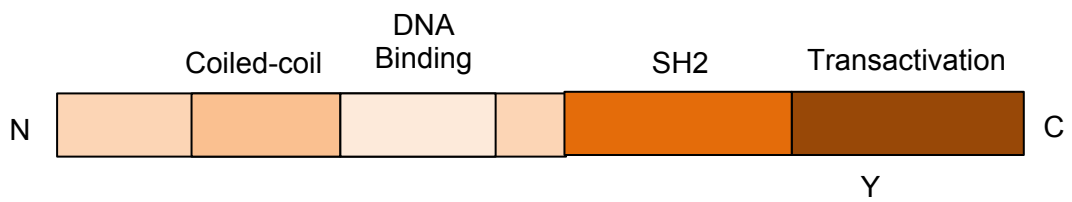


**Figure 1.6 Structure of the STAT family of transcription factors.** STAT family members contain several functional domains including an N-terminal protein interaction domain, a coiled-coil domain, a central DNA binding domain, an SH2-domain and a C-terminal transactivation domain containing a conserved tyrosine residue (Y) which once phosphorylated binds the SH2 domain of other STAT molecules to form STAT dimers. .

Specific phosphorylated tyrosine residues of IFNAR serve as docking sites for the SH2 domains of STATs, however STATs have also been reported to bind receptors (including IFNAR) via phosphotyrosine independent mechanisms (Darnell 1997; Nadeau, Domanski et al. 1999; Nguyen, Saleh et al. 2002; Tyler, Persky et al. 2007; Zhao, Lee et al. 2008). Following recruitment to the receptor complex, STATs are activated by phosphorylation on a highly conserved carboxyl-terminal tyrosine residue, presumably by the receptor associated JAKs (Darnell 1997). They then dimerise by SH2-phosphotyrosine interactions. STAT dimers are able to enter the nucleus and bind specific DNA elements to regulate gene expression (Darnell 1997). In addition to tyrosine phosphorylation, other STAT modifications such as serine phosphorylation of STAT1, STAT3 and STAT5 also occur which enhance their ability to regulate gene expression (Darnell 1997).

Although the STAT transcription factors were proposed to bind to similar sequences, different gene knock-outs display distinct phenotypes. In general STAT dimers bind to palindromic DNA elements with the same core motif, TTCN<sub>2-4</sub>GAA, however small differences in this sequence such as the number of N nucleotides present can have effects on the binding specificity of different STATs (Ehret, Reichenbach et al. 2001). The actions of the type I IFNs therefore depend largely on the level and type of STATs activated by the receptor. As discussed below, the level and type of STATs activated by the IFN receptor varies across different cell types and may therefore be dependent on a number of factors such as the level of receptor on the cell surface available for signaling, the presence or absence of co-activators or inhibitors and the type of IFN acting on the cell. Specific STAT transcription complexes that form in the cell following IFN stimulation will drive expression of a distinct set of genes and thus dictate the cellular response to IFN. It is therefore important to understand how the STATs are activated in response to IFN as well as the level and type of STAT activation in particular cell types.

#### **1.4.3.1 STAT1 and STAT2**

STAT1 and STAT2 have an essential role in type I IFN signaling (Meraz, White et al. 1996; Park, Li et al. 2000). After phosphorylation and activation, they complex with IRF9 to form the major transcriptional complex activated by type I IFNs, ISGF3. ISGF3 binds IFN stimulated response elements (ISRE) located within the promoters of IFN

stimulated genes (ISGs). STAT1 also forms homodimers, which bind Gamma Activated Sequences (GAS).

The generation of STAT1 and STAT2 null mice demonstrate the importance of these transcription factors in type I IFN signaling (Meraz, White et al. 1996; Park, Li et al. 2000). STAT1 null mice do not show any overt developmental abnormalities however they do have a complete lack of responsiveness to type I and II IFNs and are highly sensitive to viral infection (Meraz, White et al. 1996). STAT2 null mice are also highly sensitive to viral infection and have several immune defects due to absent type I IFN signaling including a lack of the type I IFN autocrine activation loop and defects in macrophage and T-cell responses (Park, Li et al. 2000). In particular, the T-cell specific marker Ly-6C, induced in response to IFN $\alpha$ , was reduced in STAT2 null mice and failed to be induced by IFN $\alpha$  (Park, Li et al. 2000). This implicates the importance of STAT2 in driving T-cell responses to IFN. In addition to absent ISGF3 formation in fibroblasts from STAT2 null mice, there are also defects in the induction of GAS driven target genes. Similar results are observed in a STAT2 deficient tumour cell line (Leung, Qureshi et al. 1995). These results suggest that STAT2 is required for type I IFN induced STAT1 activation. However, in contrast to fibroblasts, the analysis of macrophages taken from STAT2 null mice show that STAT1 activation is independent of STAT2 which highlights tissue specific differences and the complexity of type I IFN signaling (Park, Li et al. 2000).

The mutational analysis of IFNAR has highlighted key residues and regions involved in STAT recruitment and activation. Although STAT1 and STAT2 docking onto IFNAR1 has been reported (Abramovich, Shulman et al. 1994; Yan, Krishnan et al. 1996; Li, Leung et al. 1997; Krishnan, Singh et al. 1998; Nadeau, Domanski et al. 1999), it does not appear essential for a full type I IFN response. Studies using mutated mu-*Ifnar1* over-expressed in *Ifnar1*<sup>-/-</sup> MEFs show that mutations of all intracellular tyrosine residues and truncations of the receptor below the TYK2 binding domain still enables normal STAT1, STAT2 and STAT3 phosphorylation and ISRE gene induction (Zhao, Lee et al. 2008). Similarly, the mutation of all tyrosine residues of hu-IFNAR1 results in a functional receptor (Gibbs, Takahashi et al. 1996). The reported docking of STAT1 and STAT2 to the non-conserved tyrosine residue Tyr466 of hu-IFNAR1 and the weak docking of STAT1 to the non-conserved tyrosine residue Tyr481 of hu-IFNAR1 therefore appear redundant to IFN signaling (Yan, Krishnan et al. 1996; Li, Leung et al. 1997; Nadeau, Domanski et al. 1999). It has been suggested there is threshold level of

STAT activation required for the IFN response and that STAT binding sites on the IFNAR2 receptor chain alone are sufficient for this level of activation (Nadeau, Domanski et al. 1999). This indicates tyrosine phosphorylation of IFNAR1 is not required for mediating STAT activation and ISRE gene induction. IFNAR1's primary role may therefore be the recruitment of TYK2 to the receptor complex as truncations immediately prior to the TYK2 binding region abrogate signaling (Zhao, Lee et al. 2008). In addition to TYK2 recruitment, IFNAR1 may also have a role in the recruitment of other signaling molecules to the receptor complex, mediating the activation of non-STAT pathways.

IFNAR2 therefore appears the most important receptor chain for STAT recruitment (Kotenko, Izotova et al. 1999; Nadeau, Domanski et al. 1999; Russell-Harde, Wagner et al. 2000; Wagner, Velichko et al. 2002; Zhao, Lee et al. 2008). Following IFN stimulation, IFNAR2 is rapidly phosphorylated (Platanias, Uddin et al. 1994). The individual mutation of each tyrosine of IFNAR2 has no effect, however, the mutation of all tyrosines of IFNAR2 results in a receptor unable to signal (Russell-Harde, Wagner et al. 2000; Wagner, Velichko et al. 2002). The reconstitution of tyrosine residues back onto IFNAR2 reveal that Tyr512 and Tyr337, individually, are able to mediate STAT1 and STAT2 phosphorylation, ISGF3 formation and ISG induction in response to IFN $\alpha$  and IFN $\beta$  (Wagner, Velichko et al. 2002). Studies using mutated mu-*Ifnar2* over-expressed in *Ifnar2*<sup>-/-</sup> MEFs yields similar results. Mutation of the conserved distal tyrosine 510 of mu-*Ifnar2* (corresponding to human Tyr512) results in reduced IFN $\alpha$  induced STAT1, STAT2 and STAT3 phosphorylation. Mutation of the more proximal tyrosine 335 (corresponding to human Tyr337) also shows a modest reduction in STAT phosphorylation. In contrast to the human receptor in which individual tyrosines can induce ISG induction, individual mutations of Tyr335 and Tyr510 result in significantly reduced ISG induction suggesting both tyrosine residues are required for a sufficient level of STAT activation. As expected, the mutation of both Tyr510 and Tyr335 completely abrogates STAT1, STAT2 and STAT3 phosphorylation and target gene induction (Zhao, Lee et al. 2008).

A constitutive STAT2 docking site on IFNAR2 has also been reported (Nadeau, Domanski et al. 1999; Nguyen, Saleh et al. 2002). This maps to amino acids 418-444 of hu-IFNAR2 and interacts with non-phosphorylated STAT2 (Nguyen, Saleh et al. 2002). There have been mixed reports about the function of this STAT binding site; some studies report it has a positive signaling role whereas others report it acts to negatively

regulate STAT activation. Ngyugen et al found that STAT phosphorylation is enhanced with the mutation of conserved amino acid residues within this region and it is therefore likely involved in negative regulation (Nguyen, Saleh et al. 2002). Another study found a truncation at amino acid 462 allowed for IFN signaling, however a truncation at amino acid 417 abolished all signaling in response to IFN $\alpha$  suggesting this region is required for STAT activation (Russell-Harde, Wagner et al. 2000). A study by Domanski et al found that 417 and 346 truncations of IFNAR2 demonstrate antiviral activity in response to IFN $\alpha$  but not IFN $\beta$ , whereas truncations at 462 allow signaling in response to both IFNs (Domanski, Nadeau et al. 1998). This suggests that the STAT binding region is required for IFN $\beta$  signaling but not IFN $\alpha$ . In another study by Domanski et al, hu-IFNAR2 truncated at amino acid 346 (removal of Tyr512 and the constitutive STAT binding region) is still able to signal and trigger an anti-viral state in response to IFN $\alpha$  (Domanski, Fish et al. 1997), however when combined with mutations at other STAT binding sites (on either IFNAR1 or IFNAR2) signaling is reduced (Nadeau, Domanski et al. 1999). This suggests a positive role for the STAT2 constitutive binding site and that perhaps at least one site on IFNAR2 is required for signaling but when only one binding site on IFNAR2 is present, the STAT docking sites on IFNAR1 are also needed. This supports the theory of a threshold level of STAT activation being required for the IFN response. The differences found across these studies may be due to technical differences such as the cell type used. Different cells have different receptor expression and composition as well as different expression of surface proteins that may modulate receptor function and responses. Also, it is evident that the different type I IFNs signal differentially and this may also contribute to the different responses seen.

#### **1.4.3.2 STAT3**

STAT3 has anti-apoptotic, pro-proliferative and both anti- and pro-inflammatory properties. It has been implicated as an oncogene as it is found constitutively expressed in a number of cancers, and is able to transform a number of cell lines. It is also essential in development as STAT3 null mice die during early embryogenesis. STAT3 is activated by a number of cytokines including the IL-6-type cytokines, which utilise the gp130 receptor (Akira 1999; Velichko, Wagner et al. 2002). STAT3 is also activated by the type I and II IFNs resulting in STAT3:STAT3 and STAT1:STAT3 transcription complexes (Yang, Shi et al. 1996; Owczarek, Hwang et al. 1997; Velichko, Wagner et al. 2002). In response to IFN $\alpha$ , STAT3 is tyrosine phosphorylated and serine phosphorylated (Yang, Shi et al. 1996). The IFNAR1 associated TYK2, has been

reported as critical for IFN $\beta$  mediated STAT3 tyrosine phosphorylation (Rani, Leaman et al. 1999). STAT3 has been reported to associate with phosphorylated IFNAR1 upon IFN $\alpha$  stimulation through an interaction with the STAT3 SH2 domain (Yang, Shi et al. 1996). However, like STAT1 and STAT2, truncations and mutations of tyrosine residues within mu-Ifnar1 still enables STAT3 phosphorylation following IFN stimulation indicating the interaction between STAT3 and mu-Ifnar1 is not necessary (Zhao, Lee et al. 2008). STAT3 association with specific tyrosine residues on IFNAR2, however, is essential for its phosphorylation (Velichko, Wagner et al. 2002; Zhao, Lee et al. 2008). The mutation of all tyrosines within hu-IFNAR2 abolishes IFN $\alpha$  induced activation of STAT3, which indicates that STAT3 binding to IFNAR2c, via a phosphotyrosine dependent interaction, is critical for its activation (Velichko, Wagner et al. 2002). These tyrosines have been mapped to Tyr337 and Tyr512 of hu-IFNAR2c, these are the same tyrosine residues in hu-IFNAR2c that are critical to STAT1 and STAT2 binding (Velichko, Wagner et al. 2002; Wagner, Velichko et al. 2002; Zhao, Lee et al. 2008). STAT3 binding to corresponding tyrosine residues of mu-Ifnar2 has also been demonstrated (Zhao, Lee et al. 2008). The mutation of these tyrosines results in the abrogation of STAT3 phosphorylation and formation of downstream signaling complexes in response to IFN $\alpha$  (Velichko, Wagner et al. 2002; Zhao, Lee et al. 2008). The use of a *STAT2*<sup>-/-</sup> cell line also indicates that, unlike STAT1 activation, STAT3 does not require the presence of STAT2 to be activated by type I IFNs (Velichko, Wagner et al. 2002).

#### 1.4.3.3 STAT4

STAT4 plays an important role in human Th1 development. STAT4 activation in CD4<sup>+</sup> T cells results in the regulation of adaptive immune responses by promoting secretion of IFN $\gamma$  (Farrar, Smith et al. 2000). IFN $\alpha$  and IFN $\beta$  can promote Th1 development in the human but not the murine system. A major species difference is that IL-12 is unique in activating STAT4 in murine CD4<sup>+</sup> T cells, whereas in human CD4<sup>+</sup> T cells both IL-12 and IFN $\alpha$  can activate STAT4, thereby inducing IFN $\gamma$  production (Farrar, Smith et al. 2000). Farrar et al hypothesised that this may be due to differences in the structure of human and mouse IFNAR as tyrosine residues across the species are not well conserved. However STAT4 does not directly interact with phosphotyrosines on either subunit of the IFNAR receptor (Farrar, Smith et al. 2000). Rather a more complex mechanism exists in which the STAT4 N-terminal domain forms a pre-associated complex with the cytoplasmic domain of hu-IFNAR2 but not mu-Ifnar2 (Tyler, Persky et

al. 2007). The region on hu-IFNAR2 has been mapped to amino acids 299 – 333. Interestingly this region is well conserved in mu-Ifnar2, yet STAT4 fails to bind (Tyler, Persky et al. 2007). In addition it has been found that in cells lacking STAT2, STAT4 phosphorylation by IFN $\alpha$  is inhibited (Farrar, Smith et al. 2000). This is similar to that seen with STAT1 activation in response to IFN $\alpha$  being dependent on STAT2. STAT4 activation by IFNAR may therefore be through an additional interaction with STAT2 upon IFN $\alpha$  stimulation (Farrar, Smith et al. 2000).

#### 1.4.3.4 STAT5 Transcription Factors

The STAT5 transcription factors play an important role in type I IFN signaling (Uddin, Lekmine et al. 2003). There are two distinct genes which encode the two isoforms of STAT5; STAT5a and STAT5b (Grimley, Dong et al. 1999). These are tyrosine phosphorylated upon IFN stimulation resulting in STAT5a and STAT5b homodimers and heterodimers (Grimley, Dong et al. 1999). Full activation of STAT5 however also requires serine phosphorylation and both Stat5a and Stat5b are serine phosphorylated in response to IFN $\alpha$  and IFN $\beta$  in a MAP-kinase and PI 3'-kinase independent manner (Uddin, Lekmine et al. 2003). Signaling assays with *Stat5a* and *Stat5b* null mouse embryonic fibroblasts using a luciferase reporter construct with 8 x GAS repeats demonstrate that Stat5 is required for type I IFN dependent reporter activity (Uddin, Lekmine et al. 2003). In addition to forming homodimers or STAT5a and STAT5b heterodimers, STAT5 has also been found to associate with other proteins and regulate transcription. For example, the type I IFN activated Crk family member, CrkL has been found to form a heterodimer with STAT5, functioning as a nuclear adaptor protein (Fish, Uddin et al. 1999). STAT5 reportedly interacts with TYK2 constitutively and upon IFN-induced phosphorylation acts as a docking site for the SH2 domain of CrkL (Fish, Uddin et al. 1999). Consequent studies using *Crkl*<sup>-/-</sup> mice have found it to be critical for IFN $\alpha$  dependent induction of some STAT5-GAS driven genes such as the growth inhibitory protein PML (Lekmine, Sassano et al. 2002). STAT5a and STAT5b have also been found important for activation of the PI3K signaling cascade, promoting cell proliferation and survival. This is mediated via Grb associated binder 2 protein, Gab2, which forms an interaction with STAT5 (Nyga, Pecquet et al. 2005). Although this has not been directly linked to type I IFN signaling, it may represent an alternative pathway for activation of STAT5 independently of the IFNAR associated kinases TYK2 and JAK1. Indeed, GAB2 is tyrosine phosphorylated upon IFN $\alpha$ 2 stimulation and is thought to compete with IFNAR2 for interaction with IFNAR1 (Baychelier, Nardeux et al. 2007).

The interaction site is believed to coincide with a region of Gab2 containing p85-PI3K binding sites (Baychelier, Nardeux et al. 2007).

#### **1.4.3.5 STAT6**

Although not much data exists on the role of STAT6 in type I IFN signaling a number of studies have reported its activation in response to IFN in a cell type specific manner (Gupta, Jiang et al. 1999; Eriksen, Sommer et al. 2004). Gupta et al found STAT6 is phosphorylated and forms an ISGF3 like complex with STAT2 and IRF9 in response to IFN $\alpha$  in a number of B-cell lines including Ramos and Daudi cells but not in non B-cell lines such as WI38 or WISH cells (Gupta, Jiang et al. 1999). In addition, Erikson et al found IFN $\alpha$  has a synergistic effect with IL-4 on STAT6 activation at early time points in CD4<sup>+</sup> and CD8<sup>+</sup> T cell lines, greatly increasing IL-4 induced STAT6 phosphorylation (Eriksen, Sommer et al. 2004).

#### **1.4.4 STAT Independent Type I IFN Signaling**

STAT independent signaling pathways are also activated by the type I IFNs. A number of these pathways are demonstrated in Figure 1.7. Tyrosine residues on IFNAR that are not important for STAT recruitment may therefore be involved in the recruitment of other SH2 containing proteins to the receptor and the activation of non-STAT, type I IFN induced, pathways. Phospho-tyrosine independent mechanisms of signal molecule recruitment also exist. For example there have been reports of the IFN $\alpha$  induced recruitment and activation of CREB-binding protein by the IFNAR receptor complex resulting in the acetylation of IFNAR2 to create protein docking sites (Tang, Gao et al. 2007). Discussed below are a number of pathways activated by type I IFN signaling that are independent of STAT activation.

Insulin Receptor Substrate proteins 1 (IRS1) and IRS2 are tyrosine phosphorylated by type I IFNs in a JAK-dependent manner and have been found to interact with TYK2 via their PH domains (Platanias, Uddin et al. 1996). Activation of IRS1 and IRS2 results in downstream activation of phosphatidylinositol and PI 3-Kinases. Activation of the PI 3-Kinase pathway in interferon signaling appears to mediate antiviral responses and also plays a role in the serine phosphorylation (727) of STAT1 (Platanias, Uddin et al. 1996). Type I IFNs also induce the phosphorylation of Crk proteins. CrkL and CrkII expression is necessary for the IFN $\alpha$ -mediated suppression of hematopoietic progenitors (Platanias, Uddin et al. 1999). These CrkL and CrkII mediated anti-proliferative effects

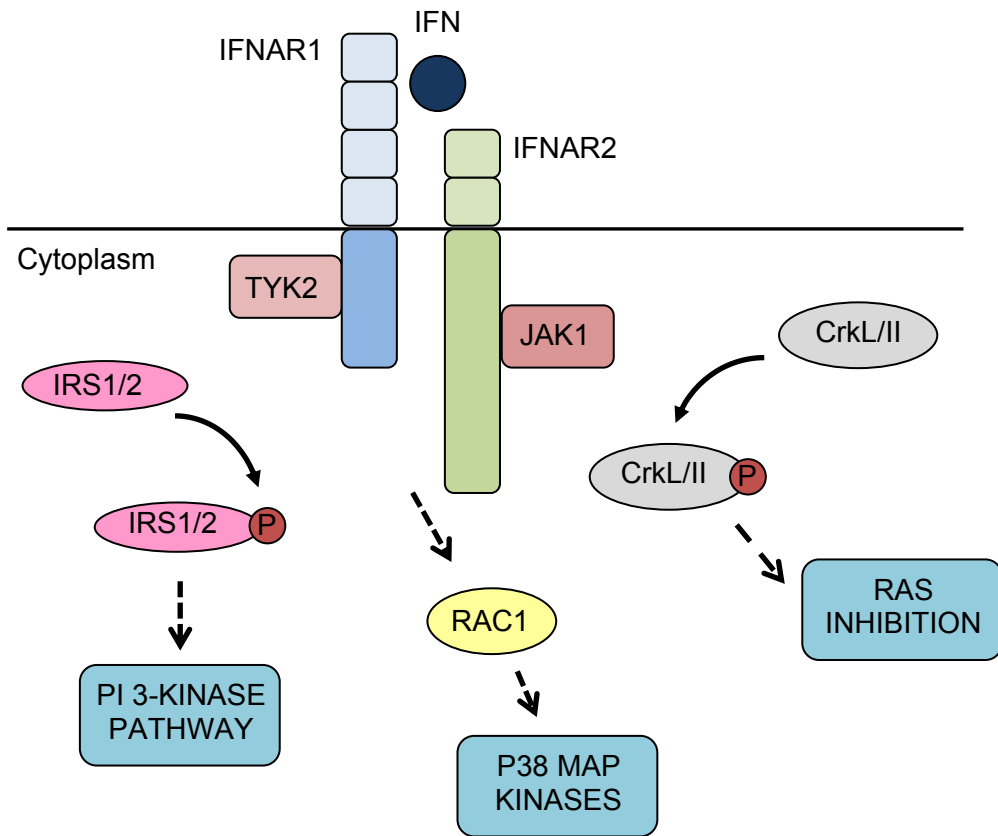


**Figure 1.7. JAK/STAT independent pathways activated by the type I IFNs.** Type I IFN signaling results in the activation of a number of JAK/STAT independent pathways. These include activation of the PI3-Kinase pathway via IRS1 and IRS2, activation of the p38 map kinases via RAC1 and RAS inhibition via CrkL and CrkLII.

of IFN $\alpha$  may be an effect of Rap1 activation (a RAS antagonist), which is downstream of Crk proteins and induced in response to IFN (Platanias, Uddin et al. 1999; Lekmine, Sassano et al. 2002). As mentioned previously, CrkL has been found to dimerise with STAT5 and is critical for IFN $\alpha$ -dependent induction of some GAS driven genes (Fish, Uddin et al. 1999). Type I IFNs can also mediate p38 MAP kinase phosphorylation through Rac1 (Uddin, Lekmine et al. 2000). This is hypothesised to be via JAK mediated tyrosine phosphorylation of Vav, resulting in Rac1 activation. The role of p38 MAP kinases in type I IFN signaling is not clear. It has been linked to mediating antiviral activities, serine phosphorylation of STAT1 as well gene induction by histone modification through serine phosphorylation and acetylation (Uddin, Lekmine et al. 2000).

*Ifnar1*<sup>-/-</sup> and *Ifnar2*<sup>-/-</sup> mice, both unable to activate STATs, have distinct phenotypes and differential gene activation profiles in response to IFN signaling. This suggests each receptor is able to transduce specific signals and may be a result of the above mentioned or novel type I IFN induced signaling pathways (Hertzog et al, unpublished data).

### **1.5 Summary of IFN Signaling Mechanism**

Type I IFN signaling results in the formation of a receptor complex involving interactions between many signaling molecules including the receptor components IFNAR1 and IFNAR2 as well as TYK2, JAK1 and STAT transcription factors. The receptor associated JAKs have multiple functions such as receptor stabilisation and tyrosine phosphorylation of both the receptor and recruited signaling molecules (such as STATs). STATs mediate many of the biological actions of the type I IFNs. All 7 STAT family members can be activated by the type I IFNs although the mechanism of receptor-STAT interactions is complex and appears to vary across different species, cell types and with use of different type I IFNs. STATs are generally found to interact with specific tyrosine residues of IFNAR through their SH2 domains although constitutive STAT binding sites on IFNAR have also been identified. The key tyrosine residues of IFNAR involved in STAT recruitment are the conserved tyrosine residues Tyr337 and Tyr512 of hu-IFNAR2. It is likely that there is a threshold level of STAT activation required for a biological response and that multiple STAT binding sites on IFNAR are required to obtain such a level of STAT activation. The level and type of

STATs activated will ultimately define the response of the cell to IFN through the formation of STAT hetero or homo-dimers or other complexes such as ISGF3 and the regulation of genes containing distinct elements to which these complexes can bind. IFN-induced genes have a diverse range of activities that mediate the anti-pathogenic and immunomodulatory functions of the type I IFNs and these are discussed below.

## **1.6 Type I IFN Functions**

Type I IFNs are predominantly known for their potent anti-viral and anti-pathogenic functions through co-ordinated activation of innate and adaptive immune responses. This complex immune regulation requires IFN control of a diverse range of cellular functions and the regulation of a complex network of genes and signaling pathways to exhibit cell specific antiviral, antiproliferative, antitumour and immunomodulatory activities.

### **1.6.1 Antiviral Functions**

IFNs were originally discovered based on their antiviral activity (Lindenmann, Burke et al. 1957). Upon production, IFN acts in a paracrine, autocrine and endocrine or systemic manner on infected cells to regulate the expression of a multitude of genes, many with antiviral activities. These act to control the infection within the cell, limiting replication and release of the virus. Many antiviral genes are up-regulated in response to IFN signaling, primarily through IFN induced ISGF3 and STAT1 binding to ISRE and GAS elements within the genes promoters, respectively. A study by Schoggins et al which screened hundreds of ISGs for anti-viral activity found that different viruses are targeted by a unique set of ISGs encompassing a range of antiviral activities (Schoggins, Wilson et al. 2011). The function of some of the best characterised antiviral genes activated by the type I IFNs are discussed below.

#### **1.6.1.1 PKR**

RNA-dependent protein kinase (PKR) is a serine/threonine protein kinase induced by the type I IFNs (Meurs, Chong et al. 1990). The importance of its anti-viral functions is evident in PKR deficient mice which have an increase susceptibility to viral infection (Nakayama, Plisch et al. 2010). PKR contains two N-terminal dsRNA binding motifs and a C-terminal protein kinase domain. PKR exists in an inactive state, mostly in the

cytoplasm. Binding of PKR to dsRNA unmasks its catalytic ATP binding site resulting in the auto-phosphorylation of PKR on multiple serine and threonine residues (Thomis and Samuel 1993). Once activated, PKR phosphorylates the protein synthesis initiation factor eIF2 $\alpha$ , preventing the recycling of eIF2 $\alpha$  required for ongoing translation (Meurs, Watanabe et al. 1992; Thomis and Samuel 1993). Subsequently this results in the inhibition of mRNA translation and therefore inhibition of viral replication within the cell.

#### **1.6.1.2 2',5'-OAS and RNase-L**

The 2',5'-oligoadenylate synthetases (2',5'-OASs) and RNase L are IFN inducible genes involved in viral RNA degradation. 2',5'-OAS proteins are dsRNA activated enzymes which convert ATP to 2',5'-linked oligoadenylates with a 2',5' phosphodiester bonds (Chakrabarti, Jha et al. 2011). Binding of 2',5'-oligoadenylates to the endoribonuclease, RNase L, results in dimerisation of RNase L monomers through their kinase-like domains, resulting in functional RNase L able to cleave viral RNAs (Chakrabarti, Jha et al. 2011). In addition to the cleavage of viral RNAs, RNase L cleaves some self RNA and produces small RNAs which activate intracellular receptors such as RIG-1 and MDA-5 (Chakrabarti, Jha et al. 2011). The importance of the 2',5'-OAS/RNase-L pathway in IFN signaling is evident in RNase L deficient mice which have reduced anti-viral effects following IFN $\alpha$  treatment (Zhou, Paranjape et al. 1997). These mice also have an enlarged thymus and spleen due to a suppression of apoptosis indicating this pathway is also involved in controlling cell death which may act to eliminate infected cells or modulate the immune cell repertoire (Zhou, Paranjape et al. 1997).

#### **1.6.1.3 Mx Proteins**

The Mx proteins are involved in the inhibition of a range of viruses (Netherton, Simpson et al. 2009). They were initially discovered in an inbred mouse strain unusually resistant to influenza A virus (Lindenmann 1962). Their expression is strictly dependent on type I IFNs as mice deficient in IFN or IFNAR are also deficient in Mx proteins (Haller, Staeheli et al. 2007). Mx proteins consist of three domains, an N-terminal GTPase domain, a middle linker domain and a C-terminal GTPase effector domain. Mx proteins are involved in mediating vesicle budding, organogenesis and cytokinesis and exert their antiviral activities by sequestering viral nucleocapsid proteins in the cytoplasm and blocking their movement into the nucleus (Haller, Staeheli et al. 2007).

#### **1.6.1.4 ISG15**

Interferon stimulated gene 15 (ISG15) is a ubiquitin-like protein involved in the inhibition of a range of DNA and RNA viruses. The importance of ISG15 in viral control is evident in knockout mice which have increased susceptibility to influenza A virus, Herpes and Sendai virus (Lenschow, Lai et al. 2007). In a similar pathway to ubiquitination, ISG15 is conjugated to target proteins in a process called ISGylation (Zhang and Zhang 2011). ISG15 is initially cleaved to reveal a C-terminal LRLRGG motif. Adenylation of this motif and a cascade of enzymatic reactions involving E1, E2 and E3 enzymes results in the transfer of ISG15 onto a lysine residue of its target substrate. ISGylation of target proteins renders them inactive, likely affecting the proteins stability, function or localisation (Zhang and Zhang 2011).

#### **1.6.2 Immunomodulatory Functions**

In addition to innate immune responses activated by type I IFNs in which they directly target and activate anti-viral pathways within infected cells, the type I IFNs also activate adaptive immune responses in order to target and clear infected cells and generate protective memory. Type I IFN modulates host adaptive immune responses by acting on multiple cell types including T-cells, B-cells and antigen presenting cells. Type I IFN has been shown to act both directly and indirectly in modulating T- and B- cell functions. Indirect mechanisms are predominantly through IFN mediated recruitment and maturation of antigen presenting cells such as monocytes, macrophages and dendritic cells, which in turn stimulate T- and B-cell functions through antigen presentation.

The type I IFN producing cells, pDCs, are central to IFN mediated immune-regulation. As mentioned previously, pDCs express high levels of TLR7 and TLR9 as well as IRF7 and thus respond rapidly to pathogen recognition. Type I IFN mRNA can be detected at 4 hours post-viral infection and peaks at 12 hours. At 6 – 12 hours post infection, about 50% of total mRNA expressed by pDCs encodes for type I IFN however after the first 24 hours of viral stimulation, IFN production is reduced (Liu 2005). Upon recognition of pathogen and the production of large amounts of IFN pDCs subsequently differentiate into DCs to trigger adaptive immune responses (Liu 2005). Such adaptive immune responses include modulation of the function of natural killer (NK) cells, B-cells, T-cells and myeloid DCs (Liu 2005). pDCs are located in prime areas of adaptive-immune responses. They are produced in the bone marrow from hematopoietic stem cell

progenitors and after leaving the bone marrow follow a migration behaviour much like that of B and T lymphocytes migrating into T cell-rich areas of secondary lymphoid tissue and mucosa-associated lymphoid tissue (MALT) as well as through marginal zones of the spleen (Liu 2005). pDCs differentiate into mature DCs through two known pathways; the virus induced pathway and the IL-3 dependent pathway. The resultant mature DC will depend on the type of maturation signals it receives (Rissoan, Soumelis et al. 1999). The virus-induced pathway involves the production of IFN $\alpha$  and TNF $\alpha$ , which act in an autocrine fashion to promote DC survival and differentiation (Kadowaki and Liu 2002). In an IFN $\alpha$  dependent manner, the resultant DCs promote human naïve CD4 $^{+}$  allogenic T-cells to undergo strong proliferation and differentiation into IFN $\gamma$  and IL-10 producing cells. This creates a TH1-like immune response, however, unlike myeloid DCs, this is independent of IL-12 (Rissoan, Soumelis et al. 1999; Kadowaki and Liu 2002). The other pathway is IL-3 dependent and results in an anti-parasitic adaptive TH2 immune response. It is proposed that IL-3 is produced by basophils, eosinophils and mast cells during parasitic infection, which acts on pDC IL-3 receptors. IL-3 dependent mature DCs prime naïve CD4 $^{+}$  T-cells to produce TH2 cytokines IL-4, IL-5, and IL-10 (Rissoan, Soumelis et al. 1999; Kadowaki and Liu 2002; Liu 2005).

Type I IFNs also promote the presentation of viral antigens on conventional dendritic cells via up-regulation of MHC class I and II molecules as well as other co-stimulatory molecules including CD83, CD40, CD80 and CD86 resulting in potent antigen presenting cells (Luft, Pang et al. 1998; Gallucci, Lolkema et al. 1999; Paquette, Hsu et al. 2002). This results in enhanced presentation of antigen to T- and B-cells and thus an increased adaptive immune response. For example, virus induced IFN enhances CD8 $^{+}$  T-cell responses through activation of cross-priming in antigen presenting cells (Le Bon, Etchart et al. 2003).

In addition to modulation of T-cell and B-cell function via indirect methods, such as through antigen presenting cells, type I IFN also acts directly on T-cells and B-cells to modulate their function. The direct effects of IFN on T-cells and B-cells have primarily been studied through the use of cells with a selective deletion of *Ifnar1*. Direct modulation of CD4 $^{+}$  and CD8 $^{+}$  T-cell function has been shown *in vivo* with the use of *Ifnar1* $^{-/-}$  or *Ifnar1* $^{+/+}$  T-cells expressing transgenic receptors specific for LCMV antigenic peptides. Adoptive transfer of *Ifnar1* $^{-/-}$  LCMV-specific CD4 $^{+}$  and CD8 $^{+}$  T-cells into recipient mice results in reduced expansion and generation of memory T-cells following LCMV infection as compared to *Ifnar1* $^{+/+}$  LCMV-specific T-cells (Kolumam, Thomas et

al. 2005; Aichele, Unsoeld et al. 2006; Havenar-Daughton, Kolumam et al. 2006). This was due to increased apoptosis rather than a reduction in the cells ability to proliferate (Kolumam, Thomas et al. 2005; Aichele, Unsoeld et al. 2006; Havenar-Daughton, Kolumam et al. 2006). IFN administration (through injection) to mouse models that are selectively deficient for *Ifnar1* in B-cells or T-cells also demonstrate the importance of direct IFN stimulation in generating adaptive immune responses. *In vivo* studies demonstrate that IFN $\alpha$  stimulation enhances the antibody response (increased production of IgM and all subclasses of IgG) to soluble antigen whereas this is dramatically reduced in mice with B-cells or T-cells selectively deficient for *Ifnar1* (Le Bon, Thompson et al. 2006).

The direct effects of IFN on T-cell survival, proliferation and differentiation have been further characterised in a number of studies. The response of the cell however depends largely on the timing of IFN stimulation as well as the activation state of the cell at the time. Activated T-cells have an increased susceptibility to cell death compared to resting T-cells and evidence suggests IFN can antagonise cell death pathways associated with T-cell activation. As mentioned above, IFN stimulation of LCMV-specific activated T-cells *in vivo* results in reduced apoptosis of T-cells resulting in expansion and generation of memory T-cells. IFN $\alpha$  has also been found to enhance survival of activated CD4<sup>+</sup> and CD8<sup>+</sup> T-cells *in vitro* (Marrack, Kappler et al. 1999; Dondi, Rogge et al. 2003). In subsequent studies, IFN was found to protect T-cells from intrinsic mitochondrial-dependent apoptosis early upon TCR-CD28 activation via the up-regulation of Bcl-2 and the down regulation of Bax (Dondi, Roue et al. 2004). Interestingly, these studies also show that IFN sensitizes cells to the extrinsic apoptotic pathway through partial activation of caspase 8 and up-regulation of Fas, thereby increasing the sensitivity of the cell to antigen induced cell death (Dondi, Roue et al. 2004). This however occurs 24 hours later than mechanisms which enhance T-cell survival and thus may be a means of controlling the response during chronic infection. In addition to the modulation of cell survival, IFN also has effects on cell proliferation. For example, IFN prolongs the proliferation and expansion of antigen-specific CD8<sup>+</sup> T cells during cross priming and the presence of IFNAR on the CD8<sup>+</sup> T cells was essential to this effect. The cytokines IL-2 and IL-15 have been identified as activators of CD8<sup>+</sup> T cell responses. IFN was also found to up-regulate expression of these cytokines yet neither of these were required for the effect of IFN $\alpha$  on CD8<sup>+</sup> T cell cross priming (Le Bon, Durand et al. 2006).

The timing of exposure to IFN relative to antigen is also an important factor in determining the response of the cell to IFN. In comparison to the effects of IFN on activated T-cells, IFN suppresses expansion of resting T-cells (Marrack, Kappler et al. 1999; Dondi, Rogge et al. 2003). One such mechanism, in the context of resting naïve CD4<sup>+</sup> T-cells, is through delaying entry into cell division pathways (Dondi, Rogge et al. 2003).

Furthermore, Lin et al found that IFN treatment severely inhibits B-cell and T-cell development at early stages (Lin, Dong et al. 1998). In IFN-treated newborn mice, bone marrow and splenic cellularity were decreased and B lineage cells were diminished by greater than 80%. Thymic cellularity was also decreased with IFN treatment by greater than 80%. In *Ifnar1<sup>-/-</sup>* mice T- and B-cell development was unaffected by IFN treatment, showing that this effect is through the IFNAR receptor. Furthermore, it was found that the inhibitory effect of IFN $\alpha$  on T- and B-cell development was through IFN inhibition of IL-7 induced growth and survival (Lin, Dong et al. 1998). Evidence suggests IFN $\alpha$  is constitutively expressed by resident pDCs in the thymus and may play a role in the regulation of T-cell development and differentiation (Colantonio, Epeldegui et al. 2011). In the absence of infection, the constitutive expression of IFN $\alpha$  in the thymus may therefore be a means to suppress adaptive immune responses.

## **1.7 Clinical Applications of the Type I IFNs**

Type I IFNs are used in the clinical setting for the treatment of a range of diseases including viral infections, cancers and some autoimmune diseases. The role of IFN in these diseases however is complex, often having opposing roles depending on the disease.

### **1.7.1 Treatment of Viral Infections**

Type I IFN is used in the treatment of viral infections, most commonly hepatitis B and C (Roffi, Mels et al. 1995; Mazzella, Saracco et al. 1999). Pegylated-IFN $\alpha$  in combination with ribavirin leads to viral eradication in 50% of treated patients (Vezali, Aghemo et al. 2011). As discussed above, IFN treatment results in the induction of the innate immune response including many antiviral genes as well as adaptive immune responses

following viral infection. The innate and adaptive immune responses elicited by IFN $\alpha$  likely act together to eliminate virus.

### 1.7.2 Treatment of cancer

IFN $\alpha$  was one of the first cytokines used for clinical oncology and has been used in the treatment of over 14 cancers including haematological malignancies (hairy cell leukemia, chronic myeloid leukemia, and some B- and T-cell lymphomas) and some solid tumors (melanoma, renal carcinoma, and Kaposi's sarcoma) (Talpaz, Kantarjian et al. 1987; Paredes and Krown 1991; Rizza, Moretti et al. 2010). While IFN treatment has been replaced with other cytokines in some of these diseases it is still widely used in cancer immunotherapy (in particular for melanoma). IFN acts to control cancer by modulating adaptive immune responses as well as through a direct interaction with tumour cells. For example, IFN can prime the tumour for apoptosis while IFN-DCs are highly effective at taking up antigen from apoptotic cells and cross-priming CD8 $^+$  T cell responses to antigen.

Anti-angiogenesis properties of IFNs also play a role in modulating tumour growth (Indraccolo 2010). IFN can promote down-regulation of angiogenesis factors such as bFGF, IL-8 and VEGF. In addition IFN has been found to directly affect endothelial cell proliferation and migration. IFN expression at the site of tumour formation disrupts the tumour microvasculature resulting in tumour hypoxia. The anti-angiogenic effect of IFN on established tumours however is minimal and most likely plays a role in inhibiting tumour formation through disruption of the development of the tumour vasculature rather than modulating established tumour vasculature (Indraccolo 2010).

Recent studies have implicated IFN in controlling breast cancer metastasis to bone (Bidwell, Slaney et al. 2012). In a mouse model of spontaneous bone metastasis, a large subset of genes suppressed in bone metastases compared to primary tumour cells were found to be targets of IRF7. Subsequently the expression of IRF7 in tumour cells or treatment with IFN resulted in reduced bone metastases and increased survival. Furthermore metastasis was enhanced in *Irfar1* $^{-/-}$  mice or mice deficient in NK and CD8 $^+$  T-cells indicating this suppression is through IFN activation of immunosurveillance. Clinical evidence also indicates that patients with high levels of IRF7 regulated genes in primary tumours have reduced bone metastasis and prolonged survival (Bidwell, Slaney et al. 2012).

### **1.7.3 Autoimmune Disease**

IFN has been implicated in the pathogenesis of autoimmune diseases such as Systemic Lupus Erythematosus and Sjogrens syndrome (Hooks, Moutsopoulos et al. 1979; Ronnblom 2011). In addition, IFN $\alpha$  treatment, in some cases, results in the development of inflammatory diseases such as rheumatoid arthritis, multiple sclerosis and type I diabetes (Ronnblom 2011). Interestingly, in contradiction to this, IFN $\beta$  has protective, anti-inflammatory effects and is used for the treatment of some autoimmune diseases such as multiple sclerosis (Ann Marrie and Rudick 2006). The differential effects of IFN in these diseases may be due to systemic versus local type I IFN activity. IFN $\alpha$  activity is more systemic and thought to contribute more to autoimmune disease than IFN $\beta$ , which is produced locally and has an anti-inflammatory role (Crow 2010; Sozzani, Bosisio et al. 2010; Choubey and Moudgil 2011). For example, many patients with systemic autoimmune disease have high levels of systemic IFN $\alpha$  and IFN $\alpha$ -induced gene induction (Ronnblom 2011). In the context of rheumatoid arthritis, a subgroup of patients with systemically increased IFN inducible genes have a more destructive form of the disease. In contrast, IFN $\beta$  produced locally in the joint results in reduced cartilage and bone destruction (Crow 2010). Indeed a higher IFN $\beta$ :IFN $\alpha$  ratio is associated with a better clinical response to TNF treatment in rheumatoid arthritis (Crow 2010).

As outlined in Chapter 1.6.2, IFN $\alpha$  has various roles in activating T-cells and B-cells either directly or indirectly. IFN $\alpha$  has been found to contribute to the pathogenesis of autoimmune disease through stimulating an increase in numbers of auto-reactive T-cells and B-cells which are major mediators of autoimmune disease (Conrad 2003). IFN $\alpha$  activation of auto-reactive T-cells may be through a number of mechanisms such as enhancing functions of antigen presenting cells to increase cross-priming of self-reactive T-cells as well as by acting directly on T-cells to promote T-cell activation and survival (Conrad 2003).

### **1.7.4 Side Effects of type I IFN treatment**

Apart from the development of autoimmune disease with IFN $\alpha$  treatment, other aberrant side effects are also observed, which often cause patients to decline or cease IFN therapy. Toxicities associated with IFNs result in the development of flu like symptoms (fever, headache, chills, fatigue) as well as haematological changes and neuropsychiatric disturbances (Calvaruso, Mazza et al. 2011). Thus improvements in

therapy may arise from the design of IFN or related factors that can achieve effective responses with minimum toxicity. In order to achieve this, the mechanism of type I IFN signaling and its negative regulation must be well understood. Below we investigate the mechanisms of the regulation of IFN signaling.

### **1.8 Regulation of Type I IFN Signaling**

Chronic activation of the immune system, due to increased type I IFN signaling can lead to serious inflammatory disease such as septic shock and autoimmune disease (Karaghiosoff, Steinborn et al. 2003; Sakaguchi, Negishi et al. 2003). Type I interferon signaling must therefore be tightly controlled to exert an appropriate immune response to pathogenic infection. A number of regulatory mechanisms exist to control type I IFN signaling. These mechanisms act at all points throughout the IFN signaling pathway including at the level of receptors, intracellular signaling molecules and transcription. The negative regulators; suppressor of cytokine signaling (SOCS)1 and SOCS3 play an important role in controlling type I IFN signaling responses, as discussed in detail in the next section of this literature review. Outlined below are other mechanisms involved in the control of IFN signaling.

One such mechanism of IFN regulation occurs at the level of receptor activation. As discussed in section 1.1, soluble mu-Ifnar2 and short membrane bound hu-IFNAR2 are able to antagonise IFN signaling *in vitro* however *in vivo* evidence to date does not support this (Pfeffer, Basu et al. 1997; Hardy, Owczarek et al. 2001). Other mechanisms that control IFN signaling target intracellular signaling molecules. For example protein inhibitor of activated STAT (PIAS1) inhibits tyrosine phosphorylated STAT1 mediated gene expression following IFN signaling (Liu, Liao et al. 1998). In addition to targeting the IFN receptor and intracellular signaling molecules, mechanisms also exist to control IFN synthesis. For example, some tumour cells are able to suppress IFN signaling via the release of Prostaglandin E2 or the production of cAMP phosphodiesterases, which reduce cAMP, an important second messenger in IFN synthesis (Chadha, Ambrus et al. 2004).

microRNA regulation has recently emerged as an important mechanism involved in controlling IFN signaling (David 2010). Cellular miRNA control of virus replication was initially reported in the context of the retrovirus, primate foamy virus type 1 (PFV-1),

which accumulated in human cells following suppression of RNA silencing (Lecellier, Dunoyer et al. 2005). Furthermore the HIV-1 Tat proteins were reported to evade defence mechanisms through suppression of RNA silencing (Bennasser, Le et al. 2005). Subsequent studies supported a role for miRNAs in controlling virus replication as the inhibition or removal of Dicer, a key enzyme in the generation of miRNAs, resulted in enhanced replication of VSV and influenza A virus (Matskevich and Moelling 2007; Otsuka, Jing et al. 2007). Two mechanisms for the type I IFN control of virus replication via miRNAs have been proposed. One mechanism involves IFN induction of antiviral miRNAs and the other involves IFN inhibition of cellular miRNAs that support viral replication. Evidence exists to support both mechanisms. For example, IFN $\beta$  stimulation of the hepatic cell line, Huh7, resulted in induction of multiple miRNAs including miR-196, miR-296, miR-351, miR-431 and miR-448. These miRNAs matched sequences within the HCV genome and expression of their corresponding synthetic forms inhibited HCV replication *in vivo* (Pedersen, Cheng et al. 2007). In contrast to this, the liver specific miRNA, miR-122, which enhances replication of hepatitis C virus, is reduced in response to IFN $\alpha$  and IFN $\beta$  stimulation of Huh7 cells (Pedersen, Cheng et al. 2007).

In addition to IFN mediated miRNA control of viral replication, IFN induced miRNAs may also contribute to activation or inhibition of the expression of molecules involved in the IFN response thereby serving as activators or inhibitors of IFN signaling. Recent studies within our lab have demonstrated that type I IFN induces widespread miRNA expression and predicted targets of these miRNAs include many components of the type I IFN pathway and IFN induced genes (Sam Forster, unpublished data). As for SOCS1, which is induced by IFN and acts in a negative regulatory loop to control IFN signaling, miRNAs may also be induced by IFN and act back to negatively control excessive IFN signaling by targeting major components of the IFN pathway. Evidence for a negative feedback loop by miR-155 has been reported in pDCs whereby IFN $\alpha$  can induce miR-155 and miR-155 attenuates IFN $\alpha$  and IFN $\beta$  production by repressing TAB2 expression (Zhou, Huang et al. 2010). These regulatory mechanisms however involve quite a complex network of interactions as miR-155 has also been shown to suppress SOCS1 expression in macrophages, thereby enhancing type I signaling (Wang, Hou et al. 2010). Other miRNAs have also been linked to negatively controlling the type I IFN pathway such as miR-221 and miR-222 which attenuate STAT1 and STAT2 expression and phosphorylation in response to IFN $\alpha$  as well as miR-146a which attenuates transcriptional transduction through the type I IFN receptor and has been

shown to target both STAT1 and IRF5 (Tang, Luo et al. 2009; Zhang, Han et al. 2010). The induction of these miRNAs by IFN however has not yet been demonstrated.

In addition to homeostatic regulation of IFN signaling, viruses have evolved to antagonise type I IFN production or signaling and thus evade the IFN-mediated immune response. Mechanisms may include sequestering or cleaving signaling molecules or targeting signaling molecules for proteosomal degradation (Versteeg and Garcia-Sastre 2010). For example, respiratory syncytial virus produces NS1 and NS2 which block IRF3 phosphorylation and subsequent IFN production while Herpesviruses produce pM27 which binds STAT2 and induces its ubiquitination and degradation (Hengel, Koszinowski et al. 2005). Furthermore, the vaccinia virus encodes a secreted protein with three immunoblobin domains that functions as a soluble receptor for IFN and attenuates IFN antiviral responses (Alcami, Symons et al. 2000). In addition the expression of proteins able to inhibit components of the innate immune system, viruses have evolved to encode miRNAs that attenuate innate immune responses, although none have yet been linked to the type I IFN pathway (David 2010).

### **1.9 Suppressors of Cytokine Signaling (SOCS)**

SOCS1 was discovered in 1997 by three independent research groups. Starr et al, discovered SOCS1 by its ability to generate a stable clone of M1 cells unresponsive to IL-6 induced macrophage differentiation (Starr, Willson et al. 1997); Endo et al, discovered SOCS1 by its ability to bind to the JAK2 JH1 domain (Endo, Masuhara et al. 1997); and Naka et al, discovered SOCS1 via screening of a cDNA library with an antibody generated against the SH2 domain of STAT (Naka, Narazaki et al. 1997). This protein was consequently named SOCS1, JAK-binding protein (JAB) and STAT-induced STAT-inhibitor 1 (SSI-1), respectively (Endo, Masuhara et al. 1997; Naka, Narazaki et al. 1997; Starr, Willson et al. 1997). A protein homology search by Starr et al identified three other related proteins including cytokine-inducible SH2-containing protein (CIS), discovered in 1995 by Yoshimura et al, and SOCS2 and SOCS3 (Yoshimura, Ohkubo et al. 1995; Starr, Willson et al. 1997). Sequence homology between these proteins then led to the discovery of a total of eight family members, named SOCS1-SOCS7 and CIS (Hilton, Richardson et al. 1998).

#### **1.9.1 SOCS Structure**

All SOCS family members contain a C-terminal homologous region called the SOCS box, a central SH2 domain and a non-homologous N-terminal region (Starr, Willson et al. 1997; Hilton, Richardson et al. 1998). The SOCS proteins may be grouped in pairs according to similarity. These are CIS and SOCS2, SOCS1 and SOCS3, SOCS4 and SOCS5, and SOCS6 and SOCS7. The general structure of SOCS1 and SOCS3 are demonstrated in Figure 1.8.

The SOCS box is a highly conserved region of 40 amino acids which has been identified in numerous proteins (Hilton, Richardson et al. 1998). The SOCS box has been implicated in the ubiquitination and targeting of proteins for proteosomal degradation through interactions with elongins B and C (Zhang, Farley et al. 1999). Other studies however suggest that the SOCS box has a role in the stabilization of SOCS1 through its interactions with elongins B and C and that it is not necessary for signal inhibition (Narazaki, Fujimoto et al. 1998; Nicholson, Willson et al. 1999). These studies were performed in over expression systems however and *in vivo* mouse models have shown that the deletion of the SOCS box results in partial loss of function of SOCS1 with mice having an increased responsiveness to IFN $\gamma$  (Zhang, Metcalf et al. 2001).

The N-terminal region of SOCS1 and SOCS3 contain a kinase inhibitory region (KIR). A number of studies have demonstrated that both the SH2 domain and the KIR domain are required for the inhibitory function of SOCS1 (Narazaki, Fujimoto et al. 1998; Nicholson, Willson et al. 1999; Yasukawa, Misawa et al. 1999; Haque, Harbor et al. 2000). Mutational analysis and modeling of the SOCS1 interaction with the JH1 domain of JAK2 has helped predict a mechanism by which SOCS1 inhibits JAK kinase activity; the SH2 domain of SOCS1 binds to a phosphotyrosine on the JAK kinase while the KIR domain stabilizes this association through an interaction with the catalytic pocket of the JH1 domain (Yasukawa, Misawa et al. 1999; Giordanetto and Kroemer 2003). The KIR domain somewhat resembles the activation loop of JAK kinases and is believed to act as a pseudo-substrate preventing access of ATP and other substrates to the JAK catalytic pocket thereby inhibition JAK function (Yasukawa, Misawa et al. 1999; Giordanetto and Kroemer 2003).

### **1.9.2 SOCS1 Expression**

The primary site of SOCS1 expression is within thymocytes, particularly CD4+CD8+ T-cells (Marine, Topham et al. 1999). SOCS1 is also expressed, but to a much lesser

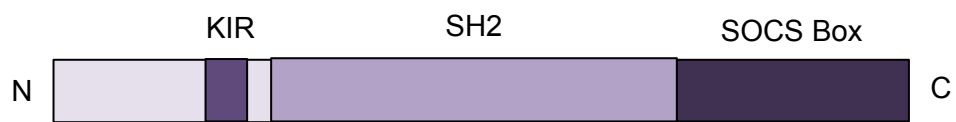


**Figure 1.8 Structure of SOCS1 and SOCS3.** SOCS1 and SOCS3 consist of an N-terminal region containing the Kinase Inhibitory Region (KIR), a central SH2 domain and a C-terminal SOCS Box.

extent, in bone marrow, spleen and peripheral blood. Expression within the thymus is independent of cytokine signaling and T-cell receptor engagement, suggesting it may be developmentally regulated (Marine, Topham et al. 1999). In addition to its high expression in thymocytes, SOCS1 expression can be induced in response to a range of cytokines including IL-2, IL-4, IL-6, IL-10, IL-21, LIF, EPO, G-CSF, FGF, GH, OSM, IFN- $\alpha$ , IFN- $\beta$  and IFN $\gamma$  (Naka, Narazaki et al. 1997; Starr, Willson et al. 1997; Sakamoto, Yasukawa et al. 1998; Sporri, Kovanen et al. 2001; Jegalian and Wu 2002; Ding, Chen et al. 2003; Ben-Zvi, Yayon et al. 2006; Strengell, Lehtonen et al. 2006). This expression is largely cell type specific, however, SOCS1 is strongly induced by IFN $\alpha$ , IFN $\beta$  and IFN $\gamma$  in a broad variety of cells lines (Sakamoto, Yasukawa et al. 1998). In addition to cytokine induced stimulation, SOCS1 may also be induced by other factors such as pathogen derived stimuli (e.g LPS and CpG DNA) (Dalpke, Opper et al. 2001; Kinjyo, Hanada et al. 2002). The expression of SOCS proteins in response to cytokine signaling is mediated by the STAT family of proteins. STAT dimers bind to elements within the promoter regions of SOCS genes. The promoter region of SOCS1 contains Specificity Protein 1 (SP1), ISRE, GAS and STAT3 and STAT6 binding elements (Naka, Narazaki et al. 1997; Sakamoto, Yasukawa et al. 1998; Schluter, Boinska et al. 2000).

### **1.9.3 SOCS1 Inhibition of Interferon Signaling**

SOCS1 and SOCS3 are negative regulators of the type I and type II interferon JAK-STAT signaling pathway (Song and Shuai 1998). SOCS1 and SOCS3 mRNA expression is induced in response to IFN $\gamma$  and IFN $\alpha$  signaling (Song and Shuai 1998). In a negative feedback loop, SOCS1 and SOCS3 have both been shown to inhibit interferon signaling, however SOCS1 demonstrates a much more potent inhibitory response (Song and Shuai 1998). The inhibitory effects of SOCS1 are demonstrated by the inactivation of signaling molecules involved in the JAK-STAT signaling pathway. For example, in cells overexpressing SOCS1, decreased JAK1, TYK2 and STAT1 phosphorylation is observed in response to type I interferons and decreased STAT1 phosphorylation is observed in response to type II interferon (Sakamoto, Yasukawa et al. 1998; Song and Shuai 1998). The negative regulation of interferons by SOCS1 is also demonstrated by the inhibition of antiviral and antiproliferative effects of IFN $\alpha$ , IFN $\beta$  and IFN $\gamma$  stimulation in cells overexpressing SOCS1 (Sakamoto, Yasukawa et al. 1998; Song and Shuai 1998).

The critical importance of SOCS1 in the regulation of cytokine signaling has been demonstrated with the generation of *Socs1*<sup>-/-</sup> mice. Within 10 days of birth, *Socs1*<sup>-/-</sup> mice are significantly smaller than their wild type littermates, and die before reaching 3 weeks of age due to a severe inflammatory syndrome (Starr, Metcalf et al. 1998). Abnormalities are observed in a number of organs. Most notable are severe lymphoid deficiencies within the peripheral blood and the lymphoid organs as well as major fatty degeneration, necrosis and monocytic infiltration of the liver (Starr, Metcalf et al. 1998). Monocytic infiltration of the lungs, heart and pancreas is also observed (Starr, Metcalf et al. 1998).

*Socs1*<sup>-/-</sup> mice show both increased type I and II interferon signaling. IFN $\gamma$  responsive genes are up-regulated in *Socs1*<sup>-/-</sup> mice; this is due to both an increased expression of IFN $\gamma$  and a hyper-responsiveness of cells to IFN $\gamma$  (Alexander, Starr et al. 1999; Fenner, Starr et al. 2006). ISGs are also up-regulated in *Socs1*<sup>-/-</sup> mice and the treatment of BMMs from *Socs1*<sup>-/-</sup>*Ifn* $\gamma$ <sup>-/-</sup> mice with IFN $\alpha$  results in prolonged tyrosine phosphorylation of STAT1 (Fenner, Starr et al. 2006). This is due to a hyper-responsiveness of cells to the type I interferons (Fenner, Starr et al. 2006).

The inflammatory phenotype of *Socs1*<sup>-/-</sup> mice is largely due to dis-regulated IFN $\gamma$  signaling and is comparable to the effects observed with the administration of IFN $\gamma$  to neonatal mice (Alexander, Starr et al. 1999). Consequently, the neonatal lethality of *Socs1*<sup>-/-</sup> mice can be rescued by the administration of anti-IFN $\gamma$  antibody or via the generation of *Socs1*<sup>-/-</sup>*Ifn* $\gamma$ <sup>-/-</sup> mice (Alexander, Starr et al. 1999). The contribution of interferon signaling to the inflammatory phenotype, however, is complex. Knockout studies have found that type I interferon signaling also contributes to the inflammatory phenotype of *Socs1*<sup>-/-</sup> mice and that this is specific to IFNAR1 signaling (Fenner, Starr et al. 2006). *Socs1*<sup>-/-</sup>*Ifnar1*<sup>-/-</sup> mice survive past 3 weeks of age and do not display the inflammatory syndrome of *Socs1*<sup>-/-</sup> mice whereas *Socs1*<sup>-/-</sup>*Ifnar2*<sup>-/-</sup> mice all die by 3 weeks of age and display a phenotype similar to *Socs1*<sup>-/-</sup> mice (Fenner, Starr et al. 2006). This raises questions about the contribution of type I and type II interferon signaling towards the inflammatory phenotype, as the knockout of either pathway abolishes the inflammatory phenotype of *Socs1*<sup>-/-</sup> mice. This may be due to the pathways working in synergy with each other. One theory is that IFNAR1 associates with IFNGR which would explain why the knockout of IFNAR1 and not IFNAR2 abolishes inflammation (Fenner, Starr et al. 2006). Other data suggests that priming by

type I IFN is necessary for maintaining STAT1 levels basally and in the absence of this priming effect IFN $\gamma$  is unable to signal efficiently (Gough, Messina et al. 2010).

Compared to wild type mice, *Socs1*<sup>-/-</sup> mice have a significantly greater ability to resolve viral infection (Fenner, Starr et al. 2006), a characteristic which is due to a hyper-responsiveness of cells solely to the type I interferons, not IFN $\gamma$  (Fenner, Starr et al. 2006). The administration of antibody against IFN $\alpha$  and IFN $\beta$  to 5 – 10 day old *Socs1*<sup>-/-</sup> *Ifny*<sup>-/-</sup> mice prior to infection with SFV results in the death of all mice within 4 days compared to an 84% survival rate of SFV challenged, but untreated, *Socs1*<sup>-/-</sup> *Ifny*<sup>-/-</sup> mice (Fenner, Starr et al. 2006). Similarly, *Socs1*<sup>-/-</sup> *Ifnar1*<sup>-/-</sup> mice which have reduced type I interferon signaling are highly susceptible to viral infections and die within 4 days (Fenner, Starr et al. 2006).

#### **1.9.4 Mechanisms of SOCS1 inhibition**

Overall, these data suggest that IFNAR1, specifically, is a target for negative regulation by SOCS1 (Fenner, Starr et al. 2006). In other signaling systems, the SOCS proteins have been shown to inhibit receptor signaling by a number of mechanisms. In the IFN $\gamma$  signaling pathway, SOCS1 binds a phosphotyrosine residue (Tyr441) of the interferon gamma receptor 1 and is believed to restrict signaling by its kinase inhibitory region (KIR) interacting with the receptor associated JAK1 (Qing, Costa-Pereira et al. 2005). SOCS3 inhibition of gp130 signaling is through binding to a receptor phosphotyrosine and blocking the recruitment of signaling molecules (Nicholson, De Souza et al. 2000). In other systems, SOCS proteins have been found to directly interact with receptor associated JAK kinases. For example, in studies with recombinant proteins, SOCS1 has been shown to bind phosphorylated TYK2 and the SH2 domain of SOCS1 is required for this interaction (Narazaki, Fujimoto et al. 1998). In addition to the SH2 domain, the KIR domain is also required for SOCS1 inhibition of TYK2 auto-phosphorylation (Narazaki, Fujimoto et al. 1998).

The mechanism of SOCS1 inhibition of IFN signaling is yet to be elucidated. Based on other systems, SOCS1 may inhibit signaling in a number of ways, whether it is by binding directly to the receptor, receptor associated JAKs or other adaptors. It may inhibit signaling by the KIR blocking kinase function of receptor associated kinases or by blocking the recruitment of other signaling molecules such as STATs.

### 1.9.5 SOCS1 and Immune Cell Development

SOCS1 plays an important role in immune cell development and differentiation. As mentioned previously, the major site of SOCS1 expression is within thymocytes, and occurs in a developmentally regulated manner (Marine, Topham et al. 1999). *Socs1*<sup>-/-</sup> mice have altered T-cell counts. At 4 days post birth, *Socs1*<sup>-/-</sup> mice have a reduced double positive T-cell population and by 10 days post birth T-cells are largely CD4 or CD8 single positive cells. The perinatal lethal phenotype of *Socs1*<sup>-/-</sup> mice can be rescued by crossing onto a recombination activating gene 2 (RAG2)-deficient background, thus indicating a significant contribution of T-cells in the development of the phenotype of *Socs1*<sup>-/-</sup> mice (Marine, Topham et al. 1999). Studies involving mice with specific T-cell lineage SOCS1 deficiency have helped further refine the role of SOCS1 in thymic T-cell development (Chong, Cornish et al. 2003; Zhan, Davey et al. 2009). Mice with a specific deletion of SOCS1 from thymocytes do not display multi-organ failure suggesting that the inflammatory phenotype of SOCS1 is not due solely to the direct effect of SOCS1 on T-cell function. Nevertheless these mice display multiple lymphoid deficiencies (Chong, Cornish et al. 2003). SOCS1 has effects on both single positive CD4 and CD8 T-cells. Thymus-specific deletion of SOCS1 results in an enhanced CD8<sup>+</sup>:CD4<sup>+</sup> T-cell ratio (Chong, Cornish et al. 2003). The effect of SOCS1 on thymic T-cells translates downstream into altered peripheral T-cells. There is a significant increase in single positive T-cells within bone marrow and splenic T-cells display an activated phenotype responding to cytokines in the absence of T-cell receptor stimulation (Marine, Topham et al. 1999). Peripheral CD8<sup>+</sup> T-cells display increased hypersensitivity to cytokines and a memory like phenotype with the deletion of thymic SOCS1 (Chong, Cornish et al. 2003). Deletion of SOCS1 in T-cells also results in increased numbers of Foxp3<sup>+</sup> CD4<sup>+</sup> thymocytes due to increased survival of CD25<sup>+</sup>CD4<sup>+</sup> T-cells. This is independent of IFN $\alpha$  or IL-7 signaling. (Zhan, Davey et al. 2009). In addition to the direct effects of SOCS1 in T-cells, a dis-regulated cytokine network between T-cells and macrophages also contributes to the inflammatory disease (Chong et al 2005).

As mentioned previously, IFN $\gamma$  contributes largely to the phenotype of *Socs1*<sup>-/-</sup> mice. SOCS1, however, has IFN $\gamma$  independent actions in T-cell homeostasis (Cornish, Davey et al. 2003), as T-cell development in *Socs1*<sup>-/-</sup>*Ifn* $\gamma$ <sup>-/-</sup> mice is perturbed. Overall T-cell numbers in *Socs1*<sup>-/-</sup>*Ifn* $\gamma$ <sup>-/-</sup> mice are increased due to an increase in proliferation, although there is a decrease in splenic T-cell numbers (Cornish, Davey et al. 2003).

Similarly to *Socs1*<sup>-/-</sup> mice, *Socs1*<sup>-/-</sup>*Ifn* $\gamma$ <sup>-/-</sup> mice also have a reduced CD4<sup>+</sup>:CD8<sup>+</sup> T-cell ratio in lymphoid tissues as compared to control mice. As this decreased ratio was also seen in fetal thymic organ cultures of *Socs1*<sup>-/-</sup> and *Socs1*<sup>-/-</sup>*Ifn* $\gamma$ <sup>-/-</sup> embryos, it suggests that this perturbation may originate in the thymus. Comparison of proliferation and survival of T-cells in *Socs1*<sup>-/-</sup>*Ifn* $\gamma$ <sup>-/-</sup> and *Socs1*<sup>+/+</sup>*Ifn* $\gamma$ <sup>-/-</sup> mice demonstrate no difference in survival, yet proliferation of CD8<sup>+</sup> T-cells was greater than that of CD4<sup>+</sup> T cells and thus may drive the altered ratio of CD4<sup>+</sup>:CD8<sup>+</sup> T cells (Cornish, Davey et al. 2003).

As SOCS1 is involved in numerous cytokine signaling pathways, there are a number of candidate cytokines which may contribute to this altered ratio, such as IL-12, IL-7 and IL-15. As transfer of *Socs1*<sup>-/-</sup> progenitor T-cells to wild type mice also results in a reduced CD4<sup>+</sup>:CD8<sup>+</sup> ratio, the altered T-cell numbers are likely due to a hypersensitivity of T-cells to cytokines or direct cytokine secretion from T-cells themselves rather than a change in the environment of *Socs1*<sup>-/-</sup> mice such as altered cytokine levels.

## 1.10 Summary

The type I IFNs are critical in orchestrating an immune response to infection. Many pathogen detection mechanisms exist within the cell which ultimately results in type I IFN synthesis. Type I IFNs then act back on the cell to stimulate a host of anti-viral events as well as in a systemic manner to modulate cellular responses to infection. There is a tight balance between under and over activation of the immune system. Under-activation may result in an inability to clear infection while over-activation may result in uncontrolled inflammation. Considering the wide variety of effects type I IFN has in controlling immune responses it is critical that type I IFN signaling is regulated in an appropriate manner to effectively clear infection while maintaining homeostasis.

Initial signaling events at the receptor result in the phosphorylation of STATs which mediate many of the functions of the type I IFNs through transcriptional regulation. Many factors may act to control the balance of STATs activated by the type I IFNs and thus the response of the cell to IFN stimulation. The potent inhibitor, SOCS1, is one such factor which has a significant impact on IFN signaling. The mechanism of SOCS1 regulation of type I IFN signaling has yet to be determined and thus the focus of this thesis.

## CHAPTER 2

### METHODS

Note: all methods for Chapter 3 are included within Chapter 3.

#### 2.1 Mouse Models

Mice were maintained in a specific pathogen free (SPF) environment at the Monash Medical Centre Animal Facility. All mice used were female between 10 – 14 weeks of age. The following genotypes were used.

- wild type C57BL/6
- *Socs1*<sup>-/-</sup>*Ifn*γ<sup>-/-</sup> (C57BL/6 background) (Alexander, Starr et al. 1999)
- *Socs1*<sup>+/+</sup>*Ifn*γ<sup>-/-</sup> (C57BL6 background) (Alexander, Starr et al. 1999)

#### 2.2 Detection of STAT1, STAT3 and STAT5 phosphorylation in immune cell populations by Phosphoflow Cytometry.

##### 2.2.1 Collection and isolation of thymic and splenic immune cells

Mice were euthanised by CO<sub>2</sub> inhalation. The spleen and thymus were harvested and collected in a solution of Dulbecco's Phosphate Buffered Saline (DPBS) (Gibco) with 5mM EDTA (Amresco) on ice. Single cell suspensions of splenocytes or thymocytes were created by filtering through 70 µm Nylon Cell Strainers (BD Falcon) with ice cold DPBS into a clean 15 ml falcon tube (BD Falcon). Cells were then pelleted at 1000 x *g* for 5 minutes and the supernatant discarded. Cells were resuspended in 5 ml pre-warmed (37°C) red cell lysis (RCL) buffer (appendix I) and incubated at 37°C for 5 minutes to lyse red blood cells. 5 ml of ice cold DPBS was then added and the cells pelleted. The supernatant was discarded and the cells resuspended and washed in 5 mls DPBS. A 200 µl aliquot was taken from each sample for analysis and cell counting using the Sysmex cell counter according to the manufacturers' instructions (Sysmex). The cells were again pelleted and the supernatant discarded and resuspended in pre-

warmed in Dulbecco's Modified Eagle Medium (DMEM) (Gibco) with 1% Fetal Bovine Serum (FBS) (Gibco) at a concentration of  $10^7$  cells/ml. The cell suspension was incubated at 37°C with 5% CO<sub>2</sub> for 1-2 hours prior to stimulation.

### **2.2.2 Collection and Isolation of Peripheral Blood Mononuclear Cells (PBMCs)**

Prior to blood collection, 10 µl of Heparin (Sigma Aldrich) was aliquoted into a clean 1.7 ml eppendorf tube (Axygen) and placed on ice. The blood was collected via cardiac puncture and transferred to the eppendorf tube containing heparin. The blood and heparin were mixed and kept on ice to prevent blood clotting. Isolation of PBMCs was performed using Histopaque® (Sigma Aldrich). The blood was warmed to room temperature and diluted in DPBS to a volume of 3 ml. 3 ml of room temperature histopaque solution was aliquoted into a 15 ml falcon tube and the diluted blood layered on top. These were then centrifuged at 4000 x *g* for 30 minutes at room temperature to separate the plasma, white blood cells, histopaque and red blood cells and granulocytes. The cell fraction layer was then carefully collected and pooled with samples from mice with the same genotype into a 50 ml falcon tube (BD Falcon) with the addition of 40 ml DPBS. The cells were pelleted at 2000 x *g* for 10 minutes and the supernatant removed. To ensure no red blood cells remained in the cell solution, 5 ml of pre-warmed (37°C) RCL buffer was added to the cell pellet, mixed and incubated at 37°C for 5 minutes. The cells were then pelleted at 1000 x *g* for 5 minutes and the supernatant discarded. 5 ml of DPBS was then added to the cells and a 200 µl aliquot taken for analysis by the Sysmex cell counter. The cells were again pelleted at 1,000 x *g* for 5 minutes and resuspended in 1% FCS DMEM to a concentration of  $10^7$  cells per ml.

### **2.2.3 Cell Stimulation**

For each stimulation condition, 300 µl of cell solution was transferred to 15 ml falcon tubes. muIFNα (Trajanovska, Owczarek et al. 2003) diluted to the required concentration (as specified) in DMEM was added to the cell suspensions and the tubes were incubated at 37°C for the required time (as specified).

### **2.2.4 Cell Fixing and Permeabilisation**

Following stimulations, cells were fixed by adding 1 ml pre-warmed (37°C) 1% Buffered Formalin (10% Buffered Formalin (Austalian Biostain Pty. Ltd.) diluted 1/10 in DPBS) and incubated at 37°C for 10 minutes. To stop fixation, 1 ml of ice cold DPBS was added to the cells and the cells pelleted at 1,000m x g for 5 minutes at 4°C. The cells were washed again in DPBS at 4°C, pelleted and the supernatant discarded. Excess supernatant was removed so cells were in minimal volume. Cells were then vortexed to disrupt the pellet while adding 1 ml of ice cold 90% methanol (Australian Biostain) (diluted in Milli-Q H<sub>2</sub>O) to permeabilise the cells. Cells were then placed at -80°C for next day staining.

### **2.2.5 Anti-body staining**

Cells were removed from -80°C freezer and placed on ice. Cells were then pelleted at 1,000 x g for 5 mins at 4°C. The supernatant was removed and the cells resuspended in 2 ml of freshly made, ice cold, phosphoflow staining buffer (appendix I). Cells suspensions were transferred to Fluorescence Activated Cell Sorting (FACS) tubes (BD Biosciences) for ease of handling. Cells were then washed twice in staining buffer, pelleting at 1,000 x g for 5 mins at 4°C. Following washes, cells were resuspended in 240 µl staining buffer and allowed to hydrate for 1 hour, on ice. 40 µl of cells were then transferred to fresh FACS tubes for each antibody stain. The antibodies used for phosph-Stat1, phospho-Stat3 and phospho-Stat5 staining and surface marker staining are described in Table 2.1. Antibodies were prepared in a total of 10 µl staining buffer at appropriate concentrations (as specified). The diluted antibodies (in 10 µl volume) were added to the 40ul aliquots of cell suspensions and incubated for 60 minutes on ice in the dark. Following staining, cells were washed twice in 1 ml ice cold staining buffer, with centrifuge spins of 1000 x g for 5 minutes at 4°C. Following washes, cells were resuspended in 400 µl staining buffer for FACS analysis.

### **2.2.6 Data Collection and Analysis**

Data was acquired using a BD FACSCanto<sup>TM</sup>II analyser according to the manufacturers' instructions. A minimum of 10,000 cells for each sample was collected. Prior to data collection, single stained (FITC, PE or Alexa647) controls were used to compensate for any background readings. Data was analysed using the software FlowJo. Details of this analysis are outlined in section 4.1.1.

**Table 2.1: List of antibodies used for flow cytometry.**

<b>Antibody</b>	<b>Conjugation</b>	<b>Concentration</b>	<b>Dilution</b>	<b>Company</b>
Anti-phospho-STAT1 (pY701)	A647	unknown	1/5	BD Biosciences
Anti-phospho-STAT3 (pY705)	A647	unknown	1/5	BD Biosciences
Anti-phospho-STAT5 (pY694)	A647	unknown	1/5	BD Biosciences
Anti-CD4	FITC	0.5 mg/ml	1/1600	BD Biosciences
Anti-CD8	PE	0.2 mg/ml	1/100	BD Biosciences
Anti-B220	FITC	0.5 mg/ml	1/3200	BD Biosciences
Anti-MAC1	PE	0.2 mg/ml	1/1600	BD Biosciences

## **2.3 Western Blot Analysis of total STAT1, STAT3 and STAT5 protein expression**

### **2.3.1 Preparation of Cell Lysates**

Whole thymus was harvested and a single cell suspension prepared as outlined in section 2.2.1. For each thymus,  $10^7$  cells, in a total volume of 1 ml DMEM with 1% FCS, were aliquoted into wells of a 24 well plate and allowed to rest for one hour. Cells were stimulated with muIFN $\alpha$  for 0, 30, 120 and 240 minutes. At appropriate time points, 1 ml of ice cold DPBS was added to each well, the cells were detached by pipetting and transferred to a 15 ml falcon tube. Cells were pelleted at 1000 x *g* for 5 mins, washed twice in DPBS and resuspended in 200  $\mu$ l cell lysis buffer (appendix I). Cell lysates were transferred to an eppendorf tube and rotated for 1 hour at 4°C to ensure complete lysis. The nuclei was pelleted at 10,000 x *g* for 10 minutes at 4°C and the supernatant transferred to a fresh eppendorf tube.

### **2.3.2 Lowry Protein Assay**

A Lowry protein assay (Promega) was performed, according to the manufacturer's instructions, to determine the concentration of protein in the cell lysates. In a total volume of 5  $\mu$ l, 0, 1, 2, 4, 8, 10, 20 and 50  $\mu$ g Bovine Serum Albumin (BSA, Sigma Aldrich) standards were aliquoted, in triplicate, into a flat bottom 96 well plate (BD Falcon) along with the cell lysates to be tested. Lowry assay reagents (Promega) were added to the wells, according to the manufacturer's instructions, and incubated at RT for 15 mins. The absorbance at 490 nm was determined using a FluoStar Optima plate reader, according to the manufacturer's instructions. A standard curve was generated using the BSA samples and the protein content of the cell lysates determined.

### **2.3.3 SDS-Polyacrylamide Gel Electrophoresis (SDS-PAGE)**

SDS-PAGE was performed using the BIO-RAD SDS-PAGE apparatus. Proteins were separated using 8% SDS-PAGE gels (appendix I). 40  $\mu$ g of lysate samples (heated at 95°C for 5 mins with 5 x Sample buffer (appendix I)) were loaded onto the SDS-PAGE gel and electrophoresed at 80 V in SDS-PAGE running buffer (appendix I) until adequate separation was achieved. A BenchMark molecular weight marker (Invitrogen) was run alongside protein samples for calculation of molecular weight.

### **2.3.4 Protein Transfer to Nitrocellulose Membrane**

Resolved protein from SDS-PAGE was transferred onto a nitrocellulose membrane (Immobilon-FL, Millipore) for immunoblot analysis. This was performed in wet transfer buffer (appendix I) using the wet transfer technique with BIO-RAD apparatus, according to the manufacturer's instructions. The transfers were run at 100 V for 70 minutes.

### **2.3.5 Immunoblotting**

Membranes were blocked for 1 hour at RT in Odyssey Blocking Buffer (OBB, LI-COR Biosciences). Membranes were then placed in roller tubes (Starstedt) and incubated with either rabbit anti-muSTAT1 (Cell Signalling), mouse anti-muSTAT3 (Cell Signalling) or rabbit anti-muSTAT5 (Cell Signalling) antibodies diluted 1:1000 in OBB overnight at 4°C. Membranes were washed 3 x 10 mins in PBS with 0.1% Tween (PBST) at RT, placed into clean roller tubes and incubated with secondary antibody, 800 nm fluorescence labelled anti-mouse-IgG or anti-rabbit-IgG antibodies (LI-COR Biosciences), diluted 1:1500 in OBB with 0.1% Tween for 1 hour at RT. Membranes were wash 3 x 10 mins at RT in PBST. Protein was visualised using the Odyssey Infrared Imaging System (LI-COR Biosciences), at wavelength 800 nm, according to the manufacturer's instructions. Membranes were then stripped of antibody by incubation with stripping buffer (appendix I) for 10 mins at 55°C. Membranes were re-blocked in OBB and incubated with anti-B-tubulin antibody (Abcam) diluted 1:1000 in OBB overnight at 4°C. Membranes were washed and incubated with secondary antibody, 800 nm fluorescence labelled anti-mouse-IgG, diluted 1:1000 in OBB with 0.1% Tween. Membranes were then washed and protein visualised using Odyssey, on wavelength 880, according to the manufacturer's instructions. Odyssey Infrared Imaging System, at wavelength 800 nm, according to the manufacturer's instructions.

## **2.4 Microarray**

A flow chart of the microarray procedure is outlined in Figure 2.1 and explained in detail below.

### **2.4.2 IFN Treatment**

muIFN $\alpha$  was diluted in 200  $\mu$ l DPBS to contain a total of 1000 IU. Mice were injected i.p using a 26 gauge needle with 200  $\mu$ l DPBS with muIFN $\alpha$  (1000 IU) or with 200  $\mu$ l DPBS for controls.

### **2.4.3 Organ Collection**

Mice were euthanized by CO<sub>2</sub> inhalation at 3 and 6 hours post IFN $\alpha$  stimulation. Mice injected with DPBS were euthanized at the 6 hour time point. Following euthanasia the thymus was harvested, snap frozen in liquid nitrogen then stored at -80°C.

### **2.4.4 RNA isolation from Whole Thymus**

The thymi were removed from -80°C and placed on dry ice. Samples were weighed and transferred to 50 ml falcon tubes with 1 ml of TRIzol reagent (Invitrogen). The tissue was homogenised in TRIzol using a T24 Ultra-Turrax (IKA) homogeniser. Following homogenisation, samples were transferred to 15 ml falcon tubes and 200  $\mu$ l of chloroform (Sigma) added to each tube. Samples were vortexed for 15 seconds and incubated at room temperature for 3 minutes. Samples were centrifuged at 10,000 x *g* for 15 minutes at 4°C. Following centrifugation, the aqueous phase (top layer) containing the RNA was transferred to a fresh eppendorf tube. 500  $\mu$ l of isopropanol (Merck) was added to each tube and the samples mixed and incubated for 10 minutes at room temperature to precipitate the RNA. The samples were then centrifuged at 10,000 x *g* for 10 minutes at 4°C and the supernatant discarded. The RNA was washed once with 1 ml of 70% ethanol (Labchem) (diluted in 0.1% v/v diethylpyrocarbonate (DEPC) treated Milli-Q H<sub>2</sub>O (appendix I)), mixed by vortexing and centrifuged at 7,500 x *g* for 5 minutes at 4°C. The supernatant was discarded and the RNA pellet air dried for 5 -10 minutes. 400  $\mu$ l of DEPC treated H<sub>2</sub>O was then added and the RNA redissolved at 55°C for 10 minutes. RNA was then stored at -80°C.

	0 hour	3 hours	6 hours
WT	PBS (n=3)	IFN $\alpha$ (n=3)	IFN $\alpha$ (n=3)
<i>Socs1<sup>+/+</sup>Ifny<sup>-/-</sup></i>	PBS (n=3)	IFN $\alpha$ (n=3)	IFN $\alpha$ (n=3)
<i>Socs1<sup>-/-</sup>Ifny<sup>-/-</sup></i>	PBS (n=3)	IFN $\alpha$ (n=3)	IFN $\alpha$ (n=3)



**Sample Preparation**  
Harvest, extract and label RNA



**Hybridisation**  
Agilent 4 x 44k mouse chips



**Quality Control**  
RNA Integrity



**Scan Chips**  
Log intensity calculated



**Analysis**  
Samples loaded into Genespring GX for analysis

**Figure 2.1: Flow chart of the microarray procedure.**

#### **2.4.5 RNA clean up**

To remove any contaminants from the RNA samples, these were cleaned using a Qiagen RNeasy Mini Kit (with an on-column DNase1 digestion) according to the manufacturers' instructions. RNA was eluted in a total volume of 50  $\mu$ l in DEPC treated H<sub>2</sub>O.

#### **2.4.6 RNA Quality Control**

Analysis of the RNA integrity and the presence of contaminants were performed using Experion RNA StdSens Analysis Kit (BIO-RAD) according to the manufacturers' instructions.

#### **2.4.7 Reverse Transcription of RNA to cDNA**

Reverse transcription of RNA to cDNA was performed with the SuperScript<sup>TM</sup>III First-Strand Synthesis System (Invitrogen). RNA (1  $\mu$ g) was combined with 50 ng random hexamers (Invitrogen) and 1  $\mu$ l of 10 mM dNTP mix (Invitrogen) (total concentration 1mM) in a total volume of 10  $\mu$ l. The samples were incubated at 65°C for 5 minutes, cooled on ice for 5 minutes and then pulse spun. 10  $\mu$ l of freshly made cDNA Synthesis Mix was then added to each sample, consisting of 2  $\mu$ l of 10 x Reverse Transcriptase buffer (Invitrogen), 2  $\mu$ l of 0.1 M DTT (Invitrogen) (total concentration 0.01mM), 4  $\mu$ l of 25 mM MgCl<sub>2</sub> (Invitrogen) (total concentration 5 mM), 1  $\mu$ l of 40 U/  $\mu$ l RNaseOUT<sup>TM</sup> (Invitrogen) and 1  $\mu$ l of SuperScript<sup>TM</sup>III Reverse Transcriptase (Invitrogen). The samples were incubated at room temperature for 10 minutes followed by 50°C for 50 minutes. The reactions were heat inactivated at 85°C for 5 minutes. 1  $\mu$ l of RNase H (Invitrogen) was added to each sample and samples were incubated at 37°C for 20 minutes. Samples were diluted 1 in 5 in DEPC treated H<sub>2</sub>O. This dilution allows for 2  $\mu$ l of sample to be used for each PCR or qRT-PCR. Samples were stored at -20°C until use.

#### **2.4.8 GAPDH PCR**

A GAPDH PCR was performed on cDNA samples to ensure no genomic DNA contamination. 1  $\mu$ l of cDNA was added to 10  $\mu$ l of 5 x Green Taq buffer (Promega), 1  $\mu$ l of 10mM dNTP (Promega), 1  $\mu$ l of 5' and 3' GAPDH primers (appendix II), 3  $\mu$ l of MgCl<sub>2</sub> (Promega), 0.3  $\mu$ l of Flexi Taq Polymerase (Promega) and made up to 50  $\mu$ l with

DEPC treated H<sub>2</sub>O. All PCR reactions were carried out in a MyCycler™ Thermal Cycler (BIO-RAD)

- PCR reaction conditions
- Denaturation: 94°C, 30 seconds      1 cycle
- Denaturation: 94°C, 30 seconds
- Annealing: 55°C, 30 seconds      } 35 cycles
- Extension: 72°C, 30 seconds
- Extension: 72°C, 5 minutes      1 cycle

#### **2.4.9 Quantitative Real Time PCR (qRT-PCR)**

The Applied Biosystems 7900HT Fast Real-time PCR system and Syber Green were used for qRT-PCR. Each reaction was performed in a total volume of 10 µl including 2 µl cDNA, 5 µl of Syber Green PCR Master Mix (Applied Biosystems) and 0.2 µM each of forward and reverse primers as indicated. The total volume was made to 10 µl with DEPC treated H<sub>2</sub>O. The primers used for each gene are indicated in appendix II. For each gene analysed a control of 18S was also performed for each sample. Each 10 µl reaction was performed in triplicate in a MicroAmp™ Optical 384-well reaction plate and sealed with MicroAmp™ Optical adhesive film. The thermal cycling protocol was as follows: 50°C for 2 minutes, 95°C for 10 minutes followed by 40 cycles of 95°C for 15 seconds and 60°C for 1 minute. Cycle threshold (Ct) values for all probes were exported and  $\Delta\Delta Ct$  for each sample calculated relative to 18S. Fold induction of  $\Delta\Delta Ct$  values was calculated relative to a chosen sample (as indicated).

#### **2.5.10 Microarray Procedure**

The methods described in section 2.5.10 were performed by Jodee Gould, CIID, MIMR.

##### **2.5.10.1 Spike In**

600 ng of RNA was diluted in nuclease free water to a total volume of 7.3 µl. The spike in mix was prepared by heating at 37°C for 5 mins. Three fold serial dilutions of the spike in mix were prepared and 3 µl was added to each RNA sample along with 1.2 µl T7 promoter primer to make a final volume of 11.5 µl. The samples were denatured by incubating at 65°C for 10 minutes followed by ice for 5 minutes and a pulse spin.

### **2.5.10.2 cDNA synthesis**

8.5 µl of cDNA mix was added to each sample and consists of 4 µl 5X first strand buffer, 2 µl 0.1M DTT, 1 µl 10mM dNTP mix, 1 µl MMLV-RT and 0.5 µl RNaseOUT. Samples were mixed by pipetting and incubated in a 40°C water bath for 2 hours. Samples were then heat inactivated by heating at 65°C for 15 minutes followed by ice for 5 minutes. Samples were stored at -20°C until the next step.

### **2.5.10.3 Cy-3 Labelling and Transcription**

60 µl of transcription mix was added to each tube consisting of 15 µl nuclease free water, 20 µl 4X transcription buffer, 6 µl 0.1mM DTT, 8 µl NTP mix, 6.4 µl 50% PEG (prewarmed 40°C for 1 minute), 0.5 µl RNaseOUT, 0.6 µl inorganic pyrophosphatase, 0.8 µl T7 RNA polymerase and 2.4 µl Cy-3-CTP. Samples were incubated in a 40°C water bath for 2 hours.

### **2.5.10.4 Purification of cRNA**

Cy3 labelled cRNA was then purified using Qiagen RNeasy mini kit. 20 µl water was added to cRNA samples for a total volume of 100 µl. 350 µl RLT (+βME 10 µl/ml) was then added and mixed by pipetting, followed by 250 µl 100% ethanol. 700 µl of cRNA was transferred to a Qiagen mini column and centrifuged at 10,000 x g for 30 seconds. Flow through was discarded. The column was transferred to a new collection tube and 500 µl RPE added. Columns were centrifuged at 10,000 x g for 30 seconds and the flow through discarded. This was then repeated with another 500 µl RPE with centrifugation 10,000 x g for 1 minute. Columns were spun for an extra 30 seconds to remove all traces of ethanol. The column was then transferred to a 1.5 ml eppendorf tube and 30 µl water added. Following a one minute incubation, columns were centrifuged 10,000 x g for 30 seconds. The eluant cRNA was then stored at -20°C until the next step.

### **2.5.10.5 Quantification of cRNA**

1 µl of cRNA from each sample was tested on the nanodrop using the RNA-40/Cy3 microarray measurement. Yield must be > 1.65 µg and specific activity > 9.0 pmol/µg.

$$\mu\text{g cRNA} = \text{mg}/\mu\text{l cRNA} \times 30\mu\text{l}(\text{elution volume})/1000$$

$$\text{specific activity} = (\text{pmol}/\mu\text{l Cy3}/ \text{ng}/\mu\text{l cRNA}) \times 1000$$

#### **2.5.10.6 Hybridisation**

For 4x 44K microarrays, 1.65 µg of Cy3 labelled cRNA , 11 µl of 10 x blocking agent, 2.2 µl of 25 x fragmentation buffer in a total volume of 55 µl made up with water. The samples were incubated at 60°C for exactly 30 minutes. The reaction was stopped by the addition 55 µl of 2 x GE Hybridisation buffer. The samples were mixed carefully by pipetting and centrifuged at 13,000 x g for 1 minute.

100 µl of sample was then used immediately for hybridisation onto the microarray slide at 65°C for 17 hours at 10 rpm.

#### **2.5.10.7 Microarray slide wash**

Disassembly was performed in GE wash buffer 1 at 25°C. Slides were then washed in GE wash buffer 1 for 1 minute at 25°C and then pre-warmed GE wash buffer 2 for 1 minute.

#### **2.5.10.8 Microarray slide scan**

Each slide was loaded into a Version B slide holder (*Agilent Technologies*) and scanned in a G2505B Series Microarray scanner (*Agilent Technologies*) using the one colour scan setting for 4x44k array slides (Scan Area 61x21.6 mm, Scan resolution 5µm, Dye channel was set to Green and Extended Dynamic Range selected at 100% and 10% Green PMT).

#### **2.5.10.9 Feature Extraction**

The scanned images were analysed with Feature Extraction Software 9.5.3.1 (*Agilent Technologies*) using default parameters (protocol GE1-v5\_95 and Grid: 014868\_D\_20060807) to obtain background subtracted and spatially detrended Processed Signal intensities. Features flagged in Feature Extraction as Feature non-uniform outliers were excluded. Ultimately, the log intensity of each spot was calculated. Log (intensity) is dependent on the gene effect, array effect, dye effect, treatment effect, effect of interaction and error. Within the analysis we are interested in the difference between log intensities of a gene under different treatment.

### 2.5.11 Data Analysis

Analysis of the microarray was performed using Genespring GX. Following feature extraction, the microarray data files were loaded into Genespring GX. Prior to statistical analysis, the data underwent a number of normalisation and quality control steps to ensure a reliable probe list was generated for analysis. A flow chart of the initial normalisation, transformation and quality control steps applied to the microarray data is demonstrated in Figure 2.2 and outlined below.

Normalisation of samples was performed to account for variations across arrays. The recommended Genespring normalisation for a one-colour Agilent array is a 'shift to the 75<sup>th</sup> percentile'. The 75<sup>th</sup> percentile was computed for every sample. The log values of the probe intensities of a sample were then subtracted by a factor so that every sample had the same 75<sup>th</sup> percentile. Following the above normalisation, baseline values for each sample were transformed to either the median of all samples or the median of its own genotypes 0 hour (as indicated). The type of baseline transformation performed is an important consideration depending on the questions to be asked of the data and the type of analysis performed.

Analysis of sample box plots enables the identification of 'abnormal' arrays. The distribution of one of the 6 hour IFN $\gamma$  time points did not follow patterns similar to the other samples and was therefore removed from the experiment. Unfortunately this only allows a sample of n=2 for this condition. Consequently some statistical analyses were unable to be performed. Where Genespring allowed the use of n=2 for statistical tests, these were performed.

Prior to data analysis, filtering of entities was performed based on gene expression intensities and the presence of flags. Entities were filtered for only those within the 15<sup>th</sup> – 100<sup>th</sup> percentile of intensities values of a probe set. For entities to be included in these analyses, they must be within the 15<sup>th</sup> – 100<sup>th</sup> percentile of at least half the samples. Flags are attributes that denote the quality of the entities. Values are generated based on the feature quality of the chip, like signal saturation and signal uniformity. The entities with low significant attributes in the data file were marked as absent and high significant values marked as present. Filtering by flags allows removal of 'absent' entities.

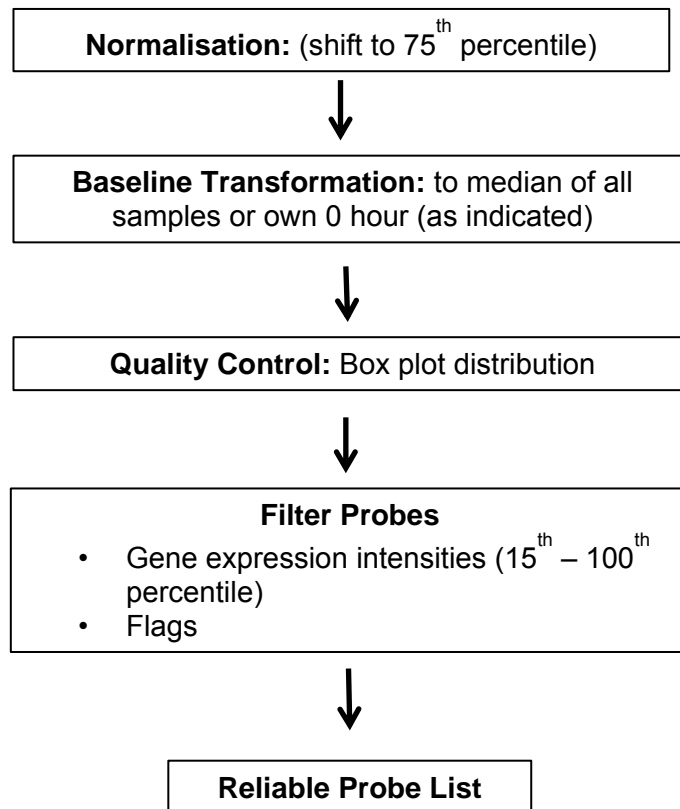


**Figure 2.2: Flow chart of the initial steps in microarray analysis using Genespring GX.**

Ultimately these steps resulted in a 'reliable' probe list on which statistical analysis was performed. Differential expression of genes across the different samples were analysed by performing a fold change cut off and applying a statistical test. A fold change cut off of greater or equal to two was used when comparing gene expression across the conditions. The type of statistical test applied was dependent on the question being asked. T-tests and one-way and two-way anovas were used (as indicated). A Benjamini Hochberg false discovery rate (FDR) multiple testing correction was also applied during the statistical analysis to minimise the detection of false positives. When a low number of genes were identified, the FDR correction was not applied (as indicated). Figure 2.3 outlines the statistical tests performed to identify genes significantly regulated following 3 and 6 hour IFN $\alpha$  treatment in the thymus of wt C57BL/6 mice. Figure 2.4 outlines the statistical tests performed to identify genes differentially expressed within *Socs1<sup>+/+</sup>Ifn $\gamma$ <sup>-/-</sup>* vs *Socs1<sup>-/-</sup>Ifn $\gamma$ <sup>-/-</sup>* mice. Figure 2.5 outlines the statistical tests performed to identify genes significantly regulated following 3 and 6 hour IFN $\alpha$  treatment in the thymus of *Socs1<sup>+/+</sup>Ifn $\gamma$ <sup>-/-</sup>* C57BL/6 mice. Figure 2.6 outlines the statistical tests performed to identify genes significantly regulated following 3 and 6 hour IFN $\alpha$  treatment in the thymus of *Socs1<sup>-/-</sup>Ifn $\gamma$ <sup>-/-</sup>* C57BL/6 mice. Figure 2.7 outlines the statistical tests performed to identify genes that interact over SOCS1 regulation and IFN $\alpha$  stimulation.

Following statistical analysis, further bioinformatics analysis was employed on the gene lists shown to be statistically different between the conditions analysed. Further refining of these lists using clustering techniques enabled grouping of similarly expressed (co-regulated) genes. The K-means algorithm was used to cluster the genes into groups with distinct profiles. K-means clustering partitions entities into k groups so that the sum of squares from points to the defined cluster centres are minimised. Euclidean distance was used as a metric and variance was used as a measure of cluster scatter. The amount of clusters generated was user-defined with the optimal number found by trial.

#### **2.5.11.1 Functional Annotation**

A web-based program called the Database of Annotation, Visualisation and Integrated Discovery (DAVID) was used to perform functional annotation clustering of gene lists (Dennis, Sherman et al. 2003). The enrichment score (ES) is a ranking calculated from the geometric mean of members p-values in a corresponding annotation cluster. The top ranked annotation groups are likely to have consistently lower p-values for their annotation members.

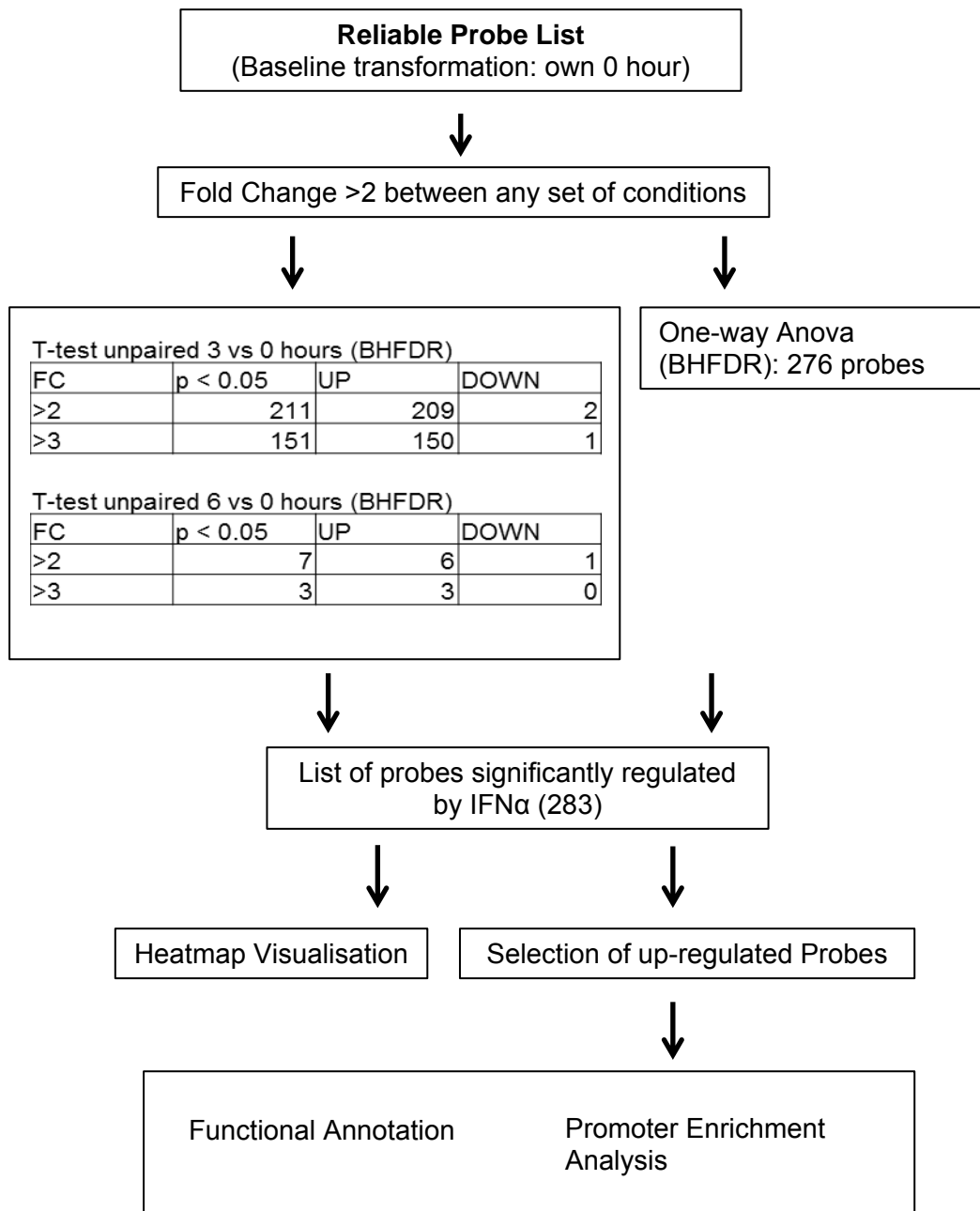


**Figure 2.3: Flow chart of analysis for the identification of genes regulated following 3 and 6 hours IFN $\alpha$  treatment, administered intraperitoneally, in the thymus of wt C57BL/6 mice**

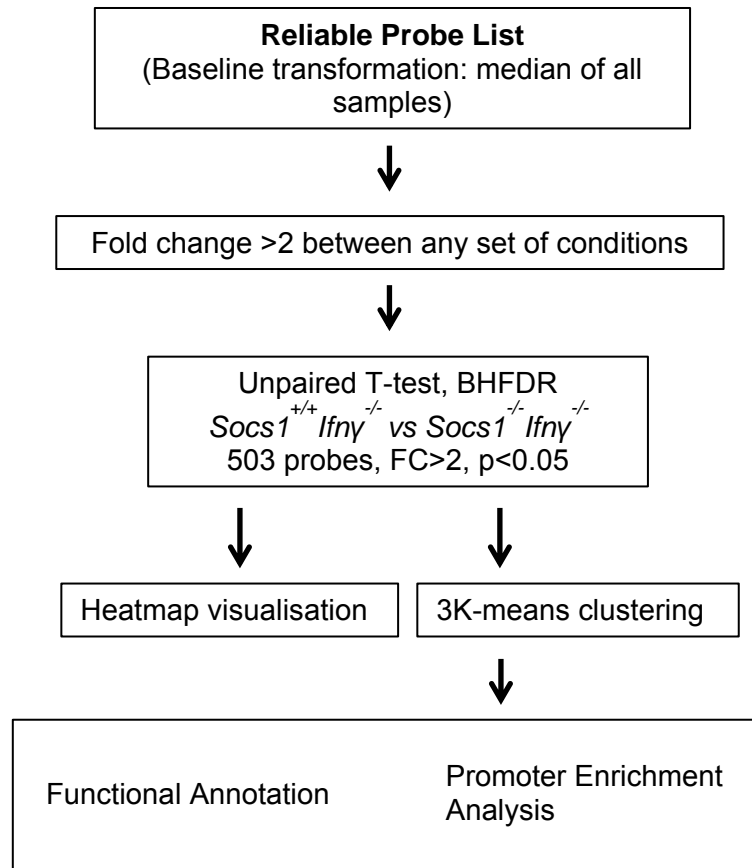


**Figure 2.4: Flow chart of analysis for the identification of genes differentially expressed within *Socs1*<sup>+/+</sup> *Ifny*<sup>-/-</sup> vs *SocS1*<sup>-/-</sup> *Ifny*<sup>-/-</sup> mice.**





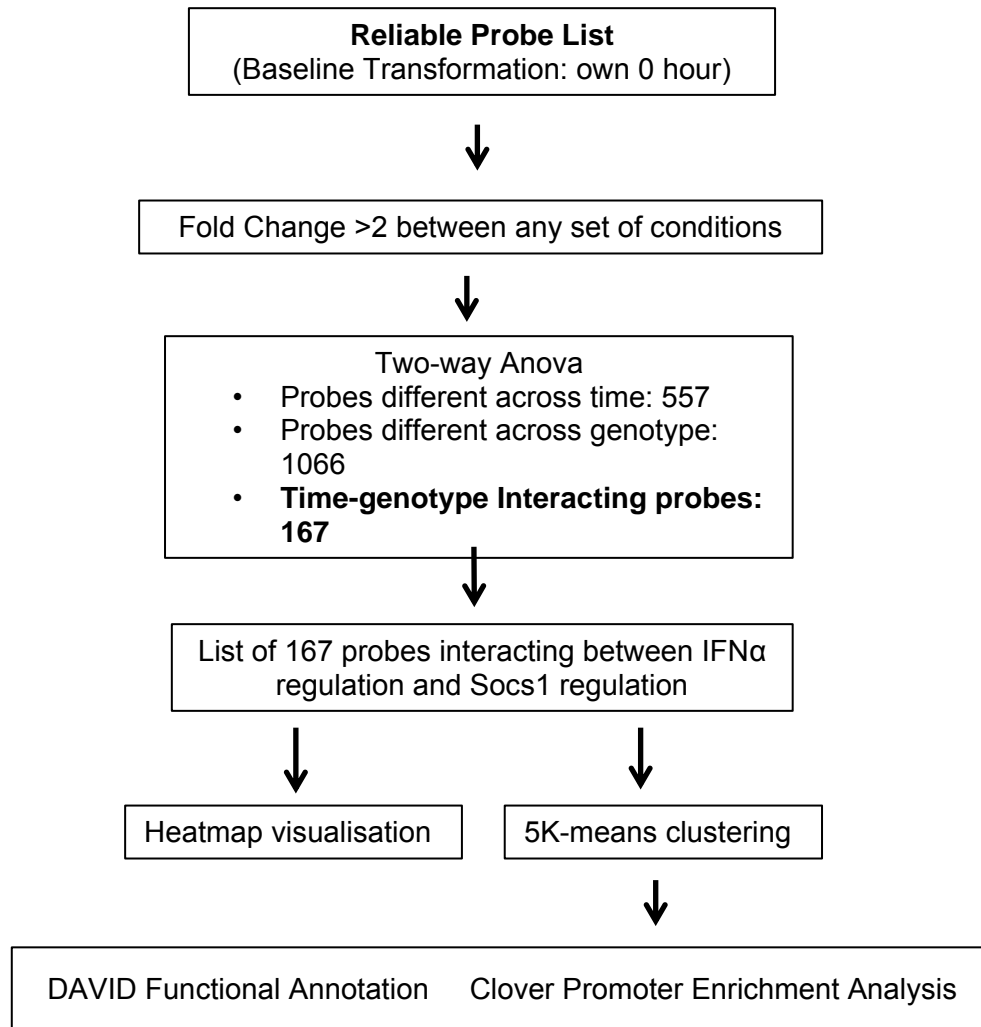


**Figure 2.7** Flow chart of anathelaysis for the identification of SOCS1/IFN regulated genes.

### 2.5.11.2 Promoter Analysis

The promoters of specific genes were analysed using the program Clover (Cis-element over-representation) (Frith, Fu et al. 2004). Clover identifies statistically over-represented sequence motifs within the promoters of specified gene sets compared with background sequences. Clover compares each motif to the sequence set and calculates a raw score indicating how strongly the motif is present in the set. For each background set clover will repeatedly extract random fragments matched by length to the target sequences and calculate raw scores for these fragments. The p-value is equal to the proportion of times that the raw score fragment set exceeds or equals the raw score target set. For each motif a separate P-value is calculated for each background file. The P-value indicates the probability that the motifs presence in the target set can be explained by chance alone. The motifs used for analysis were obtained from TRANSFAC 2010.3. TRANSFAC is a database of transcription factors containing their experimentally proven binding sites and regulated genes. Target sets: Sequences for analysis of a particular gene set were obtained from Ensemble BioMart. For each gene, 2000 base pairs upstream of the transcription start site were analysed. Background Sequence: sequences 2000 bp upstream of mouse genes (47.8% G+C) from UCSC (25 April 2003).

## CHAPTER 3

### DECLARATION

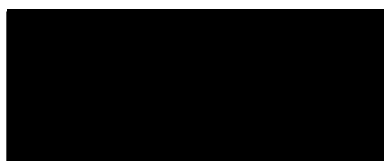
In the case of Chapter 3 the nature and extent of my contribution to the work was the following:

Nature of contribution	Extent of contribution (%)
Cloned IFNAR1 and IFNAR1 mutant expression constructs	100
Performed all luciferase assays	100
Performed all co-immunoprecipitation assays	100
Performed all ubiquitination assays	100
Performed analysis of endogenous and exogenous TYK2 expression	100
Writing of the paper	100

The following co-authors contributed to the work:

Name	Nature of contribution
Nicole de Weerd	Performed flow cytometry analysis of IFNAR1 surface levels
Jodee Gould	Cloned and performed mutagenesis of TYK2 expression constructs
Christian Schindler	Provided advice and reagents
Ashley Mansell	Provided advice and reagents
Sandra Nicholson	Provided advice and reagents
Paul Hertzog	Supervisor and lab director

Candidate's  
Signature



Date  
23/4/13

**Declaration by co-authors**

The undersigned hereby certify that:

- (1) the above declaration correctly reflects the nature and extent of the candidate's contribution to this work, and the nature of the contribution of each of the co-authors.
- (2) they meet the criteria for authorship in that they have participated in the conception, execution, or interpretation, of at least that part of the publication in their field of expertise;
- (3) they take public responsibility for their part of the publication, except for the responsible author who accepts overall responsibility for the publication;
- (4) there are no other authors of the publication according to these criteria;
- (5) potential conflicts of interest have been disclosed to (a) granting bodies, (b) the editor or publisher of journals or other publications, and (c) the head of the responsible academic unit; and
- (6) the original data are stored at the following location(s) and will be held for at least five years from the date indicated below:

**Location(s)**

The Centre for Innate Immunity and Infectious Diseases  
Monash Institute of Medical Research

Author	Signature	Date
Nicole de Weerd		15-4-2013
Jodee Gould		15-4-2013
Christian Schindler		3-22-2013
Sandra Nicholson		15/4/2013
Ashley Mansell		15/4/2013
Paul Hertzog		15/4/2013

# Suppressor of Cytokine Signaling (SOCS) 1 Inhibits Type I Interferon (IFN) Signaling via the Interferon $\alpha$ Receptor (IFNAR1)-associated Tyrosine Kinase Tyk2\*

Received for publication, June 9, 2011, and in revised form, July 11, 2011. Published, JBC Papers in Press, July 13, 2011, DOI 10.1074/jbc.M111.270207

Rebecca A. R. Piganis<sup>‡</sup>, Nicole A. De Weerd<sup>‡</sup>, Jodee A. Gould<sup>‡</sup>, Christian W. Schindler<sup>§</sup>, Ashley Mansell<sup>‡</sup>, Sandra E. Nicholson<sup>¶</sup>, and Paul J. Hertzog<sup>‡1</sup>

From the <sup>‡</sup>Centre for Innate Immunity and Infectious Disease, Monash Institute of Medical Research, Monash University, Clayton, Victoria 3168, Australia, the <sup>§</sup>Department of Microbiology and Department of Medicine, College of Physicians and Surgeons, Columbia University, Hammer Health Science Center, and the <sup>¶</sup>Walter and Elisa Hall Institute, Melbourne, Victoria 3001, Australia

Type I IFNs are critical players in host innate and adaptive immunity. IFN signaling is tightly controlled to ensure appropriate immune responses as imbalance could result in uncontrolled inflammation or inadequate responses to infection. It is therefore important to understand how type I IFN signaling is regulated. Here we have investigated the mechanism by which suppressor of cytokine signaling 1 (SOCS1) inhibits type I IFN signaling. We have found that SOCS1 inhibits type I IFN signaling not via a direct interaction with the IFN  $\alpha$  receptor 1 (IFNAR1) receptor component but through an interaction with the IFNAR1-associated kinase Tyk2. We have characterized the residues/regions involved in the interaction between SOCS1 and Tyk2 and found that SOCS1 associates via its SH2 domain with conserved phosphotyrosines 1054 and 1055 of Tyk2. The kinase inhibitory region of SOCS1 is also essential for its interaction with Tyk2 and inhibition of IFN signaling. We also found that Tyk2 is preferentially Lys-63 polyubiquitinated and that this activation reaction is inhibited by SOCS1. The consequent effect of SOCS1 inhibition of Tyk2 not only results in a reduced IFN response because of inhibition of Tyk2 kinase-mediated STAT signaling but also negatively impacts IFNAR1 surface expression, which is stabilized by Tyk2.

Interferons are a family of cytokines that elicit multifaceted effects during the host innate and adaptive immune response. The type I IFN family consists of multiple IFN $\alpha$  subtypes, IFN $\beta$  and others, that are produced in response to host viral and bacterial infection and act in an endocrine or autocrine fashion to stimulate cell antiviral responses (1). Type I IFNs signal through a common receptor, the IFN  $\alpha$  receptor (IFNAR)<sup>2</sup> which is composed of two subunits, IFNAR1 and IFNAR2 (2). The primary signaling events activated by the type I IFNs are mediated by the activation of receptor-associated JAK kinases and the recruitment of STATs to the intracellular domains of

the receptor (reviewed in Ref. 3). The kinases Tyk2 and JAK1 are associated with the intracellular domains of IFNAR1 and IFNAR2, respectively (4, 5). The JAK kinases consist of a C-terminal kinase domain, an adjacent pseudo-kinase domain, and N-terminal JH3–7 regions. The kinase domain of Tyk2 contains three conserved and functionally important residues: Tyr-1054 and Tyr-1055, which must be phosphorylated for activity, and a critical Lys-930, which is important for kinase activity (6). The JH3–7 region of Tyk2 allows association of this kinase with IFNAR1 (7). Upon IFN binding, Tyk2 and JAK1 are trans-phosphorylated (on conserved tyrosines within their kinase domain) and activated, resulting in tyrosine phosphorylation of the receptor subunits (8–10). Receptor phosphotyrosines act as docking sites for STATs, which assemble, detach from the receptor, and translocate to the nucleus as the transcription factor complex ISGF3 (composed of STAT1, STAT2, and IRF9) as well as other STAT homo- and heterodimers. Activated STAT transcriptional complexes regulate a complex network of genes and signaling pathways to exhibit cell-specific antiviral, antiproliferative, antitumor, and immunomodulatory activities (reviewed in Ref. 11).

Regulation of type I IFN signaling is critical in maintaining homeostasis and for the generation of an appropriate immune response to viral and bacterial infections. SOCS1 is a potent negative regulator of both type I and type II IFN signaling (12, 13). SOCS1<sup>-/-</sup> mice are hyperresponsive to type I IFN and have a significantly greater ability than wild-type mice to resolve viral infection independently of IFN $\gamma$  (13). SOCS1<sup>-/-</sup> mice also have a severe inflammatory phenotype because of deregulated type I and II IFN signaling. The SOCS1 protein consists of a central SH2 domain, a C-terminal SOCS box, and an N-terminal region that contains the kinase inhibitory region (KIR). The SOCS box is involved in targeted degradation, whereas the SH2 and KIR domain are involved in protein binding and inhibition of kinase activity, respectively (14, 15). SOCS1 expression is induced by the type I IFNs and then acts in a negative feedback loop to inhibit type I IFN signaling. Crosses of SOCS1<sup>-/-</sup> mice to IFNAR1<sup>-/-</sup> mice rescue the inflammatory phenotype, whereas crosses to IFNAR2<sup>-/-</sup> mice do not suggest that SOCS1 inhibits type I IFN signaling exclusively via IFNAR1 (13). Indeed, coimmunoprecipitation studies in our laboratory demonstrate that SOCS1 is associated with IFNAR1 (13).

\* This work was supported by funding from the National Health and Medical Research Council and the Victorian Government Infrastructure Support Program.

<sup>1</sup> To whom correspondence should be addressed. Tel.: [REDACTED] Fax: [REDACTED]; E-mail: [REDACTED]

<sup>2</sup> The abbreviations used are: IFNAR, IFN  $\alpha$  receptor; SOCS, suppressor of cytokine signaling; MEF, murine embryonic fibroblast; ISRE, interferon stimulated response element; TK, thymidine kinase;  $\beta$ -ME,  $\beta$ -mercaptoethanol; GAS, gamma-interferon activated sequence.

In other cytokine systems, SOCS proteins have been shown to inhibit signaling either by a direct interaction with intracellular receptors via their phosphotyrosines or indirectly via an interaction with associated JAK kinases. For example, SOCS3 binds directly to phosphotyrosine 757 on gp130 to inhibit signaling via this receptor (16). *In vivo* studies have demonstrated that this interaction is critical to maintaining the appropriate balance of STAT signaling that otherwise lead to spontaneous diseases that include gastritis and tumors, inflammatory disease of the lungs and hemopoietic abnormalities (17). Furthermore, SOCS1 has been demonstrated to inhibit IFN $\gamma$  signaling via a direct interaction with phosphotyrosine 441 on IFNGR1 (18). Evidence of indirect inhibition via interaction with JAK kinases has also been shown *in vitro* where the SH2 domain of SOCS1 binds to a phosphotyrosine residue within the Jak2 kinase domain, whereas modeling studies indicated that the KIR stabilizes this association through an interaction with the JAK catalytic pocket (19–21). SOCS1 has also previously been shown to bind and inhibit phosphorylated Tyk2 through an interaction with its SH2 and KIR domains (14). Because the SOCS proteins, including SOCS1, have the capacity to bind either to a receptor phosphotyrosine or to a JAK family member, we have undertaken to investigate the mechanism whereby SOCS1 regulates type I IFN signaling.

Our results demonstrate that rather than a direct interaction with IFNAR1, SOCS1 inhibits IFNAR signaling through an interaction with Tyk2 via its SH2 and KIR domains. Furthermore, we have discovered a novel role of SOCS1 in the inhibition of an activating Lys-63 polyubiquitination of Tyk2.

## EXPERIMENTAL PROCEDURES

**Cell Lines and Cell Culture**—IFNAR1<sup>-/-</sup> murine embryonic fibroblasts (MEFs) and HEK293T cells were cultured in DMEM (Invitrogen) supplemented with 10% FCS, 1% L-glutamine, and 1% penicillin/streptomycin and incubated at 37 °C in 5% CO<sub>2</sub>. Mice used include SOCS1<sup>-/-</sup>IFN $\gamma$ <sup>-/-</sup> and SOCS1<sup>+/+</sup>IFN $\gamma$ <sup>-/-</sup> on a C57BL/6 background as well as wild-type C57BL/6 mice and were housed in specific pathogen free conditions at Monash Medical Centre Animal Facility. Whole thymus from SOCS1<sup>-/-</sup>IFN $\gamma$ <sup>-/-</sup>, SOCS1<sup>+/+</sup>IFN $\gamma$ <sup>-/-</sup>, and wild-type mice were harvested and filtered through 70- $\mu$ m nylon cell strainers in 1% FCS DMEM to create a single cell suspension. Red blood cells were lysed in Tris-buffered NH<sub>4</sub>Cl solution for 5 min at 37 °C. Cells were washed twice, counted (Sysmex cell counter), plated at  $1 \times 10^7$  cells/ml in 1% FCS DMEM, and allowed to rest for 2 h prior to stimulations.

**Constructs and Cloning**—pEF-BOS-SOCS1-FLAG constructs are as described in (22). pEF-BOS-muIFNAR1 and mutant IFNAR1 constructs are as described in (23). hu-Tyk2-HIS and hu-Tyk2KD-GST (encoding the JH1 domain of Tyk2) were provided by Dr. Isabelle Lucet (Monash University Department of Molecular Biology and Biochemistry). Plasmids pEF-ubiquitin, pEF-Ub-K48-HA and pEF-Ub-K63-HA were a kind gift from Neal Silverman (University of Massachusetts). pEF-Ub-K63-HA contains all lysines mutated to arginine except Lys-63 and thus forms only Lys-63 ubiquitin linkages. pEF-Ub-K48-HA contains all lysines mutated to arginine except Lys-48 and thus forms only Lys-48 ubiquitin linkages.

Tyk2-HIS and Tyk2KD-GST were cloned into pEF-BOS. The Tyk2 Y1054F/Y1055F mutations were achieved by site-directed mutagenesis (QuikChange, Stratagene). Mutations were verified by DNA sequencing.

**Luciferase Assays**—A total 0.5  $\mu$ g of DNA consisting of IFNAR1 or IFNAR1 mutants (0.3 ng), SOCS1 or SOCS1 mutants (1 ng), interferon stimulated response element (ISRE) luciferase reporter (30 ng), thymidine kinase (TK)-*Renilla* reporter (100 ng) and pEF-BOS (up to 0.5  $\mu$ g) were transfected into IFNAR1<sup>-/-</sup> MEFs with FuGENE6 transfection reagent (Roche) according to the manufacturer's instructions. Transfected cells were stimulated with 50 IU/ml mu-IFN $\alpha$ 1 (24) (referred to as IFN $\alpha$  in text) for 7 h. Following stimulation, cells were lysed in reporter lysis buffer (Promega). Luciferase activity was determined using a Promega luciferase assay according to the manufacturer's instructions and TK-*Renilla* activity using Stop & Glo (Promega). Luminescence of luciferase and TK-*Renilla* was determined using a FLUOstar Optima microplate reader (BMG Technologies).

**Coimmunoprecipitation and Immunoblotting**—A total 2.5  $\mu$ g of DNA consisting of various combinations of IFNAR1 or IFNAR1 mutants (1  $\mu$ g), SOCS1-FLAG or SOCS1 mutants (500 ng), Tyk2-HIS (2  $\mu$ g), Tyk2KD-GST or Tyk2KD mutants (500 ng), ubiquitin-HA or ubiquitin mutants (200 ng), and pEF-BOS (up to 2.5  $\mu$ g) were transfected into HEK293T cells with FuGENE6 transfection reagent according to the manufacturer's instructions. For assays involving ubiquitin, cells were stimulated with MG132 for 4 h prior to harvest. Transfected HEK293T cells were harvested in lysis buffer (50 mM TRIS-HCL (pH 7.4), 1% Nonidet P-40, 150 mM NaCl, 1 mM Na<sub>3</sub>VO<sub>4</sub>, 10 mM NaF, 1 mM PMSF, and 1 protease inhibitor tablet per 50 ml of buffer) and precleared with protein G-Sepharose beads (GE Healthcare). Immunoprecipitation was performed with either monoclonal IFNAR1 antibody (Abcam) (with protein-g-Sepharose beads), glutathione beads (GE-Healthcare) (for Tyk2KD-GST) or Nickel affinity Sepharose beads (GE Healthcare) (for Tyk2-HIS). Following immunoprecipitation, Sepharose beads were washed three times in lysis buffer and boiled with 5 $\times$   $\beta$ -mercaptoethanol ( $\beta$ -ME) sample buffer to elute the bound protein. Protein lysates were analyzed by SDS-PAGE analyses and Western blotting. Blotting was performed with appropriate antibodies for the detection of IFNAR1 (anti-IFNAR1 (25), rabbit anti-mouse IgG-HRP (Dako)), SOCS1-FLAG (anti-FLAG-HRP (Sigma)), Tyk2KD-GST (anti-GST (Cell Signaling Technology, Inc.)), rabbit anti-goat IgG-HRP (Dako)), Tyk2-HIS (anti-HIS (Cell Signaling Technology, Inc.)), rabbit anti-mouse IgG-HRP, Tyk2 (anti-Tyk2 (Cell Signaling Technology, Inc.)), goat anti-rabbit IgG-HRP (Dako)) or ubiquitin (anti-HA (Rockland), goat anti-rabbit IgG-HRP).

**Endogenous Tyk2 Expression**—Thymocytes were stimulated with 10,000 IU of IFN $\alpha$  for 0, 30, and 60 min. Cells were washed and lysed in 50 mM Tris (pH 7.4), 1% Nonidet P-40, 10% glycerol, 1 mM EDTA, 1 mM Na<sub>3</sub>VO<sub>4</sub>, 1 mM NaF, 1 mM DTT, 10 mM  $\beta$ -glycerophosphate, 1 mM PMSF, and 1 $\times$  protease inhibitor tablet (Roche) per 50 ml of buffer. Lysates were incubated for 2 h at 4 °C, 5 $\times$   $\beta$ -ME sample buffer was added, and the lysates were boiled. Protein lysates were analyzed by SDS-PAGE analyses and Western blotting. Blotting was performed with appro-

appropriate antibodies for the detection of Tyk2 (anti-Tyk2, goat anti-rabbit IgG-HRP) or  $\beta$ -tubulin (anti- $\beta$ -tubulin (Abcam), rabbit anti-mouse IgG-HRP).

**Flow Cytometry**—Flow cytometry was used to measure and compare the surface levels of IFNAR1 on thymocytes from wild-type, SOCS1<sup>+/+</sup>IFN $\gamma$ <sup>-/-</sup>, and SOCS1<sup>-/-</sup>IFN $\gamma$ <sup>-/-</sup> mice. Where specified, cycloheximide (Sigma Aldrich) (to a final concentration of 20  $\mu$ g/ml) was added 15 min prior to the addition of mIFN $\alpha$  (to a final concentration of 1,000 IU/ml). One and 2 h after the addition of mIFN $\alpha$ , cells were washed and resuspended in Fc blocking antibody (eBiosciences, diluted to 1:200 in PBS with 2% FCS (wash buffer)) and incubated on ice for 20 min. Cells were then washed twice and resuspended in 100  $\mu$ l of the primary antibody (either anti-IFNAR1 (25) or isotype control antibody, both diluted to 10  $\mu$ g/ml in wash buffer, or wash buffer alone for the negative controls) and incubated on ice for 20 min. Cells were then washed twice and resuspended in 100  $\mu$ l of Alexa Fluor 488 (BD Biosciences, diluted 1:200 in wash buffer) and incubated on ice for 20 min. Following an additional two washes, cells were resuspended in 400  $\mu$ l of wash buffer containing 1  $\mu$ g/ml propidium iodide. Fluorescent staining on the cells was analyzed on a BD FACS CANTO II (BD Biosciences).

## RESULTS

**The SOCS1 SH2 Domain and N-terminal Region Are Critical for Inhibition of Type I IFN Signaling**—To determine the critical regions of SOCS1 involved in the interaction with IFNAR1, we generated a series of SOCS1 mutants and tested their effect on IFN signaling using an ISRE luciferase assay (Fig. 1). IFNAR1<sup>-/-</sup> MEFs were transiently cotransfected with an ISRE luciferase reporter, a TK-*Renilla* reporter, IFNAR1, and either FLAG-tagged SOCS1 or SOCS1 mutants. We compared the ability of SOCS1 and the SOCS1 mutant proteins to inhibit IFN $\alpha$ -induced luciferase activity. A mutation in a critical region of SOCS1 would abolish its ability to inhibit interferon signaling and thus luciferase activity. In the absence of SOCS1, IFN $\alpha$ -induced luciferase activity was robustly and reproducibly induced approximately 4-fold in this system, and the induced level is normalized to 100%. The addition of SOCS1 significantly reduced luciferase activity to approximately uninduced levels (around 30%). Deletion of the SOCS box plus SH2 domain (S1 $\Delta$ 82–212) was inactive, indicating the importance of these two domains for activity. Furthermore, deletion of the SOCS box alone (S1 $\Delta$ 170–212) retained activity, indicating the importance of the SH2 domain. This was reinforced by the lack of activity of the S1R105K mutant, which contains a mutation within the critical residue of the SOCS1 SH2 domain. The remaining constructs (S1 $\Delta$ 1–76, S1F59A, and S1D64R) demonstrate that deletion or mutation of critical residues in the KIR domain are also important for SOCS activity. Given the importance of the SH2 domain and its characteristic of binding phosphotyrosine residues in the target proteins, we next sought to determine the interacting partner of SOCS1 in the type I IFN signaling complex.

**SOCS1 Inhibits Signaling via the Tyk2 Interacting Domain of IFNAR1**—Previous genetic studies involving IFNAR1<sup>-/-</sup> SOCS1<sup>-/-</sup> and IFNAR2<sup>-/-</sup>SOCS1<sup>-/-</sup> mice indicated that

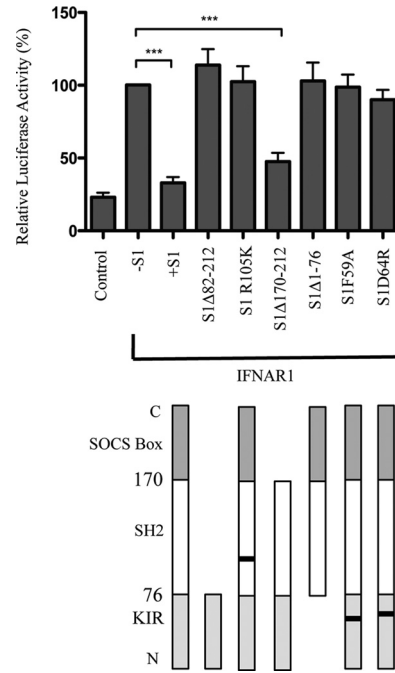


**FIGURE 1. Effect of SOCS1 variants on type I IFN signaling.** The histogram shows the relative expression of an ISRE-luciferase reporter in IFNAR1<sup>-/-</sup> MEFs transiently cotransfected with mu-IFNAR1 and either mu-SOCS1, SOCS1 $\Delta$ 82–212, SOCS1R105K, SOCS1 $\Delta$ 170–212, SOCS1 $\Delta$ 1–76, SOCS1F59A, or SOCS1D64R (represented diagrammatically in the lower panel). C represents the carboxy terminal, and N represents the amino terminal. Cells were stimulated with 50 IU/ml mu-IFN $\alpha$  for 7 h prior to luciferase readings. Luciferase activity is normalized against a TK-*Renilla* reporter to control for transfection efficiency and then expressed as a percentage of activity in the absence of SOCS1 (-S1), which is denoted as 100%. Addition of SOCS1 resulted in almost complete inhibition of IFN activity to control levels. Data are expressed as mean  $\pm$  S.E. of three experiments. \*\*\*,  $p < 0.001$ .

SOCS1 specifically regulates the type I IFN receptor via an interaction with IFNAR1 and not IFNAR2 (13). Because SH2 domains are known to associate with phosphotyrosine residues and because our results above showed that the SH2 domain is critical for SOCS1-mediated inhibition of type I IFN signaling, we investigated whether SOCS1 inhibits activity by binding to a phosphotyrosine within the intracellular domain of IFNAR1, as shown for the type II IFN receptor, IFNGR1 (18). This hypothesis was tested by a luciferase reporter assay (Fig. 2A) and coimmunoprecipitation studies (B). A series of constructs containing single and multiple tyrosine-to-phenylalanine mutations in residues in the intracellular domain of IFNAR1 were utilized to first test the ability of SOCS1 to inhibit signaling in an ISRE luciferase reporter assay (Fig. 2A). IFNAR1<sup>-/-</sup> MEFs were transiently cotransfected with an ISRE luciferase reporter, a TK-*Renilla* reporter, IFNAR1, or IFNAR1 tyrosine mutants (as specified) with and without SOCS1-FLAG. The luciferase activity induced by wild-type IFNAR1 in the absence of SOCS1 (again approximately 4-fold in these experiments) is normalized to 100%. All IFNAR1 tyrosine mutant proteins were able to induce luciferase activity to similar levels as wild-type IFNAR1 (in the absence of SOCS1), indicating that the tyrosine residues within the intracellular region of IFNAR1 are not essential for activation of ISRE signaling in this system. Also unexpectedly, in the presence of SOCS1, the luciferase activity induced by IFN stimulation of all IFNAR1 tyrosine mutant proteins was com-

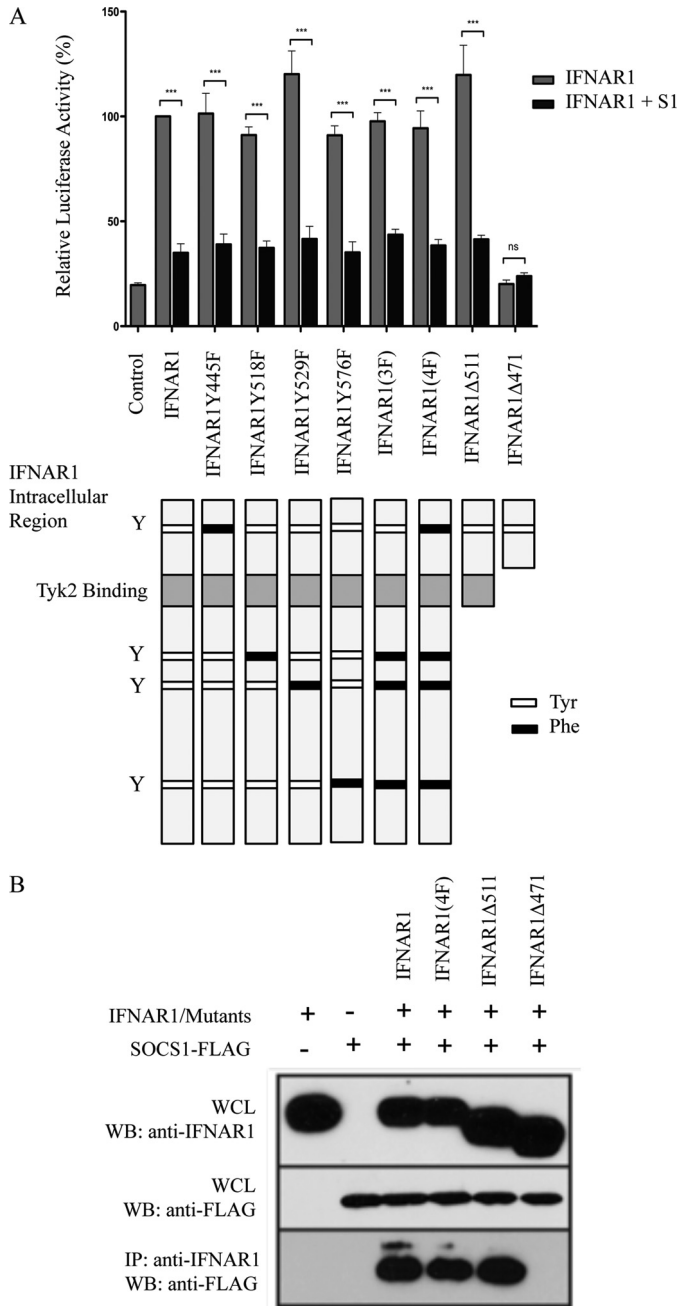


**FIGURE 2. Mapping IFNAR1 domains critical for interaction with SOCS1.** A, the histogram shows relative expression of an ISRE-luciferase reporter in IFNAR1<sup>-/-</sup> MEFs transiently cotransfected with either mu-IFNAR1, IFNAR1Y445F, IFNAR1Y518F, IFNAR1Y529F, IFNAR1Y576F, IFNAR1Y518F/Y529F/Y576F(3F), IFNAR1Y445F/Y518F/Y529F/Y576F(4F) IFNAR1Δ511, or IFNAR1Δ471 (represented diagrammatically in the lower panel) with or without mu-SOCS1. Y denotes tyrosine residues. Cells were stimulated with 50 IU/ml mu-IFN $\alpha$  for 7 h prior to luciferase readings. Luciferase activity is normalized against a TK-*Renilla* reporter to control for transfection efficiency and is expressed relative to wild-type IFNAR1 in the absence of SOCS1, which is denoted as 100%. Data are represented as mean  $\pm$  S.E. of three experiments. \*\*\*,  $p < 0.001$ . B, immunoprecipitation (IP) Western blot analyses (WB) of IFNAR1 mutants and SOCS1. IFNAR1, IFNAR1(4F), IFNAR1Δ 511, or IFNAR1Δ471 were cotransfected with SOCS1-FLAG into HEK293T cells. Following expression, immunoprecipitation of IFNAR1 or the IFNAR1 mutants was performed using anti-IFNAR1 antibody. Immunoprecipitates and whole cell lysates (WCL) were separated by SDS-PAGE and immunoblotted with anti-FLAG to detect SOCS1-FLAG. Blots are representative of triplicate experiments.

comparable with the inhibition seen with wild-type IFNAR1, including the 4F mutant whereby all four intracellular tyrosine residues of IFNAR1 are mutated to phenylalanine (approximately 30–40%). These results demonstrate that SOCS1 does not interact directly with IFNAR1 phosphotyrosine residues in its intracellular domain but rather uses an alternative mechanism for interaction. Thus, we next generated truncated forms of IFNAR1, terminating at amino acid 471 or 511, that flank the Tyk2 binding site of IFNAR1. The truncation mutant, IFNAR1Δ471, was unable to induce ISRE activity in response to IFN stimulation, consistent with the critical nature of Tyk2 for this activity. Thus, inhibition by SOCS1 could not be determined. The truncation mutant IFNAR1Δ511 was still able to signal at levels comparable with wild-type IFNAR1, with signaling still able to be inhibited by the addition of SOCS1. This suggests that SOCS1 inhibits signaling by binding to a region of IFNAR1 proximal to this truncation site.

The putative association of IFNAR1 with SOCS1 was further tested by coimmunoprecipitation studies to confirm the data above (Fig. 2B). We found that SOCS1-FLAG was coimmunoprecipitated with wild-type IFNAR1, IFNAR1(4F), and IFNAR1Δ511 but not IFNAR1Δ471. As SOCS1 was coimmunoprecipitated with IFNAR1(4F), it confirms the above conclusion that SOCS1 does not bind tyrosine residues within the intracellular domain of IFNAR1. Because SOCS1 coimmunoprecipitated with IFNAR1Δ511 but not IFNAR1Δ471, our results suggest that SOCS1 interacts with IFNAR1 either directly or indirectly within this region, likely via Tyk2.

**SOCS1 Binds Conserved Tyrosines of Tyk2 and Regulates Tyk2 Expression**—To demonstrate that SOCS1 interacted with Tyk2 and to characterize this interaction, we performed coimmunoprecipitation experiments with SOCS1-FLAG and either Tyk2KD-GST or Tyk2KD(2F)-GST in which the tyrosines at residues 1054 and 1055 were mutated to phenylalanines. The latter were included because the SOCS1 SH2 domain dependence of the IFN signal suppression would imply SOCS1-bound phosphotyrosines on Tyk2. Importantly, SOCS1-FLAG is indeed coimmunoprecipitated with Tyk2KD-GST. By contrast, Tyk2KD(2F)-GST interaction is almost completely inhibited (Fig. 3A). These results are consistent with these tyrosine residues being important for SOCS1 docking onto Tyk2. Because our results above demonstrated the importance of the KIR domain in inhibition of signaling, we investigated SOCS1 KIR mutants (SOCS1F59A and SOCS1D64R) for their binding to Tyk2 in a coimmunoprecipitation experiment. Where wild-type SOCS1 bound to Tyk2KD, these mutants failed to interact with wild-type Tyk2KD or Tyk2KD(2F), suggesting that the KIR of SOCS1 is essential for Tyk2 binding and thus inhibition of signaling.

Because SOCS1 binding can target proteins for degradation and thus impact the levels of these critical signaling molecules, we investigated the effect of SOCS1 on cellular levels of Tyk2. Firstly, Tyk2-HIS was transfected into HEK293T cells in the presence and absence of SOCS1-FLAG. In the presence of SOCS1, Tyk2 expression was reduced (Fig. 3B). Next we analyzed the effect of SOCS1 on the endogenous levels of Tyk2. Analysis of thymocytes from SOCS1<sup>-/-</sup>IFN $\gamma$ <sup>-/-</sup> and SOCS1<sup>+/+</sup>IFN $\gamma$ <sup>-/-</sup> mice demonstrated that SOCS1 modified

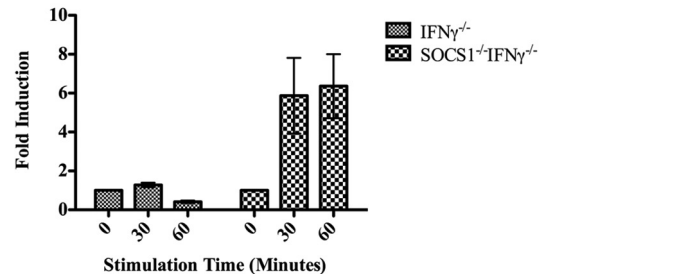
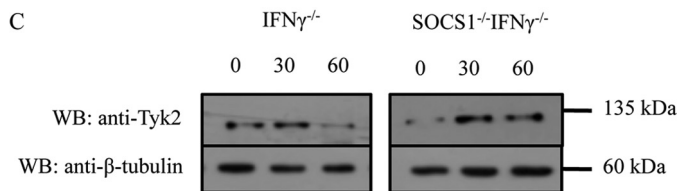
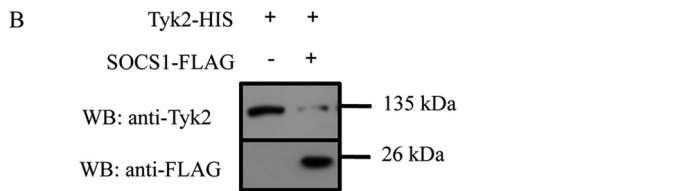
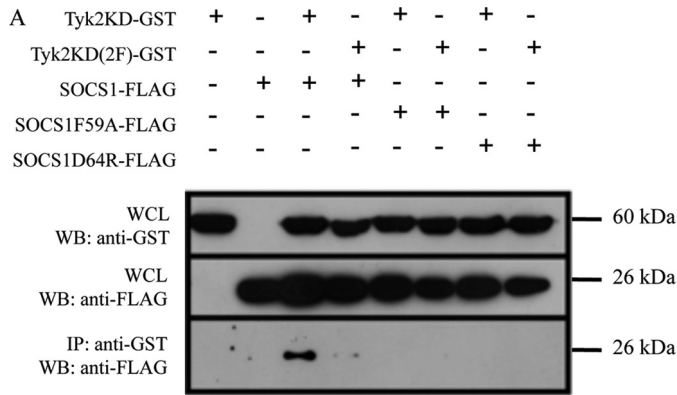


**FIGURE 3. Interaction of SOCS1 with Tyk2 and its degradation.** Western blot analyses (WB) and immunoprecipitation (IP) Western blot analyses of Tyk2 interacting with SOCS1. A, Tyk2KD or Tyk2KD(2F) were cotransfected with SOCS1-FLAG, SOCS1F59A-FLAG, or SOCS1D64R-FLAG into HEK293T cells. Following expression, immunoprecipitation of Tyk2 constructs were performed using glutathione-Sepharose beads. Immunoprecipitates and whole cell lysates (WCL) were separated by SDS-PAGE and immunoblotted with indicated antibodies. B, Tyk2-HIS was expressed  $\pm$  SOCS1-FLAG in HEK293T cells. Cells lysates were separated by SDS-PAGE and probed with the indicated antibodies. C, thymocytes from SOCS1<sup>+/+</sup>IFN $\gamma$ <sup>-/-</sup> and SOCS1<sup>-/-</sup>IFN $\gamma$ <sup>-/-</sup> mice were stimulated with IFN $\alpha$  for 0, 30, or 60 min. Cell lysates were separated by SDS-PAGE and probed with the indicated antibodies. Blots are representative of triplicate experiments. The histogram represents densitometric quantification of the Western blot analyses. Data are represented as mean  $\pm$  S.E. of three independent experiments.

the Tyk2 expression levels (Fig. 3C). In the SOCS1<sup>+/+</sup> thymocytes, Tyk2 levels were significantly reduced by 60 min after stimulation with IFN $\alpha$ . In contrast, in the SOCS1<sup>-/-</sup> thymocytes, not only was the (SOCS1-mediated) reduction in Tyk2 levels lost, but Tyk2 levels increased with IFN stimulation. Together with our overexpression data it is evident SOCS1 has an important regulatory role in type I IFN signaling through its interaction with Tyk2 and the reduction of its levels in the cell.

**SOCS1 Inhibits Lys-63 Polyubiquitination of Tyk2**—One method of SOCS1-induced degradation of binding partners is

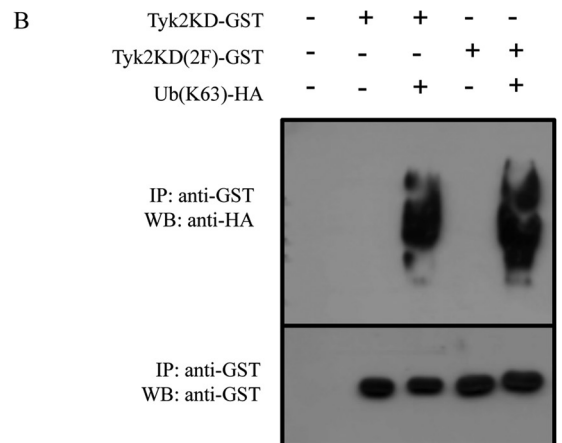
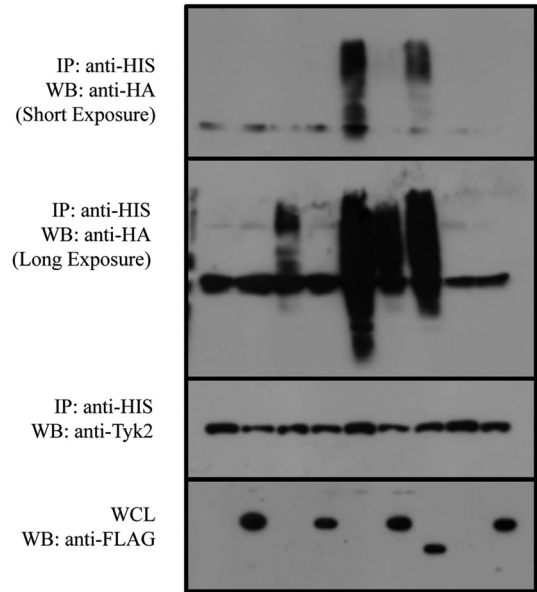


**FIGURE 4. The effect of SOCS1 on Tyk2 ubiquitination.** Western blots analyses (WB) and immunoprecipitation (IP) Western blot analyses of Tyk2 ubiquitination. A, Tyk2-HIS was expressed in HEK293T cells with ubiquitin-HA, ubiquitin(K63)-HA, or ubiquitin(K48)-HA  $\pm$  SOCS1-FLAG or SOCS1 $\Delta$ 170-212 in the presence of MG132. Cell lysates were immunoprecipitated with nickel affinity beads. Immunoprecipitates and whole cell lysates (WCL) were separated by SDS-PAGE and probed with the indicated antibodies. The second panel from the top shows a shorter exposure than the top panel. Tyk2 ubiquitination is shown in the top panel, third lane, and Lys-63 ubiquitination in the top panel and the second panel from the top, fifth lane. Inhibition by SOCS1 constructs is evident in the fourth lane (top panel) and the sixth and seventh lanes (top panel or second panel from the top). B, Tyk2KD-GST or Tyk2KD(2F)-GST were expressed in HEK293T cells  $\pm$  ubiquitin-HA. Cell lysates were immunoprecipitated with glutathione beads. Immunoprecipitates were separated by SDS-PAGE and probed with the indicated antibodies. Blots are representative of triplicate experiments.

via the SOCS box recruitment of E3 ubiquitin ligases (26, 27). Thus, we investigated the ability of Tyk2 to be ubiquitinated in the presence and absence of SOCS1. Firstly, Tyk2-HIS was overexpressed with or without ubiquitin-HA, ubiquitin-

(K63)-HA, or ubiquitin-(K48)-HA and/or SOCS1-FLAG or SOCS1 $\Delta$ 170–212-FLAG (Fig. 4A, *first through fourth lanes*). Following immunoprecipitation of Tyk2 and detection of total ubiquitination using ubiquitin-HA, we found that Tyk2 is indeed spontaneously ubiquitinated in this system and that coexpression with SOCS1 surprisingly inhibited this ubiquitination. We then investigated the type of ubiquitination using mutant ubiquitin constructs, which form Lys-63- or Lys-48-linked ubiquitin chains. These different ubiquitin linkages result in different conformations and activation of alternate pathways (28). Lys-48 linkages are primarily used for targeting the protein for degradation via the proteasome. In contrast, Lys-63 linkages have been implicated in numerous other functions, including activation of NF- $\kappa$ B-inducing kinase (29). As shown in Fig. 4A (*fifth through ninth lanes*), our data demonstrates that Lys-48-linked polyubiquitination of Tyk2 was not detected, whereas Lys-63-linked polyubiquitination was observed. In addition, the use of ubiquitin-(Lys-63)-HA resulted in increased ubiquitination of Tyk2 compared with wild-type ubiquitin-HA and may be explained either by the greater specificity of this reagent or by the mutation of lysine residues involved in negative regulation. Importantly, SOCS1 coexpression suppressed Lys-63-linked ubiquitination of Tyk2. The expression of SOCS1 $\Delta$ 170–212 (lacking the SOCS box) also inhibited Lys-63-linked polyubiquitination of Tyk2, although to a lesser extent.

We next investigated the impact of whether the phosphotyrosine residues of Tyk2 that were involved in binding SOCS1 were involved in ubiquitination. Our results show that the Tyk2 kinase domain was polyubiquitinated (Fig. 4B). Tyk2KD(2F) was also Lys-63 polyubiquitinated. As Tyk2 requires phosphorylation of these mutated tyrosine residues for its function our results suggest that Lys-63 ubiquitination of the Tyk2 kinase domain is not dependent on Tyk2 phosphorylation and activation.

**SOCS1 Expression Reduces IFNAR1 Surface Levels with IFN $\alpha$  Stimulation**—Tyk2 has been reported to be involved in stabilization of IFNAR1 at the plasma membrane (30). Because SOCS1 binds Tyk2 and modulates both its degradation and its activating ubiquitination, it is possible that the interaction of SOCS1 with IFNAR1 via its associated Tyk2 modifies cell surface expression levels. Flow cytometry was used to measure the surface expression of IFNAR1 in primary thymocytes from SOCS1 $^{-/-}$ IFN $\gamma^{-/-}$ , SOCS1 $^{+/+}$ IFN $\gamma^{-/-}$ , and wild-type mice (Fig. 5). After IFN stimulation, IFNAR1 surface levels are reduced in all three genotypes. However, in SOCS1 $^{-/-}$ IFN $\gamma^{-/-}$  thymocytes, IFNAR1 surface expression was reduced to a lesser extent than that in thymocytes from SOCS1 $^{+/+}$ IFN $\gamma^{-/-}$  and wild-type mice one and two h after IFN stimulation (Fig. 5A). Thus, SOCS1 either accelerated the internalization or degradation of the receptor or increased recycling/re-synthesis. Cycloheximide (CHX) was used, where shown, to block *de novo* protein synthesis in thymocytes from all three genotypes, thereby allowing us to measure the real rate of internalization in the absence of *de novo* protein synthesis (Fig. 5B). In the presence of cycloheximide there was again significantly more IFNAR1 present on the surface of SOCS1 $^{-/-}$  cells compared with control cells at the 1-h time point. Our results there-

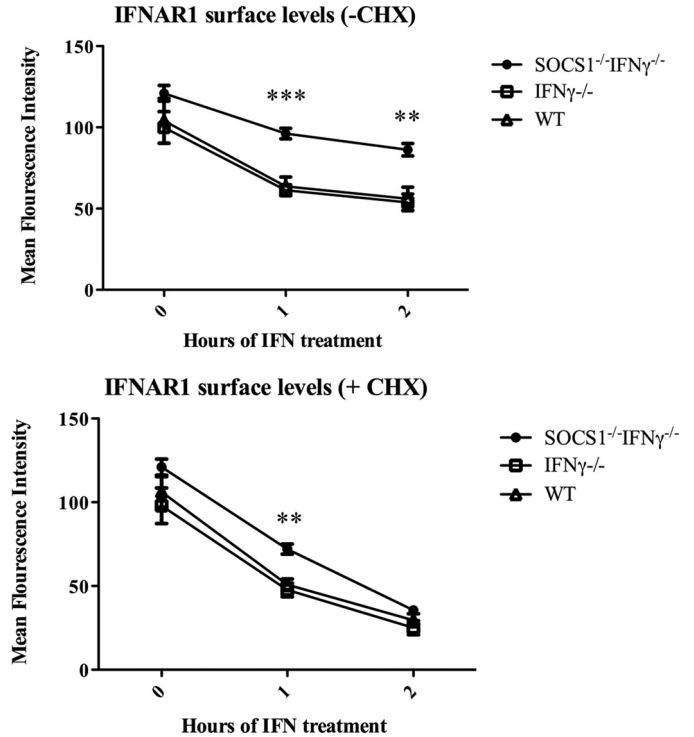


FIGURE 5. **The effect of SOCS1 on surface levels of IFNAR1.** The graphs show IFNAR1 surface levels on thymocytes from SOCS1 $^{+/+}$ IFN $\gamma^{-/-}$ , SOCS1 $^{-/-}$ IFN $\gamma^{-/-}$ , and wild-type mice stimulated with IFN $\alpha$  for 0, 1, or 2 h. Cells were probed with anti-IFNAR1 antibody and analyzed by flow cytometry to detect IFNAR1 surface levels in the presence and absence of cycloheximide (CHX). Data are represented as mean  $\pm$  S.E. of four experiments. \*\*\*,  $p < 0.001$ ; \*\*,  $p < 0.005$ .

fore demonstrate that the surface levels of IFNAR1 during a response are modulated by SOCS1, likely through its interaction with Tyk2.

## DISCUSSION

SOCS1 regulation of type I IFN signaling is critical in maintaining an appropriate immune response and to survival. The data presented here complement our previous *in vivo* data, which demonstrate that SOCS1 regulates signaling through the IFNAR1 component of the receptor. We now add mechanistic data showing how this occurs. Indeed, SOCS1 regulation of type I IFN signaling is mediated via an interaction with the IFNAR1-associated kinase Tyk2 and not by direct interaction with receptor tyrosine kinases. This distinguishes the mechanism of SOCS1 regulation of type I IFN signaling from how it modulates type II IFN $\gamma$  signaling. This study suggests that in the type I IFN system none of the intracellular tyrosine residues within IFNAR1 are important for the negative regulation of type I IFN signaling via SOCS1. Indeed, they are not required for driving ISRE (STAT1/STAT2/IRF9)-dependent signaling nor for STAT3 signaling as shown recently and thus not for gamma-interferon activated sequence (GAS) element activation (23, 31). It would be interesting to investigate the impact of these residues in the receptors and of SOCS1 on other type I IFN signaling pathways. Consequently, these results demonstrate that for the type I IFN signaling complex the interaction of SOCS1 is mediated indirectly via an adaptor molecule. Within the type I IFN system, SOCS1 requires its KIR and SH2

domains for its inhibitory function, indicating a requirement for SOCS1 interaction with the kinase and phosphotyrosine residues. Our coimmunoprecipitation studies demonstrated that the Tyk2 binding region of IFNAR1 was required for the interaction with SOCS1. Previous studies have found a direct interaction between Tyk2 and SOCS1 and a requirement of the Tyk2 SH2 domain and SOCS1 KIR domain (14), but these studies were not performed in the context of the type I IFN receptor signaling complex as described herein. Here we show that SOCS1 binds conserved tyrosine residues within the Tyk2 catalytic region (Tyr-1054 and Tyr-1055), which are phosphorylated in response to IFN $\alpha$  and are required for Tyk2 activation (6). Mutation of these residues from tyrosine to phenylalanine resulted in almost complete inhibition of the interaction between Tyk2 and SOCS1. Our results therefore suggest that the SOCS1 interaction with Tyk2 is limited to the activated, phosphorylated kinase behaving in a negative feedback manner. In addition to a requirement of the SH2 domain, we also found that the KIR domain of SOCS1 is important for binding to Tyk2 and for its inhibitory action of IFN signaling. Modeling studies have proposed that the KIR domain of SOCS1 mimics the activation loop of Jak2 and obstructs its catalytic groove (19). This region is highly conserved across JAK family members, and thus it is probable that the KIR domain of SOCS1 can also interact with and inhibit Tyk2 catalytic function.

The SOCS box has been implicated previously in the recruitment of E3 ubiquitin ligases and the consequent ubiquitination and destruction of target proteins (26, 27). We therefore aimed to investigate the effect of SOCS1 on Tyk2 ubiquitination and, quite interestingly, found that SOCS1 expression inhibited rather than facilitated the ubiquitination of Tyk2. Analysis of the type of ubiquitination of Tyk2 found that it was Lys-63-linked and not Lys-48-linked ubiquitination. In other signaling systems, Lys-63-linked ubiquitination is associated with activation of target proteins. For example, Lys-63 ubiquitination of the NF- $\kappa$ B-inducing kinase by zinc finger protein 91 contributes to stabilization and tyrosine phosphorylation of the kinase (29). Thus, SOCS1 may exert its negative effects on Tyk2 in part via inhibiting an activating or stabilizing Lys-63 ubiquitination. A mutant SOCS1 protein lacking the SOCS box was also able to inhibit the Lys-63 ubiquitination of Tyk2 and, thus, the SOCS box does not appear to be essential for this function. The mechanism of SOCS1 inhibition of ubiquitination may be via blocking the ubiquitination site of Tyk2, which we found was located within the Tyk2 kinase domain, the same region of Tyk2 to which SOCS1 binds. As SOCS1 coexpression with Tyk2 resulted in reduced Tyk2 levels, it is probable that inhibition of this ubiquitination by SOCS1 destabilizes Tyk2. As SOCS1 did not enhance ubiquitination, as might have been expected, the SOCS1 SOCS box appears to not have a critical role in the regulation of Tyk2. Our luciferase assay supports this conclusion because SOCS1 lacking the SOCS box still enabled significant inhibition of type I IFN signaling. The affinity of the SOCS1 SOCS box for E3 ubiquitin ligases is significantly weaker than that of the other SOCS family members (15). Deletion of the SOCS1 SOCS box in mice, however, resulted in reduced function of SOCS1 in response to IFN $\gamma$  (32). This may be attributed to the SOCS box stabilizing SOCS1 through

recruitment of other proteins. In our overexpression assays we saw slight, although not statistically significant, differences between wild-type SOCS1 and the SOCS box mutant. Perhaps *in vivo* a more significant role of the SOCS box in type I IFN signaling would be seen.

The Lys-63 linked ubiquitination of Tyk2 is also a novel finding and warrants further investigation. A candidate residue for ubiquitination is lysine 930, located within the Tyk2 kinase domain. A mutation of this residue destabilizes Tyk2 and reduces kinase activity (6).

In addition to facilitating IFN signal transduction by activation of STAT interactions with the receptor, Tyk2 is required for the stabilization of IFNAR1 at the plasma membrane. We postulated that the SOCS1 interaction with Tyk2 may therefore result in the destabilization of Tyk2 and the dissociation of Tyk2 from IFNAR1, leading to reduced surface levels of the receptor. In human cells lacking Tyk2, IFNAR1 is only weakly expressed at the cell surface and is instead found localized in perinuclear endosomal compartments, constituting early and recycling endosomes (30). An internalization motif of human IFNAR1, located within the Tyk2 binding site, is polyubiquitinated and targeted for degradation (33). Increased expression of Tyk2 results in increased localization of IFNAR1 to the cell surface and reduced degradation of IFNAR1 due in part to reduced endocytosis (30). In our overexpression experiments we found that SOCS1 reduced Tyk2 expression and that in primary thymocytes the absence of SOCS1 resulted in increased endogenous Tyk2 expression 1 h after IFN stimulation. Analysis of IFNAR1 internalization in thymocytes demonstrated a role for SOCS1 in controlling IFNAR1 surface expression following IFN $\alpha$  stimulation. Although not significantly different basally, IFNAR1 internalization/recycling is reduced in cells lacking SOCS1 following 1-h IFN $\alpha$  stimulation and correlates with increased endogenous expression of Tyk2. SOCS1 therefore has a role in effecting the surface expression of IFNAR1 during an interferon response. SOCS1 association of Tyk2 following its phosphorylation and activation may result in destabilization of Tyk2 and exposure of the IFNAR1 internalization motif with subsequent IFNAR1 internalization and reduced IFN signaling.

Together these studies demonstrate the mechanism of SOCS1 inhibition of type I IFN signaling. An understanding of this mechanism may lead to novel approaches to manipulate the type I IFN response and thus contribute to better therapeutic treatments of IFN-mediated diseases or enhancement of the beneficial therapeutic effects of IFN.

## REFERENCES

1. Samuel, C. E. (2001) *Clin. Microbiol. Rev.* **14**, 778–809
2. de Weerd, N. A., Samarajiva, S. A., and Hertzog, P. J. (2007) *J. Biol. Chem.* **282**, 20053–20057
3. Platanius, L. C., and Fish, E. N. (1999) *Exp. Hematol.* **27**, 1583–1592
4. Colamonici, O. R., Uyttendaele, H., Domanski, P., Yan, H., and Krolewski, J. J. (1994) *J. Biol. Chem.* **269**, 3518–3522
5. Domanski, P., Fish, E., Nadeau, O. W., Witte, M., Platanius, L. C., Yan, H., Krolewski, J., Pitha, P., and Colamonici, O. R. (1997) *J. Biol. Chem.* **272**, 26388–26393
6. Gauzzi, M. C., Velazquez, L., McKendry, R., Mogensen, K. E., Fellous, M., and Pellegrini, S. (1996) *J. Biol. Chem.* **271**, 20494–20500
7. Gauzzi, M. C., Barbieri, G., Richter, M. F., Uzé, G., Ling, L., Fellous, M., and

- Pellegrini, S. (1997) *Proc. Natl. Acad. Sci. U.S.A.* **94**, 11839–11844
8. Barbieri, G., Velazquez, L., Scrobogna, M., Fellous, M., and Pellegrini, S. (1994) *Eur. J. Biochem.* **223**, 427–435
  9. Müller, M., Briscoe, J., Laxton, C., Guschin, D., Ziemiecki, A., Silvennoinen, O., Harpur, A. G., Barbieri, G., Witthuhn, B. A., and Schindler, C. (1993) *Nature* **366**, 129–135
  10. Constantinescu, S. N., Croze, E., Wang, C., Murti, A., Basu, L., Mullersman, J. E., and Pfeffer, L. M. (1994) *Proc. Natl. Acad. Sci. U.S.A.* **91**, 9602–9606
  11. Schindler, C., Levy, D. E., and Decker, T. (2007) *J. Biol. Chem.* **282**, 20059–20063
  12. Alexander, W. S., Starr, R., Fenner, J. E., Scott, C. L., Handman, E., Sprigg, N. S., Corbin, J. E., Cornish, A. L., Darwiche, R., Owczarek, C. M., Kay, T. W., Nicola, N. A., Hertzog, P. J., Metcalf, D., and Hilton, D. J. (1999) *Cell* **98**, 597–608
  13. Fenner, J. E., Starr, R., Cornish, A. L., Zhang, J. G., Metcalf, D., Schreiber, R. D., Sheehan, K., Hilton, D. J., Alexander, W. S., and Hertzog, P. J. (2006) *Nat. Immunol.* **7**, 33–39
  14. Narazaki, M., Fujimoto, M., Matsumoto, T., Morita, Y., Saito, H., Kajita, T., Yoshizaki, K., Naka, T., and Kishimoto, T. (1998) *Proc. Natl. Acad. Sci. U.S.A.* **95**, 13130–13134
  15. Babon, J. J., Sabo, J. K., Zhang, J. G., Nicola, N. A., and Norton, R. S. (2009) *J. Mol. Biol.* **387**, 162–174
  16. Nicholson, S. E., De Souza, D., Fabri, L. J., Corbin, J., Willson, T. A., Zhang, J. G., Silva, A., Asimakis, M., Farley, A., Nash, A. D., Metcalf, D., Hilton, D. J., Nicola, N. A., and Baca, M. (2000) *Proc. Natl. Acad. Sci. U.S.A.* **97**, 6493–6498
  17. Jenkins, B. J., Grail, D., Nheu, T., Najdovska, M., Wang, B., Waring, P., Inglese, M., McLoughlin, R. M., Jones, S. A., Topley, N., Baumann, H., Judd, L. M., Giraud, A. S., Boussioutas, A., Zhu, H. J., and Ernst, M. (2005) *Nat. Med.* **11**, 845–852
  18. Qing, Y., Costa-Pereira, A. P., Watling, D., and Stark, G. R. (2005) *J. Biol. Chem.* **280**, 1849–1853
  19. Giordanetto, F., and Kroemer, R. T. (2003) *Protein Eng.* **16**, 115–124
  20. Endo, T. A., Masuhara, M., Yokouchi, M., Suzuki, R., Sakamoto, H., Mitsui, K., Matsumoto, A., Tanimura, S., Ohtsubo, M., Misawa, H., Miyazaki, T., Leonor, N., Taniguchi, T., Fujita, T., Kanakura, Y., Komiyama, S., and Yoshimura, A. (1997) *Nature* **387**, 921–924
  21. Yasukawa, H., Misawa, H., Sakamoto, H., Masuhara, M., Sasaki, A., Wakioka, T., Ohtsuka, S., Imaizumi, T., Matsuda, T., Ihle, J. N., and Yoshimura, A. (1999) *EMBO J.* **18**, 1309–1320
  22. Nicholson, S. E., Willson, T. A., Farley, A., Starr, R., Zhang, J. G., Baca, M., Alexander, W. S., Metcalf, D., Hilton, D. J., and Nicola, N. A. (1999) *EMBO J.* **18**, 375–385
  23. Zhao, W., Lee, C., Piganis, R., Plumlee, C., de Weerd, N., Hertzog, P. J., and Schindler, C. (2008) *J. Immunol.* **180**, 5483–5489
  24. Trajanovska, S., Owczarek, C. M., Stanton, P. G., and Hertzog, P. J. (2003) *J. Interferon Cytokine Res.* **23**, 351–358
  25. Sheehan, K. C., Lai, K. S., Dunn, G. P., Bruce, A. T., Diamond, M. S., Heutel, J. D., Dungo-Arthur, C., Carrero, J. A., White, J. M., Hertzog, P. J., and Schreiber, R. D. (2006) *J. Interferon Cytokine Res.* **26**, 804–819
  26. Kamura, T., Sato, S., Haque, D., Liu, L., Kaelin, W. G., Jr., Conaway, R. C., and Conaway, J. W. (1998) *Genes Dev.* **12**, 3872–3881
  27. Zhang, J. G., Farley, A., Nicholson, S. E., Willson, T. A., Zugaro, L. M., Simpson, R. J., Moritz, R. L., Cary, D., Richardson, R., Hausmann, G., Kile, B. J., Kent, S. B., Alexander, W. S., Metcalf, D., Hilton, D. J., Nicola, N. A., and Baca, M. (1999) *Proc. Natl. Acad. Sci. U.S.A.* **96**, 2071–2076
  28. Tenno, T., Fujiwara, K., Tochio, H., Iwai, K., Morita, E. H., Hayashi, H., Murata, S., Hiroaki, H., Sato, M., Tanaka, K., and Shirakawa, M. (2004) *Genes Cells* **9**, 865–875
  29. Jin, X., Jin, H. R., Jung, H. S., Lee, S. J., Lee, J. H., and Lee, J. J. (2010) *J. Biol. Chem.* **285**, 30539–30547
  30. Ragimbeau, J., Dondi, E., Alcover, A., Eid, P., Uzé, G., and Pellegrini, S. (2003) *EMBO J.* **22**, 537–547
  31. Russell-Harde, D., Wagner, T. C., Rani, M. R., Vogel, D., Colamonici, O., Ransohoff, R. M., Majchrzak, B., Fish, E., Perez, H. D., and Croze, E. (2000) *J. Biol. Chem.* **275**, 23981–23985
  32. Zhang, J. G., Metcalf, D., Rakar, S., Asimakis, M., Greenhalgh, C. J., Willson, T. A., Starr, R., Nicholson, S. E., Carter, W., Alexander, W. S., Hilton, D. J., and Nicola, N. A. (2001) *Proc. Natl. Acad. Sci. U.S.A.* **98**, 13261–13265
  33. Kumar, K. G., Barriere, H., Carbone, C. J., Liu, J., Swaminathan, G., Xu, P., Li, Y., Baker, D. P., Peng, J., Lukacs, G. L., and Fuchs, S. Y. (2007) *J. Cell Biol.* **179**, 935–950

**CHAPTER 4**

**CHARACTERISATION OF IFN $\alpha$  INDUCTION OF STAT  
PHOSPHORYLATION IN IMMUNE CELL POPULATIONS AND ITS  
REGULATION BY SOCS1**

The primary signaling pathway activated by the type I IFNs is the JAK/STAT signaling pathway (Stark, Kerr et al. 1998). Following IFN binding to IFNAR, JAK1 and TYK2 undergo cross-activation events resulting in the phosphorylation of intracellular receptor tyrosine residues of IFNAR1 and IFNAR2 (Constantinescu, Croze et al. 1994; Stark, Kerr et al. 1998). STATs are then recruited to specific phosphorylated receptor tyrosine residues via their SH2 domain. The recruitment of STATs to the activated receptor allows receptor associated kinases to phosphorylate STAT proteins. Phosphorylation of STATs leads to the formation of STAT homo and/or hetero-dimers which form transcriptionally active complexes (Levy and Darnell 2002). There are seven STAT family members (STAT1, 2, 3, 4, 5a, 5b and 6) in human and mice, all of which can be activated in response to type I IFN (van Boxel-Dezaire, Rani et al. 2006). Many combinations of STAT dimers can form in response to type I IFN signaling. The transcription factor ISGF3 is a common IFN induced STAT complex and is composed of STAT1, STAT2 and IRF9. Activated STAT complexes translocate to the nucleus and regulate gene transcription (Stark and Darnell 2012). The profile of STAT activation, in response to IFN $\alpha$ , therefore dictates the transcriptional response of the cell. The response of the cell to IFN can be quite different depending on the type of cell, or state of the cell, that IFN is acting on. For example IFN $\alpha$  can have pro- or anti-proliferative effects on T-cells depending on the activation state of the T-cell at the time of stimulation (Dondi, Roue et al. 2004). It is therefore important to understand the level and type of STATs activated in response to IFN $\alpha$  in different cell types to provide insight as to how the cell might respond.

It is also important to understand how SOCS1 effects IFN-induced STAT activation. As discussed in Chapter 1, SOCS1 is a potent negative regulator of type I IFN signaling and over-expression of SOCS1 results in reduced antiviral and anti-proliferative effects of IFN $\alpha$  (Fenner, Starr et al. 2006). Chapter 3 demonstrates SOCS1 binds to the receptor associated kinase TYK2 and regulates IFN signaling. Previous studies have also shown SOCS1 reduces IFN induced TYK2 and STAT1 phosphorylation as well as

downstream gene induction (Fenner, Starr et al. 2006). I therefore aimed to further investigate the effect of SOCS1 on STAT activation in different immune cell types as SOCS1 alteration of STAT activation may have important consequences for downstream gene regulation and the response of the cell to IFN.

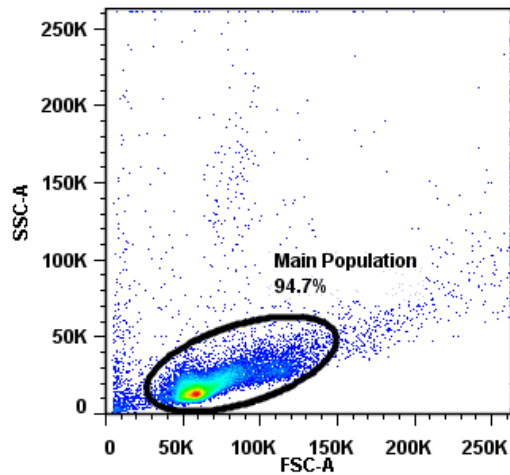
I employed phosphoflow cytometry studies to determine STAT phosphorylation in response to IFN $\alpha$  in different immune cell types. This involved staining of cells with cell surface markers (to identify cell types) and anti-phospho-STAT antibodies (to identify STAT phosphorylation). I looked at immune cells of the thymus, spleen and blood from wt mice to determine STAT1, STAT3 and STAT5 phosphorylation in response to IFN $\alpha$  stimulation. Due to the availability of reagents I was unable to analyse STAT2 phosphorylation or separate differences between STAT5A and STAT5B phosphorylation. To study the effects of SOCS1, I utilised *Socs1<sup>-/-</sup>Ifn $\gamma$ <sup>-/-</sup>* and *Socs1<sup>+/+</sup>Ifn $\gamma$ <sup>-/-</sup>* mice to compare the differences in IFN $\alpha$  induced STAT1, STAT3 and STAT5 phosphorylation in the presence or absence of SOCS1. *Socs1<sup>-/-</sup>Ifn $\gamma$ <sup>-/-</sup>* and *Socs1<sup>+/+</sup>Ifn $\gamma$ <sup>-/-</sup>* mice were used to analyse the effects of SOCS1 on IFN $\alpha$  signaling as *Socs1<sup>-/-</sup>* mice are not viable (die of severe inflammation within 3 weeks of birth). These genotypes have previously been used to study SOCS1 regulation of type I IFN signaling both *in vitro* and *in vivo* (Fenner, Starr et al. 2006).

As described in Chapter 2.2, immune cells were isolated from the thymus, spleen or blood of mice and stimulated with IFN $\alpha$  for the indicated time points *in vitro*. Following stimulations, cells were fixed, permeabilised and stained with cell surface marker antibodies coupled with anti-phospho-STAT (pSTAT) antibodies. Cell surface marker antibodies used on thymic cells include anti-CD4-FITC and anti-CD8-PE (BD Biosciences). Surface marker antibodies on spleen and blood include anti-CD4-FITC, anti-CD8-PE, anti-B220-FITC and anti-MAC1-PE (BD Biosciences). The pSTAT antibodies used include pSTAT1(pY701)-alexa647, pSTAT3(pY705)-alexa647 or pSTAT5(pY694)-alexa647 (BD Biosciences). The software program FlowJo was used for the analysis of phosphoflow cytometry data. Cells were initially gated on forward scatter (FSC) and side scatter (SSC) to select cell populations of the expected size and granularity and exclude smaller, presumably dead, cells or debris. A dead cell stain could not be performed because the cells were permeabilised for the uptake of antibody. Channel compensations were performed with single colour controls to adjust for any cross-over between channel fluorescence. Cells were then gated on surface marker expression. Thymic cells were gated on CD4 or CD8 expression to isolate

CD4+CD8+, CD4+CD8-, CD4-CD8+ and CD4-CD8- T-cell populations (Figure 4.1). PBMCs were gated on CD4 or CD8 expression to isolate CD4+CD8- and CD4-CD8+ T-cell populations (Figure 4.2b). PBMCs were also gated on B220 and MAC1 surface expression to identify B220+ cells (B-cells and pDCs), MAC1+ cells (macrophages/DCs/NK cells) and MAC1++ cells (monocytes) (Figure 4.2c). Splenic cells were gated on CD4, CD8 or MAC1 expression (Figure 4.3). This enabled the isolation of CD4+CD8- and CD4-CD8+ T-cells populations as well as CD4-CD8- cells (mostly B-cells), MAC1+ cells (macrophages/DCs/NK cells) and MAC1++ cells (monocytes/neutrophils).

Following cell type gating based on surface marker expression, a histogram of alexa647 mean fluorescence intensity (MFI) was plotted against cell count for each stimulation time point. As demonstrated in Figure 4.4, the data was analysed via two methods. A) MFI of the cell populations and B) the percentage of positive cells (cells with increased pSTAT levels compared to basal pSTAT levels). For MFI based analysis, the MFI of alexa647 fluorescence was calculated from the histogram (Figure 4.4a). MFI data was plotted as raw MFI or change in MFI relative to basal levels (as indicated), against stimulation time. The data generated from this method of analysis indicates the total pSTAT levels within the given cell population. For the calculation of the percentage of positive cells (percentage of cells with increased pSTAT expression above unstimulated controls), alexa-647 fluorescence for each cell population was plotted as a histogram and a cell gate was placed on the unstimulated cell populations so that between 0 and 2 % of unstimulated cells were in the positive gate (Figure 4.4b). For each stimulation time point, the percentage of positive cells was calculated as the percentage of cells in the positive gate relative to the total cell count and then plotted against stimulation time. The data generated by this method of analysis gives an indication of the percentage of a particular cell population with up-regulated pSTAT levels. The calculation of the percentage of positive cells has been performed previously, by van Boxel-Dezaire et al, for the analysis of IFN induction of STAT phosphorylation in populations of immune cells from human subjects (van Boxel-Dezaire, Zula et al. 2010). I therefore employed this method of analysis to enable comparison between IFN-induction of STAT phosphorylation in their human data and my data on mouse immune cell populations.

### A. Thymus



### B. CD4 and CD8 Populations

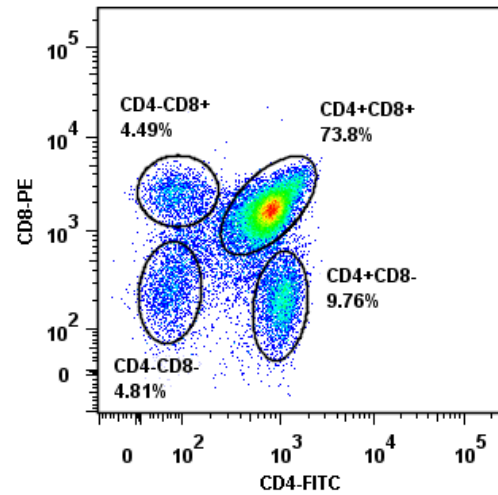
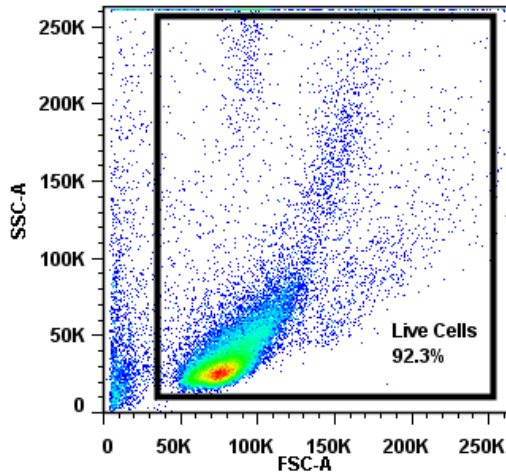
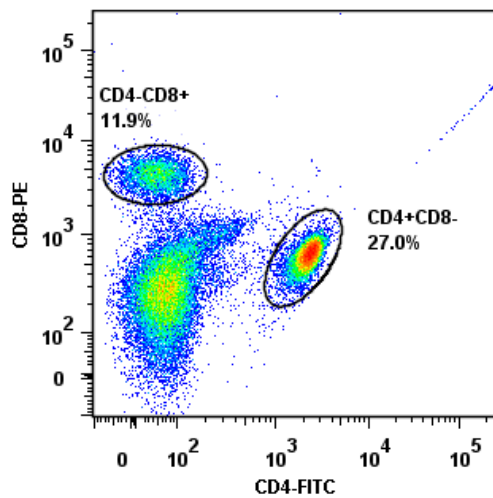


**Figure 4.1: Gating of thymic CD4/CD8 T-cell populations.** **A.** The main population of cells within the thymus were selected based on forward scatter (FSC) and side scatter (SSC) to select cells of the expected size and granularity. **B.** The main population of cells were then separated based on CD4-FITC and CD8-PE fluorescence.

### A. Peripheral Blood Mononuclear Cells (PBMCs)



### B. CD4 and CD8 Populations



### C. B220 and MAC1 Populations

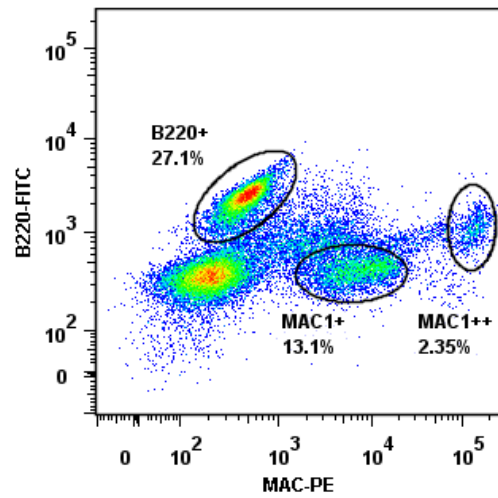
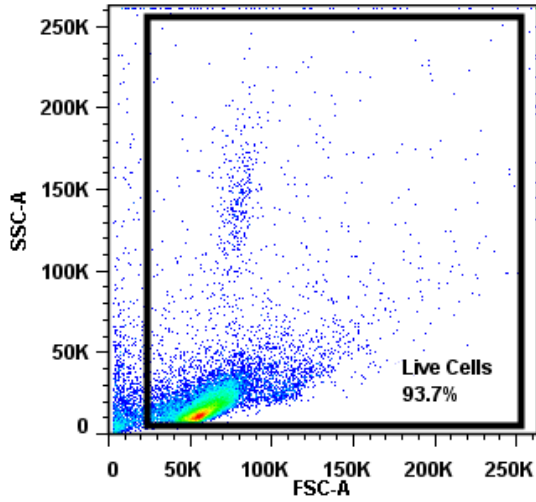


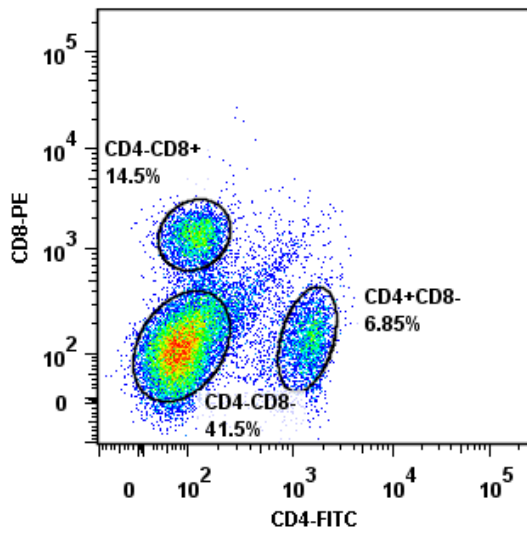
**Figure 4.2: Gating of PBMC CD4, CD8, B220 and MAC1 cell populations.**

**A.** Live cells were selected based on forward scatter (FSC) and side scatter (SSC) to select cells of the expected size and granularity. These cells were then separated based on **B.** CD4-FITC and CD8-PE fluorescence or **C.** B220-FITC or MAC1-PE fluorescence.

### A. Splenic Cells



### B. CD4 and CD8 Populations



### C. MAC1 Populations

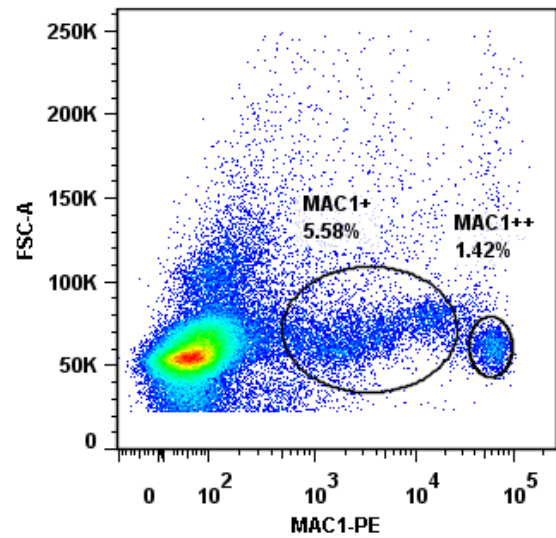


**Figure 4.3: Gating of splenic CD4, CD8 and MAC1 cell populations. A.** Live cells were selected based on forward scatter (FSC) and side scatter (SSC). These cells were then separated based on **B.** CD4-FITC and CD8-PE fluorescence or **C.** MAC1-PE fluorescence.

**A. Mean Fluorescence Intensity (MFI)**

**B. Percentage of Increased Cells**

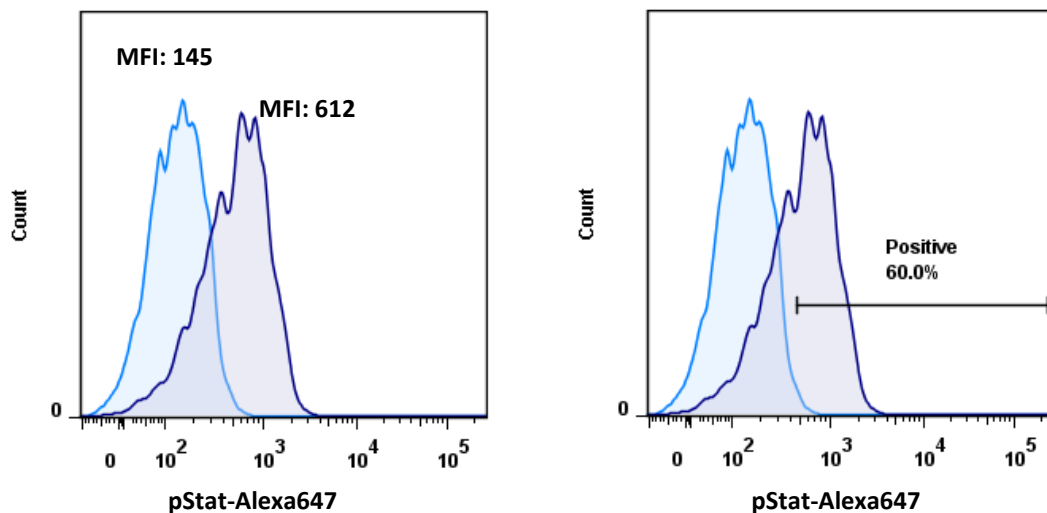


**Figure 4.4: Methods of Phosphoflow Cytometry Analysis.** A histogram of alexa-647 (representing pStat levels) was plotted for unstimulated (light blue) and stimulated (purple) cell populations. Data was analysed via two methods. **A.** The MFI (mean fluorescence intensity) of alexa647 of the unstimulated and stimulated cell populations were calculated. **B.** The percentage of positive cells were calculated by placing a gate on the unstimulated cell populations so that between 0 and 2 % of unstimulated cells were in the positive gate. For each stimulation time point, the percentage of positive cells was calculated as the percentage of cells in the positive gate.

#### **4.1 Basal MFI of pSTAT1, pSTAT3 and pSTAT5 in thymic CD4/CD8 T-cell subsets**

The different CD4/CD8 T-cell populations in the thymus had different basal levels of pSTAT1. Basal pSTAT1 levels were greatest in CD4-CD8+ T-cells (MFI 300), followed by CD4+CD8- (MFI 194), CD4-CD8- (MFI 140) and CD4+CD8+ (MFI 58) T-cells (Figure 4.5a). Basal pSTAT1 levels were not significantly different ( $p > 0.05$ ) between CD4+CD8- and CD4-CD8+ T-cells. Basal pSTAT1 levels of CD4+CD8- and CD4-CD8+ T-cells were both significantly higher ( $p < 0.05$ ) than that of CD4+CD8+ T-cells.

The different CD4/CD8 T-cell populations in the thymus also had different basal levels of pSTAT3. Basal pSTAT3 levels were greatest in CD4-CD8- (MFI 158) T-cells, followed by CD4-CD8+ T-cells (MFI 131), CD4+CD8- (MFI 98) and CD4+CD8+ (MFI 51) T-cells (Figure 4.5b). Basal pSTAT3 levels were significantly different ( $p < 0.05$ ) between CD4+CD8- and CD4-CD8+ T-cells. Basal pSTAT3 levels of CD4+CD8- and CD4-CD8+ were both significantly higher than that of CD4+CD8+ T-cells.

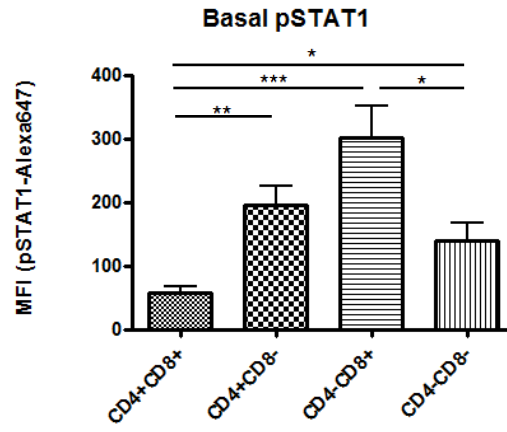
The different CD4/CD8 T-cell populations in the thymus also had different basal levels of pSTAT5. Basal pSTAT5 levels were greatest in CD4-CD8+ T-cells (MFI 1745), followed by CD4+CD8- (MFI 1304), CD4-CD8- (MFI 1299) and CD4+CD8+ (MFI 695) T-cells (Figure 4.5c). Basal pSTAT5 levels were not significantly different between CD4+CD8- and CD4-CD8+ T-cells. Basal pSTAT5 levels of CD4+CD8-, CD4-CD8+ and CD4-CD8- T-cell were significantly higher than that of CD4+CD8+ T-cells.

CD4+CD8+ T-cells displayed the lowest level of basal pSTAT1, pSTAT3 and pSTAT5. Although not significant, CD4-CD8+ T-cells displayed a trend of higher pSTAT1, pSTAT3 and pSTAT5 basal levels than CD4+CD8- T-cells.

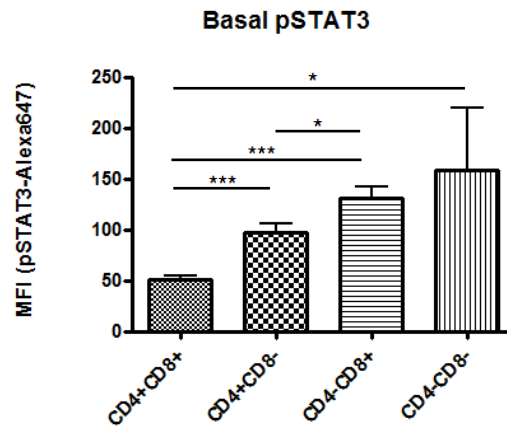
Comparison of the basal MFI's of the different STATs, in the same cell types, demonstrates large differences between pSTAT1 and pSTAT3 compared to pSTAT5 (Figure 4.5). Basal pSTAT5 MFI's are at least 5 times higher than basal pSTAT1 MFI's. This however may be due to technical differences such as differences in antibody affinities and background staining rather than a reflection of total pSTAT levels and thus cannot be taken as conclusive.

**Figure 4.5: Basal Stat1, Stat3 and Stat5 phosphorylation levels in thymic CD4/CD8 T-cell subsets.** Thymus was harvested from wt C57BL/6 mice and a single cell suspension created. Cells were incubated with surface marker antibodies (anti-CD4-FITC and anti-CD8-PE) in combination with **A.** pStat1-Alexa647, **B.** pStat3-Alexa647 or **C.** pStat5-Alexa647. Cell subsets were separated based on surface marker expression of CD4-FITC and CD8-PE. The alexa647 MFI was calculated for each cell subset. Data is presented as mean +/- SEM of N = 3-5 separate experiments. \* =  $p \leq 0.05$ , \*\* =  $p \leq 0.01$ , \*\*\* =  $p \leq 0.005$ .

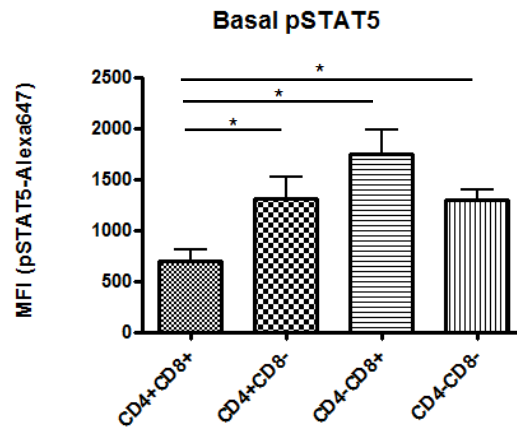
A.



B.



C.



## 4.2 Dose Response to IFN $\alpha$ – Thymic CD4/CD8 T-cell Subsets

A dose response of STAT phosphorylation was analysed in CD4/CD8 T-cell subsets of the thymus (Figure 4.6). Cells were stimulated with 100, 1000, 3000 or 10,000 IU/ml of IFN $\alpha$  for 15 minutes. The data is represented as change in MFI of stimulated cells compared to unstimulated cells as well as the percentage of positive cells (percentage of cells with increased pSTAT expression compared to unstimulated controls).

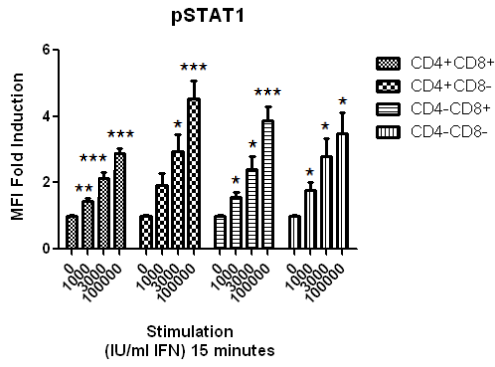
IFN $\alpha$  induction of STAT1, STAT3 and STAT5 phosphorylation occurred in a dose dependent manner. The increase in pSTAT1 MFI (Figure 4.6 A1) was greater than that of pSTAT3 (Figure 4.6 B1) in response to all doses of IFN $\alpha$  and the increase in pSTAT3 MFI was greater than that of pSTAT5 (Figure 4.6 C1). The stimulation of cells with 100 IU/ml of IFN $\alpha$  resulted in no change in STAT1, STAT3 or STAT5 phosphorylation levels compared to unstimulated controls (not shown). At 1000 IU/ml, a significant increase in STAT1 phosphorylation (1.5-2-fold,  $p < 0.05$ ) was observed in all T-cell populations except CD4+CD8- T-cells. At 3000 IU/ml and 10,000 IU/ml of IFN $\alpha$ , STAT1 phosphorylation levels were significantly increased in all CD8/CD4 T-cell populations (2-3-fold and 3-5-fold, respectively). In contrast to STAT1, IFN $\alpha$  induction of STAT3 and STAT5 phosphorylation was very low and only significant with the higher 10,000 IU/ml dose of IFN $\alpha$  (1.5-2-fold).

In terms of the percentage of positive cells, less than 20% of cells showed up-regulation of pSTAT1 with 1000 IU/ml of IFN $\alpha$  (Figure 4.6 A2). With 3000 IU/ml of IFN $\alpha$ , a significant percentage of cells (10-50%,  $p < 0.05$ ) showed up-regulation of pSTAT1 and with 10,000 IU/ml of IFN $\alpha$  this was increased (35-70%,  $p < 0.05$ ). In contrast to pSTAT1, the percentage of cells up-regulating pSTAT3 and pSTAT5 were low. 5-25% of cells showed up-regulation of pSTAT3 ( $p < 0.05$ ) (Figure 4.6 B2) and 10-35% of cells showed up-regulation of pSTAT5 ( $p < 0.05$ ) (Figure 4.6 C2) with 10,000 IU/ml IFN $\alpha$ .

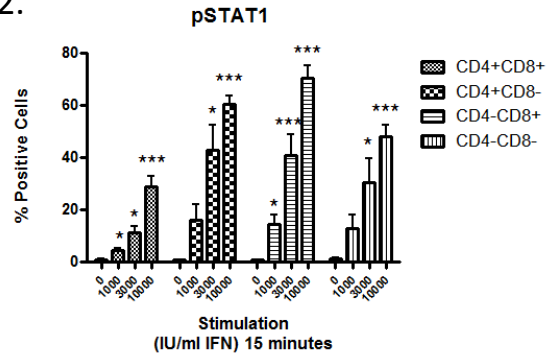
STAT1, STAT3 and STAT5 were phosphorylated in the thymus in response to IFN $\alpha$  stimulation in a dose dependent manner. These data indicate STAT1 phosphorylation occurs at lower doses of IFN $\alpha$  than that required to induce STAT3 and STAT5 phosphorylation. STAT1 phosphorylation levels were also induced to a greater degree over unstimulated controls than that of STAT3 and STAT5 phosphorylation when stimulated with the same amount of IFN $\alpha$ . In addition, more cells were also able to induce STAT1 phosphorylation than STAT3 and STAT5 phosphorylation when stimulated with the same amount of IFN $\alpha$ . STAT1 therefore appears more sensitive to

**Figure 4.6: Dose response of IFN $\alpha$  on Stat1, Stat3 and Stat5 phosphorylation in thymic CD4/CD8 T-cell subsets.** Thymus was harvested from wt C57BL/6 mice and a single cell suspension created. Cells were left untreated or stimulated with 1000, 3000 or 10,000 IU/ml of IFN $\alpha$  for 15 minutes. Following cell fixation and permeabilisation, cells were incubated with surface marker antibodies (anti-CD4-FITC and anti-CD8-PE) in combination with **A.** pStat1-Alexa647, **B.** pStat3-Alexa647 or **C.** pStat5-Alexa647. Cell subsets were separated based on surface marker expression of CD4-FITC and CD8-PE. The alexa647 MFI was calculated for each cell subset and stimulation dose. Data is represented as **Panel 1.** fold induction of MFI (MFI stimulation/MFI basal) and **Panel 2.** percentage of positive cells. Data is presented as mean +/- SEM of N = 3-5 separate experiments. \* =  $p \leq 0.05$ , \*\* =  $p \leq 0.01$ , \*\*\* =  $p \leq 0.005$ .

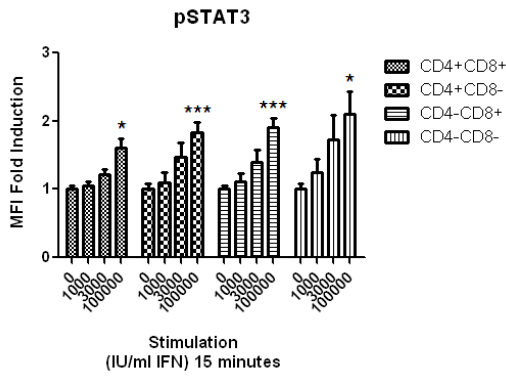
A1.



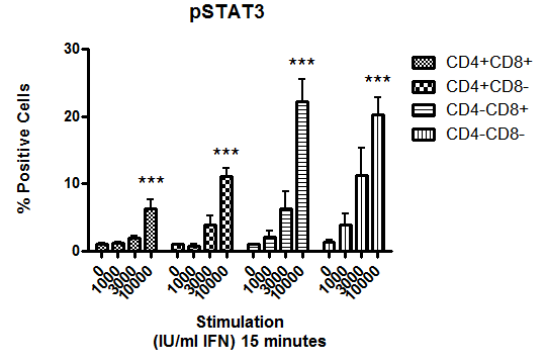
A2.



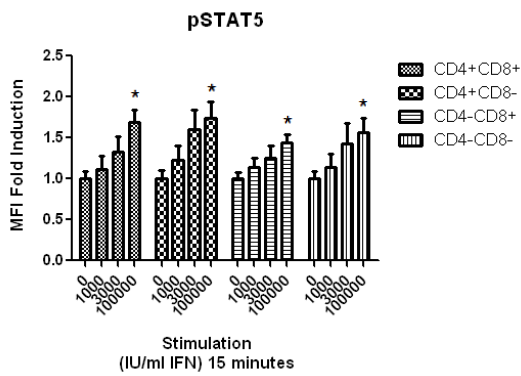
B1.



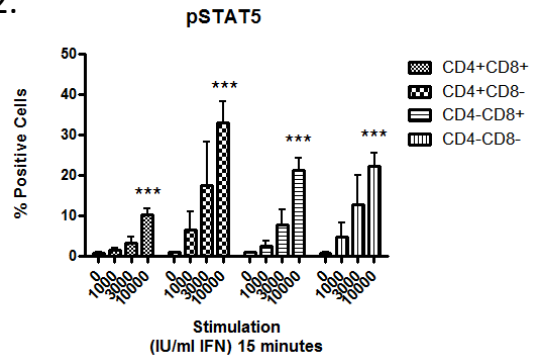
B2.



C1.



C2.



IFN $\alpha$  induced phosphorylation than STAT3 and STAT5. This is explored in more detail below, with a time-course of IFN $\alpha$  treatment. As stimulation with 10,000 IU/ml of IFN $\alpha$  resulted in significant induction of STAT1, STAT3 and STAT5 phosphorylation in all CD4/CD8 T-cell subsets analysed, this concentration was chosen for subsequent experiments.

### **4.3 Time Course – Thymic CD4/CD8 T-cell subsets**

A time-course of STAT1, STAT3 and STAT5 phosphorylation in response to 10,000 IU/ml IFN $\alpha$  was analysed in immune cell subsets of the thymus and blood.

#### **4.3.1 Time course of STAT1 phosphorylation in the thymus**

The highest levels of STAT1 phosphorylation were obtained following 15 minutes IFN $\alpha$  stimulations and were greatest in CD4-CD8+ T-cells (MFI 1384), followed by CD4+CD8- (MFI 847), CD4-CD8- (MFI 540) and CD4+CD8+ T-cells (MFI 223) (Figure 4.7 A). This follows the same pattern as the basal levels. At 15 minutes post-stimulation, STAT1 phosphorylation was increased 4.8-fold in CD4-CD8+ T-cells, 4.6-fold in CD4+CD8- T-cells, 3.9-fold in CD4-CD8- T-cells and 3.8-fold in CD4+CD8+ T-cells. At 30 minutes post-stimulation, pSTAT1 levels were slightly decreased than at 15 minutes. At subsequent time points, pSTAT1 levels were reduced. The largest drop occurred between 30 and 60 minutes post-stimulation. By 120 minutes post-stimulation, pSTAT1 levels were returned to near basal levels.

The percentages of cells with increased STAT1 phosphorylation, above basal levels, were analysed (Figure 4.7 B). CD4-CD8+ T-cells were the most significant responders (70%) followed by CD4+CD8- (59%), CD4-CD8- (52%) and CD4+CD8+ T-cells (37%). A similar percentage of cells were increased for pSTAT1 at 30 minutes post-stimulation. By 60 minutes stimulation, there is an approximately 30% reduction in the amount of cells expressing pSTAT1 and by 120 minutes this is reduced further.

#### **4.3.2 Time course of STAT3 phosphorylation in the thymus**

The highest levels of pSTAT3 were obtained following 15-30 minutes IFN $\alpha$  stimulations and were greatest in CD4-CD8+ T-cells (MFI 271), followed by CD4-CD8- (MFI 243), CD4+CD8- (MFI 183) and CD4+CD8+ T-cells (MFI 97) (Figure 4.8 A). This follows the

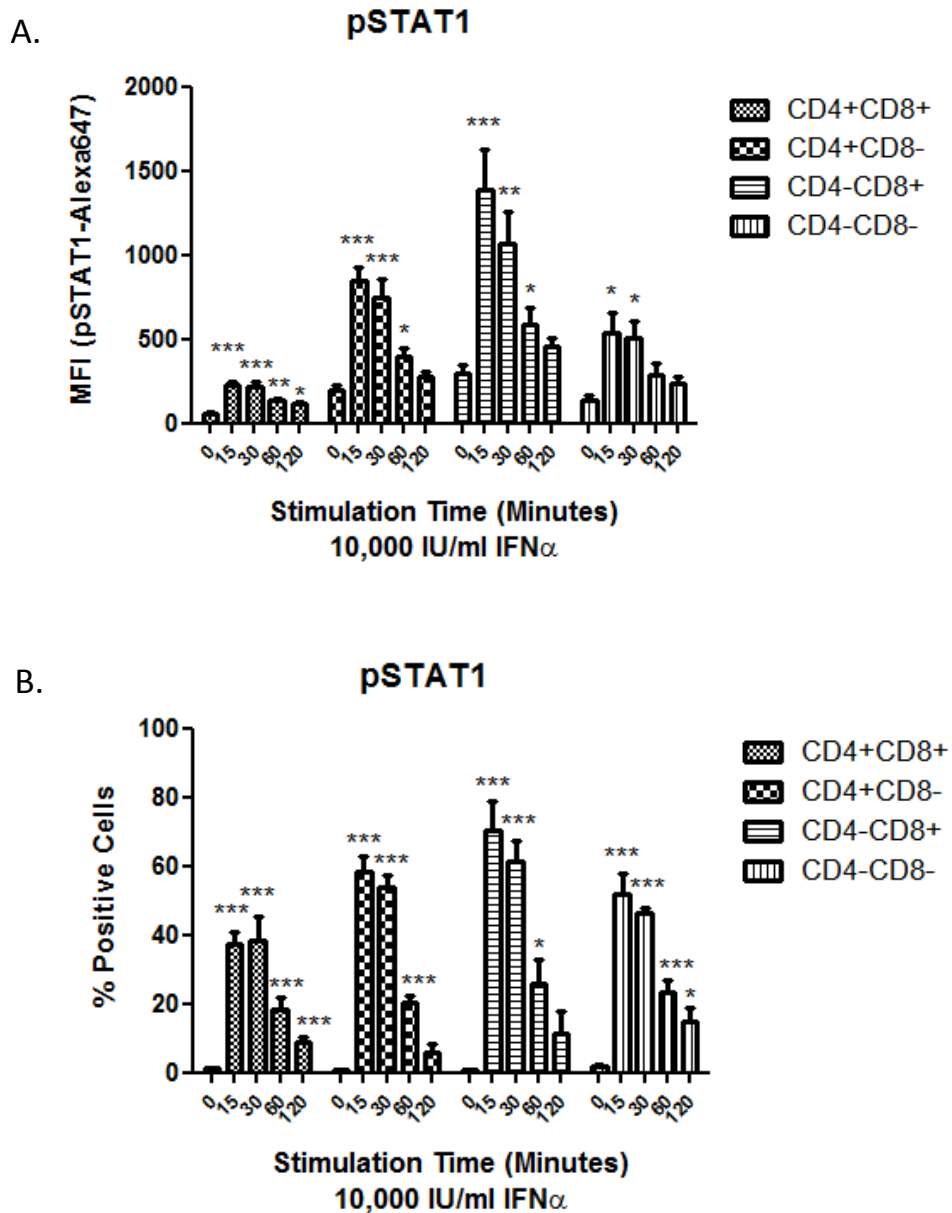


**Figure 4.7: Time course of IFN $\alpha$  induced Stat1 phosphorylation in thymic CD4/CD8 T-cell subsets.** Thymus was harvested from wt C57BL/6 mice and a single cell suspension created. Cells were left untreated or stimulated with 10,000 IU/ml of IFN $\alpha$  for 15, 30, 60 or 120 minutes. Following cell fixation and permeabilisation, cells were incubated with surface marker antibodies (anti-CD4-FITC and anti-CD8-PE) in combination with pStat1-Alexa647. Cell subsets were separated based on surface marker expression of CD4-FITC and CD8-PE. The alexa647 MFI was calculated for each cell subset and time point. Data is represented as **A.** MFI and **B.** percentage of positive cells. Data is presented as mean  $\pm$  SEM of N = 3-5 separate experiments. \* =  $p \leq 0.05$ , \*\* =  $p \leq 0.01$ , \*\*\* =  $p \leq 0.005$ .

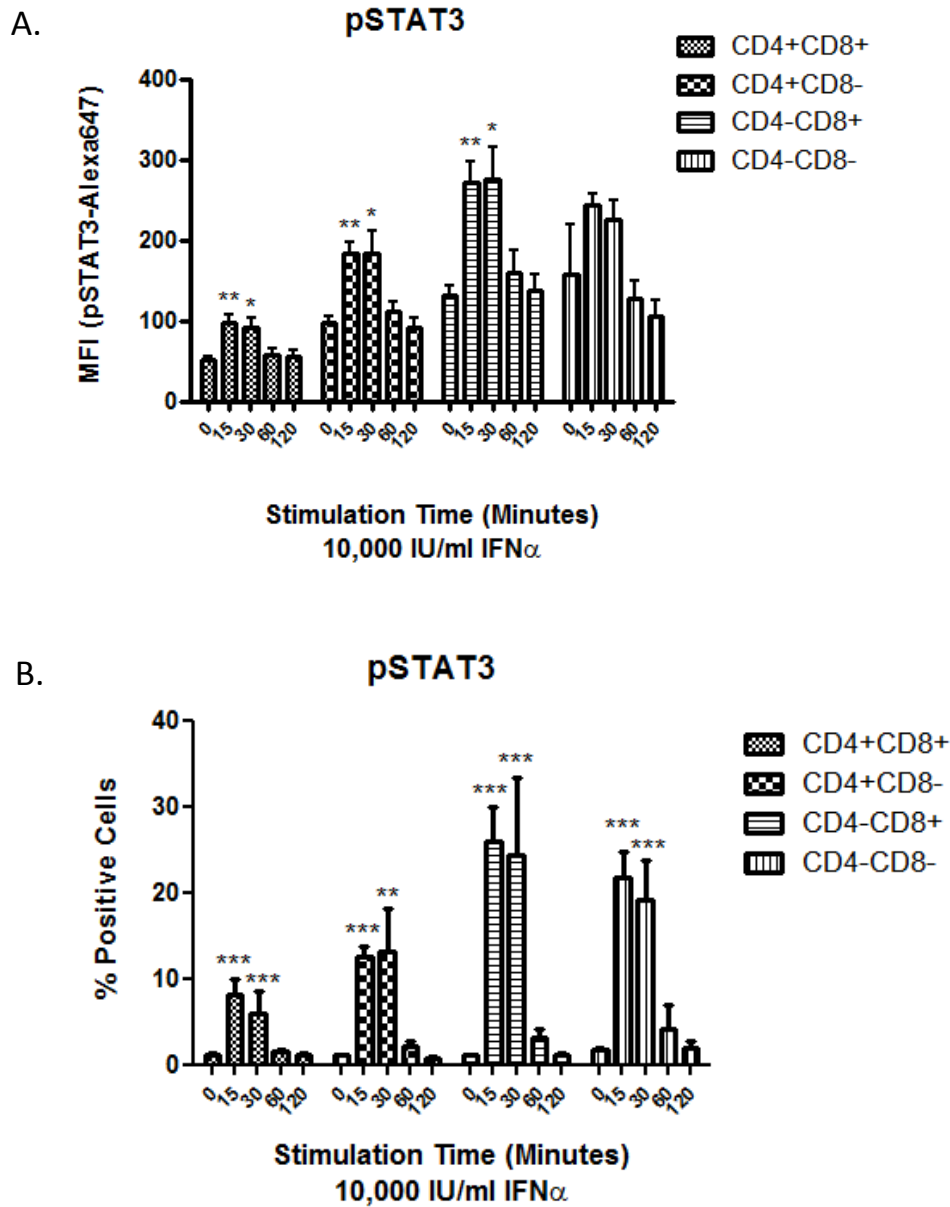


**Figure 4.8: Time course of IFN $\alpha$  induced Stat3 phosphorylation in thymic CD4/CD8 T-cell subsets.** Thymus was harvested from wt C57BL/6 mice and a single cell suspension created. Cells were left untreated or stimulated with 10,000 IU/ml of IFN $\alpha$  for 15, 30, 60 or 120 minutes. Following cell fixation and permeabilisation, cells were incubated with surface marker antibodies (anti-CD4-FITC and anti-CD8-PE) in combination with pStat3-Alexa647. Cell subsets were separated based on surface marker expression of CD4-FITC and CD8-PE. The alexa647 MFI was calculated for each cell subset and time point. Data is represented as **A.** MFI and **B.** percentage of positive cells. Data is presented as mean +/- SEM of N = 3-5 separate experiments. \* =  $p \leq 0.05$ , \*\* =  $p \leq 0.01$ , \*\*\* =  $p \leq 0.005$ .

same pattern as the basal levels. At 15 minutes post-stimulation, STAT3 phosphorylation was increased 2-fold in CD4-CD8<sup>+</sup> T-cells and 1.9-fold in CD4-CD8<sup>-</sup>, CD4+CD8<sup>-</sup> and CD4+CD8<sup>+</sup> T-cells.

The percentages of cells increased for pSTAT3, above basal levels, were also analysed (Figure 4.8 B). CD4-CD8<sup>+</sup> T-cells were the most significant responders (26%) followed by CD4-CD8<sup>-</sup> (22%), CD4+CD8<sup>-</sup> (13%) and CD4+CD8<sup>+</sup> T-cells (8%). The percentage of positive cells for pSTAT3 remain similar at 30 minutes post-IFN $\alpha$  stimulation followed by a drop to near basal levels at 60 minutes post-IFN $\alpha$  stimulation.

#### **4.3.3 Time course of STAT5 phosphorylation in the thymus**

The highest levels of pSTAT5 were obtained following 15-30 minutes IFN $\alpha$  stimulations and were greatest in CD4-CD8<sup>+</sup> T-cells (MFI 2359), followed by CD4+CD8<sup>-</sup> (MFI 2082), CD4-CD8<sup>-</sup> (MFI 2046) and CD4+CD8<sup>+</sup> T-cells (MFI 1186) (Figure 4.9 A). This follows the same pattern as the basal levels. At 15 minutes post-stimulation, STAT5 phosphorylation was increased 1.74-fold in CD4+CD8<sup>+</sup> T-cells, 1.64-fold in CD4+CD8<sup>-</sup> T-cells, 1.59-fold in CD4-CD8<sup>-</sup> T-cells and 1.46 fold in CD4-CD8<sup>+</sup> T-cells.

The percentages of cells increased for pSTAT5, above basal levels, were also analysed (Figure 4.9 B). CD4+CD8<sup>-</sup> T-cells were the most significant responders (33%) followed by CD4-CD8<sup>+</sup> (28%), CD4-CD8<sup>-</sup> (26%) and CD4+CD8<sup>+</sup> T-cells (12%). A significant percentage of cells were increased for pSTAT5 at 30 minutes post-stimulation. There is then a dramatic drop in pSTAT5 positive cells at 60 minutes post-IFN $\alpha$  stimulation to near basal levels.

#### **4.3.4 Summary and Discussion – IFN $\alpha$ induced STAT phosphorylation in thymocytes**

STAT phosphorylation peaked at 15-30 minutes post-IFN $\alpha$  stimulation and reduced over-time with the largest reduction between 30 and 60 minutes post-IFN $\alpha$  stimulation. By 120 minutes post-stimulation, most STAT phosphorylation levels were reduced to near basal. Previous studies have shown IFN induces JAK1, TYK2 and IFNAR phosphorylation within 1-5 minutes and this is reduced by 60 minutes post stimulation (Constantinescu, Croze et al. 1994; Plataniias, Uddin et al. 1994). The kinetics of STAT phosphorylation are consistent with STAT activation occurring downstream of JAK and

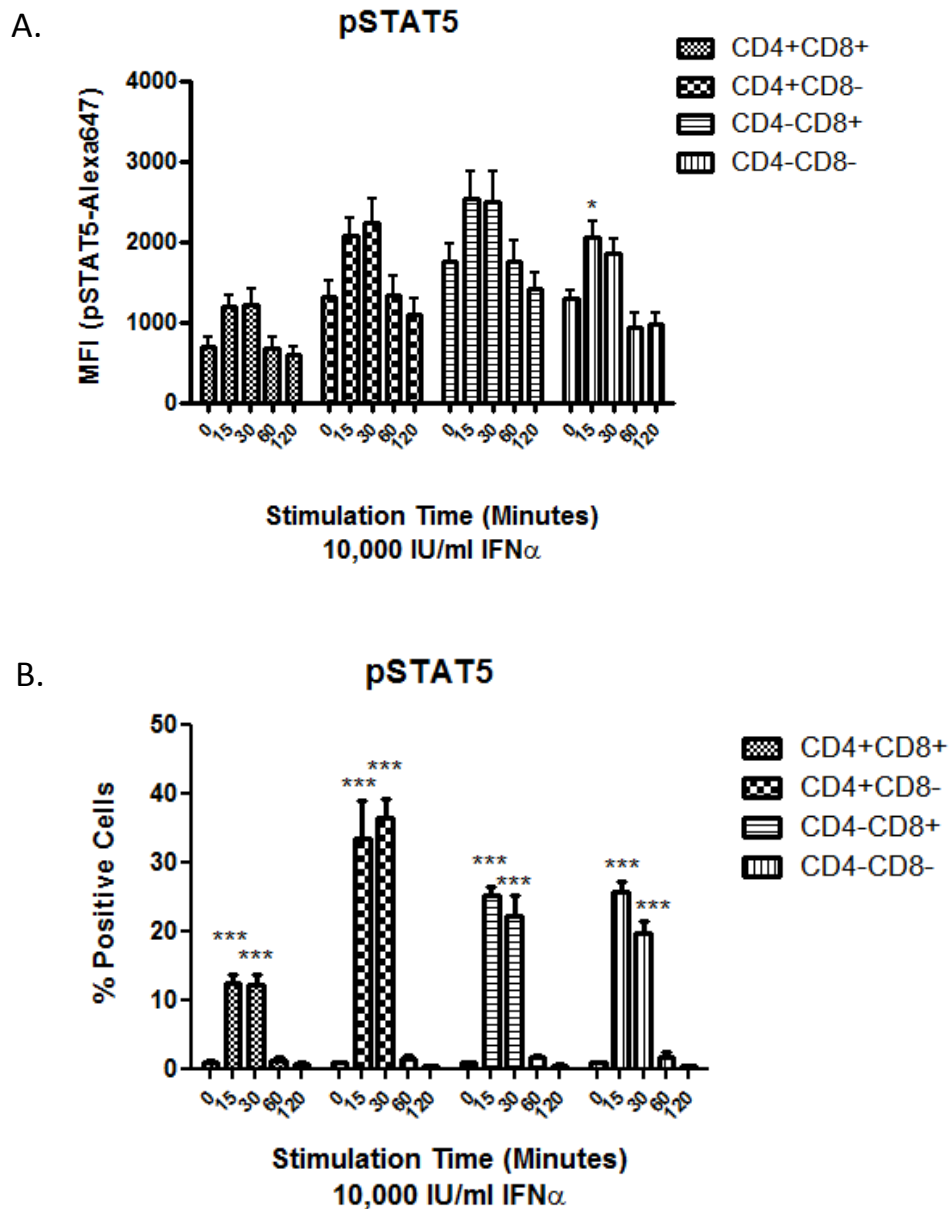


**Figure 4.9: Time course of IFN $\alpha$  induced Stat5 phosphorylation in thymic CD4/CD8 T-cell subsets.** Thymus was harvested from wt C57BL/6 mice and a single cell suspension created. Cells were left untreated or stimulated with 10,000 IU/ml of IFN $\alpha$  for 15, 30, 60 or 120 minutes. Following cell fixation and permeabilisation, cells were incubated with surface marker antibodies (anti-CD4-FITC and anti-CD8-PE) in combination with pStat5-Alexa647. Cell subsets were separated based on surface marker expression of CD4-FITC and CD8-PE. The alexa647 MFI was calculated for each cell subset and time point. Data is represented as **A.** MFI and **B.** percentage of positive cells. Data is presented as mean  $\pm$  SEM of N = 3-5 separate experiments. \* =  $p \leq 0.05$ , \*\* =  $p \leq 0.01$ , \*\*\* =  $p \leq 0.005$ .

IFNAR phosphorylation and indicate primary signalling events occur rapidly and transiently.

STAT1 phosphorylation underwent the highest induction in response to IFN $\alpha$ , followed by STAT3 and STAT5. Similarly, more cells showed induction of STAT1 phosphorylation than STAT3 and STAT5. Despite phosphorylated STAT3 displaying a greater induction than STAT5 in terms of the total level of STAT phosphorylation, the percentage of cells with increased STAT5 phosphorylation was greater than that with increased STAT3 phosphorylation. These results indicate that a larger number of cells within the thymus are able to phosphorylate STAT5 in response to IFN $\alpha$  than STAT3 although the level of STAT3 phosphorylation within a responding cell is greater than that of STAT5.

A complex network of cytokine signalling and a balance of STAT activation plays a large role in T-cell selection and differentiation within the thymus (Adamson, Collins et al. 2009). The balance of activated STATs will likely dictate the level of each transcription factor complex that forms and thus resultant gene expression and cellular changes. Phosphorylated STAT1 may form ISGF3, STAT1 homodimers or STAT1:STAT3 heterodimers. The higher phosphorylation of STAT1 than STAT3 and STAT5 indicate IFN stimulation of the thymus will predominantly result in ISGF3 or STAT1:STAT1 mediated responses. As STAT1 knock out studies have shown that it is important in mediating viral resistance, the up-regulation of STAT1 by IFN $\alpha$  is consistent with the anti-viral effects of the type I IFNs (Meraz, White et al. 1996).

STAT2 phosphorylation was unable to be studied due to the availability of required reagents. A number of studies however have previously shown that IFN induction of STAT2 phosphorylation is required for STAT1 phosphorylation to proceed and it is thus likely that STAT2 is also phosphorylated in these cell types in response to IFN (Leung, Qureshi et al. 1995). Due to the reagents available, differences in STAT5A and STAT5B phosphorylation were also unable to be analysed. Although these proteins are very similar in structure and there is still considerable overlap in the genes they are able to regulate, differences in control of gene expression have been found and thus in future studies it would be interesting to determine whether IFN $\alpha$  induces both STAT5A and STAT5B similarly (Basham, Sathe et al. 2008).

It is evident the level of STAT1, STAT3 and STAT5 phosphorylation in response to IFN $\alpha$  is cell type specific. Different immune cell subsets of the thymus contain different

levels of basal phosphorylated STATs and a different response to IFN $\alpha$  induced STAT phosphorylation. I found that thymic CD4-CD8<sup>+</sup> and CD4<sup>+</sup>CD8<sup>-</sup> T-cells displayed the highest levels of pSTAT1, pSTAT3 and pSTAT5 basally and following IFN $\alpha$  stimulations compared to CD4-CD8<sup>-</sup> and CD4<sup>+</sup>CD8<sup>+</sup> T-cell sub-populations. The single positive T-cells within the thymus are therefore likely to be more responsive to IFN $\alpha$  stimulation than less mature CD4-CD8<sup>-</sup> and CD4<sup>+</sup>CD8<sup>+</sup> T-cells.

Previous studies have implicated that type I IFN has a role in controlling T-cell differentiation and survival within the thymus. One study indicates that IFN $\alpha$  is expressed constitutively in the thymus by resident pDCs and that it may play a role in negative T-cell selection within the medulla, increasing the susceptibility of T-cells to cell death and reducing the threshold needed for negative selection (Colantonio, Epeldegui et al. 2011). In support of this, another study has shown the deletion of either IFNAR1 or STAT1 in thymocytes results in the impaired deletion of auto-reactive T-cells within the thymus (Moro, Otero et al. 2011). This negative selection occurs at the level of CD4<sup>+</sup>CD8<sup>+</sup> thymocytes however evidence indicates that mature thymocytes may mediate this selection process (Moro, Otero et al. 2011). Indeed, the ability of all thymocytes to induce STAT1 phosphorylation following IFN $\alpha$  indicate that IFN $\alpha$  may also have a greater range of effects on thymocytes than at the level of CD4<sup>+</sup>CD8<sup>+</sup> T-cell selection alone. As mentioned above, the greatest induction of STAT phosphorylation was found in the single positive CD4<sup>+</sup>CD8<sup>-</sup> or CD4-CD8<sup>+</sup> T-cells which have already undergone selection processes indicating a role for IFN $\alpha$  in modulating the effects of the more mature thymocytes as well.

It should be noted the high doses of IFN $\alpha$  used for stimulation in our studies may reflect levels seen following an infection rather than basal expression levels. As only STAT1 phosphorylation was seen at lower doses of IFN $\alpha$  treatment in our studies, low level constitutive IFN $\alpha$  expression in the thymus may be mediated by STAT1 alone, not STAT3 or STAT5. Another important consideration is the ability of IFN $\alpha$  to prime STAT1 expression and mediate cross-talk between different cytokine pathways that utilise STAT1 (Gough, Messina et al. 2010). In the context of the thymus, the constitutive expression of IFN $\alpha$  in the thymus may mediate effects of other cytokines pathways that play a role in T-cell differentiation such as IFN $\gamma$ .

The induction of STAT3 and STAT5 phosphorylation at the higher doses of IFN $\alpha$  indicate that these STATs may be activated and mediate T-cell effects during infection

when high doses of IFN $\alpha$  are produced. An important consideration however in these studies is the absence of T-cell activation through the TCR. As discussed in chapter 1, IFN $\alpha$  can have different effects depending on the activation state of the T-cell at the time. The IFN $\alpha$  induced phosphorylation of STAT1, STAT3 or STAT5 during an infection may differ to the results seen here when acting on inactive T-cells. In the absence of infection, IFN $\alpha$  expression acts to inhibit T-cell function. During early stages of T-cell differentiation and development in the thymus, IFN $\alpha$  is found to have an inhibitory effect on T-cell expansion as IFN $\alpha$  treatment of newborn mice results in a greater than 80% reduction in thymic cellularity. This inhibitory effect was found to occur at stages when T-cell growth and survival is mediated by IL-7 signaling (Lin, Dong et al. 1998). Interestingly IL-7 predominantly activates STAT5 signaling pathways. As IFN $\alpha$  also activates STAT5 in the thymus, perhaps there is cross-talk between these two pathways at the level of STAT activation. For example STAT5 activation by IFN $\alpha$  may result in a reduced amount of STAT5 available for IL-7 signaling. In the context of IFN mediated STAT5 signaling, STAT5 has been found to form complexes with a number of other transcription factors or binding proteins which may inhibit the amount of STAT5 available to form typical STAT5A/B homo or hetero dimers and thus limit typical STAT5 signaling. This however is purely speculative and additional studies are required to elucidate this hypothesis.

Interestingly we found that not all cells of a particular population induced STAT phosphorylation in response to IFN $\alpha$ . This was particularly evident with STAT3 and STAT5 which in some cases showed less than 20% of cells responding. A study by Zhao et al showed that in response to viral infection, only a portion of cells up-regulate IFN $\beta$  gene expression (Zhao, Zhang et al. 2012). They found that this variability was due to the stochastic variability of the cells themselves within a population, such as the expression of a number of factors within the cell including those involved in viral replication and expression, viral detection, signaling pathways and also the level of transcription factor expression (Zhao, Zhang et al. 2012). The response of a cell to IFN may therefore also be dependent on a range of factors within the cell such as the level of receptor expression, the level of STAT expression as well as the presence of co-activators or inhibitors. The differences observed between different cell populations are also likely to be impacted by these factors.

#### **4.4 Basal MFI of pSTAT1, pSTAT3 and pSTAT5 in PBMC CD4/CD8 T-cell subsets**

The basal levels of phosphorylated STAT1, STAT3 and STAT5 within PBMC CD4+CD8- and CD4-CD8+ T-cells were not significantly different between cell types (Figure 4.10). For pSTAT1, CD4+CD8- T-cells displayed a basal MFI of 229 whereas CD4-CD8+ T-cells displayed a basal MFI of 222. For pSTAT3 CD4+CD8- T-cells displayed a basal MFI of 138 whereas CD4-CD8+ T-cells displayed a basal MFI of 141. For pSTAT5, CD4+CD8- T-cells displayed an MFI of 1310 whereas CD4-CD8+ T-cells displayed an MFI of 1590.

Basal pSTAT levels in B220+ cells were slightly reduced compared to basal pSTAT levels in T-cells, although not significant. B220+ cells displayed a basal pSTAT1 MFI of 142, a basal pSTAT3 MFI of 94 and a basal pSTAT5 MFI of 1120.

Basal pSTAT1 levels in MAC1+ cells were slightly reduced compared to that of T-cells (222-229), with an MFI of 170. In comparison pSTAT3 and pSTAT5 levels were slightly increased as compared to T-cells and B220+ cells, with MFIs of 300 and 2187, respectively.

MAC1++ cells displayed relatively high basal levels of pSTAT1, pSTAT3 and pSTAT5 compared to T-cells, B220+ cells and MAC1+ cells, with MFIs of 478, 690 and 6690 respectively. The high basal levels of pSTATs in the MAC1++ cells indicate these cells are highly activated as basal pSTAT levels are similar to those found with IFN $\alpha$  stimulation in other cell types.

#### **4.5 Time Course of IFN $\alpha$ induced STAT phosphorylation in PBMC CD4+/CD8+, B220+ and MAC1+ and MAC1++ cell Subsets**

The phosphorylation of STAT1, STAT3 and STAT5 in response to IFN $\alpha$  in peripheral CD4+/CD8+ T-cells, B220+ cells, MAC1+ and MAC1++ cells was analysed.

##### **4.5.1 Time course of STAT1 phosphorylation in the blood**

The highest level of pSTAT1 was reached in CD4-CD8+ T-cells (MFI 1059) followed by CD4+CD8- T-cells (MFI 733) (Figure 4.11 A). These had induction levels, above basal, at 15 minutes post-IFN $\alpha$  stimulation of 4.7-fold and 3.2-fold, respectively. The percentage of cells increased for pSTAT1 above basal levels was also analysed (Figure 4.11 B). CD4-CD8+ T-cells were the most significant responders (75%)

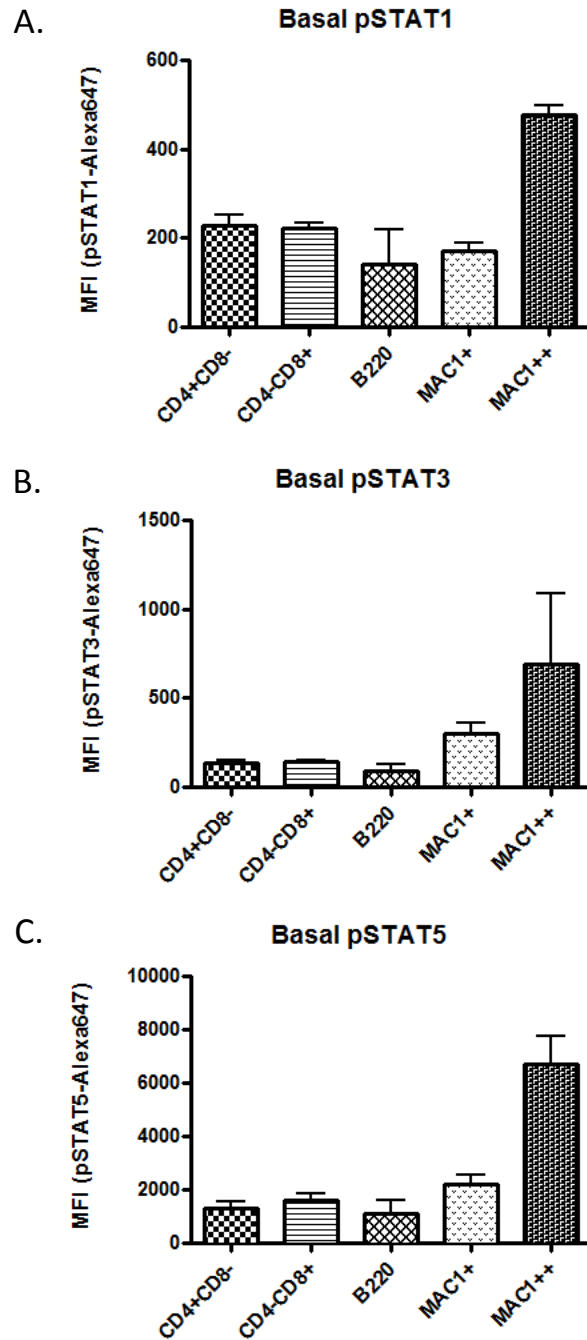


**Figure 4.10: Basal Stat1, Stat3 and Stat5 phosphorylation levels in PBMC CD4/CD8 T-cell subsets, B220 positive or MAC1 positive cells.** Blood was harvested from wt C57BL/6 mice and a single cell suspension created. Following cell fixation and permeabilisation, cells were incubated with surface marker antibodies (anti-CD4-FITC and anti-CD8-PE or anti-B220-FITC and anti-MAC1-PE) in combination with **A.** pStat1-Alexa647, **B.** pStat3-Alexa647 or **C.** pStat5-Alexa647. Cell subsets were separated based on surface marker expression of FITC and PE. The alexa647 MFI was calculated for each cell subset. Data is presented as mean +/- SEM of N = 3-5 separate experiments. \* =  $p \leq 0.05$ , \*\* =  $p \leq 0.01$ , \*\*\* =  $p \leq 0.005$ .

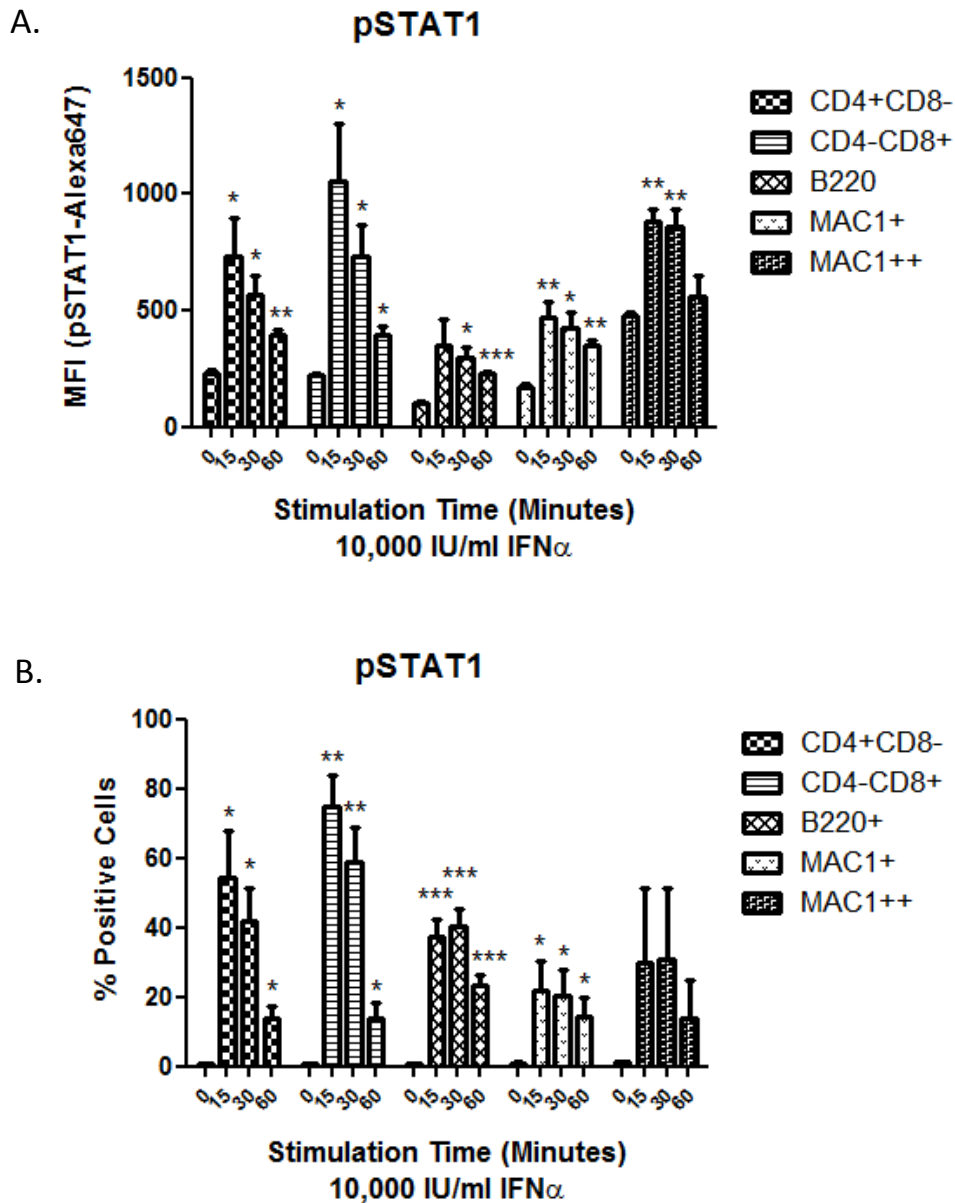


**Figure 4.11: Time course IFN $\alpha$  induced Stat1 phosphorylation in PBMC CD4/CD8 T-cell subsets, B220 positive or MAC1 positive cells.** Blood was harvested from wt C57BL/6 mice and a single cell suspension created. Cells were left untreated or stimulated with 10,000 IU/ml of IFN $\alpha$  for 15, 30 or 60 minutes. Following cell fixation and permeabilisation, cells were incubated with surface marker antibodies (anti-CD4-FITC and anti-CD8-PE or anti-B220-FITC and anti-MAC1-PE) in combination with pStat1-Alexa647. Cell subsets were separated based on surface marker expression of FITC and PE. The alexa647 MFI was calculated for each cell subset and time point. Data is represented as **A.** MFI and **B.** percentage of positive cells. Data is presented as mean +/- SEM of N = 3-5 separate experiments. \* =  $p \leq 0.05$ , \*\* =  $p \leq 0.01$ , \*\*\* =  $p \leq 0.005$ .

followed by CD4+CD8- (54%). A slightly reduced proportion of cells were positive for pSTAT1 at 30 minutes post-stimulation. By 60 minutes IFN $\alpha$  stimulation this is reduced further, however pSTAT1 levels were still significantly greater than basal levels.

B-cells (B220+) displayed up-regulation of pSTAT1 at 15-60 minutes post-IFN $\alpha$  stimulation (Figure 4.11 A). pSTAT1 levels increased 3.4-fold at 15 minutes post-IFN $\alpha$  stimulation and remained increased at 30 minutes (2.9-fold) and 60 minutes (2.2-fold) post-IFN $\alpha$  stimulation. Peak pSTAT1 levels in B-cells (350) did not reach values near that of the stimulated T-cell populations (733-1059) due to a comparatively low basal level to begin with. The percentage of B-cells positive for pSTAT1 ranged from approximately 40% with 15-30 minutes IFN $\alpha$  stimulation to approximately 25% at 60 minutes post-IFN $\alpha$  stimulation (Figure 4.11 B).

MAC1+ cells displayed up-regulation of pSTAT1 at 15-60 minutes post-IFN $\alpha$  stimulation. pSTAT1 levels increased 2.8-fold at 15 minutes post-IFN $\alpha$  stimulation and remained increased at 30 minutes (2.5-fold) and 60 minutes (2-fold) post-IFN $\alpha$  stimulation (Figure 4.11 A). The percentage of MAC1+ cells increased for pSTAT1 levels were approximately 20% at 15-30 minutes and 15% at 60 minutes post-IFN $\alpha$  stimulation (Figure 4.11 B).

MAC1++ cells displayed a 1.8-fold up-regulation of pSTAT1 15-30 minutes post-IFN $\alpha$  stimulations (Figure 4.11 A). Despite a similar trend, there was no significant induction of MAC1++ cells expressing pSTAT1 following IFN $\alpha$  stimulations, due to a large variance in results across experiments (Figure 4.11 B).

#### **4.5.2 Time course of STAT3 phosphorylation in the blood**

There was no significant induction of pSTAT3 in peripheral CD4-CD8+ or CD4+CD8- T-cells following IFN $\alpha$  stimulations (Figure 4.12 A). The percentage of cells increased for pSTAT3 above basal levels was also analysed. There was large variance in the number of cells responding across samples and therefore no significance differences were obtained (Figure 4.12 B). Despite this it is evident that the change in MFI and the percentage of positive cells were very low compared to those seen for STAT1 phosphorylation.

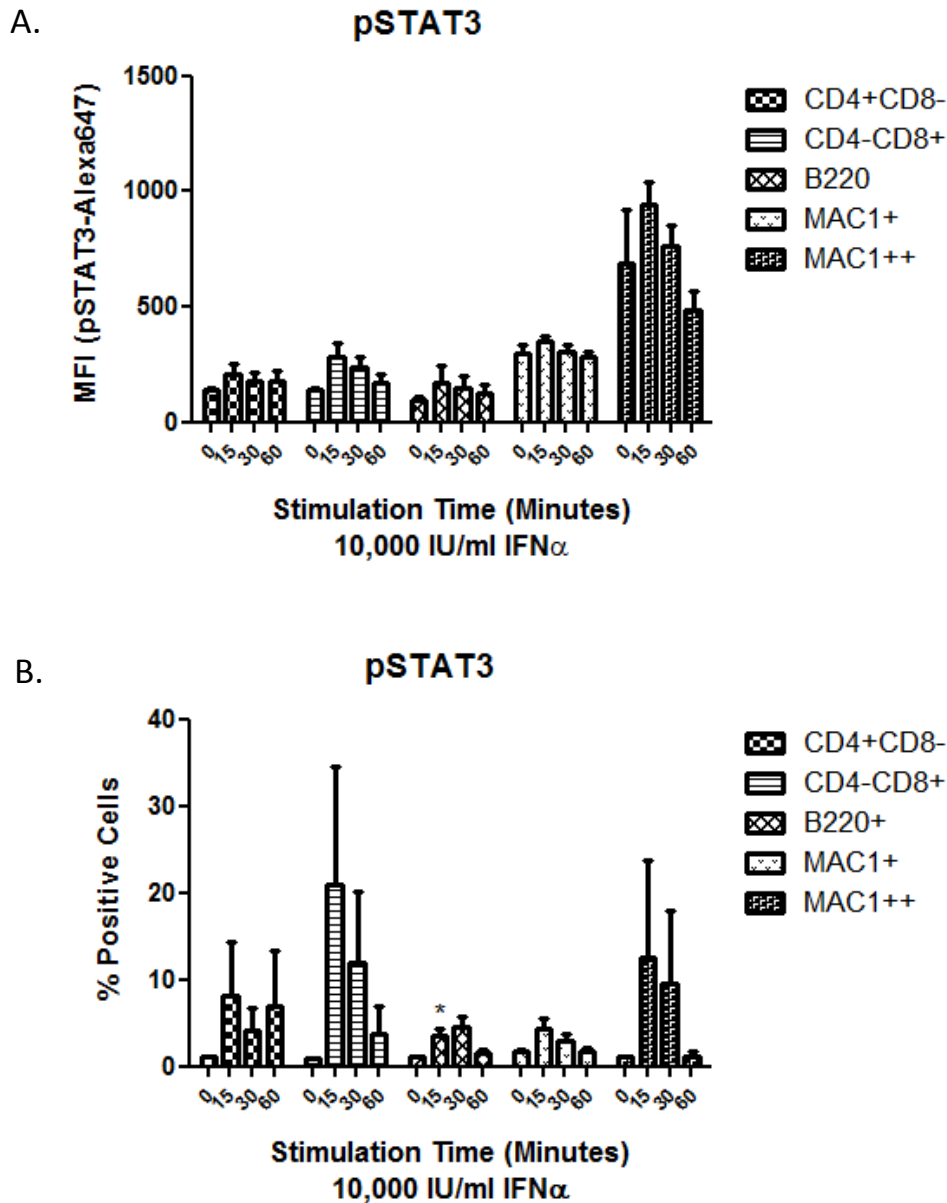


**Figure 4.12: Time course IFN $\alpha$  induced Stat3 phosphorylation in PBMC CD4/CD8 T-cell subsets, B220 positive or MAC1 positive cells.** Blood was harvested from wt C57BL/6 mice and a single cell suspension created. Cells were left untreated or stimulated with 10,000 IU/ml of IFN $\alpha$  for 15, 30 or 60 minutes. Following cell fixation and permeabilisation, cells were incubated with surface marker antibodies (anti-CD4-FITC and anti-CD8-PE or anti-B220-FITC and anti-MAC1-PE) in combination with pStat3-Alexa647. Cell subsets were separated based on surface marker expression of FITC and PE. The alexa647 MFI was calculated for each cell subset and time point. Data is represented as **A.** MFI and **B.** percentage of positive cells. Data is presented as mean  $\pm$  SEM of N = 3-5 separate experiments. \* =  $p \leq 0.05$ , \*\* =  $p \leq 0.01$ , \*\*\* =  $p \leq 0.005$ .

B220+ cells displayed no significant up-regulation of pSTAT3, in terms of MFI, in response to IFN $\alpha$  stimulation (Figure 4.12 A). At 15 minutes post-IFN $\alpha$  stimulation only 5% of B220+ cells were positive for pSTAT3 (Figure 4.12 B).

MAC1+ and MAC1++ cells did not display significant up-regulation of pSTAT3 in response to IFN $\alpha$  in terms of MFI or percentage of positive cells (Figure 4.12).

#### **4.5.3 Time course of STAT5 phosphorylation in the blood**

There was no significant induction of pSTAT5 in peripheral CD4-CD8+ or CD4+CD8- T-cells following IFN $\alpha$  stimulations (Figure 4.13 A). The percentage of cells increased for pSTAT5 above basal levels was also analysed (Figure 4.13 B). There were very few cells responding to IFN $\alpha$  in terms of pSTAT5 up-regulation. Only 6.5% of CD4+CD8- T-cells were positive for pSTAT5 ( $p < 0.05$ ) and 8% of CD4-CD8+ T-cells at 15 minutes post-IFN $\alpha$  stimulation. It is evident that the change in MFI and the percentage of positive cells were very low compared to those seen for STAT1 phosphorylation.

B220+, MAC1+ and MAC1++ cells displayed no significant up-regulation of pSTAT5 in response to IFN $\alpha$  in terms of MFI or percentage of positive cells (Figure 4.13).

#### **4.5.4 Thymic CD4/CD8 T-cells vs Periphery CD4/CD8 T-cells**

The percentage of cells up-regulated above basal levels of pSTAT1, pSTAT3 and pSTAT5 were compared following 15 minutes IFN $\alpha$  stimulation in thymic and peripheral T-cells (PBMC or splenic) (Figure 4.14). It is evident that the response to IFN $\alpha$  is cell type and tissue specific. Thymic and peripheral T-cells displayed similar levels of pSTAT1 activation in response to IFN $\alpha$ . Approximately 50-60% of CD4+CD8- and 70-80% of CD4-CD8+ thymic and PBMC T-cells displayed up-regulation of pSTAT1 at 15 minutes IFN $\alpha$  stimulation. In contrast splenic cells were less responsive as approx. 30% of CD4+CD8- and 40% of CD4-CD8+ cells were responsive to 15 minutes IFN $\alpha$  stimulation. The percentages of cells positive for pSTAT3 were relatively low (<20%) in CD4+CD8- T-cells from thymus, blood and spleen (Figure 4.14). The percentages of cells positive for pSTAT3 were similar in CD4-CD8+ T-cells from the thymus and blood however reduced in cells from the spleen. Although STAT1 and STAT3 showed similar levels of phosphorylation in response to IFN $\alpha$  between thymic and PBMC T-cells, STAT5 phosphorylation was significantly different displaying higher levels in the thymus compared to the periphery. The percentage of thymic CD4+CD8- T-cells positive for

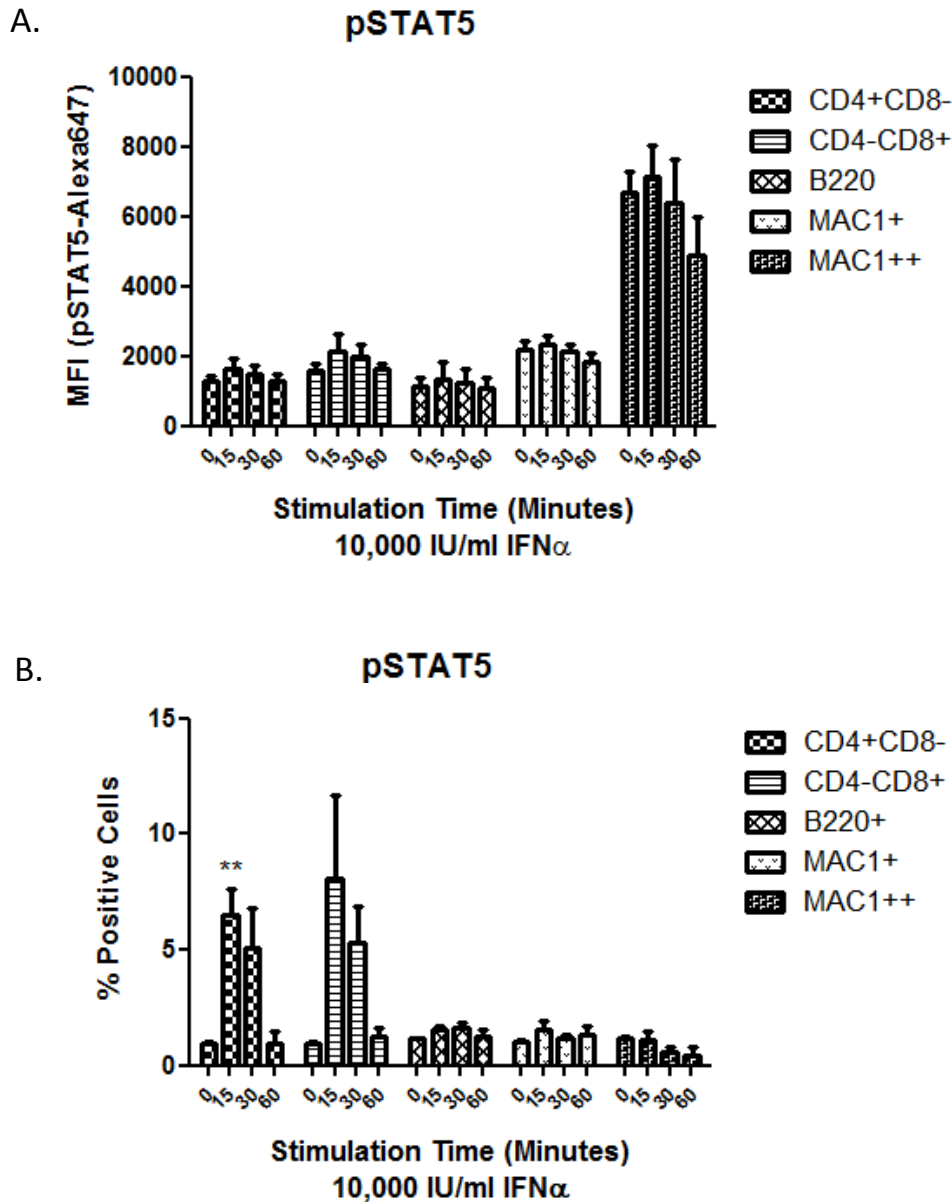


**Figure 4.13: Time course of IFN $\alpha$  induced Stat5 phosphorylation in PBMC CD4/CD8 T-cell subsets, B220 positive or MAC1 positive cells.** Blood was harvested from wt C57BL/6 mice and a single cell suspension created. Cells were left untreated or stimulated with 10,000 IU/ml of IFN $\alpha$  for 15, 30 or 60 minutes. Following cell fixation and permeabilisation, cells were incubated with surface marker antibodies (anti-CD4-FITC and anti-CD8-PE or anti-B220-FITC and anti-MAC1-PE) in combination with pStat5-Alexa647. Cell subsets were separated based on surface marker expression of FITC and PE. The alexa647 MFI was calculated for each cell subset and time point. Data is represented as **A.** MFI and **B.** percentage of positive cells. Data is presented as mean  $\pm$  SEM of N = 3-5 separate experiments. \* =  $p \leq 0.05$ , \*\* =  $p \leq 0.01$ , \*\*\* =  $p \leq 0.005$ .

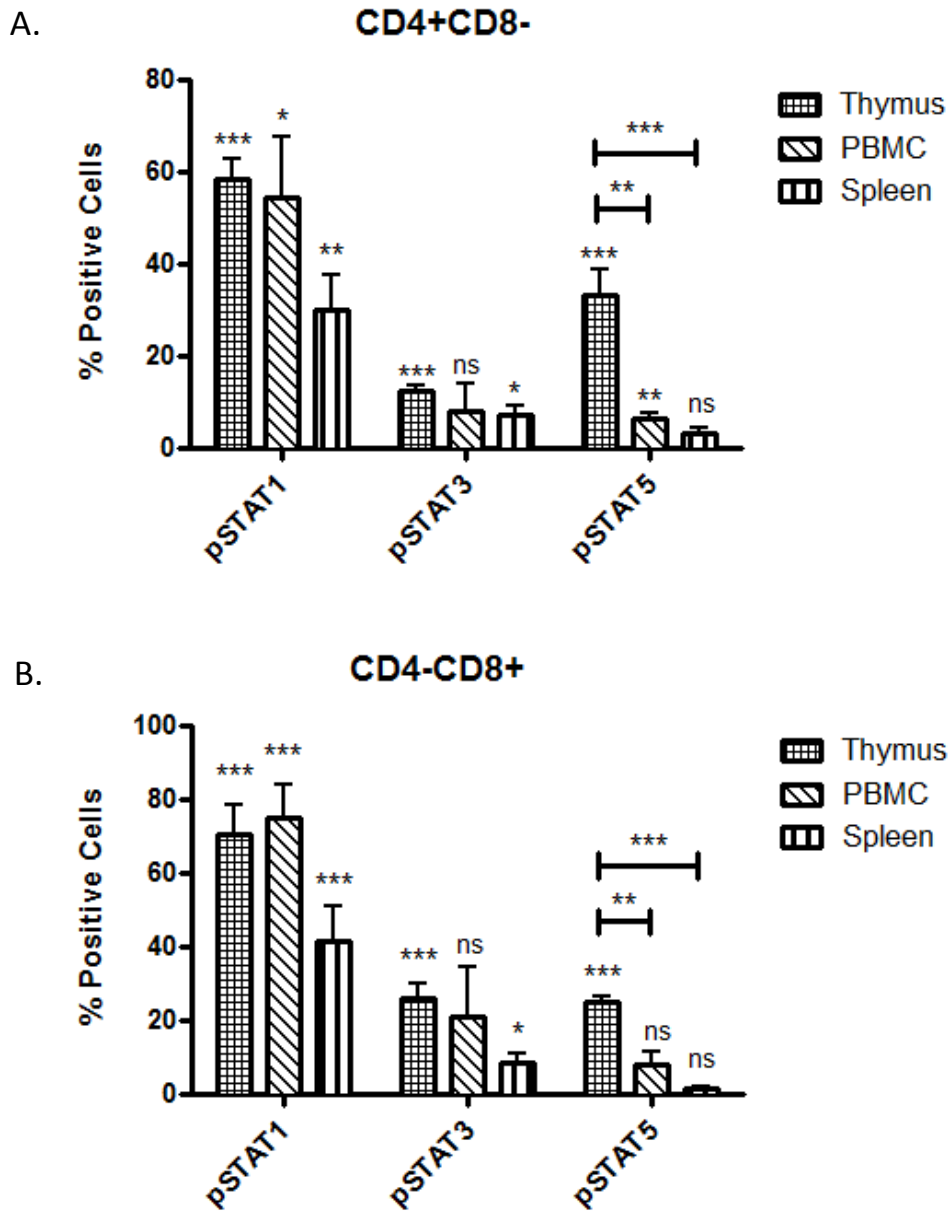


**Figure 4.14: Thymic and peripheral T-cell Stat1, Stat3 and Stat5 phosphorylation in response to 15 minutes IFN $\alpha$  stimulation.** Thymus, blood or spleen was harvested from wt C57BL/6 mice and single cell suspensions created. Cells were left untreated or stimulated with 10,000 IU/ml of IFN $\alpha$  for 15 minutes. Following cell fixation and permeabilisation, cells were incubated with surface marker antibodies (anti-CD4-FITC and anti-CD8-PE) in combination with pStat5-Alexa647. Cell subsets were separated based on surface marker expression of CD4-FITC and CD8-PE. The alexa647 MFI was calculated for **A.** CD4+CD8- and **B.** CD4-CD8+ cell populations. Data is represented as percentage of positive cells at 15 minutes IFN $\alpha$  stimulations. Data is presented as mean  $\pm$  SEM of N = 3-5 separate experiments. \* =  $p \leq 0.05$ , \*\* =  $p \leq 0.01$ , \*\*\* =  $p \leq 0.005$ .

pSTAT5, above basal levels in response to IFN $\alpha$ , were approx. 33% compared to 6.5% for PBMC CD4+CD8- T-cells and a non-significant response in the spleen. The percentage of thymic CD4-CD8+ T-cells increased for pSTAT5, above basal levels in response to IFN $\alpha$ , were approx. 25% compared to a non-significant response in PBMC and splenic CD4+CD8- T-cells.

#### **4.5.5 Summary and Discussion – IFN $\alpha$ induced STAT phosphorylation in peripheral immune cells**

STAT1 is phosphorylated in response to IFN $\alpha$  stimulation universally among the immune cell populations analysed as T-cells, B220+ cells, MAC1+ and MAC1++ cells all showed increased STAT1 phosphorylation in response to IFN $\alpha$ . T-cells and B220+ cells displayed the highest induction of STAT1 phosphorylation above basal levels. This is in contrast to pSTAT3 and pSTAT5 as T-cells, B220+ cells, MAC1+ and MAC1++ cells displayed only poor to no up-regulation of pSTAT3 and pSTAT5 in response to IFN $\alpha$ .

PBMC derived CD4+CD8- and CD4-CD8+ T-cells displayed up-regulation of pSTAT1 in response to IFN $\alpha$  in a similar manner to thymic derived T-cells. In contrast there is a large difference in the ability of thymic vs peripheral T-cells (PBMCs and splenocytes) to induce pSTAT5 and to a lesser degree pSTAT3. This may be due to intrinsic cell differences between immature T-cells isolated from the thymus and mature peripheral T-cells isolated from the blood and spleen. The result however may impact greatly on the type of response IFN $\alpha$  has on these cells. As mentioned previously, the response of the cells to IFN $\alpha$  is orchestrated in part by the level and type of STATs that are activated. Thymic T-cells may display a STAT1, STAT3 and STAT5 mediated response whereas peripheral T-cell would be skewed towards a STAT1 response. This may have important consequences in terms of the effect of IFN $\alpha$  on the function of thymic versus peripheral T-cells. As STAT5 is an important transcription factor in T-cell differentiation, the ability of thymic T-cells to induce STAT5 may therefore be indicative of IFN $\alpha$  manipulating thymic T-cell differentiation.

The profile of IFN $\alpha$  induced pSTAT upregulation in murine PBMCs is comparatively quite different to the profile of IFN $\alpha$  and IFN $\beta$  induced pSTAT upregulation in human blood leukocytes (van Boxel-Dezaire, Zula et al. 2010). Monocytes and lymphocytes derived from human blood showed a large increase in the percentage of cells up-regulating pSTAT5 and pSTAT3 whereas our results showed blunted up-regulation of

pSTAT3 and pSTAT5 in murine derived PBMCs and splenocytes (van Boxel-Dezaire, Zula et al. 2010). We also found peak pSTAT induction at 15-30 minutes post IFN $\alpha$  stimulation whereas human leukocytes displayed peak inductions at 45 minutes post IFN stimulation. These differences may be due to differences in experimental technique. Van Boxel-Dezaire et al stimulated whole blood cultures with IFN, whereas we isolated PBMC's prior to stimulation. In support of this theory, van Boxel-Dezaire has observed a blunted response following stimulation of isolated human PBMCs compared to whole human blood cultures (un-published data). The stimulation of whole mouse blood may therefore result in higher pSTAT3 and pSTAT5 up-regulation compared to the stimulation of isolated PBMCs. Future studies in mice could utilise the technique employed by van Boxel-Dezaire et al in order to make a more direct comparison to the human data.

Although these differences in technique may cause blunted responses in PBMCs, murine derived thymocytes displayed significant upregulation of pSTAT5 following IFN $\alpha$  stimulation and were harvested in a similar manner to splenocytes, which displayed a blunted response. The blunted response in splenocytes is therefore likely to be real.

#### **4.6 SOCS1 effect on IFN $\alpha$ induced STAT phosphorylation**

As mentioned above, it is important to understand the effect SOCS1 has on IFN $\alpha$  induced STAT activation to understand how SOCS1 affects the response of the cell to IFN $\alpha$ . I analysed the phosphorylation profile of STAT1, STAT3 and STAT5 in immune cell subsets of *Socs1*<sup>-/-</sup>*Ifn $\gamma$* <sup>-/-</sup> and *Socs1*<sup>+/+</sup>*Ifn $\gamma$* <sup>-/-</sup> mice to determine the effect SOCS1 has on IFN $\alpha$  induced STAT phosphorylation.

Cells were stimulated with 10,000 IU/m IFN $\alpha$  for 0, 15, 30 or 60 minutes. Cells were gated on surface marker expression and analysed for MFI of alexa647, an indicator of pSTAT1, pSTAT3 or pSTAT5 levels. The MFI was plotted against stimulation time and compared between the genotypes. The percentage of positive cells were also analysed however results showed no significant differences between the two genotypes and thus are not shown.

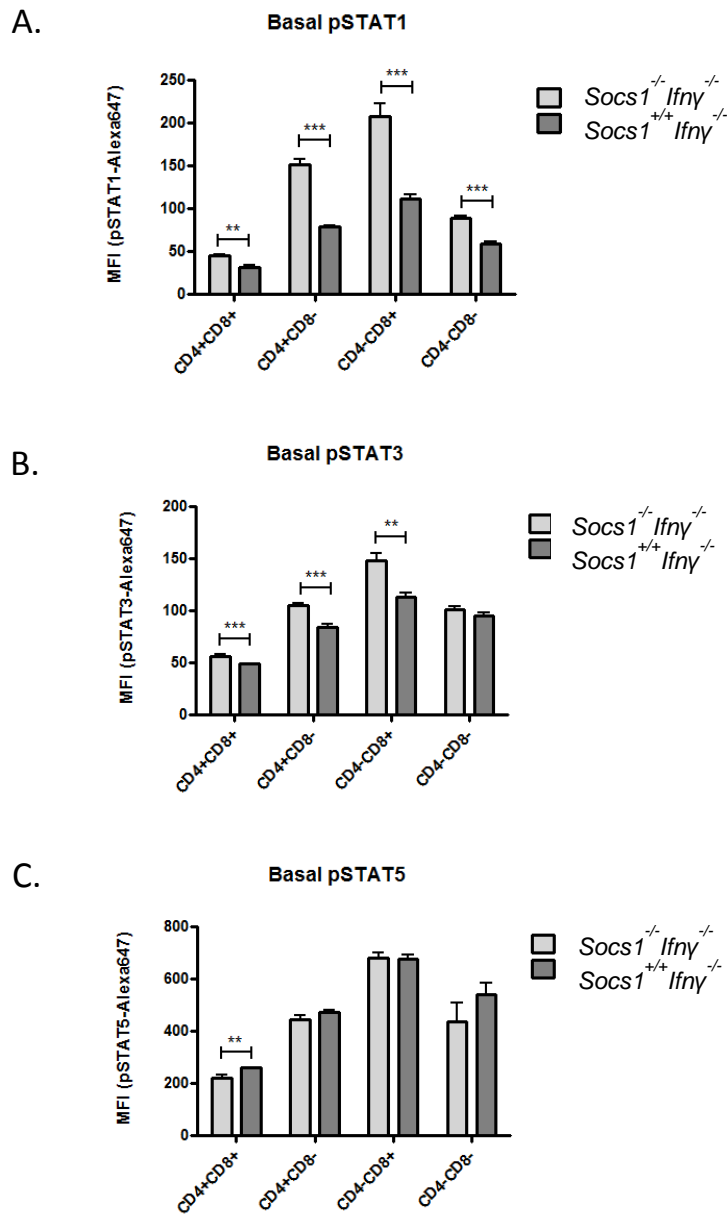


**Figure 4.15: Basal pStat1, pStat3 and, pStat5 phosphorylation levels in thymic CD4/CD8 T-cell subsets from *Socs1*<sup>-/-</sup> *Ifny*<sup>-/-</sup> and *Socs1*<sup>+/+</sup> *Ifny*<sup>-/-</sup> mice.** Thymus was harvested from *Socs1*<sup>-/-</sup> *Ifny*<sup>-/-</sup> and *Socs1*<sup>+/+</sup> *Ifny*<sup>-/-</sup> C57BL/6 mice and single cell suspensions created. Following cell fixation and permeabilisation, cells were incubated with surface marker antibodies (anti-CD4-FITC and anti-CD8-PE) in combination with **A.** pStat1-Alexa647, **B.** pStat3-Alexa647 or **C.** pStat5-Alexa647. Cell subsets were separated based on surface marker expression of CD4-FITC and CD8-PE. The alexa647 MFI was calculated for each cell subset. Data is represented as MFI. Data is presented as mean +/- SEM of N = 3-5 separate experiments. \* = p ≤ 0.05, \*\* = p ≤ 0.01, \*\*\* = p ≤ 0.005.

#### 4.6.1 STAT1 phosphorylation

Basal pSTAT1 levels in CD4/CD8 thymic T-cell subsets were significantly greater in *Socs1<sup>-/-</sup>Ifn $\gamma$ <sup>-/-</sup>* compared to *Socs1<sup>+/+</sup>Ifn $\gamma$ <sup>-/-</sup>* mice (Figure 4.15 A). In CD4+CD8- and CD4-CD8+ thymic T-cell populations, pSTAT1 basal levels were approximately 2-fold greater in the absence of SOCS1. In CD4+CD8+ and CD4-CD8- T-cells pSTAT1 basal levels were approximately 1.5-fold greater in the absence of SOCS1. Upon IFN $\alpha$  stimulation, significant pSTAT1 differences were also observed in the two genotypes. Thymic cells from *Socs1<sup>-/-</sup>Ifn $\gamma$ <sup>-/-</sup>* mice displayed higher pSTAT1 levels, at all time-points, than cells expressing SOCS1 (Figure 4.16). For CD4+CD8+ T-cells, the differences in MFI of cells from *Socs1<sup>-/-</sup>Ifn $\gamma$ <sup>-/-</sup>* compared to *Socs1<sup>+/+</sup>Ifn $\gamma$ <sup>-/-</sup>* mice were 14 ( $p < 0.01$ ) at basal (46% increase), 20.5 at 15 minutes post-stimulation (16% increase), 48.75 at 30 minutes (44% increase) and 44.48 ( $p < 0.01$ ) at 60 minutes post-stimulation (65% increase). For CD4+CD8- T-cells, the differences in MFI of cells from *Socs1<sup>-/-</sup>Ifn $\gamma$ <sup>-/-</sup>* compared to *Socs1<sup>+/+</sup>Ifn $\gamma$ <sup>-/-</sup>* mice were 72.98 ( $p < 0.005$ ) at basal levels (93% increase), 172.5 ( $p < 0.005$ ) at 15 minutes post-stimulation (51% increase), 276 ( $p < 0.05$ ) at 30 minutes (85% increase) and 146.8 ( $p < 0.005$ ) at 60 minutes post-stimulation (96% increase). For CD4-CD8+ T-cells, the differences in MFI of cells from *Socs1<sup>-/-</sup>Ifn $\gamma$ <sup>-/-</sup>* compared to *Socs1<sup>+/+</sup>Ifn $\gamma$ <sup>-/-</sup>* mice were 97.05 ( $p < 0.005$ ) at basal levels (87% increase), 193.5 ( $p < 0.05$ ) at 15 minutes post-stimulation (41% increase), 235.3 ( $p < 0.01$ ) at 30 minutes (64% increase) and 295.7 ( $p < 0.005$ ) at 60 minutes post-stimulation (77% increase). For CD4-CD8- T-cells, the differences in MFI of cells from *Socs1<sup>-/-</sup>Ifn $\gamma$ <sup>-/-</sup>* compared to *Socs1<sup>+/+</sup>Ifn $\gamma$ <sup>-/-</sup>* mice were 83.2 ( $p < 0.005$ ) at basal levels (51% increase), 109.8 ( $p < 0.005$ ) at 15 minutes post-stimulation (43% increase), 82.5 ( $p < 0.005$ ) at 30 minutes (35% increase) and 79.75 ( $p < 0.01$ ) at 60 minutes post-stimulation (56% increase).

It is evident the largest differences in pSTAT1 levels in thymic T-cells from *Socs1<sup>-/-</sup>Ifn $\gamma$ <sup>-/-</sup>* compared to *Socs1<sup>+/+</sup>Ifn $\gamma$ <sup>-/-</sup>* mice occur at 15-30 minutes post-IFN $\alpha$  stimulation. pSTAT1 levels also appear to remain elevated in the absence of SOCS1 at later time-points.

pSTAT1 induction was also investigated in spleen cells and bone marrow macrophages from *Socs1<sup>-/-</sup>Ifn $\gamma$ <sup>-/-</sup>* and *Socs1<sup>+/+</sup>Ifn $\gamma$ <sup>-/-</sup>* mice (Figures 4.17 and 4.18). CD4+CD8- and CD4-CD8+ splenic cells displayed increased levels of pSTAT following IFN $\alpha$  stimulations in the *Socs1<sup>-/-</sup>Ifn $\gamma$ <sup>-/-</sup>* compared to *Socs1<sup>+/+</sup>Ifn $\gamma$ <sup>-/-</sup>* mice. For CD4+CD8- T-cells from *Socs1<sup>-/-</sup>Ifn $\gamma$ <sup>-/-</sup>* compared to *Socs1<sup>+/+</sup>Ifn $\gamma$ <sup>-/-</sup>* mice, there is a difference in MFI of

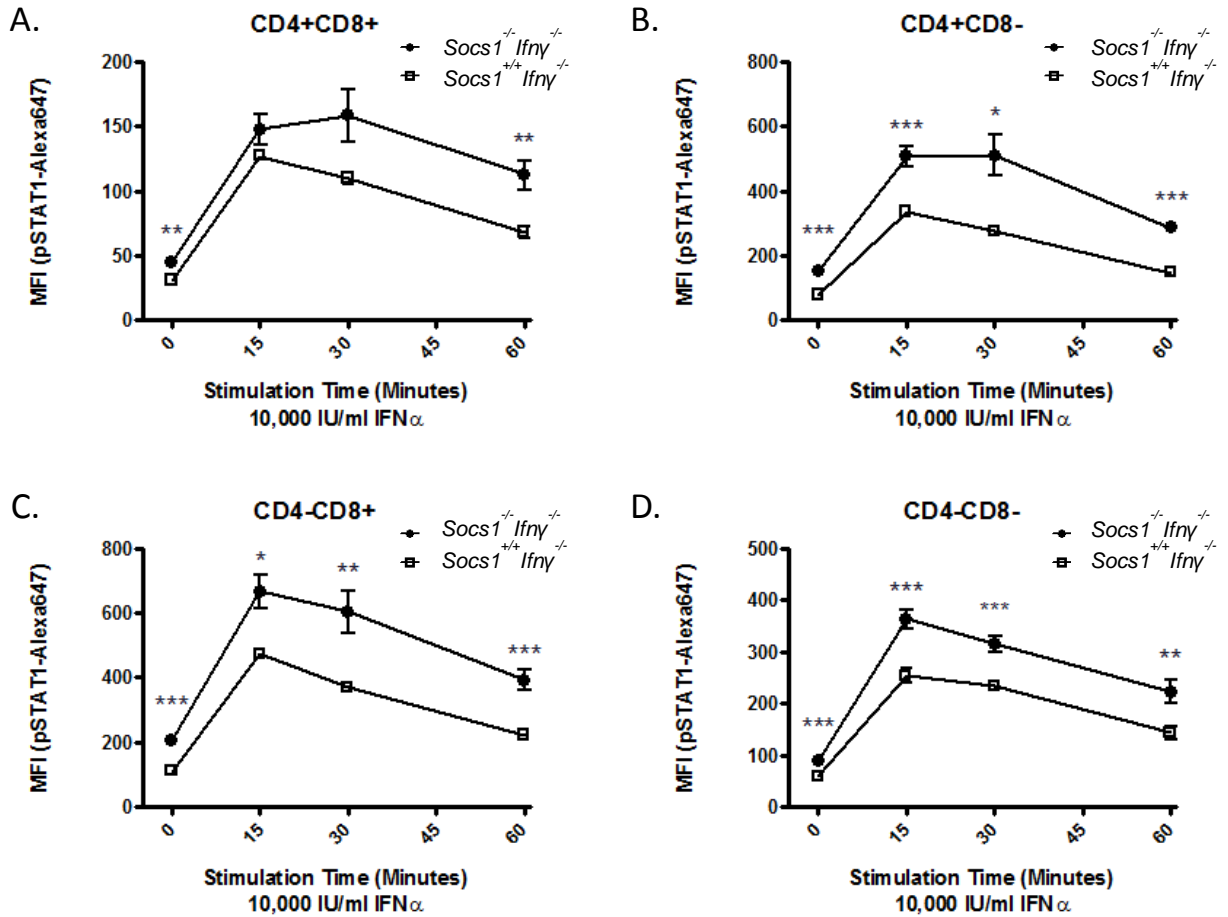


**Figure 4.16: Time course of IFN $\alpha$  induced Stat1 phosphorylation in thymic CD4/CD8 T-cell subsets from *Socs1*<sup>-/-</sup> *Ifny*<sup>-/-</sup> and *Socs1*<sup>+/+</sup> *Ifny*<sup>-/-</sup> mice.**

Thymus was harvested from *Socs1*<sup>-/-</sup> *Ifny*<sup>-/-</sup> and *Socs1*<sup>+/+</sup> *Ifny*<sup>-/-</sup> C57BL/6 mice and single cell suspensions created. Cells were left untreated or stimulated with 10,000 IU/ml of IFN $\alpha$  for 15, 30, or 60 minutes. Following cell fixation and permeabilisation, cells were incubated with surface marker antibodies (anti-CD4-FITC and anti-CD8-PE) in combination with pStat1-Alexa647. Cell subsets were separated based on surface marker expression of CD4-FITC and CD8-PE. The alexa647 MFI was calculated for each cell subset (**A.** CD4+CD8+, **B.** CD4+CD8-, **C.** CD4-CD8+ and **D.** CD4-CD8-) and time point. Data is presented as mean +/- SEM of N = 3-5 separate experiments. \* = p  $\leq$  0.05, \*\* = p  $\leq$  0.01, \*\*\* = p  $\leq$  0.005.

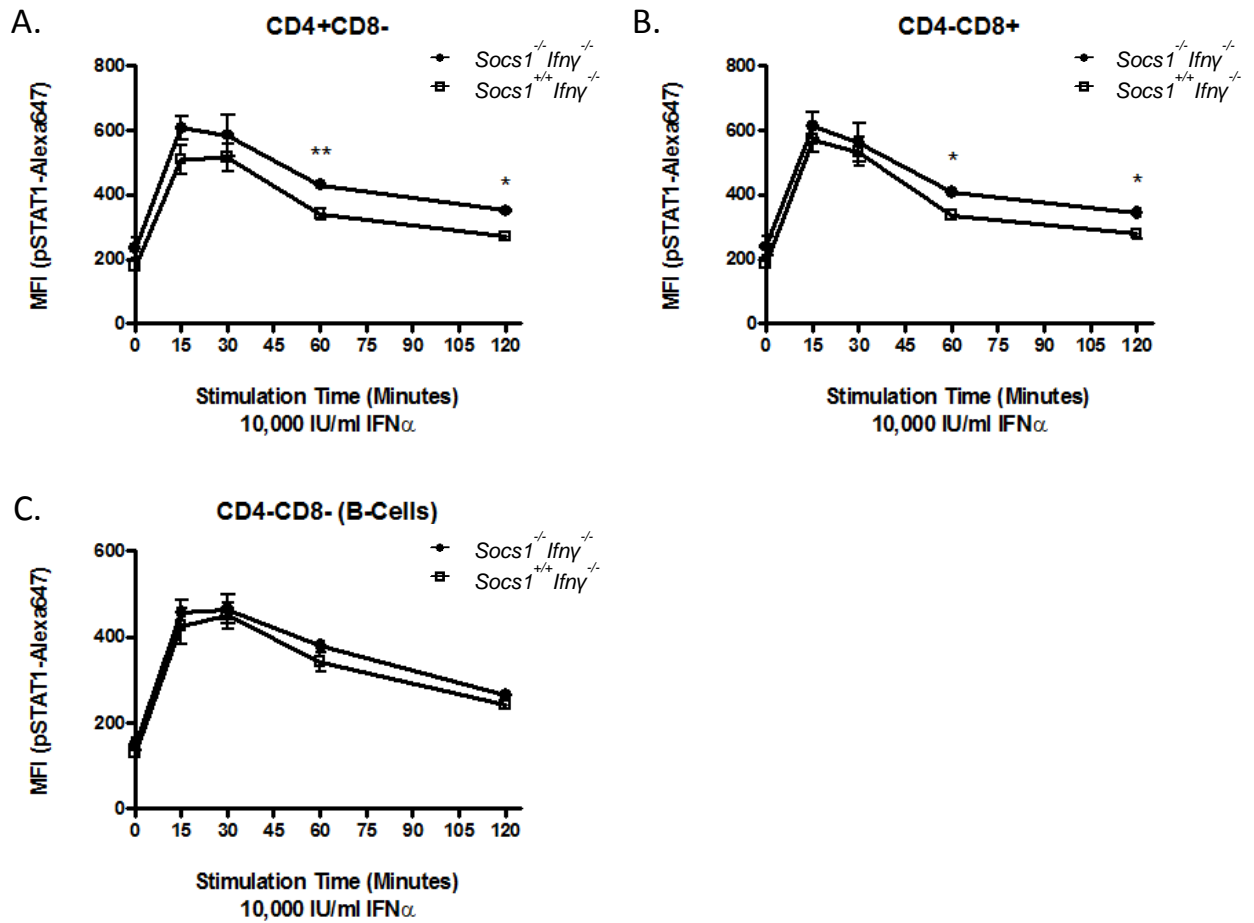


**Figure 4.17: Time course of IFN $\alpha$  induced Stat1 phosphorylation in splenic CD4/CD8 T-cell subsets and splenic B-cells from *Socs1*<sup>-/-</sup> *Ifny*<sup>-/-</sup> and *Socs1*<sup>+/+</sup> *Ifny*<sup>-/-</sup> mice.** The spleen was harvested from *Socs1*<sup>-/-</sup> *Ifny*<sup>-/-</sup> and *Socs1*<sup>+/+</sup> *Ifny*<sup>-/-</sup> C57BL/6 mice and single cell suspensions created. Cells were left untreated or stimulated with 10,000 IU/ml of IFN $\alpha$  for 15, 30, 60 or 120 minutes. Following cell fixation and permeabilisation, cells were incubated with surface marker antibodies (anti-CD4-FITC and anti-CD8-PE) in combination with pStat1-Alexa647. Cell subsets were separated based on surface marker expression of CD4-FITC and CD8-PE or MAC1-PE. The alexa647 MFI was calculated for each cell subset (**A.** CD4+CD8+, **B.** CD4+CD8- and **C.** CD4-CD8-) and time point. Data is presented as mean +/- SEM of N = 3-5 separate experiments. \* = p  $\leq$  0.05, \*\* = p  $\leq$  0.01, \*\*\* = p  $\leq$  0.005.

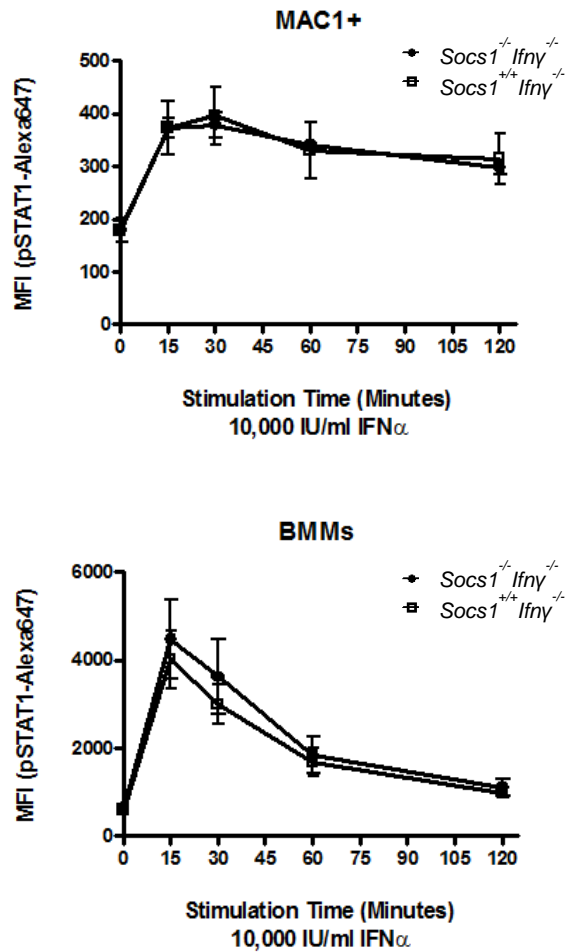


**Figure 4.18: Time course of IFN $\alpha$  induced Stat1 phosphorylation in splenic macrophages and BMMs.** The spleen was harvested from *Socs1*<sup>-/-</sup> *Ifny*<sup>-/-</sup> and *Socs1*<sup>+/+</sup> *Ifny*<sup>-/-</sup> C57BL/6 mice and single cell suspensions created. BMMs were harvested and cultured from *Socs1*<sup>-/-</sup> *Ifny*<sup>-/-</sup> and *Socs1*<sup>+/+</sup> *Ifny*<sup>-/-</sup> C57BL/6 mice. Cells were left untreated or stimulated with 10,000 IU/ml of IFN $\alpha$  for 15, 30, 60 or 120 minutes. Following cell fixation and permeabilisation, splenic cells were incubated with anti-MAC1-PE in combination with pStat1-Alexa647 and BMMs were incubated with pStat1-Alexa647 alone. Splenic cell subsets were separated based on surface marker expression of MAC1-PE. The alexa647 MFI was calculated for MAC1+ cells and BMMs at each time point. Data is presented as mean  $\pm$  SEM of N = 3-5 separate experiments. \* =  $p \leq 0.05$ , \*\* =  $p \leq 0.01$ , \*\*\* =  $p \leq 0.005$ .

58 at basal levels (33% increase), 99 at 15 minutes (19% increase), 69 at 30 minutes (13% increase), 92 ( $p < 0.01$ ) at 60 minutes (27% increase) and 82 ( $p < 0.05$ ) at 120 minutes post-IFN $\alpha$  stimulation (30% increase). For CD4-CD8+ T-cells from *Socs1<sup>-/-</sup>Ifn $\gamma$ <sup>-/-</sup>* compared to *Socs1<sup>+/+</sup>Ifn $\gamma$ <sup>-/-</sup>* mice, there is a difference in MFI of 55 (30% increase) at basal levels, 45 at 15 minutes (8% increase), 29 at 30 minutes (5% increase), 72 ( $p < 0.05$ ) at 60 minutes (21% increase) and 65 ( $p < 0.05$ ) at 120 minutes post-IFN $\alpha$  stimulation (23% increase). There were no significant differences in pSTAT1 levels observed in splenic CD4-CD8- or MAC1+ cells between the two genotypes. For BMMs there were no significant differences in pSTAT1 induction between the two genotypes.

SOCS1 mediated differences in basal STAT1 phosphorylation and IFN $\alpha$  induced STAT1 phosphorylation were greatest in thymic T-cell subsets compared to peripheral T-cells whereas there were no differences in CD4-CD8- and MAC1+ cells. This is probably due to the thymus being the tissue of highest basal SOCS1 expression (Marine, Topham et al. 1999). STAT3 and STAT5 phosphorylation were therefore also analysed in CD4+/CD8+ populations of thymic T-cells.

#### 4.6.2 STAT3 phosphorylation

Thymic pSTAT3 basal levels were significantly greater in CD4+CD8+, CD4+CD8- and CD4-CD8+ T-cells from *Socs1<sup>-/-</sup>Ifn $\gamma$ <sup>-/-</sup>* compared to *Socs1<sup>+/+</sup>Ifn $\gamma$ <sup>-/-</sup>* mice (Figure 4.15 B). The differences however were not as pronounced as for those seen with pSTAT1, with the highest difference of 1.3-fold in CD4-CD8+ cells. Upon IFN $\alpha$  stimulation pSTAT3 levels were also significantly greater in thymic cells from *Socs1<sup>-/-</sup>Ifn $\gamma$ <sup>-/-</sup>* compared to *Socs1<sup>+/+</sup>Ifn $\gamma$ <sup>-/-</sup>* mice, although like with basal levels, these were lower as compared to the differences with pSTAT1 (Figure 4.19). For CD4+CD8+ T-cells, the difference in MFI of cells from *Socs1<sup>-/-</sup>Ifn $\gamma$ <sup>-/-</sup>* compared to *Socs1<sup>+/+</sup>Ifn $\gamma$ <sup>-/-</sup>* mice were 7.45 ( $p < 0.005$ ) at basal levels (15% increase), similar at 15 minutes post-stimulation, 18.9 ( $p < 0.01$ ) at 30 minutes (27% increase) and 15.43 ( $p < 0.05$ ) at 60 minutes post-stimulation (31% increase). For CD4+CD8- T-cells, the difference in MFI of cells from *Socs1<sup>-/-</sup>Ifn $\gamma$ <sup>-/-</sup>* compared to *Socs1<sup>+/+</sup>Ifn $\gamma$ <sup>-/-</sup>* mice were 20.38 ( $p < 0.005$ ) at basal levels (24% increase), 37.5 ( $p < 0.005$ ) at 15 minutes post-stimulation (28% increase), 36.25 ( $p < 0.01$ ) at 30 minutes (31% increase) and 29.95 ( $p < 0.01$ ) at 60 minutes post-stimulation (37% increase). For CD4-CD8+ T-cells, the difference in MFI of cells from *Socs1<sup>-/-</sup>Ifn $\gamma$ <sup>-/-</sup>* compared to *Socs1<sup>+/+</sup>Ifn $\gamma$ <sup>-/-</sup>* mice were 35.25 ( $p < 0.05$ ) at basal levels (31% increase), 74.75 ( $p < 0.005$ ) at 15 minutes post-stimulation (39% increase), 61.5 ( $p < 0.01$ ) at 30

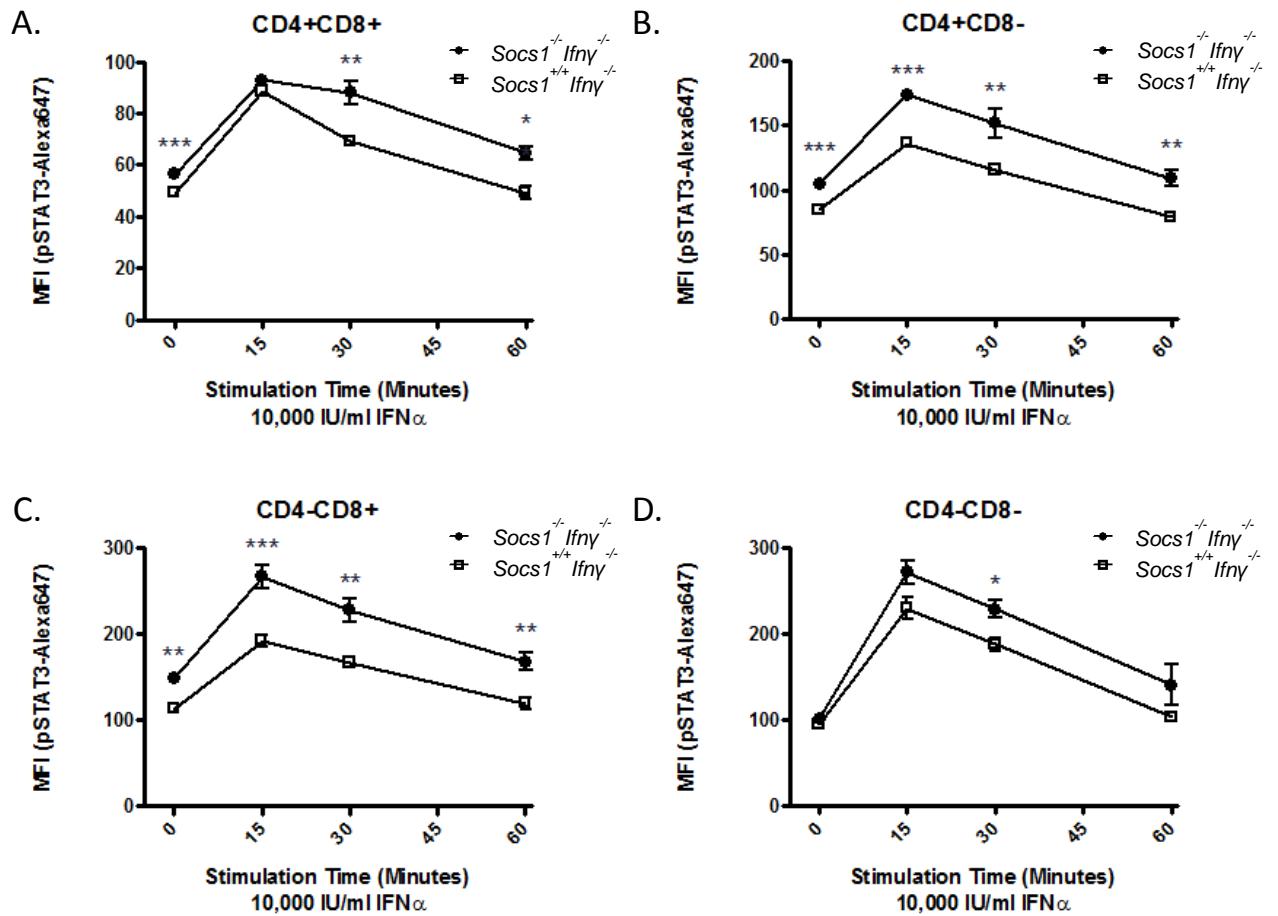


**Figure 4.19: Time course of IFN $\alpha$  induced Stat3 phosphorylation in thymic CD4/CD8 T-cell subsets from *Socs1*<sup>-/-</sup> *Ifny*<sup>-/-</sup> and *Socs1*<sup>+/+</sup> *Ifny*<sup>-/-</sup> mice.** Thymus was harvested from *Socs1*<sup>-/-</sup> *Ifny*<sup>-/-</sup> and *Socs1*<sup>+/+</sup> *Ifny*<sup>-/-</sup> C57BL/6 mice and single cell suspensions created. Cells were left untreated or stimulated with 10,000 IU/ml of IFN $\alpha$  for 15, 30, or 60 minutes. Following cell fixation and permeabilisation, cells were incubated with surface marker antibodies (anti-CD4-FITC and anti-CD8-PE) in combination with pStat3-Alexa647. Cell subsets were separated based on surface marker expression of CD4-FITC and CD8-PE. The alexa647 MFI was calculated for each cell subset (**A.** CD4+CD8+, **B.** CD4+CD8-, **C.** CD4-CD8+ and **D.** CD4-CD8-) and time point. Data is presented as mean  $\pm$  SEM of N = 3-5 separate experiments. \* =  $p \leq 0.05$ , \*\* =  $p \leq 0.01$ , \*\*\* =  $p \leq 0.005$ .

minutes (37% increase) and 48.75 ( $p < 0.01$ ) at 60 minutes post-stimulation (41% increase). For CD4-CD8- T-cells, the difference in MFI of cells from *Socs1<sup>-/-</sup>Ifn $\gamma$ <sup>-/-</sup>* compared to *Socs1<sup>+/+</sup>Ifn $\gamma$ <sup>-/-</sup>* mice were similar at basal levels, 41.75 at 15 minutes post-stimulation (18% increase), 41.25 ( $p < 0.05$ ) at 30 minutes (22% increase) and 37.8 ( $p < 0.01$ ) at 60 minutes post-stimulation (37% increase).

#### 4.6.3 STAT5 phosphorylation

In contrast to pSTAT1 and pSTAT3 (to a lesser extent), basal pSTAT5 appears independent of SOCS1 negative regulation (Figure 4.15 C). No significant differences in basal pSTAT5 were observed in CD4-CD8-, CD4+CD8- or CD4-CD8+ T-cells from *Socs1<sup>-/-</sup>Ifn $\gamma$ <sup>-/-</sup>* compared to *Socs1<sup>+/+</sup>Ifn $\gamma$ <sup>-/-</sup>* mice. A small difference (16% decrease) was observed basally in CD4+CD8+ T-cells from *Socs1<sup>-/-</sup>Ifn $\gamma$ <sup>-/-</sup>* mice as compared to *Socs1<sup>+/+</sup>Ifn $\gamma$ <sup>-/-</sup>* mice, displayed decreased STAT5 phosphorylation in cells lacking SOCS1. Upon IFN $\alpha$  stimulations, minor differences were seen in pSTAT5 induction in *Socs1<sup>-/-</sup>Ifn $\gamma$ <sup>-/-</sup>* compared to *Socs1<sup>+/+</sup>Ifn $\gamma$ <sup>-/-</sup>* mice in CD4+CD8+ and CD4+CD8- T-cells and at limited times post-stimulation, unlike STAT1 for which differences were seen at all times (Figure 4.20). With 15 minutes IFN $\alpha$  stimulation, CD4+CD8+ and CD4+CD8- T-cells contained lower pSTAT5 levels in the absence of SOCS1 with an MFI change of 231 (23% decrease) and 269 (16% decrease) respectively. This suggests SOCS1 does not have a negative regulatory role in controlling STAT5 phosphorylation early on. By 60 minutes post-stimulation, however, pSTAT5 levels were slightly increased in CD4+CD8+, CD4+CD8-, CD4-CD8+ cells lacking SOCS1 with an MFI change of 115.5 (49% increase), 215 (50% increase), and 176 (28% increase) respectively.

#### 4.6.4 Summary and Discussion

Basal STAT1 phosphorylation levels were significantly higher in thymic cells from *Socs1<sup>-/-</sup>Ifn $\gamma$ <sup>-/-</sup>* compared to *Socs1<sup>+/+</sup>Ifn $\gamma$ <sup>-/-</sup>* mice. Basal STAT3 phosphorylation levels were also higher; however this was not as pronounced as for that seen with STAT1. In comparison, there were very limited differences in basal STAT5 phosphorylation levels. Following IFN $\alpha$  stimulation, STAT1 and STAT3 phosphorylation was enhanced and prolonged in the thymus of *Socs1<sup>-/-</sup>Ifn $\gamma$ <sup>-/-</sup>* compared to *Socs1<sup>+/+</sup>Ifn $\gamma$ <sup>-/-</sup>* mice. This again was more pronounced for STAT1. This indicates a role for SOCS1 in the negative regulation of STAT1 and STAT3 phosphorylation. In contrast, IFN $\alpha$  induced STAT5 phosphorylation was lower in *Socs1<sup>-/-</sup>Ifn $\gamma$ <sup>-/-</sup>* compared to *Socs1<sup>+/+</sup>Ifn $\gamma$ <sup>-/-</sup>* mice at early time-points. These results therefore indicate SOCS1 does not negatively regulate

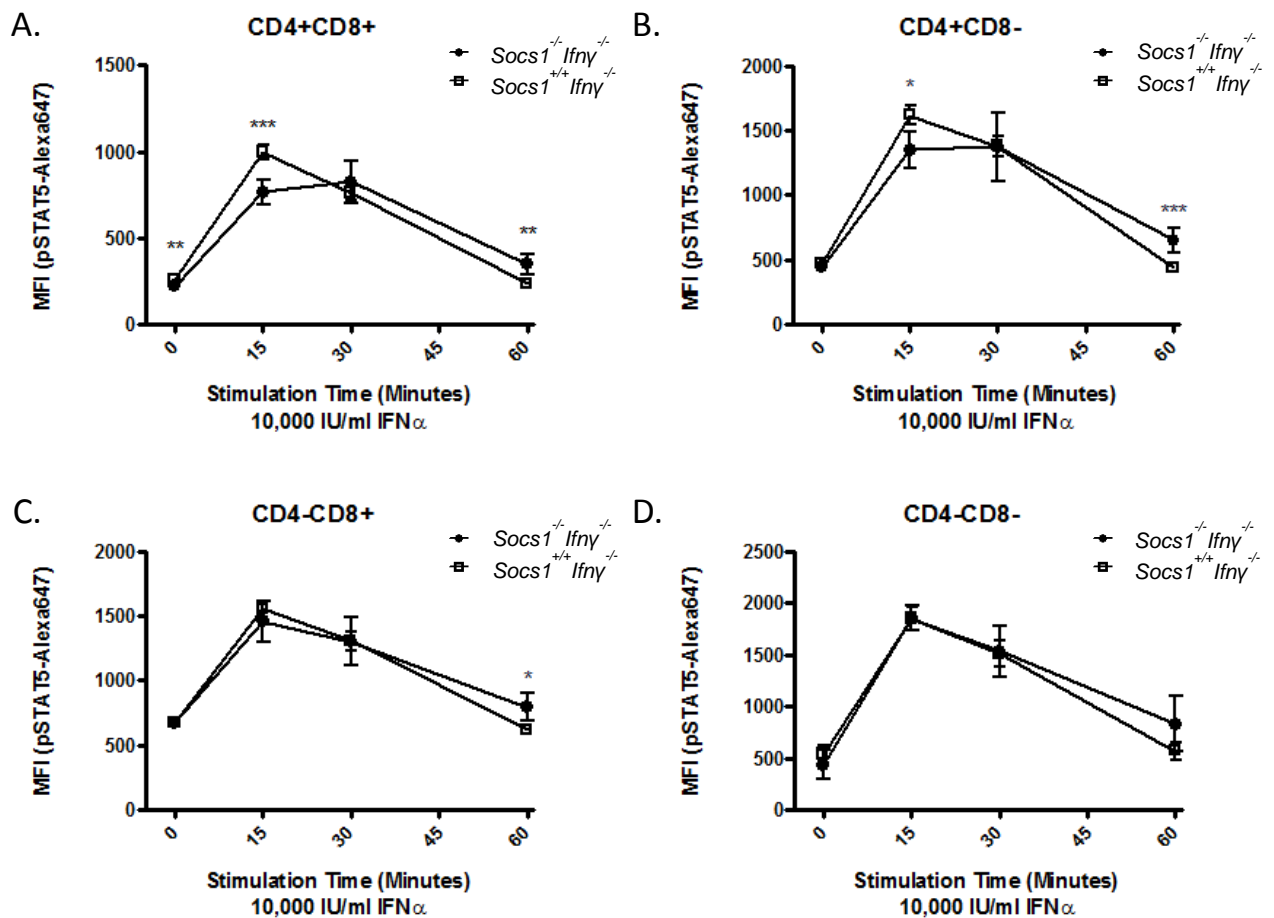


**Figure 4.20: Time course of IFN $\alpha$  induced Stat5 phosphorylation in thymic CD4/CD8 T-cell subsets from *Socs1*<sup>-/-</sup> *Ifny*<sup>-/-</sup> and *Socs1*<sup>+/+</sup> *Ifny*<sup>-/-</sup> mice.**

Thymus was harvested from *Socs1*<sup>-/-</sup> *Ifny*<sup>-/-</sup> and *Socs1*<sup>+/+</sup> *Ifny*<sup>-/-</sup> C57BL/6 mice and single cell suspensions created. Cells were left untreated or stimulated with 10,000 IU/ml of IFN $\alpha$  for 15, 30, or 60 minutes. Following cell fixation and permeabilisation, cells were incubated with surface marker antibodies (anti-CD4-FITC and anti-CD8-PE) in combination with pStat5-Alexa647. Cell subsets were separated based on surface marker expression of CD4-FITC and CD8-PE. The alexa647 MFI was calculated for each cell subset (**A.** CD4+CD8+, **B.** CD4+CD8-, **C.** CD4-CD8+ and **D.** CD4-CD8-) and time point. Data is presented as mean +/- SEM of N = 3-5 separate experiments. \* = p  $\leq$  0.05, \*\* = p  $\leq$  0.01, \*\*\* = p  $\leq$  0.005.

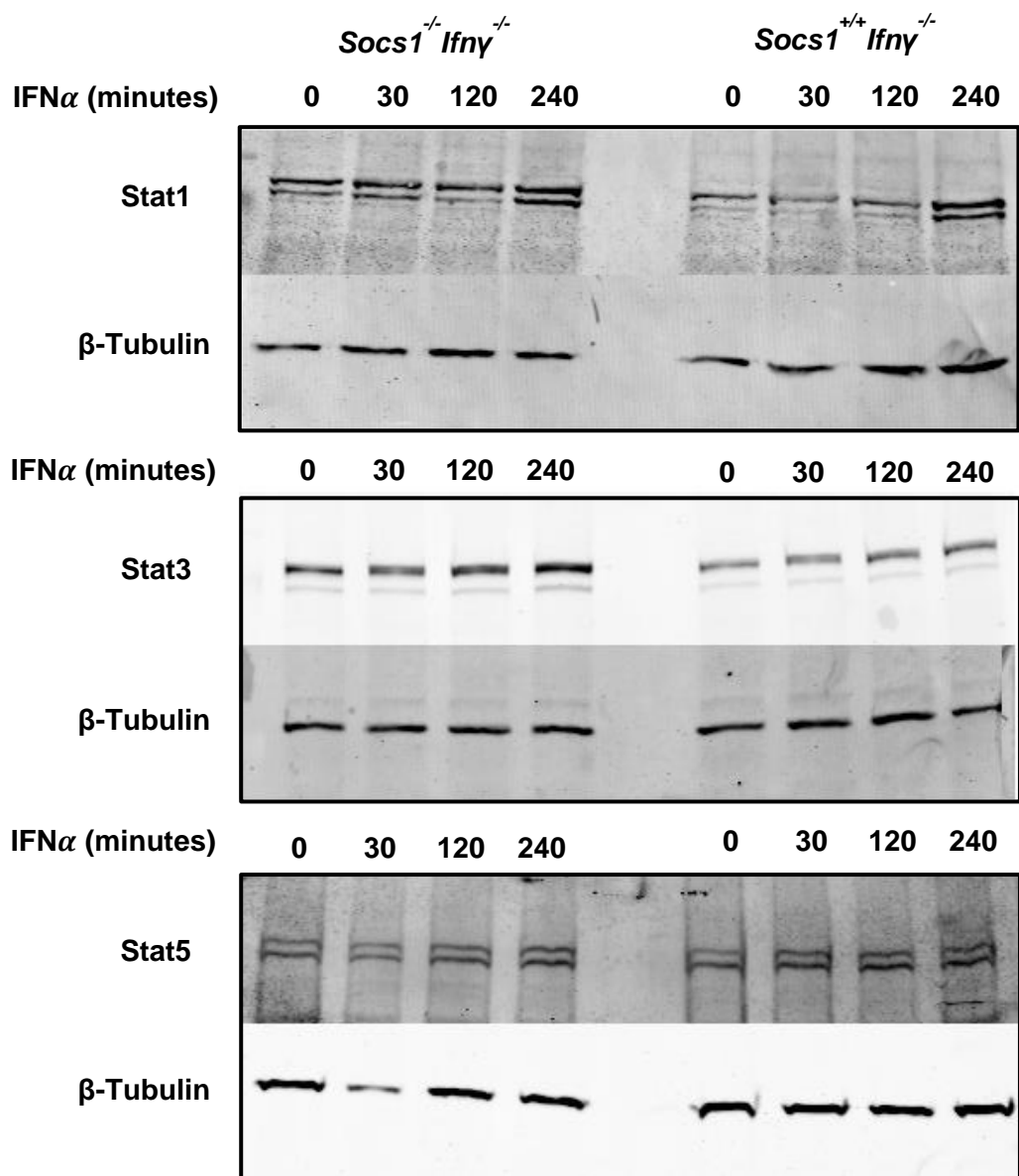
STAT5 phosphorylation basally or in the context of IFN $\alpha$  signaling at early time-points. Rather than a negative regulatory role, SOCS1 may have a minor positive regulatory role on STAT5 phosphorylation. As chapter 3 shows SOCS1 acts through TYK2, perhaps STAT5 phosphorylation is independent of TYK2. At later time points however there was increased STAT5 phosphorylation in the absence of SOCS1. As this negative change is only seen at later time-points, and is minor, these differences may be due to secondary effects of SOCS1. For example, as shown in Chapter 3, SOCS1 affects IFN $\alpha$  signaling through reduction of receptor expression at the cell surface and thus may contribute to differences in STAT5 at the later time points.

It is evident SOCS1 selectively alters the balance of STATs within the cell. As discussed previously, SOCS1 is essential in maintaining appropriate IFN $\alpha$  signaling events and in the absence of SOCS1 IFN $\alpha$  signaling proceeds unchecked resulting in uncontrolled inflammation and a high resistance to viral infection (Fenner, Starr et al. 2006). As I have shown here, SOCS1 controls both STAT1 and STAT3 phosphorylation. It is therefore likely these inflammatory events and viral resistance are mediated by STAT1 and STAT3. This is in contrast to STAT5 and may reflect the importance of IFN $\alpha$  induced STAT5 signaling to be maintained in the thymus during infection. STAT5 is a critical factor in mediating T-cell differentiation, most notably through the IL-7 signaling pathway. As mentioned previously, IFN $\alpha$  interferes with IL-7 induced growth and survival of T-cells and perhaps this is important to maintain even when other IFN $\alpha$  pathways need to be negatively controlled to maintain homeostasis (Lin, Dong et al. 1998).

#### **4.7 Total STAT1, STAT3 and STAT5 expression levels in the thymus of *Socs1*<sup>-/-</sup>*Ifn* $\gamma$ <sup>-/-</sup> and *Socs1*<sup>+/+</sup>*Ifn* $\gamma$ <sup>-/-</sup> mice.**

To identify whether the differences seen in the STAT phosphorylation of thymic cells from *Socs1*<sup>-/-</sup>*Ifn* $\gamma$ <sup>-/-</sup> compared to *Socs1*<sup>+/+</sup>*Ifn* $\gamma$ <sup>-/-</sup> mice were due to protein expression changes, the total level of STAT1, STAT3 and STAT5 protein expression was investigated in the thymus of *Socs1*<sup>-/-</sup>*Ifn* $\gamma$ <sup>-/-</sup> and *Socs1*<sup>+/+</sup>*Ifn* $\gamma$ <sup>-/-</sup> mice by western blot analysis. The thymus was harvested and a single cell suspension of 10<sup>7</sup> cells per ml was created. Cells were stimulated with 10,000 IU/ml of IFN $\alpha$  for indicated time points. Following stimulation, cells were lysed and SDS-PAGE and western blot performed to compare STAT protein expression levels between the two genotypes. STAT1, STAT3

**4.21 Total Stat1, Stat3 and Stat5 levels in the thymus of *Socs1*<sup>-/-</sup> *Ifnγ*<sup>-/-</sup> and *Socs1*<sup>+/+</sup> *Ifnγ*<sup>-/-</sup> mice following IFNα stimulation.** Whole thymus was harvested from *Socs1*<sup>-/-</sup> *Ifnγ*<sup>-/-</sup> and *Socs1*<sup>+/+</sup> *Ifnγ*<sup>-/-</sup> mice and a single cell suspension created. 10<sup>7</sup> cells per condition were stimulated with 10,000 IU/ml of IFNα for the indicated time points. Cells were lysed and proteins separated by SDS-PAGE and transferred to nitrocellulose membrane for detection by western blot analysis. Membranes were probed with anti-Stat1, Stat3 or Stat5 antibodies with an appropriate fluorescence conjugated secondary antibody for detection via odyssey. Membranes were then stripped and probed with anti-β-tubulin and appropriate fluorescence conjugated secondary antibody for detection via odyssey. Data is representative of 3 separate experiments.



and STAT5 protein expression in the thymus of *Socs1<sup>-/-</sup>Ifn $\gamma$ <sup>-/-</sup>* and *Socs1<sup>+/+</sup>Ifn $\gamma$ <sup>-/-</sup>* mice are displayed in Figure 4.21 and are representatives of triplicate experiments. Results demonstrate that STAT1 and STAT3 protein expression were higher in cells lacking SOCS1. In contrast, STAT5 expression was similar in both genotypes. These results are consistent with that of basal phospho-STAT levels where STAT1 and STAT3 phosphorylation were increased in cells lacking SOCS1 whereas STAT5 phosphorylation was similar. Some of the differences seen with STAT1 and STAT3 phosphorylation levels may therefore be attributed to total STAT levels within the cell. From this data it is also evident that STAT1 protein expression was similar to basal levels at early IFN $\alpha$  time-points and increased at 240 minutes post-IFN $\alpha$  stimulation in both genotypes. This reflects that status of STAT1 as a known IFN $\alpha$  inducible gene. In contrast STAT3 and STAT5 remained relatively similar following IFN $\alpha$  stimulation.

#### **4.8 Summary**

STAT1 phosphorylation is induced in response to type I IFN in all major T-cell populations of the thymus as well as in peripheral T-cells, B-cells and monocytes. In contrast, IFN $\alpha$  induction of STAT3 and STAT5 phosphorylation is limited to thymic T-cell populations. SOCS1 negatively regulates IFN $\alpha$  induced STAT1 and STAT3 phosphorylation but not STAT5.

## CHAPTER 5

### IFN $\alpha$ AND SOCS1 REGULATION OF GENE EXPRESSION IN THE THYMUS

Type I IFN stimulation results in the activation of multiple signaling pathways which regulate the expression of an array of genes. SOCS1 has an essential role in the regulation of type I IFN signaling (Fenner, Starr et al. 2006). Previous chapters looked at cell-type specific activation of different STAT pathways and demonstrated some that were/were not SOCS1 regulated. In this chapter I sought to complement these studies with expression profiling to examine the extent of gene regulation by IFN $\alpha$  and SOCS1 in the thymus and correlate these to the STAT signaling pathways.

To investigate the effects of IFN $\alpha$  and SOCS1 mediated gene regulation in the type I IFN pathway, the gene expression profiles of the thymus of wild type, *Socs1*<sup>-/-</sup>*Ifn $\gamma$* <sup>-/-</sup> and *Socs1*<sup>+/+</sup>*Ifn $\gamma$* <sup>-/-</sup> mice were compared in response to an IFN $\alpha$  treatment time course,. As mentioned previously, *Socs1*<sup>-/-</sup> mice are not viable and I must therefore compare *Socs1*<sup>-/-</sup>*Ifn $\gamma$* <sup>-/-</sup> mice to *Socs1*<sup>+/+</sup>*Ifn $\gamma$* <sup>-/-</sup> mice to analyse the effects of SOCS1. The thymus was chosen as the tissue to perform the microarray study since preliminary phosphoflow experiments, in the previous chapter, showed significant induction of STAT1, STAT3 and STAT5 phosphorylation in thymocytes in response to IFN $\alpha$  and that SOCS1 has the largest effect on STAT phosphorylation in immune cells from the thymus compared to other sources of immune cells (PBMCs and spleen). Furthermore evidence in the literature shows SOCS1 is most highly expressed in the thymus (Marine, Topham et al. 1999). It should be noted however that double positive CD4+CD8+ T-cells form the largest population of T-cells within the thymus and thus the microarray results will be most representative of the response of double positive T-cells to IFN $\alpha$ . This may therefore override the response that would be seen in smaller T-cell subsets such as single positive CD4+ or CD8+ T-cell populations.

This experiment consists of three different genotypes: wild type, *Socs1*<sup>-/-</sup>*Ifn $\gamma$* <sup>-/-</sup> and *Socs1*<sup>+/+</sup>*Ifn $\gamma$* <sup>-/-</sup>. Mice were injected intraperitoneally with 1000 IU of IFN $\alpha$  or with PBS (0 hour) (Chapter 2.4.2). At 3 and 6 hours later, the mice were culled and the thymus harvested (Chapter 2.4.3). Each condition was performed in triplicate to allow appropriate statistical tests to be performed. RNA extraction, purification and quality control were then performed (Chapter 2.4.4 – 2.4.6). An Agilent one-colour microarray

was performed using 4 x 44k mouse micorarray chips (Chapter 2.5.10). It should be noted that in some cases one gene may be represented by multiple probes on the microarray. The analysis may therefore refer to either probes or genes. Analysis of the microarray data was performed with Genespring GX and other bioinformatics analysis approaches (Chapter 2.5.11).

The outcome of this experiment was multi-faceted, providing information on:

- The response of the thymus to a time course of IFN $\alpha$  treatment
- Basal differences in gene expression due to SOCS1 regulation
- Type I IFN regulated genes that are SOCS1 regulated

The following chapter of this thesis analyses all three of these aspects to better understand type I IFN mediated gene regulation in the thymus, the difference between basal thymic gene expression in *Socs1<sup>-/-</sup>Ifn $\gamma$ <sup>-/-</sup>* vs. *Socs1<sup>+/+</sup>Ifn $\gamma$ <sup>-/-</sup>* mice and the consequence of SOCS1 on IFN $\alpha$  mediated gene regulation in the thymus.

### **5.1 Time Course of IFN $\alpha$ stimulation in the Thymus of Wild Type C57BL/6 mice**

The profile of gene expression in response to IFN $\alpha$  in the wild type mice was initially investigated. Normalisation, baseline transformation, filtering and statistical tests applied to the data are outlined in Chapter 2.5.11 and Figure 2.3. To summarise, samples were normalised to the 75<sup>th</sup> percentile (recommended for Agilent one-colour array) and the baseline transformed to the median of the 0hr samples for that genotype. Probes were then filtered based on expression values and flags to yield a list of 31504 probes. A cut off was performed to reduce the probe list to those probes greater or equal to a 2-fold difference between any two of the conditions. This reduced the list to 1534 probes. Two approached were used to identify genes significantly regulated with IFN $\alpha$  treatment and are described in chapter 2. A one way analysis of variance (ANOVA) with Benjamini Hochberg false discovery rate (BHFR) multiple testing correction was performed on the wild type IFN $\alpha$  time course to determine probes significantly ( $p < 0.05$ ) affected by IFN $\alpha$  treatment. This resulted in a list of 276 probes significantly regulated by type I IFN. In addition, unpaired student t-tests with BHFR multiple testing corrections were also performed on the probe list to identify probes significantly ( $p < 0.05$ ) regulated from the 0 to 3 or 0 to 6 hour time points. The probes

identified from the one way ANOVA and t-tests were combined into a single probe list (appendix IIIA). This list consists of 283 probes.

A heatmap of the gene expression profile of the 283 probes significantly changed with IFN $\alpha$  stimulation is shown in Figure 5.1. Of the 283 probes found significantly changed with IFN $\alpha$  treatment, 269 probes were up-regulated from basal levels within 3 hours. 86 of these probes were induced 2-3 fold above basal levels, 50 were induced 3-4 fold, 36 were induced 4-5 fold, 35 were induced 6-8 fold, 7 were induced 8-10 fold while 11 were induced greater than 10 fold. The most highly up-regulated genes include *Rsad2* (28.4-35 fold), *Cmpk2* (18.8-28.4 fold), *Mx2* (18 fold), *Dhx58 (RIG-I)* (14.5 fold), *Isg15* (14 fold), *Oas3* (12.8 fold), *Usp18* (11.8 fold), *Rtp4* (10.6 fold) and *Oasl1* (10.2 fold). 254 of the 269 probes up-regulated remained up-regulated with 6 hours IFN $\alpha$  treatment however most are reduced compared to 3 hours of IFN $\alpha$  treatment. Only 14 probes were down regulated with 3 hours of IFN $\alpha$  treatment. *Ucp1* was the most highly down-regulated gene (9.8 fold).

qRT-PCR, as described in Chapter 2.4.9, was utilised to validate the microarray data (Figure 5.2). Wt samples were analysed for *Isg15*, *Irgm1*, *Stat1*, *Irf7* and *Cxcl10* gene expression at 0 (PBS), 3, 6 and 24 hours following IFN $\alpha$  stimulation. The induction of each gene by IFN $\alpha$  was expressed relative to expression levels in unstimulated samples (0 hour/PBS). Results show significant induction of all genes analysed and these inductions are comparable to microarray results. RT-PCR results demonstrate *Irgm1* was induced approximately 5.5 fold above basal levels at 3 hours post IFN and 1.5 fold at 6 hours post IFN compared to a 5.8 fold and 1.3 fold induction, respectively, from microarray data. RT-PCR results demonstrate *Isg15* was induced approximately 15 fold above basal levels at 3 hours post IFN and 2.5 fold at 6 hours post IFN compared to a 14 fold and 2.3 fold induction, respectively, from microarray data. RT-PCR results demonstrate *Stat1* was induced approximately 4 fold above basal levels at 3 hours post IFN and 1.5 fold at 6 hours post IFN compared to a 3.7 fold and 1.4 fold induction, respectively, from microarray data. RT-PCR results demonstrate *Irf7* was induced approximately 5 fold above basal levels at 3 hours post IFN and 2.5 fold at 6 hours post IFN compared to a 7.3 fold and 2.3 fold induction, respectively, from microarray data. RT-PCR results demonstrate *Cxcl10* was induced approximately 3 fold above basal levels at 3 hours post IFN and not significantly at 6 hours post IFN compared to a 3.9 fold and an insignificant fold induction, respectively, from microarray data. Taken together, the magnitudes of change measured by RT-PCR were similar to

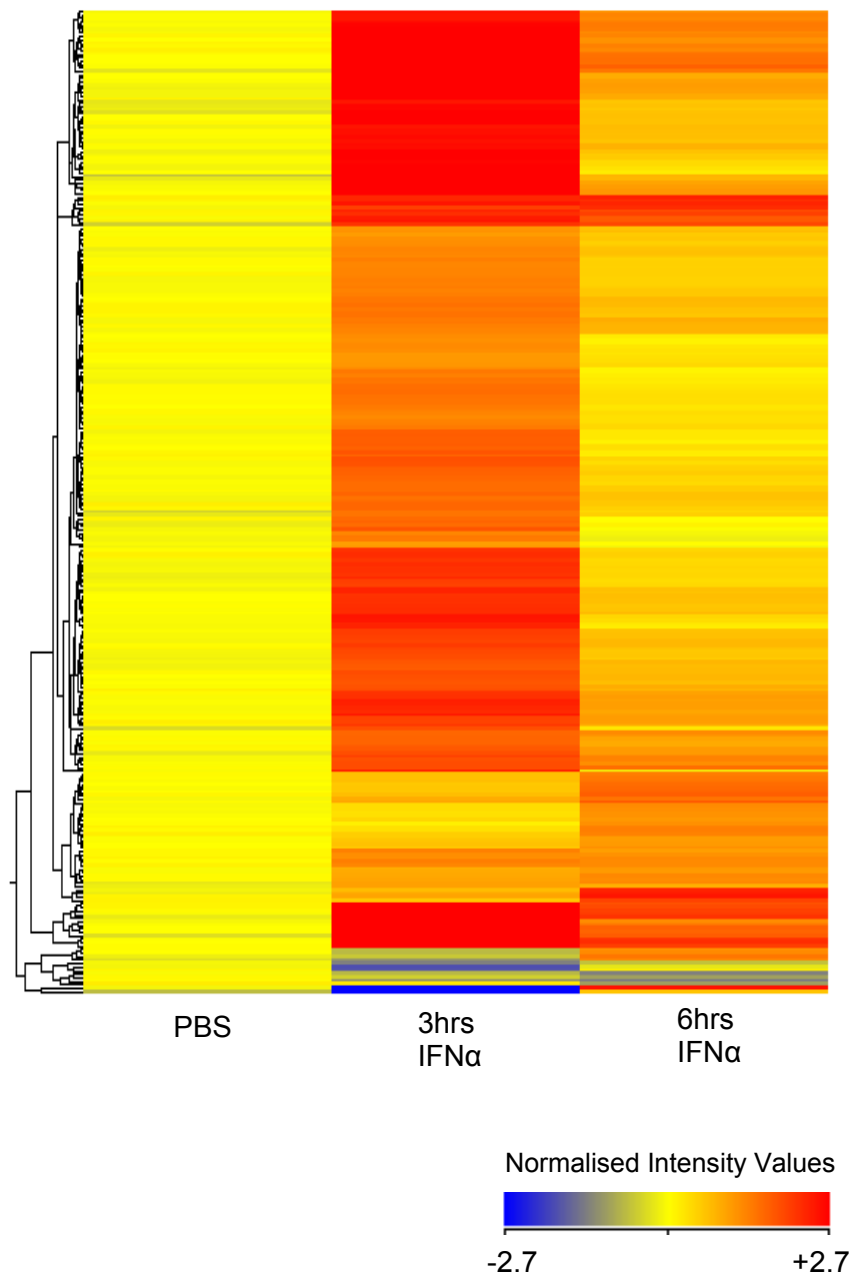
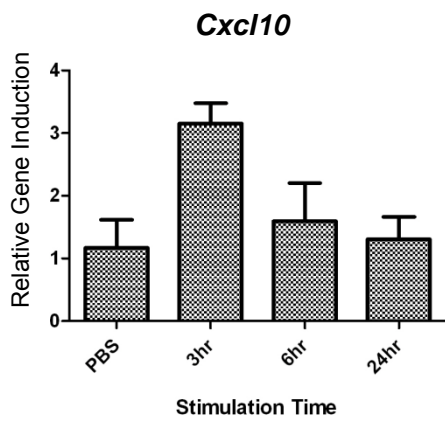
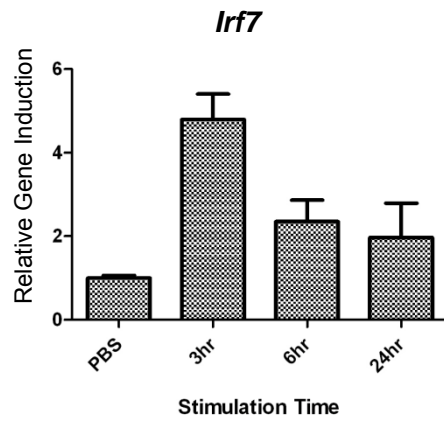
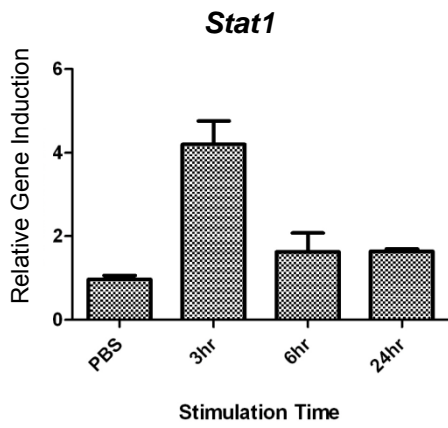
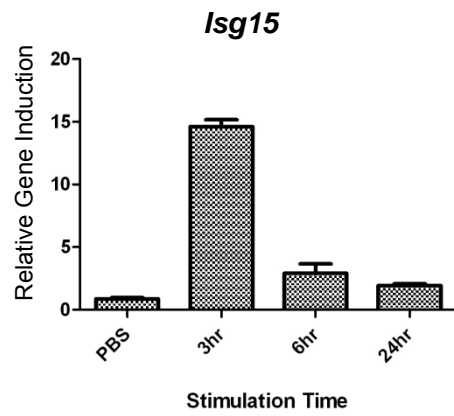
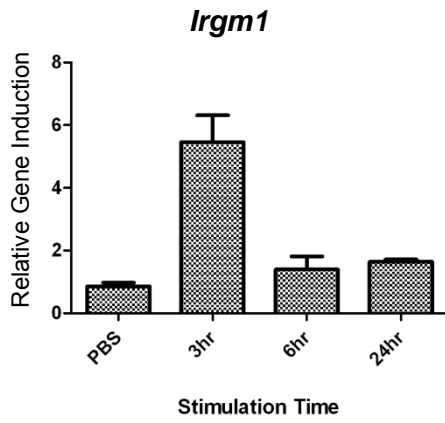


**Figure 5.1: Heatmap of IFN $\alpha$  regulated probes in the thymus of wt mice.** Statistical analysis was performed to identify probes significantly changed ( $p < 0.05$ ) in the thymus of wt mice with 3 hour and 6 hour IFN $\alpha$  stimulations (as described in Section 5.2). The heatmap of these probes was generated using hierarchical clustering in Genespring GX.

**Figure 5.2: qRT-PCR validation of microarray data.**

Quantitative RT-PCR analysis of *Irgm1*, *Isg15*, *Stat1*, *Irf7* and *Cxcl10* expression in the thymus of wt mice following 0, 3 6 and 24 hour stimulations with 1000 IU IFN $\alpha$  per mouse, administered intraperitoneally. Data is presented as mean  $\pm$  SEM of N = 3-5 separate experiments following normalisation to 18S and is expressed relative to unstimulated controls.



that measured by microarray, thus the microarray data can be considered an accurate, quantitative measure of relative gene expression changes.

To explore the function of the genes up-regulated with IFN $\alpha$  treatment, functional annotation analysis was performed with DAVID, as described in chapter 2.5.11. DAVID is a gene functional classification tool which uses a novel algorithm to cluster a set of genes or biological terms into classes of related genes or functions (Huang da, Sherman et al. 2007). This is achieved by mining and integrating data sourced from multiple independent functional annotation approaches, producing the most comprehensive functional gene classification system based on available data. This meta-analysis approach minimises annotation specific biases inherent in approaches such as Gene Ontology analysis alone. Enrichment scores (ES) for each functional group are calculated based on over-representation of the gene list compared to what would be expected by chance. A higher ES indicates the genes within that group are involved in more important roles, however all gene groups are considered important despite lower rankings (Huang da, Sherman et al. 2007). This type of analysis therefore gives an overview of the major biological functions of the genes analysed.

DAVID functional annotation analysis of the genes up-regulated with IFN $\alpha$  treatment (Table 5.1) identified a cluster of genes encoding proteins with GTP-binding and/or GTPase activities (ES 8.33) (Table 5.2). There are four classes of GTPases which include the Immunity-Related GTPases (IRGs, p47 family), the p65 family, the Mx family and the very large inducible GTPases (VLIGs), all of which are induced by IFN $\gamma$  and to a weaker degree by the type I IFNs (MacMicking 2004; Taylor, Feng et al. 2007). I have found that members of the p47, p65 and Mx GTPase families are up-regulated in thymocytes in response to IFN $\alpha$ . The different GTPases have varying roles within the cell to control pathogen infection and confer resistance to a diverse range of pathogens (Taylor, Feng et al. 2007). In the context of IFN $\alpha$  signaling, the up-regulation of GTPases is therefore likely to enhance resistance to a range of pathogens.

DAVID functional annotation also identified a cluster of genes with 2'-5'-oligoadenylate synthetase and transferase activities (ES 6.14) (Table 5.3). As discussed in Chapter 1, the 2'-5'-Oases are potent inhibitors of viral replication and known IFN inducible genes. DAVID functional annotation also identified a cluster of genes encoding proteins involved in the innate and defence response (ES 6.07) (Table 5.4). These include the

**Table 5.1: DAVID functional annotation clustering of genes up-regulated in the thymus of wt mice 3 and 6 hours post IFN $\alpha$ .** probes found to be up-regulated in the thymus of wt mice following 3 and 6 hour IFN $\alpha$  stimulations were converted to Ensemble Gene IDs with Ensemble Biomart. The Ensemble gene IDs were loaded into DAVID for functional annotation analysis with medium classification stringency.

<b>Functional Annotation</b>	<b>ES</b>
GTP-binding and/or GTPase activities	8.33
2'5'-OAS and/or transeferase activities	6.41
Innate and defence response	6.07
Purine nucleotide binding activities	4.73
Zinc finger domains and/or cation binding	4.06
PARP activity	3.25
Pyrin domains	3.24
Ubiquitination and proteolysis activity	1.91
DNA helicase activity and/or DNA repair	1.82
Cytokines and chemokines	1.83
Ubiquitin	1.16
Tetratricopetide containing domain	1.12
Positive regulation of response to stimulus and regulation of apoptosis	1.11

**Table 5.2: List of genes annotated with the GOTERM; GTPase activity or GTP binding, found up-regulated in wt mice 3 and 6 hours post IFN $\alpha$ .**

Gene Name	Ensemble Gene ID
RIKEN cDNA 9930111J21	ENSMUSG00000069893
Tgtp1	ENSMUSG00000078921
Tgtp2	ENSMUSG00000078922
BC057170	ENSMUSG00000029298
Gbp2	ENSMUSG00000028270
Gbp3	ENSMUSG00000028268
Gbp4	ENSMUSG00000079363
Gbp5	ENSMUSG00000040264
Gbp7	ENSMUSG00000040253
Irgm1	ENSMUSG00000046879
Irgm2	ENSMUSG00000069874
Igtp	ENSMUSG00000078853
Ifi47	ENSMUSG00000078920
Gbp6	ENSMUSG00000079362
Mx1	ENSMUSG00000000386
Mx2	ENSMUSG00000023341
predicted gene 12250	ENSMUSG00000082292
tubulin, alpha 3B;	ENSMUSG00000067338
tubulin, alpha 3A	ENSMUSG00000067702
pRIKEN cDNA 5830443L24 gene	ENSMUSG00000054588
predicted gene, OTTMUSG00000005523	ENSMUSG00000048852

**Table 5.3: List of genes annotated with the GOTERM; Transferase activity, found up-regulated in wt mice 3 and 6 hours post IFN $\alpha$ .**

<b>Gene Name</b>	<b>Ensemble Gene ID</b>
2'-5'OAS1A	ENSMUSG00000052776
2'-5'OAS1B	ENSMUSG00000029605
2'-5'OAS-like 1	ENSMUSG00000041827
2'-5'OAS-like 2	ENSMUSG00000029561
RIKEN cDNA 1300018I05	ENSMUSG00000024019
Cmpk2	ENSMUSG00000020638
Eif2ak2	ENSMUSG00000024079
PARP12	ENSMUSG00000038507
PARP14	ENSMUSG00000034422
PARP9	ENSMUSG00000022906
Papd7	ENSMUSG00000034575

**Table 5.4: List of genes annotated with the GOTERM; Defence Response, found up-regulated in wt mice 3 and 6 hours post IFN $\alpha$ .**

<b>Gene Name</b>	<b>Ensemble Gene ID</b>
Ddx58	ENSMUSG00000040296
Dhx58	ENSMUSG00000017830
Fcgr1	ENSMUSG00000015947
Ccl12	ENSMUSG00000035352
Ccl2	ENSMUSG00000035385
Ccl22	ENSMUSG00000031779
Ccl7	ENSMUSG00000035373
Cxcl10	ENSMUSG00000034855
Samhd1	ENSMUSG00000027639
Irgm1	ENSMUSG00000046879
Ido1	ENSMUSG00000031551
Ifi47	ENSMUSG00000078920
Ifih1	ENSMUSG00000026896
Mx1	ENSMUSG00000000386
Mx2	ENSMUSG00000023341
Rsad2	ENSMUSG00000020641
Spn	ENSMUSG000000051457
Thbs1	ENSMUSG00000040152
Tlr3	ENSMUSG00000031639
Tap1	ENSMUSG00000037321

Toll-like receptor, TLR3, as well as the RIG-I-like receptors RIG-I (Ddx58), MDA5 (Ifih1) and LPG2 (Dhx58) which play a critical role in the detection of virus infection.

Other functional clusters identified by DAVID contain genes encoding proteins with purine nucleotide binding activities (ES 4.73), zinc finger and cation binding domains (ES 4.06), PARP activity (ES 3.25), Pyrin domains (ES 3.24), DNA helicase activity and DNA repair (ES 1.82), ubiquitination and proteolysis activity (ES 1.91), cytokines and chemokines (ES 1.83), Ubiquitin (ES 1.16), tetratricopeptide containing domains (ES 1.12) as well as proteins involved in the positive regulation of response to stimulus and the regulation of apoptosis (ES 1.11). The induction of genes involved in the regulation of apoptosis suggests that IFN $\alpha$  may control apoptosis of thymocytes and modulate the T-cell repertoire. As mentioned in Chapter 4, previous studies have implicated that type I IFN has a role in controlling T-cell differentiation and survival within the thymus. One study indicates that IFN $\alpha$  is expressed constitutively in the thymus by resident pDCs and that it may play a role in negative T-cell selection within the medulla, increasing the susceptibility of T-cells to cell death and reducing the threshold needed for negative selection (Colantonio, Epeldegui et al. 2011).

From the diverse range of gene functions regulated by IFN $\alpha$ , it is evident a range of cell processes are involved in the response of the thymus to IFN $\alpha$  treatment. A large number of these genes contain anti-pathogenic and anti-viral functions and include *Gtpases*, *2'5 Oas's* and other innate immune activators or effectors including *Isg15*, *Rsad2*, *Rig-I* and *Tlr3*. Considering the potent anti-viral effects of IFN, the up-regulation of genes involved in innate immunity and host defence was expected.

The genes up-regulated by IFN $\alpha$  in wt thymus were analysed for transcription factor enrichment within their promoters. This analysis was performed to determine which transcription factors may be regulating expression of these genes, particularly which STAT family members may be involved. The analysis was performed using the program Cis-Element Over-Representation (Clover) as is outlined in Chapter 2.5.11.2. Clover analyses a sequence set to determine transcription factor binding motif over or under-representation compared to a background sequence set. The raw score (RS) calculated for each binding motif quantifies the degree of the motif's presence in the test sequences while the p-value represents the probability of obtaining the raw score by chance. A low p-value ( $p < 0.01$ ) indicates the binding motif is over-represented within the test sequences. The binding motifs tested were obtained from the

TRANSFAC database. Often one transcription factor may have multiple database entries and therefore appears multiple times in the analysis. The sequence set used for this analysis consisted of the promoter sequences 2000bp upstream of the transcript start site of the genes found up-regulated with IFN $\alpha$ . Transcription factors displaying over-representation within the promoters of these genes are presented in Table 5.5 and 5.6. Table 5.6 shows that genes up-regulated by IFN $\alpha$  contain over-representation of STAT family, IRF family and NF- $\kappa$ B transcription factor binding sites within their promoters. General IRF binding elements were most strongly over-represented (RS infinity,  $p = 0$ ). ISGF3 and ICSBP (IRF8) binding sites were also strongly over-represented (RS > 480,  $p = 0$ ). STAT3 (RS 385,  $p = 0$ ), IRF1 (RS 362,  $p = 0$ ), STAT5A (RS 325,  $p = 0.008$ ), STAT1 (RS 292,  $p = 0$ ), IRF7 (RS 170,  $p = 0$ ), NF- $\kappa$ B (RS 72.7,  $p = 0$ ) and IRF2 (RS 49.6,  $p = 0$ ) binding elements were also found to be over-represented. Table 5.6 shows over-representation of other transcription factors found to have strong association with these promoters. These include neuroD (RS 627,  $p = 0$ ), TFII-I (RS 608,  $p = 0$ ), GAGA (RS 580,  $p = 0$ ), PUR1 (RS 552,  $p = 0$ ), Blimp1 (RS 521,  $p = 0.003$ ) E2A (RS 521,  $p = 0.004$ ) and MET31 (RS 510,  $p = 0$ ) as well as a number of Ets family members which include PU.1 (RS 546,  $p = 0$ ), Ets2 (RS 537,  $p = 0$ ) and Ets1 (RS 509,  $p = 0$ ).

The enrichment of ISGF3 (STAT1/STAT2/IRF9), STAT1, STAT3 and STAT5A binding elements within the promoters of up-regulated genes was expected as the previous chapter showed STAT1, STAT3 and STAT5 were phosphorylated in all subsets of thymic T-cells following IFN $\alpha$  stimulation. The IRF family of transcription factors have a diverse range of functions from mediating innate antiviral responses to modulation of adaptive immunity such as control of hematopoietic cell differentiation (Battistini 2009). I found promoter enrichment of IRF1, IRF2, IRF7 and IRF8 (ICSBP) binding elements within the promoters of genes up-regulated upon IFN $\alpha$  stimulation. However, the general IRF binding motifs are similar to that of ISGF3 which binds the ISRE. IRF4 and IRF8, which are expressed only in immune cells have previously been shown to bind the ISRE (Ozato, Taylor et al. 2007). The presence of general IRF and IRF8 binding elements within the enrichment analysis may therefore reflect bona-fide IRF binding sites or over-representation of an ISRE.

It was unexpected to see a large number of transcription factors with stronger binding motif over-representation than the binding motifs of ISGF3 and other STAT family members. This may reflect the prevalence of sites occurring within each promoter, as

**Table 5.5: Over-represented IRF, STAT and NF- $\kappa$ B transcription factor binding elements within the promoters of genes up-regulated in the thymus of wt mice 3 and 6 hours post IFN $\alpha$ .** Clover promoter enrichment analysis was performed on sequences 2000bp upstream of the transcript start site of genes significantly up-regulated with 3 and 6 hours IFN $\alpha$  treatment in the thymus of wt mice. IRF, STAT or NF- $\kappa$ B binding elements found over-represented ( $p < 0.01$ ) and with a Raw value greater than 0 were extracted.

<b>TRANSFAC Transcription Factor Matrix</b>	<b>Raw Score</b>	<b>P-value</b>
IRF (M00972)	infinity	0
IRF (M00772)	infinity	0
ISGF3 (M00258)	484	0
ICSBP (M00258)	484	0
ICSBP (M00699)	482	0
STAT3 (M01595)	385	0
IRF-1 (M00747)	362	0
STAT (M00777)	354	0.009
STAT5A (M00499)	325	0.008
STAT1 (M01260)	292	0
IRF-7 (M00453)	170	0
STAT3 (M00497)	162	0.004
IRF-1 (M00062)	133	0
NF- $\kappa$ B (M00774)	72.7	0
STAT5A (M00457)	51.5	0.002
NF- $\kappa$ B (M00194)	50.3	0
IRF-2 (M00063)	49.6	0
NF- $\kappa$ B (M00054)	32.6	0
NF- $\kappa$ B (M00052)	24	0
NF- $\kappa$ B (M00208)	21.5	0

**Table 5.6: Over-represented transcription factor elements within IFN $\alpha$  up-regulated genes in the thymus of WT mice.** Clover promoter enrichment analysis was performed on sequences 2000bp upstream of the transcript start site of up-regulated with 3 and 6 hours IFN $\alpha$  treatment in the thymus of wt mice. IRF, STAT or NF- $\kappa$ B binding elements were excluded and the remaining top 30 elements found over-represented ( $p < 0.01$ ) were extracted.

<b>TRANSFAC Transcription Factor Matrix</b>	<b>Raw Score</b>	<b>P-value</b>
NeuroD (M01288)	672	0
TFII-I (M00706)	608	0
GAGA Factor (M00723)	580	0
PUR1 (M01721)	552	0
PU.1 (M00658)	546	0
ETS2 (M01207)	537	0
BLIMP1 (M01066)	521	0.003
E2A (M00804)	521	0.004
MET31(M01688)	510	0
c-Ets-1 (00339)	509	0
EAR2 (M01728)	499	0.003
MZF1 (M01733)	484	0.004
Ets (M00771)	478	0
Ets (M00971)	476	0
SMAD3 (M00701)	470	0
Poly (M00317)	422	0.03
Myogenin (M00712)	421	0
GCR2 (M01669)	412	0.005
RAV1 (M00344)	408	0
MET28 (M01674)	404	0
T3R (M00963)	387	0
ESE1 (M01214)	387	0
E2A (M00973)	386	0
Eve (M00629)	378	0
TAL1 (M00993)	375	0
SOX9 (M01284)	374	0.001
MAF (M00983)	370	0
Pax-4 (M00378)	368	0
NFAT2 (M01718)	367	0.008
MATH1 (M01716)	365	0

ISRE sites are typically only present once while other sites may occur multiple times in each promoter. Alternatively it may reflect IFN activation of a number of other pathways that are JAK/STAT independent. In addition to STAT and IRF promoter enrichment, we also found enrichment of NF- $\kappa$ B regulatory elements. NF- $\kappa$ B is highly activated upon TLR and cytosolic receptor stimulation, mediating innate immune responses and activating expression of type I IFNs (Martins and Calame 2008). Ets factors are a large family of transcription factors essential to the regulation of the immune system. So far a number have been implicated in the regulation of the immune system and include Ets1, Ets2, GABP, FLI1, Elf1, MEF, ESE1, PU.1 and SpiB (Gallant and Gilkeson 2006). In our promoter analysis we found enrichment of Ets1, Ets2, and PU.1. Ets1 and PU.1, which were highly enriched and have a large role in the regulation of immune cell development (Gallant and Gilkeson 2006). Further to this, IRF8 has been shown to interact with PU.1 and regulate gene expression (Tamura, Thotakura et al. 2005). We also found promoter over-representation of Blimp1 (PRDM1) binding elements. Blimp1 is a transcriptional repressor primarily known for its role in B-cell function, including the development of immunoglobulin secreting cells and the maintenance of long-lived plasma cells (Martins and Calame 2008). However, Blimp1 is also involved in T-cell function, including regulation of the survival, proliferation and differentiation of CD4+, CD8+ and CD4+ reg T-cells and can be induced by a range of cytokines (Xin, Nutt et al. 2011). The over-representation of Blimp1 binding elements indicates that Blimp1 may be induced by and mediate the effects of IFN $\alpha$  in the thymus. Alternatively, the set of genes regulated by IFN $\alpha$  may also be regulated in a different context, through Blimp1 or other transcription factors found over-represented, while sharing similar biological outcomes.

## **5.2 Thymic IFN $\alpha$ regulated genes and the Interferome**

In order to determine the extent to which this experiment had uncovered novel IFN regulated genes, I compared the data set of genes up-regulated with IFN $\alpha$  with the list of IFN regulated genes in the Interferome database. The Interferome is a database of IFN regulated genes compiled from multiple microarray analyses (Shamith A. Samarajiwa, Sam Forster, Katie Auchettl, and Paul J. Hertzog INTERFEROME: the database of interferon regulated genes Nucleic Acids Research Advance Access published on November 7, 2008). A Venn diagram was generated comparing the list of wt thymic IFN $\alpha$  regulated probes and the probes within the murine Interferome (Figure 5.3). The Interferome currently contains 3035 IFN regulated murine probes. Of the 283

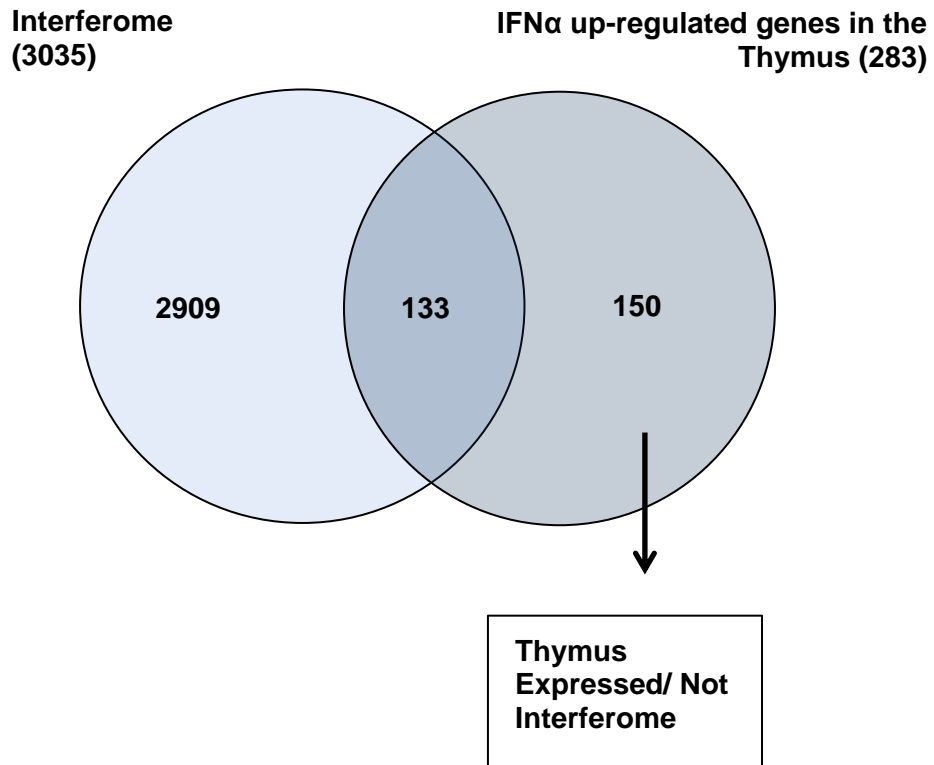


**Figure 5.3. Venn diagram of IFN $\alpha$  up-regulated probes and probes within the Interferome.** Probes found significantly regulated in the thymus of wt mice following 3 and 6 hour IFN $\alpha$  stimulations were compared to probes present within the Interferome. Of the 283 probes regulated in the thymus of wt mice following 3 and 6 hour IFN $\alpha$  stimulations, 133 were present in the Interferome whereas 150 were not.

probes identified as thymic IFN $\alpha$  regulated probes in the wild type mice, 133 are within the Interferome whereas 150 are not. Conversion of these 150 probes into ensemble IDs identifies 110 genes (appendix IIIB). These genes may represent novel IFN regulated genes with functions in the IFN response. The Interferome does not contain data from IFN stimulated thymocytes and therefore these genes may also be specific to IFN $\alpha$  regulation in the thymus.

DAVID functional annotation of the IFN $\alpha$  regulated genes absent or present from the Interferome are demonstrated in Table 5.7 and Table 5.8 respectively. For those genes absent from the Interferome, DAVID functional annotation clustering identified genes that encode proteins with 2'5'-OAS activities (ES 4.69), GTP binding and/or GTPase activities (ES 4.46), purine nucleotide binding (ES 3.68), innate immunity and the defence response with helicase activities (ES 3.21), zinc finger and/or metal binding affinities (ES 2.91), PARP activity (ES 2.13), the inflammatory response (ES 2.09) and positive regulation of apoptosis (ES 1.7), amongst others. Functional annotation clusters of the genes already present within the Interferome were very similar to those seen above and include genes that encode proteins with GTP binding and/or GTPase activities (ES 2.47), 2'5'-OAS activities (ES 2.3), purine nucleotide binding (ES 1.59) as well as zinc finger and/or metal binding (ES 0.91). There was however a lack of genes involved in inflammatory responses and genes involved in the positive regulation of apoptosis. Perhaps these functions of IFN $\alpha$  are more predominant within the thymus as compared to peripheral cells and may reflect the ability of IFN $\alpha$  to control T-cell survival and differentiation within the thymus.

Interestingly, some of the genes absent from the Interferome are still involved in typical IFN functions such as innate immunity and the defence response. Some of these are known IFN responsive genes, irrespective of expression within the thymus such as *Mx1*, the 2'5'-Oas isoform *Oas1b* and other *Oas-like* genes. The absence of some of these genes from the Interferome is therefore surprising. This may represent a gap of the gene sets currently contained within the Interferome or reflect the representation of genes on older microarray platforms that primarily comprise the Interferome database. As the Interferome is added to with increased experimental data it is likely this gap would decrease.

**Table 5.7: DAVID functional annotation clustering of the genes up-regulated in the thymus of wt mice 3 and 6 hours post IFN $\alpha$  that are *not* present within the Interferome.** The 150 probes found to be up-regulated in the thymus of wt mice following 3 and 6 hour IFN $\alpha$  stimulations and that were *not* present within the Interferome (Section 5.3) were converted to Ensemble Gene IDs with Ensemble Biomart. The Ensemble gene IDs were loaded into DAVID for functional annotation analysis with medium classification stringency.

<b>Functional Annotation</b>	<b>ES</b>
2'-5' OAS activities	4.69
GTP binding and/or GTPase activity	4.46
Purine nucleotide binding	3.68
Defence Response, Innate Immunity, Helicase	3.21
Zinc Finger and/or metal binding	2.91
PARP	2.13
Inflammatory Response	2.09
Positive Regulation of Apoptosis	1.7
Extracellular Region, secreted	1.68
Cellular Macromolecule catabolic process	1.32
Regulation of cytokine production	1.28
Tetratricopeptide region	1.26
Ubl conjugation	1.26
Glycoprotein, Signal peptide, Disulfide bond and inflammatory response	0.86

**Table 5.8: DAVID functional annotation clustering of the genes up-regulated in the thymus of wt mice 3 and 6 hours post IFN $\alpha$  that are present within the Interferome.** The 126 probes found to be up-regulated in the thymus of wt mice following 3 and 6 hour IFN $\alpha$  stimulations and that were also present within the Interferome (Section 5.3) were converted to Ensemble Gene IDs with Ensemble Biomart. The Ensemble gene IDs were loaded into DAVID for functional annotation analysis with medium classification stringency.

<b>Functional Annotation</b>	<b>ES</b>
GTP binding and/or GTPase activity	2.47
2'-5' OAS activities	2.3
Purine nucleotide binding	1.59
Zinc finger domains and/or metal binding	0.91
Transferase Activity	0.8
Immunoglobulin-like folds	0.71
Plasma membrane part	0.7

Promoter enrichment analysis of STAT family, IRF family and NF- $\kappa$ B transcription factors was performed on the list of genes that are absent (Table 5.9) or present (Table 5.10) from the Interferome. Many promoter binding elements were similar between the two lists and include ISGF3, STAT3, IRF7, IRF8 and NF $\kappa$ B binding elements. There were however some differences, notably, STAT5 was over-represented (RS 164,  $p = 0$ ) within the list of genes absent from the Interferome yet was not found within the list of genes currently within the Interferome.

Chapter 4 demonstrates that STAT3 and STAT5 are phosphorylated in the thymus in response to IFN $\alpha$  yet minimally or not at all peripheral immune cells (PBMCs and splenocytes). Considering the enrichment of STAT5 binding motifs within the promoters of genes found absent from the interferome and that the interferome does not yet contain thymic data, STAT5 may be an important transcription factor in mediating the regulation of genes within the thymus in response to IFN $\alpha$ . As STAT5 is not found to be enriched in genes currently within the interferome, it again supports the findings which suggest STAT5 is not activated in response to IFN $\alpha$  in peripheral cells. Although STAT3 binding sites were found to be enriched in both gene sets, the absence of IFN $\alpha$  induced STAT3 phosphorylation in peripheral cells, as shown in Chapter 4, suggest that STAT3 may too be important in mediating the regulation of genes within the thymus in response to IFN $\alpha$ . The identification of STAT3 binding sites within both gene lists may therefore represent the ability of STAT1 and STAT3 to regulate a similar set of genes or may be due to a redundancy of STAT sites within the TRANSFAC database. Nevertheless, it is likely that some of the differences in gene induction in thymic vs. peripheral T-cells are due to differences in STAT5 and STAT3 phosphorylation. The differences observed between the thymus and peripheral cells may be due to a number of reasons such as differences in the basal levels of STAT3 or STAT5, the presence of co-activators within thymic T-cells that are not present in peripheral cells or the presence of inhibitors within peripheral T-cells that are not present in thymic T-cells. A better understanding of the mechanisms leading to IFN induced STAT5 phosphorylation may provide an explanation as to how STAT5 is differentially regulated by IFN in different cell types.

**Table 5.9: Over-represented IRF, STAT and NF- $\kappa$ B transcription factor binding elements within the promoters of genes up-regulated in the thymus of wt mice 3 and 6 hours post IFN $\alpha$  and that were not present within the Interferome.** Clover promoter enrichment analysis was performed on sequences 2000bp upstream of the transcript start site of genes significantly up-regulated with 3 and 6 hours IFN $\alpha$  treatment in the thymus of wt mice and that were not present within the Interferome. IRF, STAT or NK- $\kappa$ B binding elements found over-represented ( $p < 0.01$ ) and with a Raw value greater than 0 were extracted.

<b>TRANSFAC Transcription Factor Matrix</b>	<b>Raw Score</b>	<b>P-value</b>
IRF (M00772)	419	0
IRF (M00972)	370	0
ISGF3 (M00258)	180	0
ICSBP (M00699)	177	0
STAT5A (M00499)	164	0
IRF8 (M01665)	89.4	0.001
STAT5A (M00493)	84.4	0
STAT4 (M00498)	80.4	0.002
STAT3 (M00497)	78.2	0.003
IRF7 (M00453)	42.1	0
NF- $\kappa$ B (M00194)	22.3	0.005

**Table 5.10: Over-represented IRF, STAT and NF-κB transcription factor binding elements within the promoters of genes up-regulated in the thymus of wt mice 3 and 6 hours post IFNα and that were present within the Interferome.** Clover promoter enrichment analysis was performed on sequences 2000bp upstream of the transcript start site of genes significantly up-regulated with 3 and 6 hours IFNα treatment in the thymus of wt mice and that were present within the Interferome. IRF, STAT or NK-κB binding elements found over-represented ( $p < 0.01$ ) and with a Raw value greater than 0 were extracted.

<b>TRANSFAC Transcription Factor Matrix</b>	<b>Raw Score</b>	<b>P-value</b>
IRF (M00772)	625	0
IRF (M00972)	550	0
ICSBP (M00699)	310	0
ISGF-3 (M00258)	306	0
STAT3 (M01595)	299	0
STAT1 (M01260)	223	0
IRF1 (M00747)	221	0
STAT (M00777)	217	0.003
IRF7 (M00453)	126	0
IRF1 (M00062)	123	0
IRF8 (M01665)	103	0.001
IRF2 (M00063)	54.8	0
NFκB (M00774)	54.7	0
NFκB (M00194)	28.1	0.001
NFκB (M00052)	25.5	0
NFκB (M00208)	14.2	0.001

### 5.3 Basal Differences in Gene Expression between *Socs1<sup>-/-</sup>Ifn $\gamma$ <sup>-/-</sup>* and *Socs1<sup>+/+</sup>Ifn $\gamma$ <sup>-/-</sup>* mice

I sought to analyse the differences in gene expression between the *Socs1<sup>-/-</sup>Ifn $\gamma$ <sup>-/-</sup>* and *Socs1<sup>+/+</sup>Ifn $\gamma$ <sup>-/-</sup>* mice. SOCS1 is involved in the regulation of a multitude of cytokine pathways. The differences observed between these mice may therefore be due to a number of cytokines. The use of *Socs1<sup>-/-</sup>Ifn $\gamma$ <sup>-/-</sup>* and *Socs1<sup>+/+</sup>Ifn $\gamma$ <sup>-/-</sup>* mice eliminates the effects SOCS1 has on type II IFN signaling and allows for viable mice to be compared. Basal differences in *Socs1<sup>-/-</sup>Ifn $\gamma$ <sup>-/-</sup>* and *Socs1<sup>+/+</sup>Ifn $\gamma$ <sup>-/-</sup>* mice therefore show a global view of SOCS1 regulation, with exception of IFN $\gamma$ . As SOCS1 is a potent inhibitor of type I IFN signaling, some of the differential expression seen basally between these mice may represent a contribution by the type I IFNs. As demonstrated in previous chapters there is increased STAT1 and STAT3 phosphorylation levels in the thymus in *Socs1<sup>-/-</sup>Ifn $\gamma$ <sup>-/-</sup>* compared to *Socs1<sup>+/+</sup>Ifn $\gamma$ <sup>-/-</sup>* mice and as such I would expect a number of STAT1 and STAT3 regulated genes will be differentially expressed.

Using Genespring, samples were normalised to the 75<sup>th</sup> percentile and the baseline transformed to median of all samples. Filtering based on gene expression and flags were performed and resulted in a list of 25,962 probes. The basal differences between the *Socs1<sup>-/-</sup>Ifn $\gamma$ <sup>-/-</sup>* and the *Socs1<sup>+/+</sup>Ifn $\gamma$ <sup>-/-</sup>* mice were investigated as described in Figure 2.4. A cut off was performed to reduce the list to those genes that are 2 fold or greater different across the two conditions. An unpaired students t-test with BHFD multiple testing correction was then performed on this gene list to identify significantly ( $p < 0.05$ ) different gene expression across the conditions. This generated a list of 503 probes that were greater than 2 fold different with 185 of these probes greater than 3 fold different as shown in appendix IIIC. A heatmap of differential basal gene expression was generated and displayed in Figure 5.4. As can be seen from the heatmap, there are groups of genes with similar expression patterns. To define the clusters of similarly expressed (co regulated) genes, K-means clustering was performed, as outlined in Chapter 2.5.11. The co-regulated gene sets were identified by applying 3K-means clustering, using Euclidean distance, to genes found basally different between the *Socs1<sup>-/-</sup>Ifn $\gamma$ <sup>-/-</sup>* and the *Socs1<sup>+/+</sup>Ifn $\gamma$ <sup>-/-</sup>* mice. The resultant basal gene clusters are shown on a scatter plot in Figure 5.5. These include a cluster of genes with increased expression in the *Socs1<sup>-/-</sup>Ifn $\gamma$ <sup>-/-</sup>* mice compared to *Socs1<sup>+/+</sup>Ifn $\gamma$ <sup>-/-</sup>* (Basal Cluster 1) as well as two clusters of genes with increased expression in the *Socs1<sup>+/+</sup>Ifn $\gamma$ <sup>-/-</sup>* mice compared to *Socs1<sup>-/-</sup>Ifn $\gamma$ <sup>-/-</sup>* mice. The difference between the last two clusters, as evidenced in

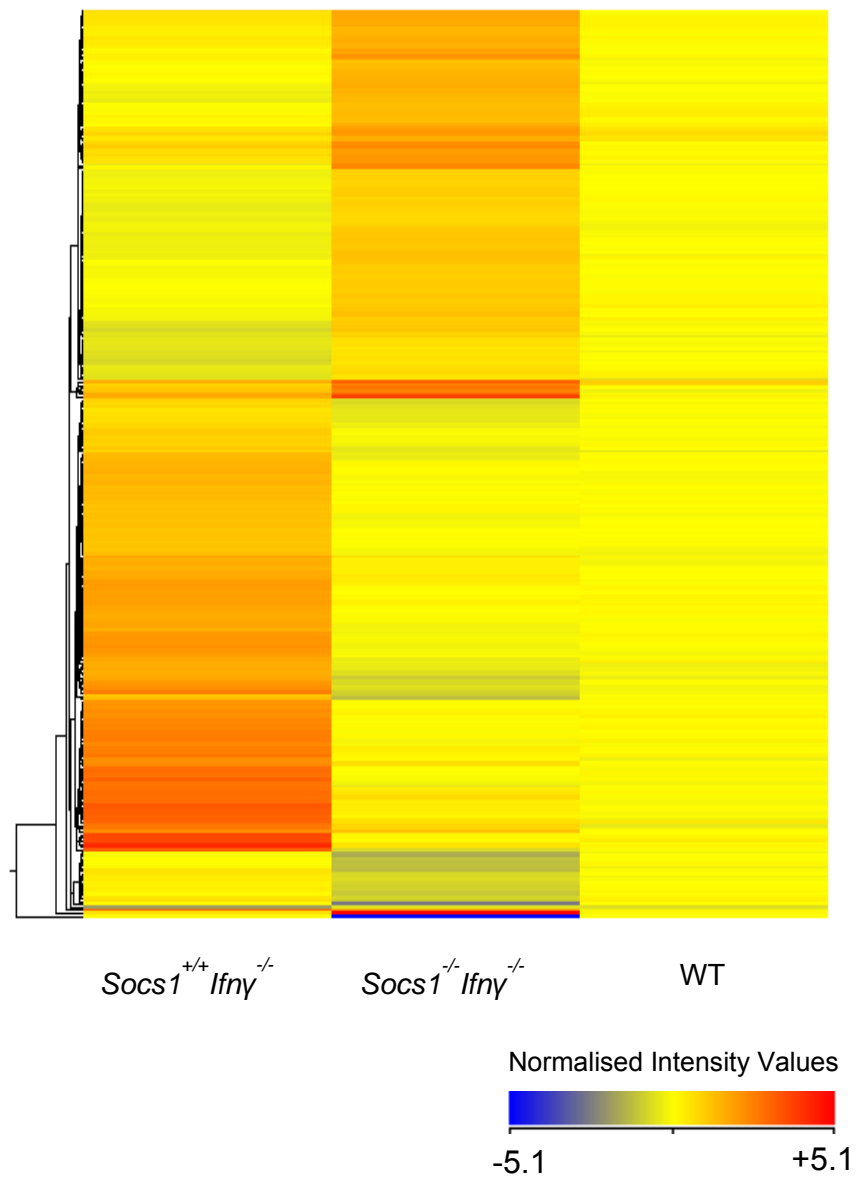
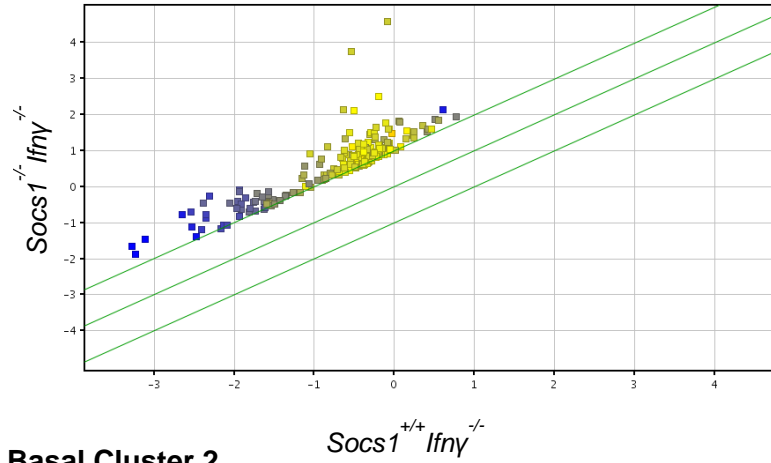


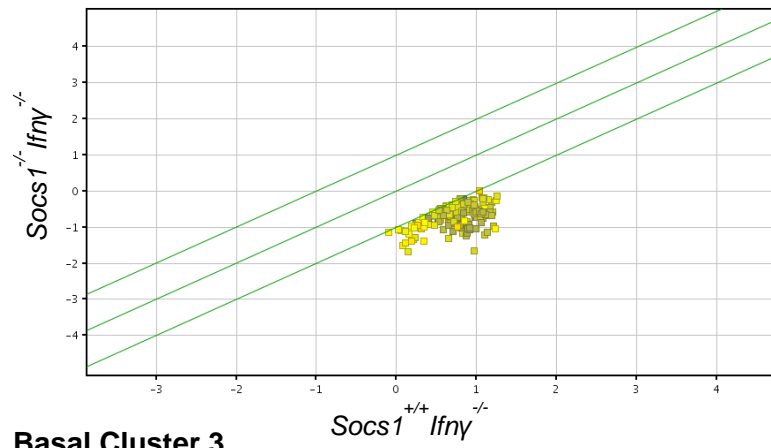
**Figure 5.4: Heatmap of basal gene expression in the thymus of *Socs1*<sup>-/-</sup> *Ifnγ*<sup>-/-</sup>, *Socs1*<sup>+/+</sup> *Ifnγ*<sup>-/-</sup> and wt mice.** Statistical analysis was performed to identify probes significantly different ( $p < 0.05$ ) in the thymus of *Socs1*<sup>+/+</sup> *Ifnγ*<sup>-/-</sup>, *Socs1*<sup>-/-</sup> *Ifnγ*<sup>-/-</sup>, and wt mice (as described in Section 5.5). The heatmap of these probes was generated using hierarchical clustering in Genespring GX.

**Figure 5.5: Scatter plots of probe clusters found differentially expressed in the thymus of *Socs1*<sup>+/+</sup>*Ifnγ*<sup>-/-</sup> and *Socs1*<sup>-/-</sup>*Ifnγ*<sup>-/-</sup> mice.** Clusters were generated by 3K-means clustering of probes differentially expressed in the thymus of *Socs1*<sup>+/+</sup>*Ifnγ*<sup>-/-</sup> and *Socs1*<sup>-/-</sup>*Ifnγ*<sup>-/-</sup> mice using Genespring GX. Scatter plots of the clusters were generated using Genespring GX. Normalised gene expression values of *Socs1*<sup>+/+</sup>*Ifnγ*<sup>-/-</sup> mice (y-axis) were plotted against normalised gene expression of *Socs1*<sup>-/-</sup>*Ifnγ*<sup>-/-</sup> mice (x-axis). Green lines represent a 2 fold induction boundary. Gene colours represent relative wt expression values.

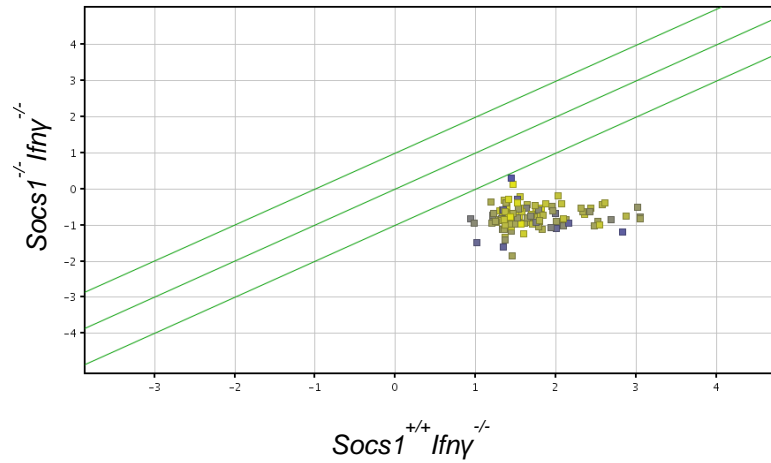
### Basal Cluster 1



### Basal Cluster 2



### Basal Cluster 3



Normalised Intensity Values (WT)

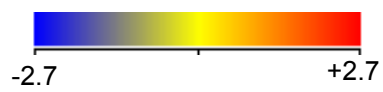


Figure 5.5, is the level of gene expression within the *Socs*<sup>+/+</sup>*Ifn* $\gamma$ <sup>-/-</sup> mice. Gene intensity values from *Socs*<sup>1+/+</sup>*Ifn* $\gamma$ <sup>-/-</sup> mice are greater in Basal Cluster 3 compared to Basal Cluster 2. In comparison gene intensity values from *Socs*<sup>1-/-</sup>*Ifn* $\gamma$ <sup>-/-</sup> mice are similar in Basal Cluster 2 and Basal Cluster 3. Functional annotation and promoter enrichment were performed on the three resultant clusters; Basal Cluster1, Basal Cluster 2, and Basal Cluster 3. Details of the results of these analyses are outlined below.

### 5.3.1 Basal Cluster 1

Basal cluster 1 consists of 224 probes most highly expressed in the *Socs*<sup>1-/-</sup>*Ifn* $\gamma$ <sup>-/-</sup> mice. As SOCS1 is not present in the *Socs*<sup>1-/-</sup>*Ifn* $\gamma$ <sup>-/-</sup> mice, these genes appear SOCS1 negatively regulated. DAVID functional annotation analysis (Table 5.11) of the up-regulated genes found a functional cluster containing genes that encode proteins with signal peptide sequences (10.05) and thus constitute secreted or membrane bound rather than intracellular proteins. In the absence of SOCS1, this may result in an increased ability of the cells to interact with their extracellular environment, likely an important cell process during an immune response. The second functional cluster contains genes that encode proteins involved in innate and adaptive immune responses (4.28). Other functional clusters contain genes that encode proteins involved in lipid metabolism (3.04), hormone regulation (2.31), PARP signaling (2.17), chemotaxis (2.12) and cellular adhesion (2.04). Promoter enrichment analysis (Table 5.12) identified multiple transcription factor binding motifs involved in innate immunity which are over-represented in Basal Cluster 1 and include IRF (RS 320, p = 0), STAT5A (RS 174, p = 0.001), ISGF3 (RS 109, p = 0) ICSBP (IRF8) (RS 108, p = 0), STAT3 (RS 84.8, p = 0) and IRF7 (RS 33.2, p = 0). Other transcription factor binding motifs over-represented include Tal-1 (RS 460, p = 0.001), GAGA (RS 335, p = 0) and MZF1 (RS 328, p = 0) as well as a number of Ets factors including PU.1 (RS 292, p = 0), Ets2 (RS 287, p = 0) and Ets1 (RS 238, p = 0).

The up-regulation of a larger set of genes in the absence of SOCS1 reflects the negative regulatory role of SOCS1 on transcription factor activation and gene expression. As SOCS1 is involved in the negative regulation of a range of cytokine pathways, the genes found up-regulated in the absence of SOCS1 are likely due to hyper-activation of these pathways. This may be due to an increase in total STAT1 or STAT3 expression levels in the absence of SOCS1, as shown in Chapter 4, and thus cytokine stimulation may result in increased phosphorylated STAT levels. Alternatively

**Tables 5.11: DAVID functional annotation of genes from Basal Cluster 1.**

The probes of Basal Cluster 1 were converted to Ensemble Gene IDs with Ensemble Biomart. The Ensemble gene IDs were loaded into DAVID for functional annotation analysis with medium classification stringency.

<b>Functional Annotation</b>	<b>ES</b>
Proteins with signal peptide sequences (secreted or membrane bound proteins) consisting of Glycoproteins and/or proteins involved in disulfide bond formation.	10.05
Innate and adaptive immune responses	4.28
Lipid Metabolism	3.04
Hormone Regulation	2.31
PARP signaling	2.17
Chemotaxis	2.12
Cellular Adhesion	2.04

**Table 5.12. Clover promoter analysis of Basal Cluster 1 displaying A) Over-represented IRF, STAT and NF- $\kappa$ B binding elements, B) Over-represented “non STAT, IRF or NF- $\kappa$ B” binding elements.** Clover promoter enrichment analysis was performed on sequences 2000bp upstream of the transcript start site of genes within basal cluster 3. Table A displays STAT, IRF or NF- $\kappa$ B binding elements found over-represented ( $p < 0.01$ ). There were no STAT, IRF or NF- $\kappa$ B binding elements found under-represented ( $p > 0.99$ ). Table B displays “non STAT, IRF or NF- $\kappa$ B” binding elements over-represented.

**A. Over-represented – IRF, STAT and NF- $\kappa$ B**

<b>TRANSFAC Transcription Factor Matrix</b>	<b>Raw Score</b>	<b>P-value</b>
IRF (M00772)	320	0
STAT (M00777)	196	0.004
STAT5A (M00499)	174	0.001
ISGF3 (M00258)	109	0
ICSBP (M00699)	108	0
STAT5A (M00493)	87.2	0.006
STAT3 (M00497)	84.8	0.009
IRF7 (M00453)	33.2	0

**B. Over-represented – Other**

<b>TRANSFAC Transcription Factor Matrix</b>	<b>Raw Score</b>	<b>P-value</b>
Tal-1 (M01591)	460	0.001
GAGA (M00723)	335	0
MZF1 (M00084)	328	0
MZF1 (M01733)	307	0
PU.1 (M00658)	292	0.001
ETS2 (M01207)	287	0
PUR1 (M01721)	286	0
ELF (M01266)	255	0
MZF1 (M00083)	242	0
c-Ets-1 (M00339)	238	0
E2A (M00972)	201	0.006
TAL1 (M00993)	183	0
c-Ets-2 (M00340)	175	0

SOCS1 has been implicated in regulating cytokine expression and thus in the absence of SOCS1 there may be an increase in cytokines and hence cytokine signaling. The over-representation of ISGF3 and other STAT binding sites within the promoters of genes negatively regulated by SOCS1 was expected as SOCS1 is typically involved in the regulation of cytokine pathways that utilise STAT signaling, including IFN $\alpha$  signaling.

### 5.3.1.1 Basal and IFN $\alpha$ regulation

In order to determine which SOCS1 negatively regulated genes are also IFN $\alpha$  induced genes, I compared the gene set of basal cluster 1 with the genes found up-regulated with IFN $\alpha$  treatment. A venn diagram comparing the genes up-regulated by IFN $\alpha$  in the wt mice and the genes basally higher in the *Socs1<sup>-/-</sup>Ifn $\gamma$ <sup>-/-</sup>* compared to the *Socs1<sup>+/+</sup>Ifn $\gamma$ <sup>-/-</sup>* mice (Basal cluster 1), found 55 probes within this group. These genes thus appear both IFN $\alpha$  and SOCS1 regulated (Figure 5.6). Conversion of these probes to Ensembl gene IDs identifies 42 unique genes (Table 5.13). DAVID functional annotation clustering of these genes (Table 5.14) identified a cluster with an enrichment score of 5.01 containing cytoplasmic genes involved in response to virus, antiviral defence and the RIG-I like pathway. The second cluster with an enrichment score of 3.55 contains genes involved in the immune response and genes that have nucleotide binding and transferase activities. Promoter enrichment analysis was performed using clover and is presented in Table 5.15. Promoters from this gene set were found to be enriched in IRF (RS 229, p = 0), ISGF3 (160, p = 0), ICSPB (IRF8) (RS 137, p = 0), IRF7 (RS 90.8, p = 0), STAT3 (RS 78.9, p = 0.001), STAT1 (67, p = 0) and STAT5A (RS 61, p = 0.001) binding motifs.

The increased expression of IFN $\alpha$  induced genes, in the absence of SOCS1, was expected as previous chapters show SOCS1 negatively regulates IFN $\alpha$  induced STAT1 and STAT3 phosphorylation. Furthermore the involvement of these genes in viral detection and defence supports previous findings that in the absence of SOCS1, mice are highly resistant to viral infection (Fenner, Starr et al. 2006). The increased expression of the 42 genes found both IFN $\alpha$  regulated and SOCS1 negatively regulated may confer viral resistance to these mice. Some of the antiviral genes within this list include *Oas1a*, *Oas1b*, *Oas2*, *Oas3*, *Oas1*, *Ddx58 (RIG-I)*, *Ddx60*, *Irf7*, *Irf9*, *Mx2*, *Isg15*, *Rsad2*, *Cmpk2*, *Gbp5*, *Rtp4* and *Usp18*. A study by Schoggins et al analysed the ability of different ISGs to inhibit a range of viruses (Schoggins, Wilson et

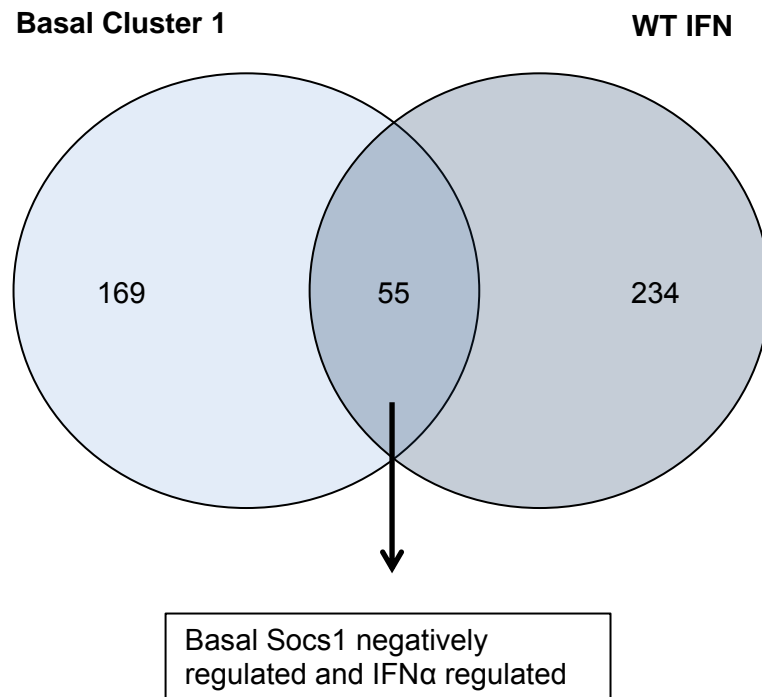


**Figure 5.6: Venn diagram of basal Socs1 negatively regulated (Basal Cluster 1) and IFN $\alpha$  regulated (IFN $\alpha$  regulated in WT mice) probes.** Probes found significantly regulated in the thymus of wt mice following 3 and 6 hour IFN $\alpha$  stimulations were compared to probes up-regulated in *Socs1*<sup>-/-</sup> *Ifn $\gamma$* <sup>-/-</sup> compared to *Socs1*<sup>+/+</sup> *Ifn $\gamma$* <sup>-/-</sup> mice (Basal Cluster 3). Of the 289 probes regulated in the thymus of wt mice following 3 and 6 hour IFN $\alpha$  stimulations 55 were also up-regulated in *Socs1*<sup>-/-</sup> *Ifn $\gamma$* <sup>-/-</sup> compared to *Socs1*<sup>+/+</sup> *Ifn $\gamma$* <sup>-/-</sup> mice.

**Table 5.13. Gene list of Basal Socs1 negatively regulated (Basal Cluster 1) and IFN $\alpha$  regulated (IFN $\alpha$  regulated in WT mice) genes with associated Ensemble gene transcript IDs.** The 55 probes found significantly regulated in the thymus of wt mice following 3 and 6 hour IFN $\alpha$  stimulations and up-regulated in *Socs1*<sup>-/-</sup> *Ifny*<sup>-/-</sup> compared to *Socs1*<sup>+/+</sup> *Ifny*<sup>-/-</sup> mice (Basal Cluster 1) were converted to Ensemble Gene IDs and associated gene names with Ensemble Biomart. This resulted in a list of 42 genes.

Gene Name	Ensembl Gene ID
Gm14446	ENSMUSG00000079339
Ddx58	ENSMUSG00000040296
AC125149.6	ENSMUSG00000079800
Rtp4	ENSMUSG00000033355
Ddx60	ENSMUSG00000037921
Hoxb5	ENSMUSG00000038700
Usp18	ENSMUSG00000030107
Oas1	ENSMUSG00000041827
Gbp5	ENSMUSG00000040264
Trim30a	ENSMUSG00000030921
Trim30d	ENSMUSG00000057596
Tgtp1	ENSMUSG00000078922
Tgtp2	ENSMUSG00000078921
Oas2	ENSMUSG00000032690
Oas3	ENSMUSG00000032661
Oas1b	ENSMUSG00000029605
Oas1a	ENSMUSG00000052776
4930599N23Rik	ENSMUSG00000073144
H2-T24	ENSMUSG00000053835
Xaf1	ENSMUSG00000040483
Mx2	ENSMUSG00000023341
Ccl12	ENSMUSG00000035352
Plscr2	ENSMUSG00000032372
Fcgr4	ENSMUSG00000059089
Gm4955	ENSMUSG00000037849
Pydc4	ENSMUSG00000073491
Crb2	ENSMUSG00000035403
9330175E14Rik	ENSMUSG00000074153
Irf9	ENSMUSG00000002325
AC133103.4	ENSMUSG00000079193
AC133103.1	ENSMUSG00000079189
Gzmb	ENSMUSG00000015437
Has1	ENSMUSG00000003665
Gm10553	ENSMUSG00000073631
A530040E14Rik	ENSMUSG00000072109
Gm10552	ENSMUSG00000073628
Irf7	ENSMUSG00000025498
Gm12250	ENSMUSG00000082292
Nlrc5	ENSMUSG00000074151
Rsad2	ENSMUSG00000020641
Cmpk2	ENSMUSG00000020638
Isg15	ENSMUSG00000035692

**Table 5.14. DAVID functional annotation of basal *Socs1* negatively regulated (Basal Cluster 1) and IFN $\alpha$  regulated (IFN $\alpha$  regulated in WT mice) genes.** The Ensemble gene IDs of the 42 genes found significantly regulated in the thymus of wt mice following 3 and 6 hour IFN $\alpha$  stimulations and up-regulated in *Socs1*<sup>-/-</sup> *Ifn $\gamma$* <sup>-/-</sup> compared to *Socs1*<sup>+/+</sup> *Ifn $\gamma$* <sup>-/-</sup> mice (Basel Cluster 1) were loaded into DAVID for functional annotation analysis with medium classification stringency.

<b>Functional Annotation</b>	<b>ES</b>
Response to virus, antiviral defence and the RIG-I like pathway	5.01
Immune response and nucleotide binding and transferase activities	3.55
GTP binding, GTPase activity	1.6
DNA binding, Transcriptional Regulation	0.37

**Table 5.15: Clover promoter enrichment analysis of genes that are Basal Socs1 negatively regulated (Basal Cluster 1) and IFN $\alpha$  regulated (IFN $\alpha$  regulated in WT mice) genes.** Clover promoter enrichment analysis was performed on sequences 2000bp upstream of the transcript start site of genes found significantly regulated in the thymus of wt mice following 3 and 6 hour IFN $\alpha$  stimulations and up-regulated in *Socs1*<sup>-/-</sup> *Ifny*<sup>-/-</sup> compared to *Socs1*<sup>+/+</sup> *Ifny*<sup>-/-</sup> mice (Basel Cluster 1). IRF, STAT or NK- $\kappa$ B binding elements found over-represented ( $p < 0.01$ ) are shown.

<b>TRANSFAC Transcription Factor Matrix</b>	<b>Raw Score</b>	<b>P-value</b>
IRF (M00772)	229	0
IRF (M00972)	193	0
ISGF3 (M00258)	160	0
ICSBP (M00699)	137	0
IRF7 (M00453)	90.8	0
STAT3 (M01595)	78.9	0.001
STAT1 (M01260)	67	0
STAT5A (M00499)	61	0.001
IRF8 (M01665)	38.9	0
IRF-1 (M00062)	33.5	0
STAT4 (M00498)	31.1	0.001
STAT3 (M00497)	30.4	0
IRF2 (M00063)	10.2	0.001

al. 2011). A number of genes were found to have broad antiviral activity such as *Ddx58* (*Rig-I*) as well as more specific antiviral activity such as *Ddx60*, *Rtp4*, *Oasl* and *Irf7*. When these genes were expressed in combination, the antiviral activity was significantly increased. The combination of expression of the IFN $\alpha$  induced antiviral genes, in the absence of SOCS1, is therefore likely to confer high viral resistance to a range of viruses.

In addition to the antiviral phenotype of *Socs1*<sup>-/-</sup>*Irfn*<sup>-/-</sup> mice, these mice also develop an autoimmune disease later in life. As discussed in chapter 1, IFN $\alpha$  is known to contribute to the onset of autoimmune disease (Hooks, Moutsopoulos et al. 1979; Ronnblom 2011). The 42 IFN $\alpha$  induced genes found basally up-regulated in the absence of SOCS1 may therefore contribute to the onset of autoimmune disease which occurs in *Socs1*<sup>-/-</sup>*Irfn*<sup>-/-</sup> mice due to a heightened immune response. As IFN $\alpha$  also plays a role in T-cell differentiation and/or selection, the absence of SOCS1 may also affect the T-cell repertoire and thus contribute to the susceptibility of these mice to developing autoimmune disease.

### 5.3.2 Basal Cluster 2

Probes within basal cluster 2 are most highly expressed in the *Socs1*<sup>+/-</sup>*Irfn*<sup>-/-</sup> mice and reduced in *Socs1*<sup>-/-</sup>*Irfn*<sup>-/-</sup> mice. In total this cluster consists of 170 probes. These probes appear to be positively regulated by SOCS1. DAVID functional annotation clustering of basal cluster 2 was performed and identified a number of functional clusters (Table 5.16). The first functional cluster contained genes that encode proteins involved in lipid binding (ES 1.52). The second functional cluster contains genes that encode proteins involved in ion binding, in particular zinc finger containing proteins (ES 1.04). The third functional cluster contains genes that encode proteins within membrane enclosed lumen such as the nucleoplasm (ES 1.02). The fourth functional cluster contains genes that encode proteins involved in DNA repair and cellular response to stress (ES 0.93). Basal cluster 2 was also analysed for promoter enrichment using clover (Table 5.17). Results indicate STAT1 (RS 22.9, p = 0.997) and STAT3 (RS 40.9, p = 1) are under-represented within this cluster, which is consistent with SOCS1 positive regulation of these genes. The Ets factors Ets1 (RS 57, p = 1) and Ets2 (RS 35.1, p = 1) were also found to be under-represented while other transcription factors including MZF1 (RS 191, p = 0.008), NF-AT (RS 82.3, p = 0.008), FOXP3 (RS 80.3, p = 0.009) and p53 (RS 70.7, p = 0) were all over-represented. The over-representation of these binding motifs

**Tables 5.16: DAVID functional annotation of genes from Basal Cluster 2.**

The probes of Basal Cluster 1 were converted to Ensemble Gene IDs with Ensemble Biomart. The Ensemble gene IDs were loaded into DAVID for functional annotation analysis with medium classification stringency.

<b>Functional Annotation</b>	<b>ES</b>
Lipid Binding	1.52
Ion Binding	1.04
Proteins within membrane enclosed lumen	1.02
DNA repair and cellular response to stress	0.93

**Table 5.17. Clover promoter analysis of Basal Cluster 2 displaying A) Under-represented IRF, STAT and NF-κB binding elements, B) Over-represented “non STAT, IRF or NF-κB” binding elements and C) Under-represented “non STAT, IRF or NF-κB” binding elements.** Clover promoter enrichment analysis was performed on sequences 2000bp upstream of the transcript start site of genes within basal cluster 1. There were no STAT, IRF or NF-κB binding elements found over-represented ( $p < 0.01$ ). Table A displays IRF, STAT and NF-κB binding elements found under-represented ( $p > 0.99$ ). Table B displays “non STAT, IRF or NF-κB” binding elements over-represented. Table C displays “non STAT, IRF or NF-κB” binding elements under-represented.

**A. Under-represented – IRF, STAT and NF-κB**

<b>TRANSFAC Transcription Factor Matrix</b>	<b>Raw Score</b>	<b>P-value</b>
STAT (M00777)	67.4	1
STAT4 (M00498)	53.5	0.992
STAT3 (M01595)	40.9	1
STAT1 (M01260)	22.9	0.997

**B. Over-represented - Other**

<b>TRANSFAC Transcription Factor Matrix</b>	<b>Raw Score</b>	<b>P-value</b>
MZF1 (M00084)	191	0.008
NF-AT (M00935)	82.3	0.008
FOXP3 (M01599)	80.3	0.009
p53 (M01652)	70.7	0

**C. Under-represented – Other**

<b>TRANSFAC Transcription Factor Matrix</b>	<b>Raw Score</b>	<b>P-value</b>
Ets (M00771)	80.1	1
c-Ets-1 (M00339)	57	1
c-Ets-2 (M00340)	35.1	1

within the promoters of genes with increased expression in the presence of SOCS1 indicates that their associated transcription factors may be SOCS1 positively regulated. This is true for Foxp3 as SOCS1 was found to prevent the loss of Foxp3 expression in regulatory T-cells (Takahashi, Nishimoto et al. 2011).

### 5.3.3 Basal Cluster 3

The 109 probes within this cluster have increased expression in *Socs1<sup>+/+</sup>Ifn $\gamma$ <sup>-/-</sup>* mice and reduced expression in *Socs1<sup>-/-</sup>Ifn $\gamma$ <sup>-/-</sup>* mice. These genes therefore appear to be SOCS1 positively regulated. DAVID functional annotation analysis of probes within basal cluster 3 was performed (Table 5.18). The first functional cluster contains genes that encode intracellular, non-membrane bound, organelle and cytoskeleton proteins (ES 2.69). The second functional cluster contains genes that encode proteins involved in histone and chromatin modification and organisation (ES 1.22). Other functional clusters include genes involved in RNA processing and regulation of transcription. Promoter enrichment analysis was performed using clover (Table 5.19). Results show that the promoter regions of the genes within basal cluster 3 are over-enriched in IRF binding motifs (RS 147,  $p = 0$ ). This is surprising as these motifs were also over-represented in Basal Cluster 1. Despite this, these genes displayed no over or under-representation of STAT elements within their promoters suggesting STAT independent mechanisms may be involved in their regulation. The highest scoring transcription factor binding elements over-represented were Blimp-1 (RS 147,  $p = 0$ ) and Tal-1 (RS 68.3,  $p = 0.004$ ) suggesting these transcription factors may be SOCS1 positively regulated.

**Tables 5.18: DAVID functional annotation of genes from Basal Cluster 3.**

The probes of Basal Cluster 2 were converted to Ensemble Gene IDs with Ensemble Biomart. The Ensemble gene IDs were loaded into DAVID for functional annotation analysis with medium classification stringency.

<b>Functional Annotation</b>	<b>ES</b>
Intracellular, non-membrane bound, organelle and cytoskeleton probes	1.89
Histone and chromatin modification and organisation	1.36
RNA processing	1.17
Regulation of Transcription	0.72

**Table 5.19. Clover promoter analysis of Basal Cluster 3 displaying A) Over-represented IRF, STAT and NF-κB binding elements, B) Over-represented “non STAT, IRF or NF-κB” binding elements and C) Under-represented “non STAT, IRF or NF-κB” binding elements.** Clover promoter enrichment analysis was performed on sequences 2000bp upstream of the transcript start site of genes within basal cluster 2. Table A displays STAT, IRF or NF-κB binding elements found over-represented ( $p < 0.01$ ). There were no STAT, IRF or NF-κB binding elements found under-represented. Table B displays “non STAT, IRF or NF-κB” binding elements over-represented. Table C displays “non STAT, IRF or NF-κB” binding elements under-represented ( $p < 0.99$ ).

**A. Over-represented – IRF, STAT and NF-κB**

<b>TRANSFAC Transcription Factor Matrix</b>	<b>Raw Score</b>	<b>P-value</b>
IRF (M00972)	142	0
IRF (M00772)	139	0
ICSBP (M00699)	38.1	0.005

**B. Over-represented – Other**

<b>TRANSFAC Transcription Factor Matrix</b>	<b>Raw Score</b>	<b>P-value</b>
BLIMP1 (M01066)	147	0
TAL-1 (M00993)	68.3	0.004

**C. Under-represented - Other**

<b>TRANSFAC Transcription Factor Matrix</b>	<b>Raw Score</b>	<b>P-value</b>
c-Ets-1 (M00339)	32.8	0.995

## 5.4 SOCS1 regulation of IFN Stimulated Genes

We aimed to identify IFN $\alpha$  regulated genes which have their expression effected by the presence or absence of SOCS1. We therefore performed analysis of probes differentially regulated in the *Socs1<sup>-/-</sup>Ifn $\gamma$ <sup>-/-</sup>* and *Socs1<sup>+/+</sup>Ifn $\gamma$ <sup>-/-</sup>* mice following IFN $\alpha$  stimulation.

To visualise IFN $\alpha$  gene induction, with respect to basal expression levels, we first performed individual analysis whereby each genotype was normalised to its own 0 hour. Statistical analysis was performed on these data sets to determine the genes which were significantly regulated by type I IFN over time (as outlined in Figures 2.5 and 2.6). 221 probes were found to be regulated by IFN $\alpha$  in the *Socs1<sup>+/+</sup>Ifn $\gamma$ <sup>-/-</sup>* mice (appendix IIID) whereas 304 probes were found to be regulated by IFN $\alpha$  in the *Socs1<sup>-/-</sup>Ifn $\gamma$ <sup>-/-</sup>* mice (appendix IIIE).

A heatmap of the 221 probes found significantly regulated with IFN $\alpha$  treatment in the thymus of *Socs1<sup>+/+</sup>Ifn $\gamma$ <sup>-/-</sup>* mice is shown in Figure 5.7. Of the 221 probes found differentially regulated with IFN $\alpha$  treatment 194 probes were up-regulated with 3 hours of IFN $\alpha$  treatment. The most highly up-regulated genes include *Rsad2* (37.4-42.2 fold), *Mx2* (26.9 fold), *Cmpk2* (23-25.1 fold), *Oas2* (13.8 fold), *Ddx60* (13.5 fold) and *Isg15* (13.3 fold). Only 9 genes were found significantly up-regulated with 6 hours of IFN $\alpha$  treatment.

A heatmap of the 304 probes found significantly regulated with IFN $\alpha$  treatment in the thymus of *Socs1<sup>-/-</sup>Ifn $\gamma$ <sup>-/-</sup>* mice is shown in Figure 5.8. Of the 304 probes differentially regulated with IFN $\alpha$  treatment, 281 probes were up-regulated with 3 hours of IFN $\alpha$  treatment. The most highly up-regulated genes include *Slfn4* (22.1 fold) *Rsad2* (20.6 – 22 fold), *Cmpk2* (13.3-14.7 fold), *Ptx3* (14 fold), *Mx1* (12.6 - 12.7 fold), *Oas2* (12.6 fold) and *Mx2* (12.4 fold). 275 probes were found to be up-regulated with 6 hours of IFN $\alpha$  treatment. The most highly expressed include *Slfn4* (10.8 fold), *Mmp13* (9.4 fold), *Oas2* (7 fold), *Oas3* (6.5 fold) and *Rsad2* (6.26 fold).

There were 87 more probes identified as being up-regulated with 3 hours IFN $\alpha$  in the *Socs1<sup>-/-</sup>Ifn $\gamma$ <sup>-/-</sup>* but not in the *Socs1<sup>+/+</sup>Ifn $\gamma$ <sup>-/-</sup>* mice, indicating a suppression of IFN $\alpha$  induced gene transcription in the presence of SOCS1. Despite this, the induction of gene expression for some genes with 3 hours of IFN $\alpha$  treatment were much lower in *Socs1<sup>-/-</sup>Ifn $\gamma$ <sup>-/-</sup>* compared to *Socs1<sup>+/+</sup>Ifn $\gamma$ <sup>-/-</sup>* mice. For example, with 3 hours IFN $\alpha$

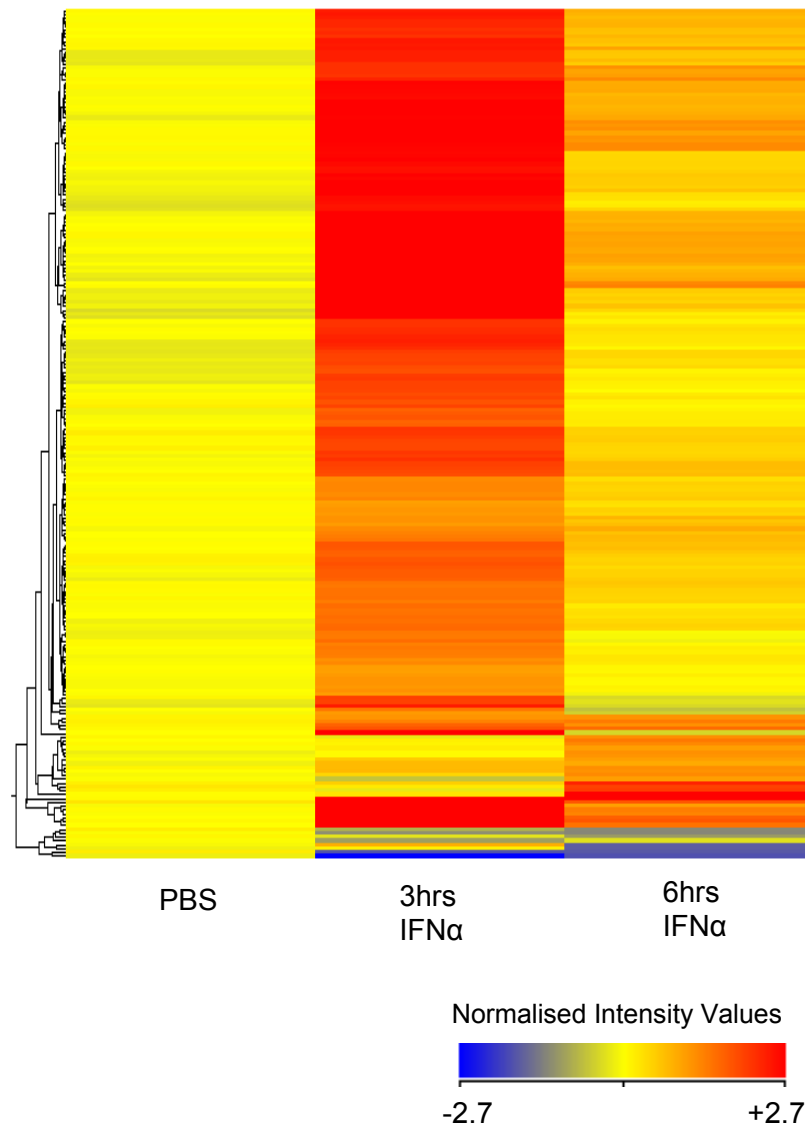


**Figure 5.7: Heatmap of IFN $\alpha$  regulated probes in *Socs1*<sup>+/+</sup> *Ifn $\gamma$* <sup>-/-</sup> mice.** Statistical analysis was performed to identify probes significantly changed ( $p < 0.05$ ) in the thymus of *Socs1*<sup>+/+</sup> *Ifn $\gamma$* <sup>-/-</sup> mice with 3 hour and 6 hour IFN $\alpha$  stimulations (as described in Section 5.7). The heatmap of these probes was generated using hierarchical clustering in Genespring GX.

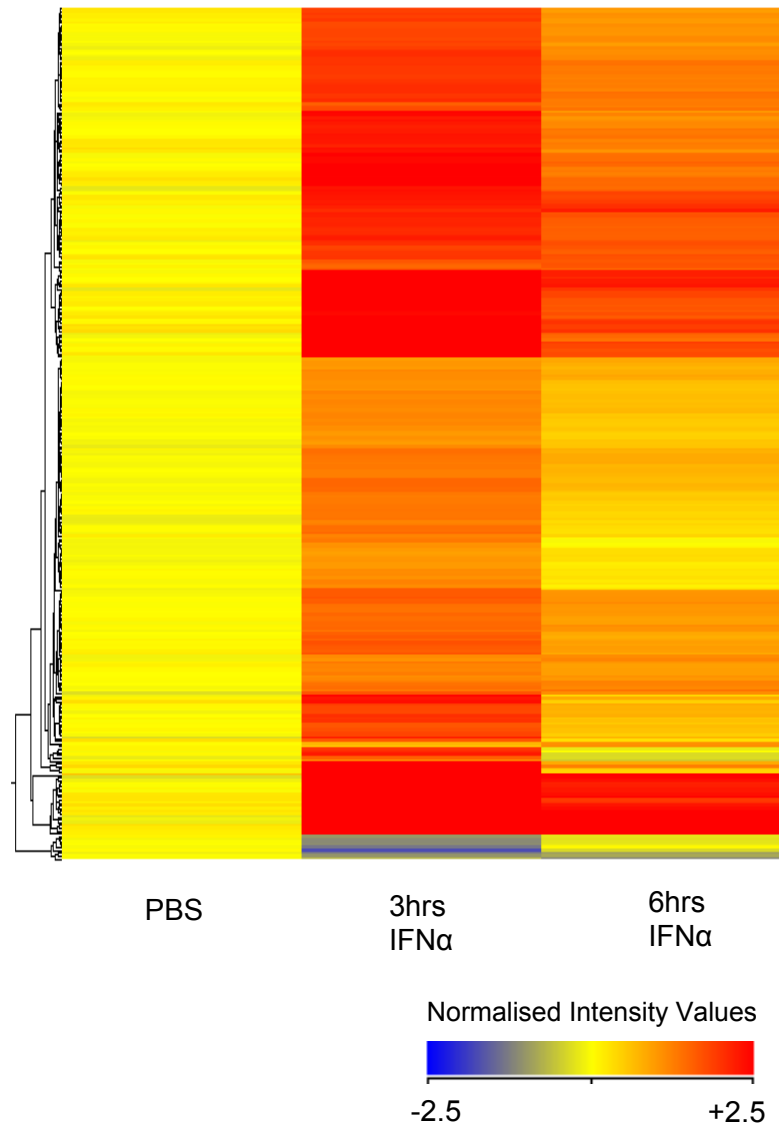


**Figure 5.8: Heatmap of IFN $\alpha$  regulated probes in *Socs1*<sup>-/-</sup> *Ifn $\gamma$* <sup>-/-</sup> mice.** Statistical analysis was performed to identify probes significantly changed ( $p < 0.05$ ) in the thymus of *Socs1*<sup>-/-</sup> *Ifn $\gamma$* <sup>-/-</sup> mice with 3 hour and 6 hour IFN $\alpha$  stimulations (as described in Section 5.7). The heatmap of these probes was generated using hierarchical clustering in Genespring GX.

treatment, *Rsad2* was induced 20.6-22 fold in *Socs1<sup>-/-</sup>Ifn $\gamma$ <sup>-/-</sup>* mice compared to 37.4 – 42.2 fold in *Socs1<sup>+/+</sup>Ifn $\gamma$ <sup>-/-</sup>* mice and *Cmpk2* was induced 14.7 fold in *Socs1<sup>-/-</sup>Ifn $\gamma$ <sup>-/-</sup>* mice compared to 23 fold in *Socs1<sup>+/+</sup>Ifn $\gamma$ <sup>-/-</sup>* mice. Other genes however were more highly induced in the *Socs1<sup>-/-</sup>Ifn $\gamma$ <sup>-/-</sup>* mice such as *Cxcl10* which was induced 6.6 compared to 4.6 fold and *Ifi44* which was induced 10.9 compared to 6.4 fold.

Functional annotation of the significantly up-regulated genes was performed on both gene sets. Functional annotation of the genes significantly up-regulated in the *Socs1<sup>+/+</sup>Ifn $\gamma$ <sup>-/-</sup>* mice is shown in Table 5.20 and the *Socs1<sup>-/-</sup>Ifn $\gamma$ <sup>-/-</sup>* mice in Table 5.21. DAVID functional annotation of the IFN $\alpha$  induced genes in *Socs1<sup>+/+</sup>Ifn $\gamma$ <sup>-/-</sup>* thymus results in clusters of genes that encode proteins with GTP binding of GTPase activities (ES 6.76), 2'5'OAS or transferase activities (ES 6.4), nucleotide binding (ES 5.4), zinc fingers (ES 3.89) and proteins involved in the RIG-I like pathway, innate immunity and defence response (ES 2.28), amongst other functions. DAVID functional annotation of the IFN $\alpha$  induced up-regulated genes in *Socs1<sup>-/-</sup>Ifn $\gamma$ <sup>-/-</sup>* thymus results in clusters of genes that encode proteins with GTPase activities (ES 7.2), proteins involved in the defence response and innate immunity (ES 6.44), nucleotide binding (ES 6.35) and zinc fingers (ES 4.06), amongst other functions. In addition to these common clusters, genes up-regulated by IFN $\alpha$  treatment in the *Socs1<sup>-/-</sup>Ifn $\gamma$ <sup>-/-</sup>* thymus clustered into functional annotation groups that were not present in the *Socs1<sup>+/+</sup>Ifn $\gamma$ <sup>-/-</sup>* thymus. These include genes that encode proteins involved in the inflammatory response (cytokines and chemokines) and apoptosis as well as genes that encode glycoproteins with signal peptides. *Socs1<sup>-/-</sup>* mice have a severe inflammatory phenotype and therefore the up-regulation of proteins involved in the inflammatory response in *Socs1<sup>-/-</sup>Ifn $\gamma$ <sup>-/-</sup>* mice is consistent with this phenotype (Starr, Metcalf et al. 1998). The ability of SOCS1 to regulate genes involved in apoptosis is also consistent with previous findings in which SOCS1 was found to affect the anti-proliferative effects of IFN $\alpha$  in human neutrophils through a suppression of STAT3 (Sakamoto, Hato et al. 2005). The expression of glycoproteins with signal peptides also indicates an increased ability of cells from *Socs1<sup>-/-</sup>Ifn $\gamma$ <sup>-/-</sup>* mice to interact with the external environment. This is likely an important process during infection in which many cells, cytokines other signaling molecules must interact and act together to amount an appropriate immune response.

Following individual analysis of *Socs1<sup>-/-</sup>Ifn $\gamma$ <sup>-/-</sup>* and *Socs1<sup>+/+</sup>Ifn $\gamma$ <sup>-/-</sup>* mice to determine IFN $\alpha$  induced gene expression, they were analysed collectively to determine genes differentially regulated between the two genotypes. Normalisation and filtering of the

**Table 5.20: DAVID functional annotation clustering of genes up-regulated in the thymus of *Socs1*<sup>+/+</sup> *Ifny*<sup>-/-</sup> mice with 3 and 6 hour IFN $\alpha$  stimulations.** Probes found to be up-regulated in the thymus of *Socs1*<sup>+/+</sup> *Ifny*<sup>-/-</sup> mice following 3 and 6 hour IFN $\alpha$  stimulations (Section 5.7) were converted to Ensemble Gene IDs with Ensemble Biomart. The Ensemble gene IDs were loaded into DAVID for functional annotation analysis with medium classification stringency.

Functional Annotation	ES
GTP binding, GTPase activity	6.76
2'5'OAS, transferase activity	6.4
Nucleotide binding	5.4
Zinc finger	3.89
PARP activity	3.18
RIG-I like pathway, innate immunity, defense response, helicase	2.28
Macromolecule catabolic process, proteolysis	1.51
Tetratricopeptide region	1.32
Ubiquitin	1.32

**Table 5.21: DAVID functional annotation clustering of genes up-regulated in the thymus of *Socs1*<sup>-/-</sup> *Ifny*<sup>-/-</sup> mice 3 and 6 hours post IFN $\alpha$ .**

Probes found to be up-regulated in the thymus of *Socs1*<sup>-/-</sup> *Ifny*<sup>-/-</sup> mice mice following 3 and 6 hour IFN $\alpha$  stimulations (Section 5.7) were converted to Ensemble Gene IDs with Ensemble Biomart. The Ensemble gene IDs were loaded into DAVID for functional annotation analysis with medium classification stringency.

Functional Annotation	ES
GTPase activity	7.2
Defense response, Innate immunity	6.44
Nucleotide binding	6.35
2'5'OAS, RNA binding, transferase activity	5.47
Zinc finger	4.06
RNA binding, ds RNA binding	3.83
Pyrin	3.76
PARP activity	3.49
Inflammatory response, Cytokine, Chemokine, taxis, extracellular space	2.22
Regulation of type I IFN production	1.61
Glycoprotein, signal peptide, disulfide bond	1.61
Apoptosis	1.56
Jak-STAT signaling pathway, Cytokine-cytokine receptor interaction	1.36
Thrombospondin repeat	1.32
Cellular macromolecule catabolic process, ISG15-protein conjugation, proteolysis	1.31
Ubiquitin	1.12

data was first performed, as described previously. The baseline was then transformed to the median of all samples. A cut off was performed to obtain only the probes that are 2 fold or greater different across any of the conditions. This reduced the probe list to 2055 genes. A two-way anova was performed on this list to analyse differences between the IFN $\alpha$  time course of gene regulation in *Socs1<sup>+/+</sup>Ifn $\gamma$ <sup>-/-</sup>* and *Socs1<sup>-/-</sup>Ifn $\gamma$ <sup>-/-</sup>* mice. A two-way anova (two-way analysis of variance) allows measurement of the effects of two parameters simultaneously (IFN $\alpha$  time-course and genotype). Three gene lists were obtained, one for each parameter and one for measuring the interaction between the two parameters. I consequently identified of a subset of genes that interact over the two parameters.

The two-way anova experiment resulted in three lists (Figure 5.9):

- Genes different across time: 557
- Genes different across genotype: 1066
- Time-genotype Interacting genes: 167

We are interested in the 167 genes that interact over the two conditions (IFN $\alpha$  timecourse and genotype) as these will be the genes that are both IFN regulated and effected by the presence of SOCS1. A heatmap of the interacting genes using hierarchical clustering was generated in Genespring (Figure 5.10). DAVID functional annotation of the interacting genes (Table 5.22) indicates these genes encode proteins involved in the innate immune response (2.81), glycoproteins with signal peptides (2.2), GTP activities (1.94), peptidase inhibitors (1.71), EGF-like domains (1.58), response to wounding (1.21) and secreted proteins (1.2). Promoter enrichment analysis was performed using clover. Promoter analysis (Table 5.23) indicates over-representation STAT3 (RS 217, p = 0.001), STAT1 (RS 156, p = 0.002), ISGF3 (RS 55, p = 0.01), NF- $\kappa$ B (RS 43.6, p = 00.003) and IRF7 (RS 17.6, p = 0) binding elements. The enrichment of ISGF3, STAT1 and STAT3 within this gene cluster is consistent with findings in Chapter 4 which demonstrate SOCS1 regulates IFN $\alpha$  induced STAT1 and STAT3 phosphorylation. Interestingly, STAT5 binding elements were not present within the promoter analysis as either over or under-represented which is consistent with findings in Chapter 4 which suggest STAT5 phosphorylation is independent of SOCS1 regulation.

We further clustered the genes identified as interacting over the two conditions. 5 K-means clustering using Euclidean distance was performed on the time-genotype

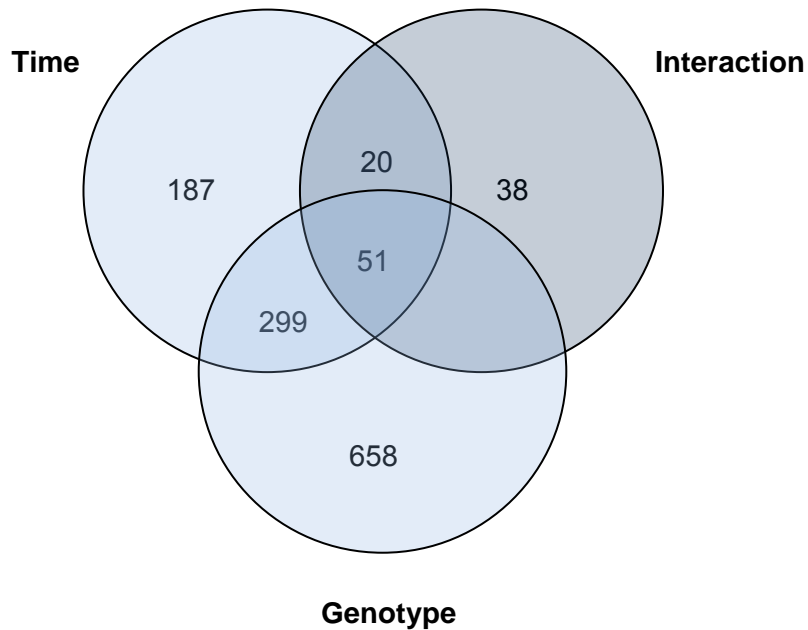


**Figure 5.9: Venn Diagram of probes found via two-way anova analysis of 3 and 6 hours IFN $\alpha$  stimulations in the thymus of *Socs1*<sup>-/-</sup> *Ifny*<sup>-/-</sup> and *Socs1*<sup>+/+</sup> *Ifny*<sup>-/-</sup> mice.** A two-way anova (non-corrected) was performed on *Socs1*<sup>-/-</sup> *Ifny*<sup>-/-</sup> and *Socs1*<sup>+/+</sup> *Ifny*<sup>-/-</sup> microarray data to analyse differences between the IFN $\alpha$  time course of gene regulation in *Socs1*<sup>-/-</sup> *Ifny*<sup>-/-</sup> and *Socs1*<sup>+/+</sup> *Ifny*<sup>-/-</sup> mice. The resultant entity sets include probes regulated over time, probes regulated over genotype and probes that interact over time and genotype. The overlap of these gene sets is displayed. 167 probes were found to interact over time and genotype.

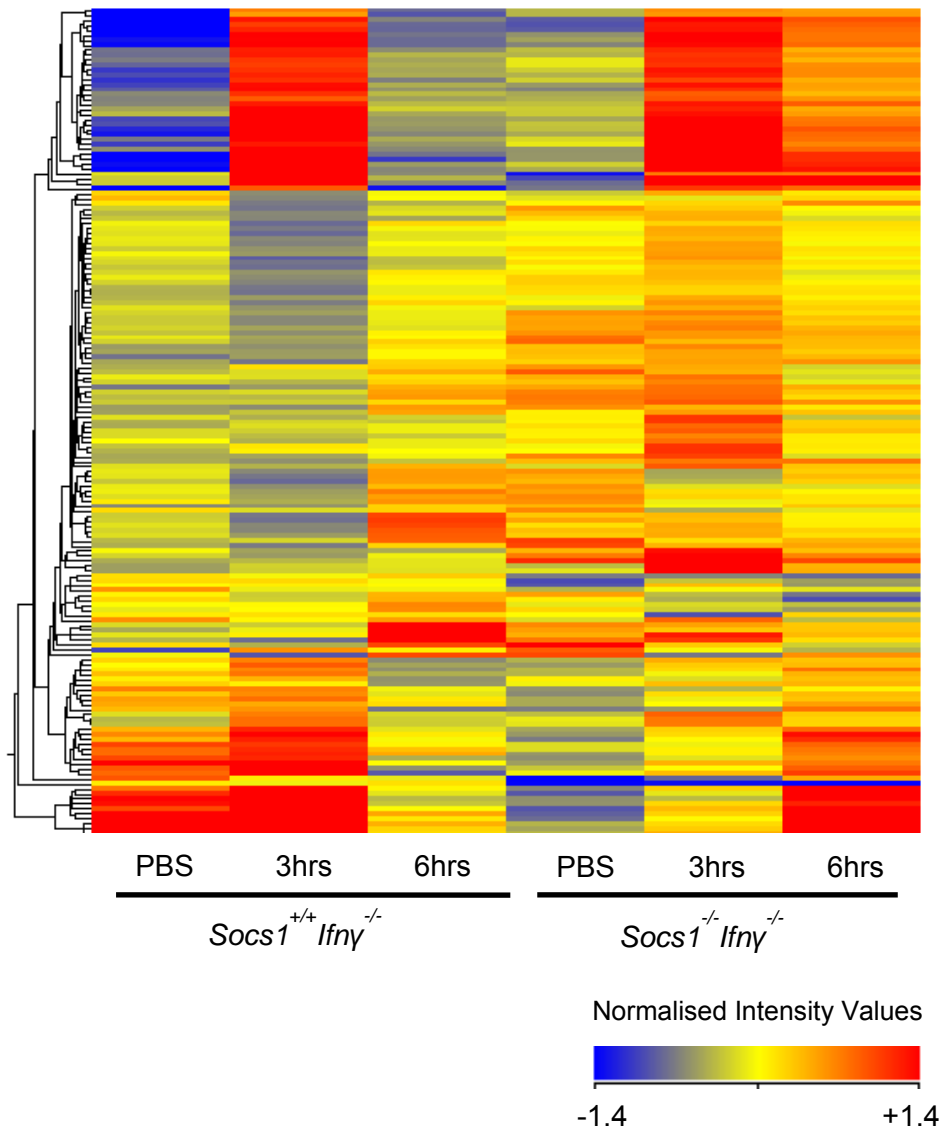


**Figure 5.10: Heatmap of genes that interact over IFN $\alpha$  and Socs1 regulation.** A heatmap was generated of the resultant entity list from two way anova analysis to determine genes that interact over IFN $\alpha$  and Socs1 regulation. The heatmap was generated in Genespring using hierarchical clustering.

**Table 5.22: DAVID functional annotation of genes that interact over IFN $\alpha$  and Socs1 regulation.** probes found to interact over IFN $\alpha$  and Socs1 regulation were converted to Ensemble Gene IDs with Ensemble Biomart. The Ensemble gene IDs were loaded into DAVID for functional annotation analysis with medium classification stringency.

<b>Functional Annotation</b>	<b>ES</b>
Immune Response, Innate Immunity	2.81
Disulfide Bond, Signal peptide, Glycoprotein	2.2
GTPase activity, GTP-binding, nucleotide binding	1.94
Peptidase Inhibitor	1.71
Positive Regulation of immune response	1.59
EGF like domain	1.58
Extracellular region, extracellular matrix	1.36
Defence Response, Response to wounding	1.21
Secreted	1.2

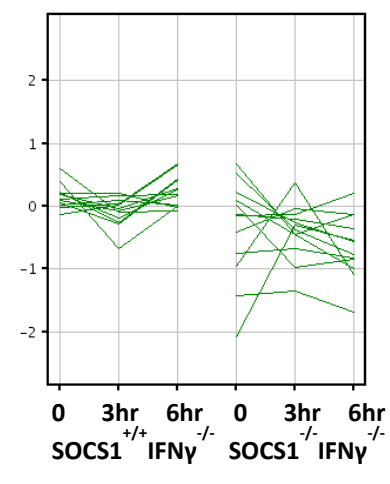
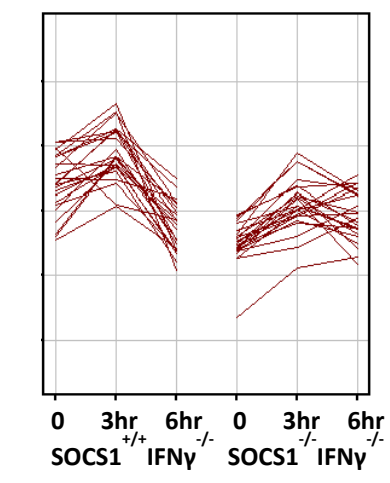
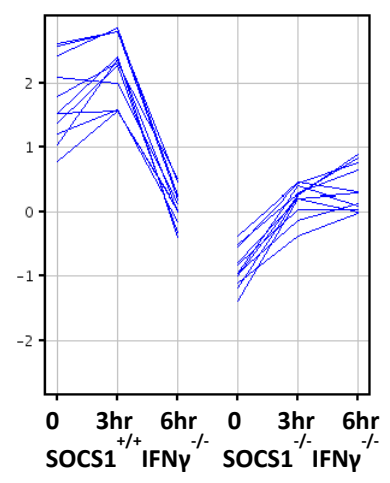
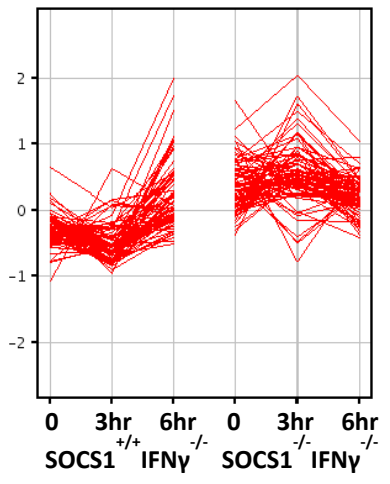
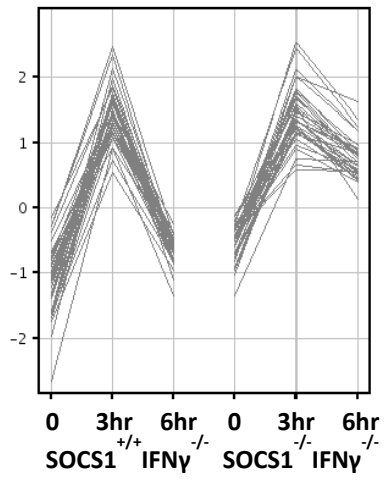
**Table 5.23: Over-represented STAT, IRF and NF- $\kappa$ B binding elements within the promoters of genes that interaction over IFN $\alpha$  and Socs1 regulation.** Clover promoter enrichment analysis was performed on sequences 2000bp upstream of the transcript start site of genes found to interact over IFN $\alpha$  and Socs1 regulation. IRF, STAT or NF- $\kappa$ B binding elements found over-represented ( $p < 0.05$ ) and with a Raw value greater than 0 were extracted.

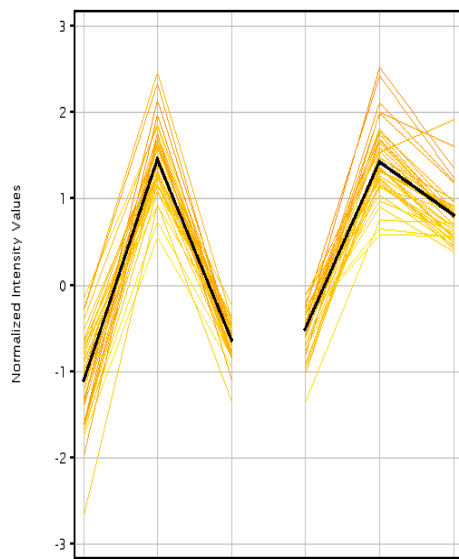
<b>TRANSFAC Transcription Factor Matrix</b>	<b>Raw Score</b>	<b>P-value</b>
STAT3 (M01595)	217	0.001
STAT1 (M01260)	156	0.002
ISGF-3 (M00258)	55	0.01
NFKB (M00774)	43.6	0.003
IRF7 (M00453)	17.6	0
NFKB (M00052)	12.8	0.006

interacting list (Figure 5.11) to identify co-regulated gene sets. Distinct expression patterns were obtained in the time-genotype interaction clusters generated. Interaction cluster 1 contains 37 co-regulated probes which have sustained expression at 6 hours in the absence of SOCS1. Conversion of this list into ensemble gene IDs using ensemble Biomart results in 23 genes. These are presented in Figure 5.12. RT-PCR analysis was performed on samples to validate microarray results (Figure 5.13). Both RT-PCR and microarray results followed similar expression patterns. In this cluster, all genes are up-regulated with IFN $\alpha$  stimulation in both genotypes. Probes from the *Socs1*<sup>-/-</sup>*Ifny*<sup>-/-</sup> mice however remain increased at 6 hours, above basal levels, while in the *Socs1*<sup>+/+</sup>*Ifny*<sup>-/-</sup> mice they are significantly reduced at this time point to near basal levels. These results therefore indicate that the removal of SOCS1 enables sustained gene expression. Most genes within this cluster represent typical interferon stimulated genes involved in antiviral immunity. For example these include *Ddx58 (Rig-I)*, *Ifi47*, *Irf9*, *Irgm1*, *Irgm2*, *Isg15*, *Oas1b*, *Stat1*, *Trim21* and *Rtp4*. Functional annotation clustering identifies four clusters of genes, however, with some overlap (Table 5.24). The functional cluster with the highest enrichment score contains genes that encode proteins with GTPase activities and proteins involved in purine nucleotide binding (ES 2.88). The second cluster contains genes that encode cytoplasmic proteins involved in antiviral defence and the RIG-I like receptor signaling pathway (ES 2.18). The third cluster contains genes that encode nucleotide binding proteins involved in the immune and defence responses (ES 1.13). The fourth cluster contains genes that encode proteins that function within the nucleus and are involved in transcription and transcriptional regulation (ES 0.81). Promoter enrichment analysis of these genes was performed using clover to identify common transcription regulatory elements (Table 5.25). Transcription factors over-represented in the promoters of these genes include IRF (RS 149, p = 0), ICSBP (IRF8) (RS 79.4, p = 0), ISGF3 (RS 71.2, p=0), STAT3 (RS 69.7, p = 0) and STAT1 (RS 54, p = 0), amongst others. Surprisingly STAT5A and STAT5B binding elements were also enriched within the promoters of these genes (RS 19.9, p = 0 and RS 16, p = 0 respectively) however this may reflect the ability of different STATs to bind similar elements or regulate a similar set of genes.

In order to determine the transcription factors that are induced by IFN $\alpha$  yet are not regulated by SOCS1, it is important to analyse the promoters of genes that are IFN $\alpha$  regulated but not SOCS1 regulated. Comparison of promoter regulatory sites within these gene lists may help identify elements which are IFN $\alpha$  but not SOCS1 responsive. 486 probes were identified as being regulated by IFN $\alpha$  yet not regulated by SOCS1

**Figure 5.11: Clusters of co-regulated probes that interact over IFN $\alpha$  and Socs1 regulation.** 5K-means clustering was performed on the list of probes found to interact over IFN $\alpha$  stimulation and Socs1 regulation using Genespring. Data is represented as normalised intensity values.





Gene Name	Ensembl Gene ID
AF067061	ENSMUSG00000079674
BC006779	ENSMUSG00000027580
BC094916	ENSMUSG00000070501
Ddx58	ENSMUSG00000040296
Ifi47	ENSMUSG00000078920
Irf9	ENSMUSG00000002325
Irgm1	ENSMUSG00000046879
Irgm2	ENSMUSG00000069874
Isg15	ENSMUSG00000035692
Mitd1	ENSMUSG00000026088
Ncoa7	ENSMUSG00000039697
Oas1b	ENSMUSG00000029605
Parp14	ENSMUSG00000034422
Parp9	ENSMUSG00000022906
Pyhin1	ENSMUSG00000043263
Rnf213	ENSMUSG00000070327
Rtp4	ENSMUSG00000033355
Stat1	ENSMUSG00000026104
Tgtp1	ENSMUSG00000078922
Tgtp2	ENSMUSG00000078921
Trim21	ENSMUSG00000030966

**Figure 5.12: Expression profile and list of genes within Interaction Cluster 1.** The expression profile of probes from interaction cluster 1 are represented as normalised intensity values, with the mean expression profile represented in black. The probes were converted to Ensembl Gene IDs and associated gene names with Ensembl Biomart.

**Figure 5.13: qRT-PCR validation of microarray data.** Quantitative RT-PCR analysis of *Irgm1*, *Stat1* and *Isg15* expression within the thymus of *Socs1*<sup>-/-</sup> *Ifnγ*<sup>-/-</sup> and *Socs1*<sup>+/+</sup> *Ifnγ*<sup>-/-</sup> mice following 0, 3 6 and 24 hour stimulations with 1000 IU IFNα per mouse, administered intraperitoneally. Data is presented as mean +/- SEM of N = 3-5 separate experiments following normalisation to 18S and is expressed relative to unstimulated controls from *Socs1*<sup>-/-</sup> *Ifnγ*<sup>-/-</sup> mice. \* = p ≤ 0.05, \*\* = p ≤ 0.01, \*\*\* = p ≤ 0.005.

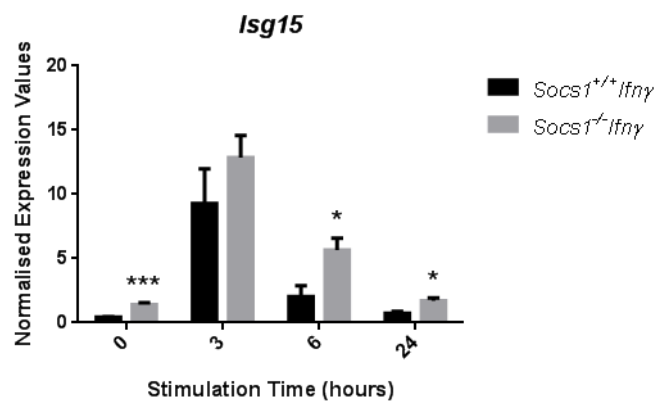
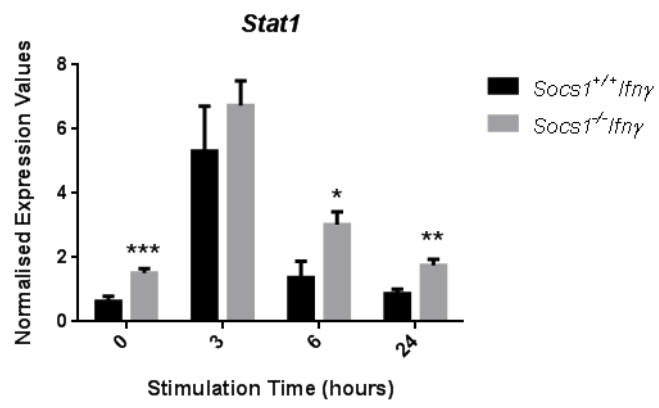
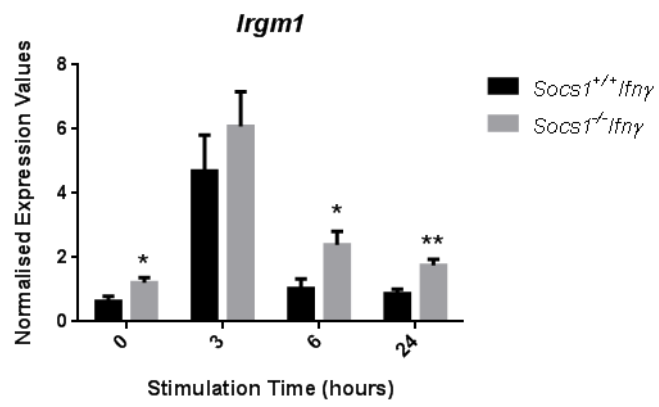


**Table 5.24: DAVID functional annotation of genes from Interaction Cluster 1.** The Ensemble gene IDs from interaction cluster 1 were loaded into DAVID for functional annotation analysis with medium classification stringency.

<b>Functional Annotation</b>	<b>ES</b>
GTPase activities and purine nucleotide binding	2.88
Cytoplasmic, involved in antiviral defence and RIG-I like receptor signaling	2.18
Nucleotide binding, involved in immune and defence responses	1.13

**Table 5.25: Over-represented STAT, IRF and NF- $\kappa$ B binding elements within the promoters of genes within Interaction Cluster 1.** Clover promoter enrichment analysis was performed on sequences 2000bp upstream of the transcript start site of genes within interaction cluster 1. IRF, STAT or NF- $\kappa$ B binding elements found over-represented ( $p < 0.01$ ) and with a Raw value greater than 0 were extracted.

<b>TRANSFAC Transcription Factor Matrix</b>	<b>Raw Score</b>	<b>P-value</b>
IRF (M00772)	149	0
IRF (M00972)	114	0
ICSBP (M00699)	79.4	0
ISGF3 (M00258)	71.2	0
STAT3 (M01595)	69.7	0
STAT (M00777)	55.5	0
IRF7 (M00453)	55.1	0
STAT1 (M01260)	54	0
STAT1:STAT1 (M01212)	32.9	0
IRF1 (M00062)	27.4	0
IRF8 (M01665)	26	0.001
STAT5A (M00457)	19.9	0
NFKB (M00774)	17.2	0
STAT5B (M00459)	16	0
NFKB (M00194)	10.4	0.004
STATx (M00223)	8.3	0.006
NFKB (M00208)	6.73	0.001
STAT (M00259)	5.86	0.002
STAT3 (M00225)	0.472	0

over a time-course of IFN $\alpha$  stimulation (Time minus Interaction). This is presented in Figure 5.14. DAVID functional annotation of this list demonstrates these genes encode proteins that have 2'5'OAS, RNA binding and transferase activities (4.51) and are involved in the inflammatory response with cytokine or chemokine functions (3.41) (Table 5.26). Promoter analysis was performed to identify transcription factors over- or under-represented within the promoters of these genes (Table 5.27). ISGF3 was not found to be over-enriched; a reflection of the negative regulation of ISGF3 by SOCS1. Surprisingly the promoter regions of these genes were still enriched in STAT1 (RS 451,  $p = 0$ ) and STAT3 (RS 614,  $p = 0$ ) binding elements. This may reflect that the genes with these binding sites within their promoters may also be regulated by other factors which are not SOCS1 regulated and thus their expression is maintained in the absence of SOCS1. Alternatively this may reflect a redundancy of STAT1, STAT3 and STAT5 sites within the transfac binding site definitions. The over-representation of STAT5A (RS 524,  $p = 0$ ) and STAT5B (RS 61.9,  $p = 0$ ) was consistent with our findings in previous chapters showing STAT5 phosphorylation is not negatively regulated by SOCS1.

Overall these microarray studies support a negative regulatory role for SOCS1 in IFN $\alpha$  induced STAT1 and STAT3 activation. We have identified a subset of IFN $\alpha$  induced genes suppressed by SOCS1. Promoter analysis of these genes indicates over-representation of ISGF3, STAT1 and STAT3 binding elements. STAT5A or STAT5B binding elements were not found to be over-represented, thus supporting a role for SOCS1 in the negative control of STAT1 and STAT3 but not STAT5. Further clustering of these genes identified a cluster which displayed sustained expression in the absence of SOCS1. This cluster contained genes involved largely in the innate defense response. Promoter analysis of these genes found enrichment of ISGF3, STAT1, STAT3 and STAT5A binding elements. STAT5B binding elements were not found to be enriched. As the promoters of these genes are enriched in ISGF3, STAT1 and STAT3 binding sites, it is likely that prolonged STAT1 and STAT3 phosphorylation and activation in the absence of SOCS1 contributes to prolonged expression of these genes.

By selectively controlling STAT activation, SOCS1 may selectively control the transcriptional response. The STAT family members have critical roles in regulation of the immune system and the balance of STATs activated in a cell will dictate the response of the cell to IFN. SOCS1 alteration of this balance will thus affect the

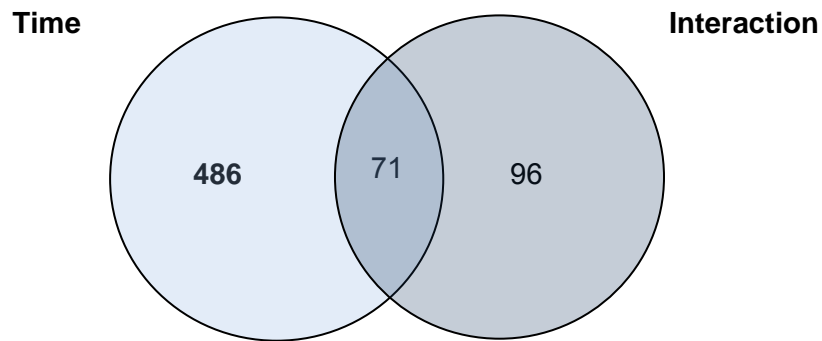


**Figure 5.14: Venn diagram of probes found via two-way anova analysis of 3 hour and 6 hour IFN $\alpha$  stimulation in the thymus of *Socs1*<sup>-/-</sup> *Ifn $\gamma$* <sup>-/-</sup> and *Socs1*<sup>+/+</sup> *Ifn $\gamma$* <sup>-/-</sup> mice.** A two-way anova (non-corrected) was performed on *Socs1*<sup>-/-</sup> *Ifn $\gamma$* <sup>-/-</sup> and *Socs1*<sup>+/+</sup> *Ifn $\gamma$* <sup>-/-</sup> microarray data to analyse differences between the IFN $\alpha$  time course of gene regulation in *Socs1*<sup>-/-</sup> *Ifn $\gamma$* <sup>-/-</sup> and *Socs1*<sup>+/+</sup> *Ifn $\gamma$* <sup>-/-</sup> mice. A venn diagram of the number of probes found regulated over time (557) and .found to interact over IFN $\alpha$  and *Socs1* regulation (167) was generated. 486 probes were found to be regulated by time alone (time minus interaction).

**Table 5.26: DAVID Functional Annotation clustering of genes found regulated by IFN $\alpha$  yet not by Socs1 (Time – Interaction).** Probes found regulated by IFN $\alpha$  yet not Socs1 (Time – Interaction) were converted to Ensemble Gene IDs with Ensemble Biomart. The Ensemble genes IDs loaded into DAVID for functional annotation analysis with medium classification stringency.

<b>Functional Annotation</b>	<b>ES</b>
2'5 OAS, RNA binding, Transferase Activity	4.51
Inflammatory response, cytokine-cytokine receptor interaction, Chemokine activity, chemotaxis	3.41

**Table 5.27: Promoter Enrichment of genes found regulated by IFN $\alpha$  yet not by Socs1 (Time minus Interaction).** Clover promoter enrichment analysis was performed on sequences 2000bp upstream of the transcript start site of genes found regulated by IFN $\alpha$  yet not Socs1 (Time – Interaction). IRF, STAT or NF- $\kappa$ B binding elements found over-represented ( $p < 0.01$ ) and with a Raw value greater than 0 were extracted.

<b>TRANSFAC Transcription Factor Matrix</b>	<b>Raw Score</b>	<b>P-value</b>
STAT3 (M01595)	614	0
STAT (M00777)	563	0
IRF1 (M00972)	555	0
IRF3 (M01279)	543	0
STAT5A (M00499)	524	0
STAT1 (M01260)	451	0
IRF8 (M01665)	263	0
STAT3 (M00497)	252	0
STAT4 (M01666)	235	0
IRF7 (M00453)	174	0
IRF1 (M00062)	110	0
STAT5A (M00457)	93.6	0
STAT5B (M00459)	61.9	0
NF- $\kappa$ B (M00194)	58.5	0
IRF2 (M00063)	42.3	0
NF- $\kappa$ B (M00054)	29.2	0.002
NF- $\kappa$ B (M00208)	23.2	0.007

response of the cell. STAT1 is typically involved in innate immunity, STAT3 in inflammation and STAT5 typically has immunomodulatory functions and is involved in adaptive immunity (Akira 1999; Adamson, Collins et al. 2009). SOCS1 selective regulation would therefore suppress STAT1 and STAT3 mediated innate defense and inflammatory functions while allowing the immunomodulatory functions of STAT5 to proceed. This may allow sustained IFN $\alpha$  immunomodulatory functions and adaptive immune responses while the initial innate response is dampened with SOCS1 expression.

## CHAPTER 6

### DISCUSSION

Suppressor of cytokine signaling (SOCS)1 has emerged as an important factor in controlling IFN signaling to limit potential toxicity and optimise effective signaling. This thesis has characterised the mechanism by which SOCS1 inhibits type I IFN signaling in the form of STAT activation and the transcription of IFN stimulated genes.

SOCS1 gene expression is up-regulated in response to type I IFN signaling and it acts in a negative feedback loop to suppress the actions of the type I IFNs. This was initially investigated by Fenner et al in which *in vivo* genetic studies showed that the deletion of SOCS1 resulted in mice being highly resistant to viral infection, a consequence of enhanced type I IFN signaling. In addition, they showed that SOCS1 regulation was mediated through the IFNAR1 component of the IFN receptor rather than IFNAR2 (Fenner, Starr et al. 2006). As shown in Chapter 3, SOCS1 inhibits type I IFN induction of ISGF3 mediated gene transcription through an interaction with the IFNAR1 associated JAK, TYK2, rather than through a direct interaction with the receptor itself. I propose a model in which SOCS1 binds to conserved tyrosine residues within the catalytic region of TYK2 through its SH2 domain and inhibits TYK2 kinase function through its kinase inhibitory region. I also propose that the interaction of SOCS1 with TYK2 inhibits an activating/stabilising Lys-63 ubiquitination of TYK2, resulting in reduced levels of TYK2 and thus reduced stabilisation of IFNAR1 at the cell surface. Subsequently type I IFN signaling is reduced initially through an inhibition of TYK2 kinase function and therefore TYK2 mediated STAT activation and later through a reduction in the level of receptor available for signaling at the cell surface.

The responses of cells to type I IFNs are dependent on the activation of a complex network of transcription factors and signaling pathways. The STAT family of transcription factors are major mediators of type I IFN signaling, dictating the transcription of a multitude of IFN stimulated genes by binding to distinct DNA regulatory elements. The response of a particular cell to IFN is therefore dependent on the type and level of STAT activation. All 6 members of the STAT family can be activated by the type I IFNs, although in a cell type specific manner (van Boxel-Dezaire, Rani et al. 2006). The activation of particular STATs in response to IFN is

dependent on a range of factors such as the level of basal STAT expression and phosphorylation within the cell, the concentration of receptor on the cell surface, the type and level of IFN acting on the cell as well as the presence or absence of co-activators and inhibitors (Zhao, Zhang et al. 2012). The data within this thesis demonstrates that SOCS1, a potent inhibitor of type I IFN signaling, alters the balance of STAT activation within the cell, resulting in an altered transcriptional response.

The results presented in Chapter 4 demonstrate the downstream consequences of SOCS1 inhibition of IFN $\alpha$  signaling in terms of STAT phosphorylation. IFN $\alpha$  stimulation of wt mice resulted in STAT1, STAT3 and STAT5 phosphorylation in thymocytes. In mice with a deletion of SOCS1, STAT1 and STAT3 phosphorylation were increased whereas STAT5 phosphorylation was not, indicating an ability of SOCS1 to selectively regulate IFN $\alpha$  mediated phosphorylation of STATs. As seen in Chapter 5, IFN $\alpha$  induces expression of a range of genes within thymocytes whose promoters are enriched in STAT1, STAT3 and STAT5 binding elements. In the absence of SOCS1, IFN $\alpha$  mediated gene expression is altered. A subset of genes found regulated by IFN $\alpha$  and SOCS1 were enriched in STAT1 and STAT3 binding elements but not STAT5 which again supports the ability of SOCS1 to negatively regulate STAT1 and STAT3 but not STAT5 phosphorylation.

The set of genes found basally increased in the absence of SOCS1 and that were also induced by IFN $\alpha$ , primarily had antiviral functions. In addition, the expression of a set of IFN $\alpha$  induced genes with antiviral functions was sustained for longer in the absence of SOCS1. The function of SOCS1 may therefore primarily be in the control of IFN $\alpha$  induced antiviral functions. The suppression of IFN $\alpha$  induced antiviral functions by SOCS1 has previously been demonstrated (Song and Shuai 1998; Fenner, Starr et al. 2006). These suppressive effects are likely mediated by the suppression of STAT1 phosphorylation as previous studies have shown that STAT1 is essential in the control of viral infection through type I and II IFN signaling pathways and gene expression data from Chapter 5 showed enrichment of STAT1 binding elements in the promoters of these genes (Meraz, White et al. 1996; Park, Li et al. 2000). SOCS1 control of IFN $\alpha$  induced STAT1 phosphorylation was observed in all immune cell populations analysed (both thymic T-cells and peripheral T-cells, B-cells and monocytes) and thus the regulation of antiviral genes would also be expected in these cell types.

In addition to the control of antiviral genes, the STAT family members also have other critical roles in the regulation of the immune system and the balance of different phosphorylated STATs within a cell will influence the response of the cell to IFN. For example tyrosine phosphorylated STAT1 may form a combination of dimers with other tyrosine phosphorylated STATs in response to IFN $\alpha$  such as STAT1:STAT1, STAT1:STAT2 or STAT1:STAT3 and regulate a different set of genes. In addition, tyrosine phosphorylated STAT5A or STAT5B may form homo or heterodimers with each other or heterodimers with CrkL to regulate transcription (Lekmine, Sassano et al. 2002). The formation of any one of these particular dimers will be defined by the level of activated STATs in the cell available for dimer formation. In addition to STAT tyrosine phosphorylation, however, other post-translational STAT modifications also occur which may influence the function of STATs, the formation of dimers and their transcriptional potential. These include STAT serine phosphorylation, arginine methylation, lysine acetylation, threonine glycosylation and lysine SUMOylation (Brierley and Fish 2005). Several STAT family members including STAT1, STAT3, STAT4, STAT5a and STAT5b require specific serine phosphorylation at the C-terminal region for their full transcriptional potential (Brierley and Fish 2005). Specifically, STAT1 requires serine phosphorylation at serine727 for its full transcriptional activity and this occurs through type I IFN activation of the protein kinase C (PKC) isoform PKC $\delta$  (Uddin, Sassano et al. 2002). In addition, IFN induced serine phosphorylation of STAT5a and STAT5b at serine725/730 respectively is required for its full transcriptional activity (Uddin, Lekmine et al. 2003). Arginine methylation has also been found to increase the transcriptional activity of STAT1 in response to IFN. For example STAT1 Arg31 methylation by protein arginine methyl-transferase (PRMT1) results in increased STAT1-DNA binding and in the absence of STAT1 arginine methylation there is an increased association of phosphorylated STAT1 with the STAT inhibitor PIAS1 (Mowen, Tang et al. 2001). Furthermore, cells deficient in methyl-thioadenosine phosphorylase (MTAP), which is involved in the de-methylation pathway, are less responsive to the anti-proliferative effects of IFN $\alpha$  and IFN $\beta$  (Mowen, Tang et al. 2001). A number of studies have also demonstrated that STAT1 acetylation negatively regulates IFN responses. IFN and histone deacetylase inhibitors (HDACIs) were found to regulate the acetylation of STAT1 by the histone acetyltransferase (HAT) CBP in a number of tumour cell lines (Kramer, Baus et al. 2006). Furthermore this acetylation counteracts IFN-induced STAT1 phosphorylation, nuclear translocation and transcriptional activity (Kramer, Knauer et al. 2009). As can be seen, these different

modifications of STATs can greatly influence their function. Considering the large range of cytokines that stimulate STAT activation, these different modifications may also provide a framework for cross-talk between different cytokines that act on a particular cell. Future studies looking at the role of IFN $\alpha$  induced STATs in T-cell responses could consider these different modifications and how they influence STAT mediated transcription in response to IFN $\alpha$ . Furthermore investigation of the ability of SOCS1 to regulate these modifications may provide further insight into the role of SOCS1 in the negative regulation of IFN $\alpha$  signaling.

Previous studies have shown cross-talk between the type I and II IFN pathways exists at the level of STAT1 expression with type I IFN priming STAT1 expression to levels that enable type II signaling (Gough, Messina et al. 2010). SOCS1 regulation of type I IFN signaling results in reduced STAT1 expression and tyrosine phosphorylation and is therefore likely to reduce type II IFN signaling as well, suggesting that SOCS1 may mediate cross-talk between these two cytokine families through control of STAT1 (Fenner, Starr et al. 2006). As SOCS1 also negatively regulates IFN $\alpha$  mediated STAT3 phosphorylation perhaps there is also cross-talk between pathways that utilize STAT3 for signaling such as the IL-6 or IL-10 pathways.

In addition to the ability of tyrosine phosphorylated STATs to form dimers and regulate transcription, the ability of un-phosphorylated STATs to regulate gene transcription distinct from phosphorylated STATs has also been reported (Yang and Stark 2008). As shown in Chapter 4, IFN $\alpha$  stimulation of thymocytes results in increased total STAT1 levels within the cell. In addition, thymocytes deficient in SOCS1 have increased total STAT1 and STAT3 levels. Transcriptional changes following IFN $\alpha$  stimulation of thymocytes as well as the transcriptional changes mediated by SOCS1 may therefore include genes regulated by un-phosphorylated STATs. The genes regulated by un-phosphorylated STATs however are likely to be induced at later time points than analysed in Chapter 5 as this regulation would follow the initial IFN mediated increase in STAT concentration. SOCS1 may therefore regulate un-phosphorylated STAT mediated gene expression through regulation of the IFN mediated increase in STAT concentration.

As IFN $\alpha$  stimulation of peripheral immune cells induced only STAT1 phosphorylation while IFN $\alpha$  stimulation of thymocytes induced STAT1, STAT3 and STAT5 phosphorylation, STAT3 and STAT5 may be important in mediating the IFN $\alpha$  response

in immature thymocytes rather than in mature peripheral immune cells and perhaps these STATs play a role in mediating IFN $\alpha$  effects on T-cell differentiation or maturation. A number of studies have shown that STAT3 and STAT5 are critical in mediating T-cell differentiation. Conditional STAT3 or STAT5 knockouts indicate these STATs reciprocally regulate T-reg and Th17 cell differentiation. STAT3 activation by IL-6 and TGF $\beta$  results in the development of Th17 cells while a deletion of STAT3 in T-cells causes a decrease in ROR-gamma expression and an increase in Foxp3 expression which promotes T-reg cell development (Mathur, Chang et al. 2007; Yang, Panopoulos et al. 2007; Yang, Nurieva et al. 2008). In contrast, IL-2 mediated activation of STAT5 drives T-reg development through STAT5 directly binding the promoter and inducing expression of Foxp3 while it inhibits Th17 differentiation through an inhibition of IL-17 production (Zorn, Nelson et al. 2006; Burchill, Yang et al. 2007; Yao, Kanno et al. 2007). In addition to STAT3 and STAT5, STAT1 also has effects on T-reg cell development as a deletion of STAT1 results in impaired functionality and numbers of T-reg cells and an increased susceptibility to autoimmune disease (Nishibori, Tanabe et al. 2004). Considering STAT1, STAT3 and STAT5 are up-regulated by IFN $\alpha$  and that they have differential roles in T-reg and Th17 development, a critical balance of each STAT may determine the ultimate outcome of IFN $\alpha$  signaling. A number of studies have shown that IFN $\alpha$  delays T-reg cell generation (Golding, Rosen et al. 2010; Pace, Vitale et al. 2010) while other studies have shown that IFN $\alpha$  suppresses Th17 cell differentiation (Moschen, Geiger et al. 2008; Hirohata, Shibuya et al. 2010). These studies however involved human peripheral T-cells and may not reflect the effect of IFN $\alpha$  on T-reg and Th17 cell differentiation in the thymus of mice. Subsequent studies could delve further into the role of type I IFN on specific T-cell subsets and the effect this has on the overall immune response. This could be achieved by analysing the response to infection in mouse models with a deletion of IFNAR in specific T-cell subsets such as T-reg or Th17 cells. Furthermore the combination of these studies with different STAT knockouts could provide further insight into the role of the different STATs in particular T-cell populations in response to IFN $\alpha$  signaling.

Further to the role of IFN $\alpha$  and STATs in T-cell differentiation, the ability of SOCS1 to negatively regulate IFN $\alpha$  induced STAT1 and STAT3 but not STAT5 may alter the balance of STATs within the cell and therefore alter the differentiation pathways of Treg and Th17 cells. Indeed SOCS1 has been implicated in maintaining Foxp3 expression in T-reg cells (through suppression of IFN $\gamma$ -STAT1 signaling) and in

suppressing IFN $\gamma$  and IL-17 production by T-regs (through suppression of STAT3) (Takahashi, Nishimoto et al. 2011). In addition STAT5 has been found to be phosphorylated to a higher degree in SOCS1 deficient T-reg cells compared to wt T-reg cells (consistent with results within this thesis) and this is associated with an increase in T-reg cell numbers (Lu, Thai et al. 2009). During times of chronic IFN $\alpha$  stimulation and the expression of SOCS1, the ability of SOCS1 to negatively regulate STAT1 and STAT3 but not STAT5 may tip the balance towards STAT5 mediated effects driving T-reg cell development and suppressing Th17 cell development. This scenario ties in with the contribution of IFN $\alpha$  signaling to the inflammatory phenotype of *Socs1*<sup>-/-</sup> mice and their susceptibility to autoimmunity (Fenner, Starr et al. 2006). Whether this inflammation is driven by a lack of T-reg cells, however, remains to be determined.

SOCS1 is not the only negative regulator of type I IFN signaling. For example recent studies have also highlighted the importance of considering the effect of miRNA on IFN $\alpha$  signaling. This may be particularly important in the thymus as the thymic epithelial microRNA network has been shown to modify expression of IFNAR and thus IFN $\alpha$  signaling pathways that control infection associated thymic involution (Papadopoulou, Dooley et al. 2012). A microarray analysis, as performed in Chapter 5, provides a readout of the mRNA present within the cell through quantification of the association of mRNA with specific probes. The mRNA levels measured by microarray analysis, in steady state, reflect the balance of mRNA synthesis, stability and degradation. As discussed in chapter 1, miRNA is believed to have an effect on many components of the type I IFN pathway through regulation of the stability and degradation of mRNA. One such method for the analysis of miRNA expression involves next generation sequencing which can provide a total readout of the RNA expressed within the cell including mRNA, miRNA and long non-coding RNA. Future studies looking at the type I IFN response may therefore employ this method to provide a better understanding of the complex regulatory pathways activated by the IFNs and how these are controlled (ie. whether miRNA expression is controlled by SOCS1). Next generation sequencing could also be employed in combination with Chromatin IP studies (ChIP-Seq) to determine the specific sites of STAT binding following IFN $\alpha$  stimulation.

Although prediction models were used in Chapter 5 to identify STAT binding sites within gene promoters, these methods have their limitations. For example Clover

analysis employed in Chapter 5 relies on pre-defined binding sites and thus these studies are limited to the information contained within the TRANSFAC database. In addition, a pre-defined region must be selected on which the analysis is performed. In Chapter 5, a region of 2000bp upstream of the transcript site was selected and thus any potential binding sites outside of this region were not considered. Furthermore many of the STAT binding sites are similar in sequence and therefore competition for binding may occur which cannot be identified by prediction models. The use of ChIP-seq studies on different STATs following IFN $\alpha$  treatment would identify the exact sites to which these STATs bind. These studies could also be performed on a *Socs1*<sup>-/-</sup> background and thus also identify how SOCS1 controls STAT-DNA binding. A combination of ChIP-Seq studies with next generation sequencing of the RNA profile induced in the cell will also provide insight into how these STATs cooperatively regulate gene expression.

In addition to the analysis of STAT activation and STAT-DNA binding following IFN stimulation, future studies could also focus on non-STAT pathways induced by the IFNs. Promoter enrichment analysis of genes regulated by IFN found enrichment of binding elements associated with transcription factors such as Ets family members including Ets1, Ets2 and PU.1 as well as Blimp1 indicating these factors may also be regulated by IFN. As these transcription factors have previously been linked to T-cell regulation it is possible they may mediate T-cell responses following IFN stimulation (Gallant and Gilkeson 2006; Xin, Nutt et al. 2011). ChIP-Seq studies could be used to identify changes in DNA binding of these transcription factors following IFN stimulations. Furthermore the analysis of IFN signaling in mouse models with deletions of these transcription factors would identify whether they are required for the IFN response.

As IFN $\alpha$  induced STAT5 phosphorylation, in the thymus, was independent of SOCS1 negative regulation at early time points, we hypothesise that the mechanism of STAT5 phosphorylation by IFNAR differs to that of STAT1 and STAT3 phosphorylation mechanisms which are regulated by SOCS1. Our finding that SOCS1 binds to and inhibits TYK2 suggests that STAT1 and STAT3 require TYK2 for activation whereas STAT5 may use a different mechanism. Furthermore, as STAT1 and STAT3 require IFNAR2 tyrosine phosphorylation for their activation, STAT5 activation may be mediated by IFNAR1 (Zhao, Lee et al. 2008). SOCS1 inhibition of TYK2 may therefore result in reduced IFNAR2 tyrosine phosphorylation and reduced recruitment of STAT1

and STAT3 to IFNAR2 while IFNAR1 phosphorylation and STAT5 recruitment may continue uninhibited in the presence of SOCS1. Future studies could examine the effect SOCS1 has on IFNAR1 and IFNAR2 phosphorylation following stimulation to determine if this is the case. Alternatively, other kinases or adaptor proteins may also be interacting with the IFN receptor to mediate STAT5 phosphorylation. Evidence within the literature suggests that the adaptor protein GAB2 may be involved in IFN induced STAT5 activation. GAB2 has been linked, although independently, with constitutively binding IFNAR1 (Baychelier, Nardeux et al. 2007) and binding to STAT5 (Nyga, Pecquet et al. 2005). GAB2 is phosphorylated upon IFN $\alpha$  stimulation (Baychelier, Nardeux et al. 2007) and has many tyrosine phosphorylation sites to which STAT5 could potentially bind. Furthermore, in the context of IL-2 signaling, GAB2 has also been found to associate with CrkL (which can form dimers with phosphorylated STAT5) as well as p85 (part of the PI3-kinase complex which is also induced by IFN $\alpha$ ) and SHP-2 (a tyrosine phosphatase involved in the negative regulation of IFN $\alpha$ ) (Gesbert, Guenzi et al. 1998). GAB2 may therefore act as an adaptor for STAT5 and other signaling components activated by IFN (in a similar manner to IL-2 signaling) bringing them into close proximity with IFNAR associated kinases to mediate phosphorylation. Future studies involving knockout or knockdown of GAB2 may help elucidate the exact components acting at the receptor that are involved in STAT5 activation. Alternatively tyrosine kinase inhibitors that target specific JAK kinases or other tyrosine kinases shown to interact with IFNAR may also help elucidate the kinases involved in IFN $\alpha$  induced STAT5 phosphorylation.

Overall, these findings provide the foundation for selectively controlling the IFN response through control of STAT activation. Although further research is needed into the precise signaling mechanisms that occur at the receptor, it is evident that manipulation of IFN $\alpha$  signaling could be achieved by modulation of the STATs it activates. This could be achieved by a number of mechanisms including blocking or mutating specific STAT1 and STAT3 binding sites on the receptor such as Tyr510 of mu-Ifnar2. Indeed mouse models with selective tyrosine to phenylalanine mutations of residues within IFNAR1 and IFNAR2 would help elucidate the precise tyrosines required for IFN signaling *in vivo* and dispel any contradictory evidence that exists about IFNAR-STAT binding from *in vitro* studies. Other mechanisms which take into account how SOCS1 regulates IFN induced STAT activation could also be utilized to control IFN $\alpha$  signaling such as manipulating the level of SOCS1 expression within the cell, blocking SOCS1 binding to TYK2, altering the ability of the cell to activate Lys-63

ubiquitination pathways and thus altering SOCS1 mediated reduction of TYK2 and IFNAR1 surface levels or by using specific TYK2 or JAK1 inhibitors. As discussed in Chapter 1, IFNs are used in the clinic to treat a range of diseases such as viral infections, cancer and autoimmune disease (Hooks, Moutsopoulos et al. 1979; Talpaz, Kantarjian et al. 1987; Paredes and Krown 1991; Roffi, Mels et al. 1995; Mazzella, Saracco et al. 1999; Rizza, Moretti et al. 2010; Ronnblom 2011). There are however many adverse side effects of IFN treatment such as the development of flu-like symptoms, hematological changes and neuropsychiatric disturbances which often result in patients ceasing treatment (Calvaruso, Mazza et al. 2011). By altering the level of STATs activated by IFNs it may be possible to alter the IFN response to achieve desired clinical outcomes while reducing adverse effects.

## REFERENCES

- Abramovich, C., L. M. Shulman, et al. (1994). "Differential tyrosine phosphorylation of the IFNAR chain of the type I interferon receptor and of an associated surface protein in response to IFN-alpha and IFN-beta." Embo J **13**(24): 5871-5877.
- Adamson, A. S., K. Collins, et al. (2009). "The Current STATus of lymphocyte signaling: new roles for old players." Curr Opin Immunol **21**(2): 161-166.
- Agalioti, T., S. Lomvardas, et al. (2000). "Ordered recruitment of chromatin modifying and general transcription factors to the IFN-beta promoter." Cell **103**(4): 667-678.
- Aichele, P., H. Unsoeld, et al. (2006). "CD8 T cells specific for lymphocytic choriomeningitis virus require type I IFN receptor for clonal expansion." J Immunol **176**(8): 4525-4529.
- Akira, S. (1999). "Functional roles of STAT family proteins: lessons from knockout mice." Stem Cells **17**(3): 138-146.
- Akira, S., S. Uematsu, et al. (2006). "Pathogen recognition and innate immunity." Cell **124**(4): 783-801.
- Alcami, A., J. A. Symons, et al. (2000). "The vaccinia virus soluble alpha/beta interferon (IFN) receptor binds to the cell surface and protects cells from the antiviral effects of IFN." J Virol **74**(23): 11230-11239.
- Alexander, W. S., R. Starr, et al. (1999). "SOCS1 is a critical inhibitor of interferon gamma signaling and prevents the potentially fatal neonatal actions of this cytokine." Cell **98**(5): 597-608.
- Ann Marrie, R. and R. A. Rudick (2006). "Drug Insight: interferon treatment in multiple sclerosis." Nat Clin Pract Neurol **2**(1): 34-44.
- Barbieri, G., L. Velazquez, et al. (1994). "Activation of the protein tyrosine kinase tyk2 by interferon alpha/beta." Eur J Biochem **223**(2): 427-435.
- Basham, B., M. Sathe, et al. (2008). "In vivo identification of novel STAT5 target genes." Nucleic Acids Res **36**(11): 3802-3818.
- Basu, L., C. H. Yang, et al. (1998). "The antiviral action of interferon is potentiated by removal of the conserved IRTAM domain of the IFNAR1 chain of the interferon alpha/beta receptor: effects on JAK-STAT activation and receptor down-regulation." Virology **242**(1): 14-21.
- Battistini, A. (2009). "Interferon regulatory factors in hematopoietic cell differentiation and immune regulation." J Interferon Cytokine Res **29**(12): 765-780.
- Baychelier, F., P. C. Nardeux, et al. (2007). "Involvement of the Gab2 scaffolding adapter in type I interferon signalling." Cell Signal **19**(10): 2080-2087.

- Ben-Zvi, T., A. Yaron, et al. (2006). "Suppressors of cytokine signaling (SOCS) 1 and SOCS3 interact with and modulate fibroblast growth factor receptor signaling." J Cell Sci **119**(Pt 2): 380-387.
- Bennasser, Y., S. Y. Le, et al. (2005). "Evidence that HIV-1 encodes an siRNA and a suppressor of RNA silencing." Immunity **22**(5): 607-619.
- Bidwell, B. N., C. Y. Slaney, et al. (2012). "Silencing of Irf7 pathways in breast cancer cells promotes bone metastasis through immune escape." Nat Med.
- Brierley, M. M. and E. N. Fish (2005). "Stats: multifaceted regulators of transcription." J Interferon Cytokine Res **25**(12): 733-744.
- Burchill, M. A., J. Yang, et al. (2007). "IL-2 receptor beta-dependent STAT5 activation is required for the development of Foxp3+ regulatory T cells." J Immunol **178**(1): 280-290.
- Cajean-Feroldi, C., F. Nosal, et al. (2004). "Identification of residues of the IFNAR1 chain of the type I human interferon receptor critical for ligand binding and biological activity." Biochemistry **43**(39): 12498-12512.
- Calvaruso, V., M. Mazza, et al. (2011). "Pegylated-interferon-alpha(2a) in clinical practice: how to manage patients suffering from side effects." Expert Opin Drug Saf **10**(3): 429-435.
- Carmody, R. J. and Y. H. Chen (2007). "Nuclear factor-kappaB: activation and regulation during toll-like receptor signaling." Cell Mol Immunol **4**(1): 31-41.
- Chadha, K. C., J. L. Ambrus, Jr., et al. (2004). "Interferons and interferon inhibitory activity in disease and therapy." Exp Biol Med (Maywood) **229**(4): 285-290.
- Chakrabarti, A., B. K. Jha, et al. (2011). "New insights into the role of RNase L in innate immunity." J Interferon Cytokine Res **31**(1): 49-57.
- Chill, J. H., S. R. Quadt, et al. (2004). "NMR backbone dynamics of the human type I interferon binding subunit, a representative cytokine receptor." Biochemistry **43**(31): 10127-10137.
- Choe, J., M. S. Kelker, et al. (2005). "Crystal structure of human toll-like receptor 3 (TLR3) ectodomain." Science **309**(5734): 581-585.
- Chong, M. M., A. L. Cornish, et al. (2003). "Suppressor of cytokine signaling-1 is a critical regulator of interleukin-7-dependent CD8+ T cell differentiation." Immunity **18**(4): 475-487.
- Choubey, D. and K. D. Moudgil (2011). "Interferons in autoimmune and inflammatory diseases: regulation and roles." J Interferon Cytokine Res **31**(12): 857-865.
- Cohen, B., D. Novick, et al. (1995). "Ligand-induced association of the type I interferon receptor components." Mol Cell Biol **15**(8): 4208-4214.

- Colamonici, O., H. Yan, et al. (1994). "Direct binding to and tyrosine phosphorylation of the alpha subunit of the type I interferon receptor by p135tyk2 tyrosine kinase." Mol Cell Biol **14**(12): 8133-8142.
- Colamonici, O. R., H. Uyttendaele, et al. (1994). "p135tyk2, an interferon-alpha-activated tyrosine kinase, is physically associated with an interferon-alpha receptor." J Biol Chem **269**(5): 3518-3522.
- Colantonio, A. D., M. Epeldegui, et al. (2011). "IFN-alpha is constitutively expressed in the human thymus, but not in peripheral lymphoid organs." PLoS One **6**(8): e24252.
- Conrad, B. (2003). "Potential mechanisms of interferon-alpha induced autoimmunity." Autoimmunity **36**(8): 519-523.
- Constantinescu, S. N., E. Croze, et al. (1994). "Role of interferon alpha/beta receptor chain 1 in the structure and transmembrane signaling of the interferon alpha/beta receptor complex." Proc Natl Acad Sci U S A **91**(20): 9602-9606.
- Cornish, A. L., G. M. Davey, et al. (2003). "Suppressor of cytokine signaling-1 has IFN-gamma-independent actions in T cell homeostasis." J Immunol **170**(2): 878-886.
- Crow, M. K. (2010). "Type I interferon in organ-targeted autoimmune and inflammatory diseases." Arthritis Res Ther **12 Suppl 1**: S5.
- Dalpke, A. H., S. Opper, et al. (2001). "Suppressors of cytokine signaling (SOCS)-1 and SOCS-3 are induced by CpG-DNA and modulate cytokine responses in APCs." J Immunol **166**(12): 7082-7089.
- Darnell, J. E., Jr. (1997). "STATs and gene regulation." Science **277**(5332): 1630-1635.
- David, M. (2010). "Interferons and microRNAs." J Interferon Cytokine Res **30**(11): 825-828.
- de Weerd, N. A., S. A. Samarajiwa, et al. (2007). "Type I interferon receptors: biochemistry and biological functions." J Biol Chem **282**(28): 20053-20057.
- Dennis, G., Jr., B. T. Sherman, et al. (2003). "DAVID: Database for Annotation, Visualization, and Integrated Discovery." Genome Biol **4**(5): P3.
- Ding, Y., D. Chen, et al. (2003). "Suppressor of cytokine signaling 1 inhibits IL-10-mediated immune responses." J Immunol **170**(3): 1383-1391.
- Domanski, P., E. Fish, et al. (1997). "A region of the beta subunit of the interferon alpha receptor different from box 1 interacts with Jak1 and is sufficient to activate the Jak-Stat pathway and induce an antiviral state." J Biol Chem **272**(42): 26388-26393.
- Domanski, P., O. W. Nadeau, et al. (1998). "Differential use of the betaL subunit of the type I interferon (IFN) receptor determines signaling specificity for IFNalpha2 and IFNbeta." J Biol Chem **273**(6): 3144-3147.

- Domanski, P., M. Witte, et al. (1995). "Cloning and expression of a long form of the beta subunit of the interferon alpha beta receptor that is required for signaling." J Biol Chem **270**(37): 21606-21611.
- Dondi, E., L. Rogge, et al. (2003). "Down-modulation of responses to type I IFN upon T cell activation." J Immunol **170**(2): 749-756.
- Dondi, E., G. Roue, et al. (2004). "A dual role of IFN-alpha in the balance between proliferation and death of human CD4+ T lymphocytes during primary response." J Immunol **173**(6): 3740-3747.
- Dostert, C., E. Meylan, et al. (2008). "Intracellular pattern-recognition receptors." Adv Drug Deliv Rev **60**(7): 830-840.
- Dzionek, A., Y. Sohma, et al. (2001). "BDCA-2, a novel plasmacytoid dendritic cell-specific type II C-type lectin, mediates antigen capture and is a potent inhibitor of interferon alpha/beta induction." J Exp Med **194**(12): 1823-1834.
- Ehret, G. B., P. Reichenbach, et al. (2001). "DNA binding specificity of different STAT proteins. Comparison of in vitro specificity with natural target sites." J Biol Chem **276**(9): 6675-6688.
- Endo, T. A., M. Masuhara, et al. (1997). "A new protein containing an SH2 domain that inhibits JAK kinases." Nature **387**(6636): 921-924.
- Eriksen, K. W., V. H. Sommer, et al. (2004). "Bi-phasic effect of interferon (IFN)-alpha: IFN-alpha up- and down-regulates interleukin-4 signaling in human T cells." J Biol Chem **279**(1): 169-176.
- Farrar, J. D., J. D. Smith, et al. (2000). "Recruitment of Stat4 to the human interferon-alpha/beta receptor requires activated Stat2." J Biol Chem **275**(4): 2693-2697.
- Fenner, J. E., R. Starr, et al. (2006). "Suppressor of cytokine signaling 1 regulates the immune response to infection by a unique inhibition of type I interferon activity." Nat Immunol **7**(1): 33-39.
- Fish, E. N., S. Uddin, et al. (1999). "Activation of a CrkL-stat5 signaling complex by type I interferons." J Biol Chem **274**(2): 571-573.
- Fitzgerald, K. A., D. C. Rowe, et al. (2003). "LPS-TLR4 signaling to IRF-3/7 and NF-kappaB involves the toll adapters TRAM and TRIF." J Exp Med **198**(7): 1043-1055.
- Frith, M. C., Y. Fu, et al. (2004). "Detection of functional DNA motifs via statistical over-representation." Nucleic Acids Res **32**(4): 1372-1381.
- Gallant, S. and G. Gilkeson (2006). "ETS transcription factors and regulation of immunity." Arch Immunol Ther Exp (Warsz) **54**(3): 149-163.
- Gallucci, S., M. Lolkema, et al. (1999). "Natural adjuvants: endogenous activators of dendritic cells." Nat Med **5**(11): 1249-1255.

- Gauzzi, M. C., G. Barbieri, et al. (1997). "The amino-terminal region of Tyk2 sustains the level of interferon alpha receptor 1, a component of the interferon alpha/beta receptor." Proc Natl Acad Sci U S A **94**(22): 11839-11844.
- Gauzzi, M. C., L. Velazquez, et al. (1996). "Interferon-alpha-dependent activation of Tyk2 requires phosphorylation of positive regulatory tyrosines by another kinase." J Biol Chem **271**(34): 20494-20500.
- Gazziola, C., N. Cordani, et al. (2005). "The relative endogenous expression levels of the IFNAR2 isoforms influence the cytostatic and pro-apoptotic effect of IFNalpha on pleomorphic sarcoma cells." Int J Oncol **26**(1): 129-140.
- Gesbert, F., C. Guenzi, et al. (1998). "A new tyrosine-phosphorylated 97-kDa adaptor protein mediates interleukin-2-induced association of SHP-2 with p85-phosphatidylinositol 3-kinase in human T lymphocytes." J Biol Chem **273**(29): 18273-18281.
- Ghislain, J., C. A. Lingwood, et al. (1994). "Evidence for glycosphingolipid modification of the type 1 IFN receptor." J Immunol **153**(8): 3655-3663.
- Gibbs, V. C., M. Takahashi, et al. (1996). "A negative regulatory region in the intracellular domain of the human interferon-alpha receptor." J Biol Chem **271**(45): 28710-28716.
- Giordanetto, F. and R. T. Kroemer (2003). "A three-dimensional model of Suppressor Of Cytokine Signalling 1 (SOCS-1)." Protein Eng **16**(2): 115-124.
- Golding, A., A. Rosen, et al. (2010). "Interferon-alpha regulates the dynamic balance between human activated regulatory and effector T cells: implications for antiviral and autoimmune responses." Immunology **131**(1): 107-117.
- Gough, D. J., N. L. Messina, et al. (2010). "Functional crosstalk between type I and II interferon through the regulated expression of STAT1." PLoS Biol **8**(4): e1000361.
- Grimley, P. M., F. Dong, et al. (1999). "Stat5a and Stat5b: fraternal twins of signal transduction and transcriptional activation." Cytokine Growth Factor Rev **10**(2): 131-157.
- Gupta, S., M. Jiang, et al. (1999). "IFN-alpha activates Stat6 and leads to the formation of Stat2:Stat6 complexes in B cells." J Immunol **163**(7): 3834-3841.
- Gutterman, J. U. (1994). "Cytokine therapeutics: lessons from interferon alpha." Proc Natl Acad Sci U S A **91**(4): 1198-1205.
- Haller, O., P. Staeheli, et al. (2007). "Interferon-induced Mx proteins in antiviral host defense." Biochimie **89**(6-7): 812-818.
- Haque, S. J., P. C. Harbor, et al. (2000). "Identification of critical residues required for suppressor of cytokine signaling-specific regulation of interleukin-4 signaling." J Biol Chem **275**(34): 26500-26506.

- Hardy, M. P., C. M. Owczarek, et al. (2004). "Characterization of the type I interferon locus and identification of novel genes." Genomics **84**(2): 331-345.
- Hardy, M. P., C. M. Owczarek, et al. (2001). "The soluble murine type I interferon receptor Ifnar-2 is present in serum, is independently regulated, and has both agonistic and antagonistic properties." Blood **97**(2): 473-482.
- Havenar-Daughton, C., G. A. Kolumam, et al. (2006). "Cutting Edge: The direct action of type I IFN on CD4 T cells is critical for sustaining clonal expansion in response to a viral but not a bacterial infection." J Immunol **176**(6): 3315-3319.
- Hemmi, H., T. Kaisho, et al. (2003). "The roles of Toll-like receptor 9, MyD88, and DNA-dependent protein kinase catalytic subunit in the effects of two distinct CpG DNAs on dendritic cell subsets." J Immunol **170**(6): 3059-3064.
- Hengel, H., U. H. Koszinowski, et al. (2005). "Viruses know it all: new insights into IFN networks." Trends Immunol **26**(7): 396-401.
- Hertzog, P. J., L. A. O'Neill, et al. (2003). "The interferon in TLR signaling: more than just antiviral." Trends Immunol **24**(10): 534-539.
- Hilton, D. J., R. T. Richardson, et al. (1998). "Twenty proteins containing a C-terminal SOCS box form five structural classes." Proc Natl Acad Sci U S A **95**(1): 114-119.
- Hirohata, S., H. Shibuya, et al. (2010). "Suppressive influences of IFN-alpha on IL-17 expression in human CD4+ T cells." Clin Immunol **134**(3): 340-344.
- Hoebe, K., E. M. Janssen, et al. (2003). "Upregulation of costimulatory molecules induced by lipopolysaccharide and double-stranded RNA occurs by Trif-dependent and Trif-independent pathways." Nat Immunol **4**(12): 1223-1229.
- Honda, K., A. Takaoka, et al. (2006). "Type I interferon [corrected] gene induction by the interferon regulatory factor family of transcription factors." Immunity **25**(3): 349-360.
- Honda, K., H. Yanai, et al. (2004). "Role of a transductional-transcriptional processor complex involving MyD88 and IRF-7 in Toll-like receptor signaling." Proc Natl Acad Sci U S A **101**(43): 15416-15421.
- Honda, K., H. Yanai, et al. (2005). "IRF-7 is the master regulator of type-I interferon-dependent immune responses." Nature **434**(7034): 772-777.
- Hooks, J. J., H. M. Moutsopoulos, et al. (1979). "Immune interferon in the circulation of patients with autoimmune disease." N Engl J Med **301**(1): 5-8.
- Hoshino, K., O. Takeuchi, et al. (1999). "Cutting edge: Toll-like receptor 4 (TLR4)-deficient mice are hyporesponsive to lipopolysaccharide: evidence for TLR4 as the Lps gene product." J Immunol **162**(7): 3749-3752.
- Huang da, W., B. T. Sherman, et al. (2007). "The DAVID Gene Functional Classification Tool: a novel biological module-centric algorithm to functionally analyze large gene lists." Genome Biol **8**(9): R183.

- Hwang, S. Y., P. J. Hertzog, et al. (1995). "A null mutation in the gene encoding a type I interferon receptor component eliminates antiproliferative and antiviral responses to interferons alpha and beta and alters macrophage responses." Proc Natl Acad Sci U S A **92**(24): 11284-11288.
- Indraccolo, S. (2010). "Interferon-alpha as angiogenesis inhibitor: learning from tumor models." Autoimmunity **43**(3): 244-247.
- Inohara, N. and G. Nunez (2003). "NODs: intracellular proteins involved in inflammation and apoptosis." Nat Rev Immunol **3**(5): 371-382.
- Isaacs, A. and J. Lindenmann (1957). "Virus interference. I. The interferon." Proc R Soc Lond B Biol Sci **147**(927): 258-267.
- Ishikawa, H. and G. N. Barber (2008). "STING is an endoplasmic reticulum adaptor that facilitates innate immune signalling." Nature **455**(7213): 674-678.
- Jegalian, A. G. and H. Wu (2002). "Differential roles of SOCS family members in EpoR signal transduction." J Interferon Cytokine Res **22**(8): 853-860.
- Kadowaki, N. and Y. J. Liu (2002). "Natural type I interferon-producing cells as a link between innate and adaptive immunity." Hum Immunol **63**(12): 1126-1132.
- Karaghiosoff, M., R. Steinborn, et al. (2003). "Central role for type I interferons and Tyk2 in lipopolysaccharide-induced endotoxin shock." Nat Immunol **4**(5): 471-477.
- Kato, H., S. Sato, et al. (2005). "Cell type-specific involvement of RIG-I in antiviral response." Immunity **23**(1): 19-28.
- Kato, H., O. Takeuchi, et al. (2006). "Differential roles of MDA5 and RIG-I helicases in the recognition of RNA viruses." Nature **441**(7089): 101-105.
- Kawai, T., O. Adachi, et al. (1999). "Unresponsiveness of MyD88-deficient mice to endotoxin." Immunity **11**(1): 115-122.
- Kawai, T., S. Sato, et al. (2004). "Interferon-alpha induction through Toll-like receptors involves a direct interaction of IRF7 with MyD88 and TRAF6." Nat Immunol **5**(10): 1061-1068.
- Kawai, T., K. Takahashi, et al. (2005). "IPS-1, an adaptor triggering RIG-I- and Mda5-mediated type I interferon induction." Nat Immunol **6**(10): 981-988.
- Kim, S. H., B. Cohen, et al. (1997). "Mammalian type I interferon receptors consists of two subunits: IFNAR1 and IFNAR2." Gene **196**(1-2): 279-286.
- Kim, T., S. Pazhoor, et al. (2010). "Aspartate-glutamate-alanine-histidine box motif (DEAH)/RNA helicase A helicases sense microbial DNA in human plasmacytoid dendritic cells." Proc Natl Acad Sci U S A **107**(34): 15181-15186.
- Kim, T. K. and T. Maniatis (1997). "The mechanism of transcriptional synergy of an in vitro assembled interferon-beta enhanceosome." Mol Cell **1**(1): 119-129.

- Kinjyo, I., T. Hanada, et al. (2002). "SOCS1/JAB is a negative regulator of LPS-induced macrophage activation." Immunity **17**(5): 583-591.
- Kolumam, G. A., S. Thomas, et al. (2005). "Type I interferons act directly on CD8 T cells to allow clonal expansion and memory formation in response to viral infection." J Exp Med **202**(5): 637-650.
- Kotenko, S. V., G. Gallagher, et al. (2003). "IFN-lambdas mediate antiviral protection through a distinct class II cytokine receptor complex." Nat Immunol **4**(1): 69-77.
- Kotenko, S. V., L. S. Izotova, et al. (1999). "The intracellular domain of interferon-alpha receptor 2c (IFN-alphaR2c) chain is responsible for Stat activation." Proc Natl Acad Sci U S A **96**(9): 5007-5012.
- Kramer, O. H., D. Baus, et al. (2006). "Acetylation of Stat1 modulates NF-kappaB activity." Genes Dev **20**(4): 473-485.
- Kramer, O. H., S. K. Knauer, et al. (2009). "A phosphorylation-acetylation switch regulates STAT1 signaling." Genes Dev **23**(2): 223-235.
- Krause, C. D. and S. Pestka (2005). "Evolution of the Class 2 cytokines and receptors, and discovery of new friends and relatives." Pharmacol Ther **106**(3): 299-346.
- Krishnan, K., B. Singh, et al. (1998). "Identification of amino acid residues critical for the Src-homology 2 domain-dependent docking of Stat2 to the interferon alpha receptor." J Biol Chem **273**(31): 19495-19501.
- Kumar, H., T. Kawai, et al. (2006). "Essential role of IPS-1 in innate immune responses against RNA viruses." J Exp Med **203**(7): 1795-1803.
- Lamken, P., S. Lata, et al. (2004). "Ligand-induced assembling of the type I interferon receptor on supported lipid bilayers." J Mol Biol **341**(1): 303-318.
- Le Bon, A., V. Durand, et al. (2006). "Direct stimulation of T cells by type I IFN enhances the CD8+ T cell response during cross-priming." J Immunol **176**(8): 4682-4689.
- Le Bon, A., N. Etchart, et al. (2003). "Cross-priming of CD8+ T cells stimulated by virus-induced type I interferon." Nat Immunol **4**(10): 1009-1015.
- Le Bon, A., C. Thompson, et al. (2006). "Cutting edge: enhancement of antibody responses through direct stimulation of B and T cells by type I IFN." J Immunol **176**(4): 2074-2078.
- Lecellier, C. H., P. Dunoyer, et al. (2005). "A cellular microRNA mediates antiviral defense in human cells." Science **308**(5721): 557-560.
- Lekmine, F., A. Sassano, et al. (2002). "The CrkL adapter protein is required for type I interferon-dependent gene transcription and activation of the small G-protein Rap1." Biochem Biophys Res Commun **291**(4): 744-750.

- Lenschow, D. J., C. Lai, et al. (2007). "IFN-stimulated gene 15 functions as a critical antiviral molecule against influenza, herpes, and Sindbis viruses." Proc Natl Acad Sci U S A **104**(4): 1371-1376.
- Leung, S., S. A. Qureshi, et al. (1995). "Role of STAT2 in the alpha interferon signaling pathway." Mol Cell Biol **15**(3): 1312-1317.
- Levy, D. E. and J. E. Darnell, Jr. (2002). "Stats: transcriptional control and biological impact." Nat Rev Mol Cell Biol **3**(9): 651-662.
- Li, X., S. Leung, et al. (1997). "Functional subdomains of STAT2 required for preassociation with the alpha interferon receptor and for signaling." Mol Cell Biol **17**(4): 2048-2056.
- Lin, Q., C. Dong, et al. (1998). "Impairment of T and B cell development by treatment with a type I interferon." J Exp Med **187**(1): 79-87.
- Lindenmann, J. (1962). "Resistance of mice to mouse-adapted influenza A virus." Virology **16**: 203-204.
- Lindenmann, J., D. C. Burke, et al. (1957). "Studies on the production, mode of action and properties of interferon." Br J Exp Pathol **38**(5): 551-562.
- Liu, B., J. Liao, et al. (1998). "Inhibition of Stat1-mediated gene activation by PIAS1." Proc Natl Acad Sci U S A **95**(18): 10626-10631.
- Liu, Y. J. (2005). "IPC: professional type 1 interferon-producing cells and plasmacytoid dendritic cell precursors." Annu Rev Immunol **23**: 275-306.
- Lu, L. F., T. H. Thai, et al. (2009). "Foxp3-dependent microRNA155 confers competitive fitness to regulatory T cells by targeting SOCS1 protein." Immunity **30**(1): 80-91.
- Luft, T., K. C. Pang, et al. (1998). "Type I IFNs enhance the terminal differentiation of dendritic cells." J Immunol **161**(4): 1947-1953.
- Lutfalla, G., S. J. Holland, et al. (1995). "Mutant U5A cells are complemented by an interferon-alpha beta receptor subunit generated by alternative processing of a new member of a cytokine receptor gene cluster." Embo J **14**(20): 5100-5108.
- MacMicking, J. D. (2004). "IFN-inducible GTPases and immunity to intracellular pathogens." Trends Immunol **25**(11): 601-609.
- Mamane, Y., C. Heylbroeck, et al. (1999). "Interferon regulatory factors: the next generation." Gene **237**(1): 1-14.
- Marine, J. C., D. J. Topham, et al. (1999). "SOCS1 deficiency causes a lymphocyte-dependent perinatal lethality." Cell **98**(5): 609-616.
- Marrack, P., J. Kappler, et al. (1999). "Type I interferons keep activated T cells alive." J Exp Med **189**(3): 521-530.

- Martins, G. and K. Calame (2008). "Regulation and functions of Blimp-1 in T and B lymphocytes." Annu Rev Immunol **26**: 133-169.
- Mathur, A. N., H. C. Chang, et al. (2007). "Stat3 and Stat4 direct development of IL-17-secreting Th cells." J Immunol **178**(8): 4901-4907.
- Matskevich, A. A. and K. Moelling (2007). "Dicer is involved in protection against influenza A virus infection." J Gen Virol **88**(Pt 10): 2627-2635.
- Mazzella, G., G. Saracco, et al. (1999). "Long-term results with interferon therapy in chronic type B hepatitis: a prospective randomized trial." Am J Gastroenterol **94**(8): 2246-2250.
- McKenna, S. D., K. Vergilis, et al. (2004). "Formation of human IFN-beta complex with the soluble type I interferon receptor IFNAR-2 leads to enhanced IFN stability, pharmacokinetics, and antitumor activity in xenografted SCID mice." J Interferon Cytokine Res **24**(2): 119-129.
- Meraz, M. A., J. M. White, et al. (1996). "Targeted disruption of the Stat1 gene in mice reveals unexpected physiologic specificity in the JAK-STAT signaling pathway." Cell **84**(3): 431-442.
- Meurs, E., K. Chong, et al. (1990). "Molecular cloning and characterization of the human double-stranded RNA-activated protein kinase induced by interferon." Cell **62**(2): 379-390.
- Meurs, E. F., Y. Watanabe, et al. (1992). "Constitutive expression of human double-stranded RNA-activated p68 kinase in murine cells mediates phosphorylation of eukaryotic initiation factor 2 and partial resistance to encephalomyocarditis virus growth." J Virol **66**(10): 5805-5814.
- Moro, H., D. C. Otero, et al. (2011). "T cell-intrinsic and -extrinsic contributions of the IFNAR/STAT1-axis to thymocyte survival." PLoS One **6**(9): e24972.
- Moschen, A. R., S. Geiger, et al. (2008). "Interferon-alpha controls IL-17 expression in vitro and in vivo." Immunobiology **213**(9-10): 779-787.
- Mowen, K. A., J. Tang, et al. (2001). "Arginine methylation of STAT1 modulates IFNalpha/beta-induced transcription." Cell **104**(5): 731-741.
- Muller, M., J. Briscoe, et al. (1993). "The protein tyrosine kinase JAK1 complements defects in interferon-alpha/beta and -gamma signal transduction." Nature **366**(6451): 129-135.
- Muller, U., U. Steinhoff, et al. (1994). "Functional role of type I and type II interferons in antiviral defense." Science **264**(5167): 1918-1921.
- Nadeau, O. W., P. Domanski, et al. (1999). "The proximal tyrosines of the cytoplasmic domain of the beta chain of the type I interferon receptor are essential for signal transducer and activator of transcription (Stat) 2 activation. Evidence that two Stat2 sites are required to reach a threshold of interferon alpha-induced Stat2 tyrosine phosphorylation that allows normal formation of interferon-stimulated gene factor 3." J Biol Chem **274**(7): 4045-4052.

- Nagano, Y. and Y. Kojima (1954). "[Immunizing property of vaccinia virus inactivated by ultraviolet rays]." C R Seances Soc Biol Fil **148**(19-20): 1700-1702.
- Naka, T., M. Narazaki, et al. (1997). "Structure and function of a new STAT-induced STAT inhibitor." Nature **387**(6636): 924-929.
- Nakayama, Y., E. H. Plisch, et al. (2010). "Role of PKR and Type I IFNs in viral control during primary and secondary infection." PLoS Pathog **6**(6): e1000966.
- Narazaki, M., M. Fujimoto, et al. (1998). "Three distinct domains of SSI-1/SOCS-1/JAB protein are required for its suppression of interleukin 6 signaling." Proc Natl Acad Sci U S A **95**(22): 13130-13134.
- Negishi, H., Y. Fujita, et al. (2006). "Evidence for licensing of IFN-gamma-induced IFN regulatory factor 1 transcription factor by MyD88 in Toll-like receptor-dependent gene induction program." Proc Natl Acad Sci U S A **103**(41): 15136-15141.
- Netherton, C. L., J. Simpson, et al. (2009). "Inhibition of a large double-stranded DNA virus by MxA protein." J Virol **83**(5): 2310-2320.
- Nguyen, V. P., A. Z. Saleh, et al. (2002). "Stat2 binding to the interferon-alpha receptor 2 subunit is not required for interferon-alpha signaling." J Biol Chem **277**(12): 9713-9721.
- Nicholson, S. E., D. De Souza, et al. (2000). "Suppressor of cytokine signaling-3 preferentially binds to the SHP-2-binding site on the shared cytokine receptor subunit gp130." Proc Natl Acad Sci U S A **97**(12): 6493-6498.
- Nicholson, S. E., T. A. Willson, et al. (1999). "Mutational analyses of the SOCS proteins suggest a dual domain requirement but distinct mechanisms for inhibition of LIF and IL-6 signal transduction." Embo J **18**(2): 375-385.
- Nishibori, T., Y. Tanabe, et al. (2004). "Impaired development of CD4+ CD25+ regulatory T cells in the absence of STAT1: increased susceptibility to autoimmune disease." J Exp Med **199**(1): 25-34.
- Novick, D., B. Cohen, et al. (1994). "The human interferon alpha/beta receptor: characterization and molecular cloning." Cell **77**(3): 391-400.
- Nyga, R., C. Pecquet, et al. (2005). "Activated STAT5 proteins induce activation of the PI 3-kinase/Akt and Ras/MAPK pathways via the Gab2 scaffolding adapter." Biochem J **390**(Pt 1): 359-366.
- Oganesyan, G., S. K. Saha, et al. (2006). "Critical role of TRAF3 in the Toll-like receptor-dependent and -independent antiviral response." Nature **439**(7073): 208-211.
- Otsuka, M., Q. Jing, et al. (2007). "Hypersusceptibility to vesicular stomatitis virus infection in Dicer1-deficient mice is due to impaired miR24 and miR93 expression." Immunity **27**(1): 123-134.

- Owczarek, C. M., S. Y. Hwang, et al. (1997). "Cloning and characterization of soluble and transmembrane isoforms of a novel component of the murine type I interferon receptor, IFNAR 2." J Biol Chem **272**(38): 23865-23870.
- Ozato, K., P. Taylor, et al. (2007). "The interferon regulatory factor family in host defense: mechanism of action." J Biol Chem **282**(28): 20065-20069.
- Pace, L., S. Vitale, et al. (2010). "APC activation by IFN-alpha decreases regulatory T cell and enhances Th cell functions." J Immunol **184**(11): 5969-5979.
- Papadopoulou, A. S., J. Dooley, et al. (2012). "The thymic epithelial microRNA network elevates the threshold for infection-associated thymic involution via miR-29a mediated suppression of the IFN-alpha receptor." Nat Immunol **13**(2): 181-187.
- Paquette, R. L., N. Hsu, et al. (2002). "Interferon-alpha induces dendritic cell differentiation of CML mononuclear cells in vitro and in vivo." Leukemia **16**(8): 1484-1489.
- Paredes, J. and S. E. Krown (1991). "Interferon-alpha therapy in patients with Kaposi's sarcoma and the acquired immunodeficiency syndrome." Int J Immunopharmacol **13 Suppl 1**: 77-81.
- Park, C., S. Li, et al. (2000). "Immune response in Stat2 knockout mice." Immunity **13**(6): 795-804.
- Pedersen, I. M., G. Cheng, et al. (2007). "Interferon modulation of cellular microRNAs as an antiviral mechanism." Nature **449**(7164): 919-922.
- Pfeffer, L. M., L. Basu, et al. (1997). "The short form of the interferon alpha/beta receptor chain 2 acts as a dominant negative for type I interferon action." J Biol Chem **272**(17): 11002-11005.
- Platanias, L. C., S. Uddin, et al. (1999). "CrkL and CrkII participate in the generation of the growth inhibitory effects of interferons on primary hematopoietic progenitors." Exp Hematol **27**(8): 1315-1321.
- Platanias, L. C., S. Uddin, et al. (1994). "Tyrosine phosphorylation of the alpha and beta subunits of the type I interferon receptor. Interferon-beta selectively induces tyrosine phosphorylation of an alpha subunit-associated protein." J Biol Chem **269**(27): 17761-17764.
- Platanias, L. C., S. Uddin, et al. (1996). "The type I interferon receptor mediates tyrosine phosphorylation of insulin receptor substrate 2." J Biol Chem **271**(1): 278-282.
- Poltorak, A., X. He, et al. (1998). "Defective LPS signaling in C3H/HeJ and C57BL/10ScCr mice: mutations in Tlr4 gene." Science **282**(5396): 2085-2088.
- Qing, Y., A. P. Costa-Pereira, et al. (2005). "Role of tyrosine 441 of interferon-gamma receptor subunit 1 in SOCS-1-mediated attenuation of STAT1 activation." J Biol Chem **280**(3): 1849-1853.

- Ragimbeau, J., E. Dondi, et al. (2003). "The tyrosine kinase Tyk2 controls IFNAR1 cell surface expression." Embo J **22**(3): 537-547.
- Rani, M. R., D. W. Leaman, et al. (1999). "Catalytically active TYK2 is essential for interferon-beta-mediated phosphorylation of STAT3 and interferon-alpha receptor-1 (IFNAR-1) but not for activation of phosphoinositol 3-kinase." J Biol Chem **274**(45): 32507-32511.
- Riboldi, E., R. Daniele, et al. (2011). "Human C-type lectin domain family 4, member C (CLEC4C/BDCA-2/CD303) is a receptor for asialo-galactosyl-oligosaccharides." J Biol Chem **286**(41): 35329-35333.
- Rissoan, M. C., V. Soumelis, et al. (1999). "Reciprocal control of T helper cell and dendritic cell differentiation." Science **283**(5405): 1183-1186.
- Rizza, P., F. Moretti, et al. (2010). "Recent advances on the immunomodulatory effects of IFN-alpha: implications for cancer immunotherapy and autoimmunity." Autoimmunity **43**(3): 204-209.
- Rodig, S. J., M. A. Meraz, et al. (1998). "Disruption of the Jak1 gene demonstrates obligatory and nonredundant roles of the Jaks in cytokine-induced biologic responses." Cell **93**(3): 373-383.
- Roffi, L., G. C. Mels, et al. (1995). "Breakthrough during recombinant interferon alfa therapy in patients with chronic hepatitis C virus infection: prevalence, etiology, and management." Hepatology **21**(3): 645-649.
- Ronnblom, L. (2011). "The type I interferon system in the etiopathogenesis of autoimmune diseases." Ups J Med Sci **116**(4): 227-237.
- Russell-Harde, D., T. C. Wagner, et al. (2000). "Role of the intracellular domain of the human type I interferon receptor 2 chain (IFNAR2c) in interferon signaling. Expression of IFNAR2c truncation mutants in U5A cells." J Biol Chem **275**(31): 23981-23985.
- Saha, S. K., E. M. Pietras, et al. (2006). "Regulation of antiviral responses by a direct and specific interaction between TRAF3 and Cardif." Embo J **25**(14): 3257-3263.
- Sakaguchi, S., H. Negishi, et al. (2003). "Essential role of IRF-3 in lipopolysaccharide-induced interferon-beta gene expression and endotoxin shock." Biochem Biophys Res Commun **306**(4): 860-866.
- Sakamoto, E., F. Hato, et al. (2005). "Type I and type II interferons delay human neutrophil apoptosis via activation of STAT3 and up-regulation of cellular inhibitor of apoptosis 2." J Leukoc Biol **78**(1): 301-309.
- Sakamoto, H., H. Yasukawa, et al. (1998). "A Janus kinase inhibitor, JAB, is an interferon-gamma-inducible gene and confers resistance to interferons." Blood **92**(5): 1668-1676.
- Saleh, A. Z., A. T. Fang, et al. (2004). "Regulated proteolysis of the IFNAR2 subunit of the interferon-alpha receptor." Oncogene **23**(42): 7076-7086.

- Sancho, D. and C. Reis e Sousa (2012). "Signaling by myeloid C-type lectin receptors in immunity and homeostasis." Annu Rev Immunol **30**: 491-529.
- Sato, M., N. Hata, et al. (1998). "Positive feedback regulation of type I IFN genes by the IFN-inducible transcription factor IRF-7." FEBS Lett **441**(1): 106-110.
- Sato, M., N. Tanaka, et al. (1998). "Involvement of the IRF family transcription factor IRF-3 in virus-induced activation of the IFN-beta gene." FEBS Lett **425**(1): 112-116.
- Schluter, G., D. Boinska, et al. (2000). "Evidence for translational repression of the SOCS-1 major open reading frame by an upstream open reading frame." Biochem Biophys Res Commun **268**(2): 255-261.
- Schoggins, J. W., S. J. Wilson, et al. (2011). "A diverse range of gene products are effectors of the type I interferon antiviral response." Nature **472**(7344): 481-485.
- Sheppard, P., W. Kindsvogel, et al. (2003). "IL-28, IL-29 and their class II cytokine receptor IL-28R." Nat Immunol **4**(1): 63-68.
- Shimoda, K., K. Kato, et al. (2000). "Tyk2 plays a restricted role in IFN alpha signaling, although it is required for IL-12-mediated T cell function." Immunity **13**(4): 561-571.
- Song, M. M. and K. Shuai (1998). "The suppressor of cytokine signaling (SOCS) 1 and SOCS3 but not SOCS2 proteins inhibit interferon-mediated antiviral and antiproliferative activities." J Biol Chem **273**(52): 35056-35062.
- Sozzani, S., D. Bosisio, et al. (2010). "Type I interferons in systemic autoimmunity." Autoimmunity **43**(3): 196-203.
- Sporri, B., P. E. Kovanen, et al. (2001). "JAB/SOCS1/SSI-1 is an interleukin-2-induced inhibitor of IL-2 signaling." Blood **97**(1): 221-226.
- Stark, G. R. and J. E. Darnell, Jr. (2012). "The JAK-STAT pathway at twenty." Immunity **36**(4): 503-514.
- Stark, G. R., I. M. Kerr, et al. (1998). "How cells respond to interferons." Annu Rev Biochem **67**: 227-264.
- Starr, R., D. Metcalf, et al. (1998). "Liver degeneration and lymphoid deficiencies in mice lacking suppressor of cytokine signaling-1." Proc Natl Acad Sci U S A **95**(24): 14395-14399.
- Starr, R., T. A. Willson, et al. (1997). "A family of cytokine-inducible inhibitors of signalling." Nature **387**(6636): 917-921.
- Strengell, M., A. Lehtonen, et al. (2006). "IL-21 enhances SOCS gene expression and inhibits LPS-induced cytokine production in human monocyte-derived dendritic cells." J Leukoc Biol.

- Strunk, J. J., I. Gregor, et al. (2008). "Ligand binding induces a conformational change in ifnar1 that is propagated to its membrane-proximal domain." J Mol Biol **377**(3): 725-739.
- Takahashi, R., S. Nishimoto, et al. (2011). "SOCS1 is essential for regulatory T cell functions by preventing loss of Foxp3 expression as well as IFN- $\gamma$  and IL-17A production." J Exp Med **208**(10): 2055-2067.
- Takeuchi, O. and S. Akira (2010). "Pattern recognition receptors and inflammation." Cell **140**(6): 805-820.
- Talpaz, M., H. M. Kantarjian, et al. (1987). "Clinical investigation of human alpha interferon in chronic myelogenous leukemia." Blood **69**(5): 1280-1288.
- Tamura, T., P. Thotakura, et al. (2005). "Identification of target genes and a unique cis element regulated by IRF-8 in developing macrophages." Blood **106**(6): 1938-1947.
- Tang, X., J. S. Gao, et al. (2007). "Acetylation-dependent signal transduction for type I interferon receptor." Cell **131**(1): 93-105.
- Tang, Y., X. Luo, et al. (2009). "MicroRNA-146A contributes to abnormal activation of the type I interferon pathway in human lupus by targeting the key signaling proteins." Arthritis Rheum **60**(4): 1065-1075.
- Taylor, G. A., C. G. Feng, et al. (2007). "Control of IFN-gamma-mediated host resistance to intracellular pathogens by immunity-related GTPases (p47 GTPases)." Microbes Infect **9**(14-15): 1644-1651.
- Thomis, D. C. and C. E. Samuel (1993). "Mechanism of interferon action: evidence for intermolecular autophosphorylation and autoactivation of the interferon-induced, RNA-dependent protein kinase PKR." J Virol **67**(12): 7695-7700.
- Trajanovska, S., C. M. Owczarek, et al. (2003). "Generation and characterization of recombinant unmodified and phosphorylatable murine IFN-alpha1 in the methylotropic yeast *Pichia pastoris*." J Interferon Cytokine Res **23**(7): 351-358.
- Tyler, D. R., M. E. Persky, et al. (2007). "Pre-assembly of STAT4 with the human IFN-alpha/beta receptor-2 subunit is mediated by the STAT4 N-domain." Mol Immunol **44**(8): 1864-1872.
- Uddin, S., F. Lekmine, et al. (2003). "Role of Stat5 in type I interferon-signaling and transcriptional regulation." Biochem Biophys Res Commun **308**(2): 325-330.
- Uddin, S., F. Lekmine, et al. (2000). "The Rac1/p38 mitogen-activated protein kinase pathway is required for interferon alpha-dependent transcriptional activation but not serine phosphorylation of Stat proteins." J Biol Chem **275**(36): 27634-27640.
- Uddin, S., A. Sassano, et al. (2002). "Protein kinase C-delta (PKC-delta ) is activated by type I interferons and mediates phosphorylation of Stat1 on serine 727." J Biol Chem **277**(17): 14408-14416.

- Uematsu, S. and S. Akira (2007). "Toll-like receptors and Type I interferons." J Biol Chem **282**(21): 15319-15323.
- Uze, G., G. Lutfalla, et al. (1992). "Behavior of a cloned murine interferon alpha/beta receptor expressed in homospecific or heterospecific background." Proc Natl Acad Sci U S A **89**(10): 4774-4778.
- Uze, G., G. Lutfalla, et al. (1990). "Genetic transfer of a functional human interferon alpha receptor into mouse cells: cloning and expression of its cDNA." Cell **60**(2): 225-234.
- van Boxel-Dezaire, A. H., M. R. Rani, et al. (2006). "Complex modulation of cell type-specific signaling in response to type I interferons." Immunity **25**(3): 361-372.
- van Boxel-Dezaire, A. H., J. A. Zula, et al. (2010). "Major differences in the responses of primary human leukocyte subsets to IFN-beta." J Immunol **185**(10): 5888-5899.
- Velazquez, L., M. Fellous, et al. (1992). "A protein tyrosine kinase in the interferon alpha/beta signaling pathway." Cell **70**(2): 313-322.
- Velichko, S., T. C. Wagner, et al. (2002). "STAT3 activation by type I interferons is dependent on specific tyrosines located in the cytoplasmic domain of interferon receptor chain 2c. Activation of multiple STATS proceeds through the redundant usage of two tyrosine residues." J Biol Chem **277**(38): 35635-35641.
- Versteeg, G. A. and A. Garcia-Sastre (2010). "Viral tricks to grid-lock the type I interferon system." Curr Opin Microbiol **13**(4): 508-516.
- Vezi, E., A. Aghemo, et al. (2011). "Interferon in the treatment of chronic hepatitis C: a drug caught between past and future." Expert Opin Biol Ther **11**(3): 301-313.
- Waetzig, G. H. and S. Rose-John (2012). "Hitting a complex target: an update on interleukin-6 trans-signalling." Expert Opin Ther Targets **16**(2): 225-236.
- Wagner, T. C., S. Velichko, et al. (2002). "Interferon signaling is dependent on specific tyrosines located within the intracellular domain of IFNAR2c. Expression of IFNAR2c tyrosine mutants in U5A cells." J Biol Chem **277**(2): 1493-1499.
- Wang, P., J. Hou, et al. (2010). "Inducible microRNA-155 feedback promotes type I IFN signaling in antiviral innate immunity by targeting suppressor of cytokine signaling 1." J Immunol **185**(10): 6226-6233.
- Xin, A., S. L. Nutt, et al. (2011). "Blimp1: driving terminal differentiation to a T." Adv Exp Med Biol **780**: 85-100.
- Xu, L. G., Y. Y. Wang, et al. (2005). "VISA is an adapter protein required for virus-triggered IFN-beta signaling." Mol Cell **19**(6): 727-740.
- Yamamoto, M., S. Sato, et al. (2003). "Role of adaptor TRIF in the MyD88-independent toll-like receptor signaling pathway." Science **301**(5633): 640-643.

- Yan, H., K. Krishnan, et al. (1996). "Phosphorylated interferon-alpha receptor 1 subunit (IFNaR1) acts as a docking site for the latent form of the 113 kDa STAT2 protein." Embo J **15**(5): 1064-1074.
- Yan, H., K. Krishnan, et al. (1996). "Molecular characterization of an alpha interferon receptor 1 subunit (IFNaR1) domain required for TYK2 binding and signal transduction." Mol Cell Biol **16**(5): 2074-2082.
- Yang, C. H., W. Shi, et al. (1996). "Direct association of STAT3 with the IFNAR-1 chain of the human type I interferon receptor." J Biol Chem **271**(14): 8057-8061.
- Yang, J. and G. R. Stark (2008). "Roles of unphosphorylated STATs in signaling." Cell Res **18**(4): 443-451.
- Yang, X. O., R. Nurieva, et al. (2008). "Molecular antagonism and plasticity of regulatory and inflammatory T cell programs." Immunity **29**(1): 44-56.
- Yang, X. O., A. D. Panopoulos, et al. (2007). "STAT3 regulates cytokine-mediated generation of inflammatory helper T cells." J Biol Chem **282**(13): 9358-9363.
- Yao, Z., Y. Kanno, et al. (2007). "Nonredundant roles for Stat5a/b in directly regulating Foxp3." Blood **109**(10): 4368-4375.
- Yasukawa, H., H. Misawa, et al. (1999). "The JAK-binding protein JAB inhibits Janus tyrosine kinase activity through binding in the activation loop." Embo J **18**(5): 1309-1320.
- Yoneyama, M., M. Kikuchi, et al. (2004). "The RNA helicase RIG-I has an essential function in double-stranded RNA-induced innate antiviral responses." Nat Immunol **5**(7): 730-737.
- Yoshimura, A., T. Ohkubo, et al. (1995). "A novel cytokine-inducible gene CIS encodes an SH2-containing protein that binds to tyrosine-phosphorylated interleukin 3 and erythropoietin receptors." Embo J **14**(12): 2816-2826.
- Zelensky, A. N. and J. E. Gready (2005). "The C-type lectin-like domain superfamily." FEBS J **272**(24): 6179-6217.
- Zhan, Y., G. M. Davey, et al. (2009). "SOCS1 negatively regulates the production of Foxp3+ CD4+ T cells in the thymus." Immunol Cell Biol **87**(6): 473-480.
- Zhang, C., L. Han, et al. (2010). "Global changes of mRNA expression reveals an increased activity of the interferon-induced signal transducer and activator of transcription (STAT) pathway by repression of miR-221/222 in glioblastoma U251 cells." Int J Oncol **36**(6): 1503-1512.
- Zhang, D. and D. E. Zhang (2011). "Interferon-stimulated gene 15 and the protein ISGylation system." J Interferon Cytokine Res **31**(1): 119-130.
- Zhang, J. G., A. Farley, et al. (1999). "The conserved SOCS box motif in suppressors of cytokine signaling binds to elongins B and C and may couple bound proteins to proteasomal degradation." Proc Natl Acad Sci U S A **96**(5): 2071-2076.

- Zhang, J. G., D. Metcalf, et al. (2001). "The SOCS box of suppressor of cytokine signaling-1 is important for inhibition of cytokine action in vivo." Proc Natl Acad Sci U S A **98**(23): 13261-13265.
- Zhao, M., J. Zhang, et al. (2012). "Stochastic expression of the interferon-beta gene." PLoS Biol **10**(1): e1001249.
- Zhao, W., C. Lee, et al. (2008). "A conserved IFN-alpha receptor tyrosine motif directs the biological response to type I IFNs." J Immunol **180**(8): 5483-5489.
- Zhao, W., C. Lee, et al. (2008). "A conserved IFNAR tyrosine motif directs the biological response to type I IFNs." Submitted.
- Zhou, A., J. Paranjape, et al. (1997). "Interferon action and apoptosis are defective in mice devoid of 2',5'-oligoadenylate-dependent RNase L." Embo J **16**(21): 6355-6363.
- Zhou, H., X. Huang, et al. (2010). "miR-155 and its star-form partner miR-155\* cooperatively regulate type I interferon production by human plasmacytoid dendritic cells." Blood **116**(26): 5885-5894.
- Zorn, E., E. A. Nelson, et al. (2006). "IL-2 regulates FOXP3 expression in human CD4+CD25+ regulatory T cells through a STAT-dependent mechanism and induces the expansion of these cells in vivo." Blood **108**(5): 1571-1579.

## APPENDICES I: SOLUTIONS

### 1% Buffered Formalin

10% Buffered Formalin diluted 1 in 10 in DPBS

### Cell Lysis Buffer

50 mM Tris-HCl (pH 7.4), 1% (v/v) Igepal, 10% (v/v) Glycerol, 1 mM EDTA, 1 mM  $\text{Na}_3\text{VO}_4$ , 1 mM NaF, 1 mM DTT, 4.5 mM Sodium Pyrophosphate, 10 mM  $\beta$ -Glycerophosphate, 1 mM PMSF, protease inhibitor (1 tablet per 50 mls) and made to volume with MQdH<sub>2</sub>O.

### DEPC H<sub>2</sub>O

0.1% DEPC in MQH<sub>2</sub>O, incubated at RT overnight then autoclaved

### Phosphoflow Staining Buffer

0.5% BSA, 100mM NaF, 1mM NaV, 10mM B-glycerophosphoric acid and 4.5 mM Na Pyrophosphate made to volume with DPBS.

### Red Cell Lysis (RCL) Buffer

155 mM  $\text{NH}_4\text{Cl}$ , 12 mM  $\text{NaHCO}_3$ , 0.1 mM EDTA made up to volume with MQdH<sub>2</sub>O.

### 8% SDS-PAGE Lower Gel (10mls)

2.7 mls of 30% bis-acrylamide mix, 2.5 mls of 1.5 M Tris (pH 8.8), 0.1 mls of 10% SDS, 0.1 mls of 10% ammonium persulfate, 0.006 mls of TEMED and 4.6 mls of MQdH<sub>2</sub>O.

### 5 x SDS Sample Buffer

625mM Tris, 10% (v/v) glycerol, 50mM Dithiothreitol, 2.3% (w/v) SDS, 2% (v/v)  $\beta$ -mercaptoethanol

### SDS-PAGE Running Buffer

25mM Tris-HCL, 192 mM Glycine, 0.1% (w/v) SDS, made to volume with MQdH<sub>2</sub>O.

### SDS-PAGE Upper Gel (10mls)

1.7 mls of 30% bis-acrylamide mix, 1.25 mls of 0.5 M Tris (pH 6.8), 0.1 mls of 10% SDS, 0.1 mls of 10% ammonium persulfate, 0.01 mls of TEMED and 6.8 mls of MQdH<sub>2</sub>O.

**Stripping Buffer**

62.5 mM Tris-HCl (pH 6.8), 2% (w/v) SDS, 0.1 M β-mercaptoethanol, made to volume with MQdH<sub>2</sub>O.

**Wet Transfer Buffer**

1.56 mM Tris-HCl (pH 8.1), 1.2 mM Glycine, 20% (v/v) Methanol, made to volume with MQdH<sub>2</sub>O.

## APPENDICES II: PRIMERS for PCR and RT-PCR

GAPDH Primers for conventional PCR (5' – 3' Prime)

Fwd: CTG CCA CCC AGA AGA CTG TGG

Rev: GTC ATA CCA GGA AAT CAG C

qRT-PCR Syber Primers

Target Gene	Forward Primer (5' – 3' Prime)	Reverse Primer (5' – 3' Prime)
18S	GTA ACC CGT TGA ACC CCA TT	CCA TCC AAT CGG TAG TAG CG
Isg15	TGA GAG CAA GCA GCC AGA AG	ACG GAC ACC AGG AAA TCG TT
Irgm1	GGA GCT GAA AGG TCC ACA GA	GGG GAG CAT AAT GGG TCT CT
Stat1	TCA CAT TCA CAT GGG TGG AA	CGG CAG CCA TGA CTT TGT AG
Irf7	ATC TTG CGC CAA GAC AAT TC	AGC ATT GCT GAG GCT CAC TT
Cxcl10	CTG AAT CCG GAA TCT AAG ACC A	GAG GCT CTC TGC TGT CCA TC

### APPENDICES III: GENE LISTS

#### A. IFN $\alpha$ regulated probes within the thymus of wt mice

Agilent Probe Name	GeneSymbol	Fold Change (0 vs 3 hours)	Regulation (0 vs 3 hours)	Fold Change (0 vs 6 hours)	Regulation (0 vs 6 hours)	Corrected p value, One way anova (BHFR)	Corrected p value, Unpaired T-test (0 vs 3 hours) (BHFR)	Corrected p value, Unpaired T-test (0 vs 6 hours) (BHFR)
A_52_P77093	1600014C10Rik	2.628	up	1.233	up	0.000	0.002	
A_51_P453616	1700003F17Rik	13.310	up	1.921	up	0.001	0.004	
A_51_P322473	2310042D19Rik	5.842	up	1.308	up	0.001	0.005	
A_52_P542502	2310042D19Rik	4.975	up	1.048	down	0.033	0.031	
A_52_P241640	4930599N23Rik	3.393	up	2.667	up	0.001	0.004	
A_52_P359071	4930599N23Rik	3.770	up	1.587	up	0.002	0.003	
A_51_P264132	5430416O09Rik	1.755	down	1.236	up	0.023		
A_52_P417945	9330175E14Rik	2.732	up	1.201	up	0.024	0.021	
A_51_P249471	9530028C05	2.759	up				0.045	
A_52_P61697	9930111J21Rik2	2.583	up	1.220	up	0.005	0.016	
A_51_P158072	A230050P20Rik	3.336	up	1.556	up	0.001	0.007	
A_51_P158073	A230050P20Rik	3.090	up	1.477	up	0.004	0.016	
A_52_P649038	A230050P20Rik	3.788	up	1.553	up	0.022	0.010	
A_52_P367486	A430072C10Rik	1.999	down	1.080	up	0.047		
A_52_P564444	A530064D06Rik	7.449	up	1.962	up	0.005	0.017	
A_52_P875073	A930019D19Rik	1.053	up	2.198	down	0.021		
A_51_P215143	AC154274.1	4.263	up	1.339	up	0.017	0.015	

Agilent Probe Name	GeneSymbol	Fold Change (0 vs 3 hours)	Regulation (0 vs 3 hours)	Fold Change (0 vs 6 hours)	Regulation (0 vs 6 hours)	Corrected p value, One way anova (BHFDR)	Corrected p value, Unpaired T-test (0 vs 3 hours) (BHFDR)	Corrected p value, Unpaired T-test (0 vs 6 hours) (BHFDR)
A_51_P234944	Adamts4	1.877	up	1.427	down	0.040		
A_51_P257134	Adar	4.327	up	2.047	up	0.002	0.007	
A_52_P183181	Adar	3.353	up	1.755	up	0.004	0.016	
A_51_P325281	Al607873	3.108	up	1.182	up	0.017	0.000	
A_52_P86965	Al607873	3.092	up	1.938	up	0.038	0.004	
A_52_P360742	Apol7a	2.683	up	1.803	up	0.009	0.016	
A_52_P803082	Apol9a	3.004	up	1.824	up	0.005	0.003	
A_51_P123546	Armc3	2.197	up	1.634	up	0.005	0.016	
A_51_P134627	Asb13	2.632	up	1.102	up	0.012	0.019	
A_52_P537941	Asb13	2.517	up	1.196	up	0.001	0.004	
A_52_P549985	Asb13	3.007	up	1.252	up	0.005	0.003	
A_51_P129006	B2m	1.502	up	2.405	up	0.037		
A_52_P233811	B430306N03Rik	3.227	up	1.277	up	0.005	0.005	
A_51_P165182	Batf2	3.889	up	1.704	up	0.026		
A_51_P406604	BC006779	4.826	up	1.983	up	0.002	0.000	
A_52_P321358	BC006779	5.318	up	1.540	up	0.001	0.000	
A_51_P494597	BC013712	2.572	up	1.419	up	0.037		
A_51_P460844	Blvrb	1.834	up	3.193	up	0.030		
A_51_P169693	Bst2	3.911	up	2.454	up	0.002	0.009	
A_52_P249514	Ccl12	3.902	up	1.729	up	0.004	0.016	
A_51_P286737	Ccl2	2.602	up	1.632	up	0.022	0.017	
A_51_P327996	Ccl22	1.255	up	2.160	up	0.017		
A_51_P436652	Ccl7	3.302	up	1.732	up	0.011	0.015	

Agilent Probe Name	GeneSymbol	Fold Change (0 vs 3 hours)	Regulation (0 vs 3 hours)	Fold Change (0 vs 6 hours)	Regulation (0 vs 6 hours)	Corrected p value, One way anova (BHFD R)	Corrected p value, Unpaired T-test (0 vs 3 hours) (BHFD R)	Corrected p value, Unpaired T-test (0 vs 6 hours) (BHFD R)
A_52_P208763	Ccl7	3.400	up	1.719	up	0.013	0.019	
A_51_P232682	Ccr12	2.561	up	1.218	up	0.029		
A_52_P334593	Ccr12	2.749	up	1.309	up	0.047		
A_51_P431364	Cd247	1.868	up	2.770	up	0.015		
A_51_P253074	Chit1	4.078	up	3.577	up	0.037	0.011	
A_51_P199168	Cidea	4.742	down	2.377	up	0.026		
A_51_P400190	Cmpk2	28.433	up	3.887	up	0.002	0.007	
A_52_P186937	Cmpk2	18.845	up	2.564	up	0.000	0.000	
A_51_P432641	Cxcl10	4.095	up	1.301	up	0.002	0.012	
A_52_P380369	D14Ert668e	4.913	up	1.943	up	0.000	0.001	
A_51_P393748	Ddx58	5.273	up	1.354	up	0.012	0.002	
A_52_P385536	Ddx58	5.556	up	1.652	up	0.001	0.005	
A_52_P479001	Ddx58	5.634	up	1.597	up	0.000	0.001	
A_52_P523946	Ddx58	6.126	up	1.472	up	0.011	0.001	
A_51_P197910	Ddx60	7.349	up	2.147	up	0.045	0.012	
A_51_P234274	Ddx60	8.165	up	3.117	up	0.048		
A_52_P223809	Dhx58	14.489	up	4.837	up	0.002	0.008	
A_52_P127813	E030037K03Rik	6.681	up	1.780	up	0.002	0.000	
A_52_P559919	Eif2ak2	5.953	up	1.545	up	0.001	0.003	
A_52_P475229	Ep400	1.343	up	3.434	up	0.047		
A_51_P376050	Epsti1	2.433	up	1.629	up	0.010	0.005	
A_52_P582374	Epsti1	2.863	up	1.825	up	0.022	0.007	
A_51_P167535	Fabp3	1.618	down	2.243	up	0.014		

Agilent Probe Name	GeneSymbol	Fold Change (0 vs 3 hours)	Regulation (0 vs 3 hours)	Fold Change (0 vs 6 hours)	Regulation (0 vs 6 hours)	Corrected p value, One way anova (BHFD R)	Corrected p value, Unpaired T-test (0 vs 3 hours) (BHFD R)	Corrected p value, Unpaired T-test (0 vs 6 hours) (BHFD R)
A_51_P100852	Fam26f	4.026	up	2.352	up	0.013	0.034	
A_52_P172838	Fat2	1.766	up	2.230	up	0.048		
A_51_P296755	Fcgr1	4.230	up	3.968	up	0.007	0.033	
A_52_P47846	Fcgr1	5.221	up	4.632	up	0.001	0.010	0.001
A_51_P181517	Fcgr4	4.027	up	4.589	up	0.003	0.023	0.027
A_51_P223177	Ftsjd2	2.314	up	1.345	up	0.007	0.024	
A_52_P309418	Ftsjd2	2.215	up	1.146	up	0.000	0.002	
A_51_P203955	Gbp2	3.373	up	1.802	up	0.001	0.003	
A_51_P165244	Gbp3	2.375	up	1.389	up	0.017	0.015	
A_52_P327664	Gbp5	2.724	up	1.032	up	0.014	0.006	
A_51_P463846	Gbp6	3.453	up	1.033	up	0.018	0.021	
A_51_P323180	Gbp9	3.270	up	1.257	up	0.038	0.027	
A_52_P344949	Gbp9	4.429	up	1.524	up	0.038		
A_52_P532982	Gdf15	1.842	up	2.072	up	0.001		0.030
A_52_P146457	Gm11531	1.428	up	2.024	up	0.029		
A_52_P494730	Gm12185	6.088	up	1.144	up	0.001	0.001	
A_52_P164821	Gm12250	9.549	up	2.086	up	0.001	0.004	
A_52_P378084	Gm12799	2.060	up	5.563	up	0.043		
A_51_P500082	Gm14446	6.643	up	1.740	up	0.002	0.006	
A_52_P294064	Gm14446	6.260	up	1.576	up	0.001	0.003	
A_52_P599964	Gm4955	7.676	up	2.112	up	0.001	0.001	
A_52_P427759	Gm6118	1.457	up	2.797	up	0.045		
A_51_P211467	Gpr50	1.449	up	2.927	up	0.035		

Agilent Probe Name	GeneSymbol	Fold Change (0 vs 3 hours)	Regulation (0 vs 3 hours)	Fold Change (0 vs 6 hours)	Regulation (0 vs 6 hours)	Corrected p value, One way anova (BHFDR)	Corrected p value, Unpaired T-test (0 vs 3 hours) (BHFDR)	Corrected p value, Unpaired T-test (0 vs 6 hours) (BHFDR)
A_52_P179309	Gria3	1.447	down	2.006	down	0.006		
A_51_P162794	Gzma	2.960	up	2.287	up	0.004	0.008	
A_51_P333274	Gzmb	2.484	up	1.414	up	0.029		
A_51_P432538	H2-T22	2.067	up	1.523	up	0.022		
A_52_P197826	H2-T22	2.355	up	1.149	up	0.045		
A_52_P189812	H2-T24	6.365	up	2.634	up	0.001	0.001	
A_52_P581082	H2-T24	8.122	up	3.059	up	0.001	0.003	
A_52_P64514	Herc5	3.044	up	1.373	up	0.009	0.014	
A_51_P134228	Hlf	3.479	down	1.053	up	0.005	0.019	
A_51_P375754	Hoxc10	1.089	up	2.123	up	0.029		
A_52_P522427	Hsh2d	7.068	up	1.947	up	0.001	0.004	
A_52_P663686	I830012O16Rik	8.687	up	3.286	up	0.001	0.004	
A_51_P292116	Ica1	1.813	up	2.105	up	0.033		
A_51_P307150	Ido1	2.050	up	1.135	up	0.010	0.036	
A_51_P408346	Ifi204	3.051	up	1.587	up	0.030	0.028	
A_51_P358233	Ifi2712a	1.984	up	2.108	up	0.033		
A_51_P414889	Ifi35	3.909	up	1.597	up	0.007	0.025	
A_51_P129229	Ifi47	4.453	up	1.379	up	0.000	0.002	
A_51_P387810	Ifih1	4.258	up	1.460	up	0.001	0.003	
A_52_P121468	Ifih1	4.965	up	1.447	up	0.022	0.013	
A_51_P327751	Ifit1	8.684	up	1.985	up	0.001	0.001	
A_51_P161021	Ifit2	2.701	up	1.031	down	0.042		
A_52_P542388	Ifit2	3.272	up	1.131	up	0.040	0.018	

Agilent Probe Name	GeneSymbol	Fold Change (0 vs 3 hours)	Regulation (0 vs 3 hours)	Fold Change (0 vs 6 hours)	Regulation (0 vs 6 hours)	Corrected p value, One way anova (BHFDR)	Corrected p value, Unpaired T-test (0 vs 3 hours) (BHFDR)	Corrected p value, Unpaired T-test (0 vs 6 hours) (BHFDR)
A_51_P359570	lfit3	6.923	up	2.686	up	0.001	0.003	
A_51_P450788	lgkv7-33	3.191	down	1.094	down	0.029		
A_51_P112355	lgtp	3.501	up	1.311	up	0.001	0.004	
A_51_P421876	lrf7	7.676	up	2.764	up	0.002	0.011	
A_51_P127367	lrf9	5.138	up	2.321	up	0.002	0.005	
A_52_P176013	lrf9	5.655	up	2.248	up	0.004	0.006	
A_51_P262171	lrgm1	5.748	up	1.585	up	0.000	0.001	
A_52_P126158	lrgm1	6.128	up	1.507	up	0.001	0.001	
A_51_P416295	lrgm2	4.397	up	1.418	up	0.000	0.002	
A_52_P463936	lsg15	14.072	up	2.908	up	0.000	0.002	
A_51_P510713	lsg20	2.277	up	1.225	up	0.047		
A_52_P448253	lsg20	2.368	up	1.226	up	0.038		
A_51_P511285	Kcnj9	2.284	down	2.599	down	0.040		0.027
A_51_P359636	Lgals3bp	3.679	up	1.936	up	0.016	0.040	
A_51_P500813	Lgals9	2.353	up	1.671	up	0.023	0.037	
A_52_P165856	LOC639910	4.734	up	2.030	up	0.001	0.005	
A_52_P203833	Mitd1	2.806	up	1.308	up	0.001	0.002	
A_52_P203837	Mitd1	3.263	up	1.558	up	0.001	0.003	
A_51_P499623	Mlana	2.096	up	2.057	up	0.007	0.010	
A_51_P440535	Mlkl	2.393	up	1.550	up	0.006	0.020	
A_51_P184484	Mmp13	5.714	up	4.988	up	0.016	0.049	
A_51_P377620	Mnda	2.674	up	1.165	up	0.033	0.031	
A_51_P169495	Mov10	4.087	up	1.860	up	0.002	0.009	

Agilent Probe Name	GeneSymbol	Fold Change (0 vs 3 hours)	Regulation (0 vs 3 hours)	Fold Change (0 vs 6 hours)	Regulation (0 vs 6 hours)	Corrected p value, One way anova (BHFDR)	Corrected p value, Unpaired T-test (0 vs 3 hours) (BHFDR)	Corrected p value, Unpaired T-test (0 vs 6 hours) (BHFDR)
A_52_P189772	Mpa2l	6.028	up	1.746	up	0.026	0.041	
A_52_P393488	Ms4a4c	2.183	up				0.021	
A_51_P294505	Ms4a4d	2.488	up	1.486	up	0.007	0.002	
A_52_P211956	Ms4a4d	2.923	up	2.124	up	0.002	0.001	
A_51_P422300	Ms4a6b	2.546	up	1.430	up	0.003	0.007	
A_52_P446431	Mx1	9.040	up	1.686	up	0.001	0.002	
A_52_P614259	Mx1	8.384	up	1.505	up	0.000	0.002	
A_51_P514085	Mx2	18.139	up	2.355	up	0.001	0.001	
A_52_P311903	Ncoa7	2.904	up	1.349	up	0.030	0.034	
A_52_P255300	Nhsl2	2.114	up				0.020	
A_52_P382107	Nlrc5	3.056	up	1.436	up	0.001	0.004	
A_52_P337357	Oas1a	5.031	up	3.233	up	0.007	0.026	
A_52_P110877	Oas1b	7.478	up	1.998	up	0.001	0.002	
A_51_P428529	Oas1c	3.430	up	1.769	up	0.001	0.005	
A_51_P134030	Oas1e	2.545	up	1.455	up	0.022		
A_51_P154842	Oas1f	4.061	up	4.336	up	0.011	0.022	
A_51_P277994	Oas2	9.137	up	2.711	up	0.001	0.001	
A_51_P472867	Oas3	12.771	up	3.058	up	0.000	0.002	0.030
A_52_P516296	Oas3	8.069	up	3.995	up	0.005	0.008	
A_51_P437309	Oasl1	10.200	up	2.062	up	0.001	0.006	
A_51_P387123	Oasl2	2.964	up	1.706	up	0.022	0.050	
A_52_P272217	Ogfr	2.098	up	1.312	up	0.022	0.038	
A_51_P237055	Olf1198	1.304	up	2.248	up	0.029		

Agilent Probe Name	GeneSymbol	Fold Change (0 vs 3 hours)	Regulation (0 vs 3 hours)	Fold Change (0 vs 6 hours)	Regulation (0 vs 6 hours)	Corrected p value, One way anova (BHFDR)	Corrected p value, Unpaired T-test (0 vs 3 hours) (BHFDR)	Corrected p value, Unpaired T-test (0 vs 6 hours) (BHFDR)
A_51_P386280	Olfr187	1.134	up	2.231	up	0.047		
A_52_P358720	Olfr266	1.514	up	2.509	up	0.028		
A_51_P340525	Olfr357	1.833	up	2.149	up	0.040		
A_52_P103732	Olfr741	1.430	up	2.153	up	0.003		
A_51_P389255	Olfr767	1.609	up	2.710	up	0.008		0.048
A_52_P451775	Otub2	2.170	up	1.361	up	0.008	0.026	
A_51_P120738	P2ry14	2.002	up	1.451	up	0.007	0.010	
A_52_P380329	Papd7	2.382	up	1.321	up	0.005	0.015	
A_51_P129199	Parp10	3.101	up	1.249	up	0.004	0.019	
A_51_P214747	Parp12	5.135	up	2.363	up	0.001	0.005	
A_51_P341767	Parp14	4.861	up	1.184	up	0.008	0.002	
A_51_P514712	Parp14	4.421	up	1.520	up	0.000	0.001	
A_52_P97680	Parp14	5.063	up	1.674	up	0.007	0.007	
A_51_P218984	Parp9	6.968	up	2.125	up	0.001	0.004	
A_51_P282760	Per2	2.287	down	1.444	down	0.017	0.040	
A_51_P262515	Phf11	3.538	up	2.475	up	0.003	0.003	
A_51_P199199	Pik3ap1	2.496	up	1.553	up	0.030		
A_51_P270339	Pik3ap1	2.307	up	1.605	up	0.038		
A_52_P642239	Pik3ap1	2.610	up	1.695	up	0.027		
A_51_P515883	Plac8	2.150	up	2.075	up	0.041		
A_51_P251022	Plscr2	2.683	up	1.378	up	0.001	0.003	
A_52_P372901	Plscr2	2.494	up	1.163	up	0.001	0.002	
A_51_P282799	Pml	3.979	up	1.251	up	0.013	0.032	

Agilent Probe Name	GeneSymbol	Fold Change (0 vs 3 hours)	Regulation (0 vs 3 hours)	Fold Change (0 vs 6 hours)	Regulation (0 vs 6 hours)	Corrected p value, One way anova (BHFDR)	Corrected p value, Unpaired T-test (0 vs 3 hours) (BHFDR)	Corrected p value, Unpaired T-test (0 vs 6 hours) (BHFDR)
A_52_P121087	Pml	4.044	up	1.285	up	0.004	0.018	
A_51_P428372	Ppbp	1.643	down	2.901	up	0.037		
A_51_P361535	Psme2	2.169	up	1.940	up	0.040		
A_51_P470443	Rabepk	2.022	up	1.223	up	0.002	0.004	
A_52_P193362	Rilpl1	2.388	up	2.211	up	0.037		
A_51_P177819	Rnf114	3.435	up	1.695	up	0.004	0.016	
A_51_P259378	Rnf114	2.565	up	1.431	up	0.007	0.022	
A_51_P159503	Rnf213	6.006	up	2.590	up	0.001	0.001	
A_51_P191469	Rnf31	2.168	up	1.395	up	0.022	0.043	
A_52_P514982	Rnf31	2.244	up	1.339	up	0.026	0.044	
A_52_P78183	Rnf43	2.291	up	2.715	up	0.048		
A_52_P548790	Rpl7a	1.487	up	2.895	up	0.047		
A_51_P505132	Rsad2	33.252	up	4.133	up	0.000	0.000	
A_51_P505134	Rsad2	35.023	up	4.345	up	0.000	0.000	
A_52_P670026	Rsad2	28.339	up	3.797	up	0.000	0.000	
A_51_P304170	Rtp4	10.673	up	3.700	up	0.001	0.000	
A_52_P466090	Samhd1	2.066	up	1.415	up	0.002	0.012	
A_52_P419678	Serpina3f	6.614	up	2.063	up	0.002	0.009	
A_52_P419679	Serpina3f	4.796	up	2.940	up	0.010	0.012	
A_51_P326191	Serpina3g	2.883	up	1.632	up	0.033		
A_51_P447329	Slc25a22	2.001	up	1.035	up	0.002	0.013	
A_52_P425890	Slfn1	4.544	up	1.465	up	0.001	0.005	
A_51_P423578	Slfn2	3.002	up	1.567	up	0.007	0.023	

Agilent Probe Name	GeneSymbol	Fold Change (0 vs 3 hours)	Regulation (0 vs 3 hours)	Fold Change (0 vs 6 hours)	Regulation (0 vs 6 hours)	Corrected p value, One way anova (BHFDR)	Corrected p value, Unpaired T-test (0 vs 3 hours) (BHFDR)	Corrected p value, Unpaired T-test (0 vs 6 hours) (BHFDR)
A_51_P364694	Slfn5	4.728	up	1.510	up	0.001	0.003	
A_51_P413359	Slfn5	4.753	up	1.218	up	0.033	0.004	
A_52_P543489	Slfn8	6.654	up	1.320	up	0.022	0.012	
A_51_P504988	Slfn9	6.391	up	1.398	up	0.015	0.015	
A_51_P255016	Sp100	3.508	up	1.760	up	0.035		
A_51_P305583	Sp100	2.591	up	1.472	up	0.020	0.008	
A_52_P140287	Spn	1.775	up	4.841	up	0.042		
A_52_P496503	Stat1	4.021	up	1.595	up	0.001	0.005	
A_52_P505218	Stat1	3.908	up	1.613	up	0.001	0.001	
A_52_P542540	Stat1	4.650	up	1.399	up	0.040	0.029	
A_52_P70255	Stat1	4.100	up	1.356	up	0.001	0.002	
A_52_P70261	Stat1	4.248	up	1.572	up	0.001	0.004	
A_51_P100327	Tap1	2.477	up	1.333	up	0.022	0.049	
A_51_P481777	Tcstv1	4.335	up	3.249	up	0.022	0.012	
A_51_P143200	Tcstv3	4.552	up	1.902	up	0.001	0.003	
A_51_P271835	Tdrd7	2.493	up	1.527	up	0.003	0.008	
A_51_P478722	Tgtp1	7.045	up	1.421	up	0.000	0.001	
A_52_P676510	Tgtp1	9.697	up	2.512	up	0.022		
A_52_P363951	Thbs1	2.619	up	1.075	down	0.026	0.024	
A_52_P22001	Thsd1	1.284	down	1.699	up	0.046		
A_51_P291906	Tlr3	2.116	up	1.037	up	0.046		
A_52_P799815	Tmem171	7.117	up	2.180	up	0.004	0.016	
A_51_P448741	Tnfsf10	2.854	up	1.460	up	0.001	0.006	

Agilent Probe Name	GeneSymbol	Fold Change (0 vs 3 hours)	Regulation (0 vs 3 hours)	Fold Change (0 vs 6 hours)	Regulation (0 vs 6 hours)	Corrected p value, One way anova (BHFD)	Corrected p value, Unpaired T-test (0 vs 3 hours) (BHFD)	Corrected p value, Unpaired T-test (0 vs 6 hours) (BHFD)
A_51_P503149	Tns4	1.271	up	2.218	up	0.018		
A_51_P124886	Tor1aip1	2.032	up	1.192	up	0.041		
A_51_P198179	Tor3a	3.391	up	1.652	up	0.014	0.032	
A_52_P52357	Tor3a	3.534	up	2.225	down	0.001	0.002	
A_51_P414412	Trafd1	2.152	up	1.138	up	0.044		
A_52_P267391	Trim12	2.807	up	1.235	up	0.048	0.034	
A_52_P634829	Trim12	3.145	up				0.032	
A_52_P252348	Trim14	3.813	up	1.348	up	0.002	0.002	
A_52_P640484	Trim21	3.184	up	1.194	up	0.001	0.002	
A_51_P212854	Trim25	4.243	up	1.543	up	0.000	0.001	
A_52_P654161	Trim25	4.181	up	1.553	up	0.001	0.004	
A_52_P353031	Trim26	2.058	up	1.258	up	0.013	0.033	
A_52_P353038	Trim26	2.209	up	1.285	up	0.007	0.023	
A_51_P275454	Trim30	5.517	up	1.727	up	0.002	0.004	
A_52_P442567	Trim30	7.425	up	1.880	up	0.022	0.015	
A_52_P157316	Trim34	3.549	up	1.470	up	0.010	0.001	
A_52_P278853	Trim34	3.954	up	1.553	up	0.004	0.002	
A_52_P367034	Trim34	4.370	up	1.638	up	0.002	0.003	
A_51_P244820	Trim56	2.204	up	1.117	up	0.002	0.002	
A_52_P199019	Trim6	2.179	up	1.000	down	0.017	0.030	
A_52_P199023	Trim6	2.394	up	1.027	down	0.049		
A_52_P199024	Trim6	3.329	up				0.027	
A_52_P199633	Trim79	5.541	up	1.730	up	0.005	0.005	

Agilent Probe Name	GeneSymbol	Fold Change (0 vs 3 hours)	Regulation (0 vs 3 hours)	Fold Change (0 vs 6 hours)	Regulation (0 vs 6 hours)	Corrected p value, One way anova (BHFDR)	Corrected p value, Unpaired T-test (0 vs 3 hours) (BHFDR)	Corrected p value, Unpaired T-test (0 vs 6 hours) (BHFDR)
A_52_P371494	Trim79	3.396	up	1.382	up	0.038	0.041	
A_52_P72826	Tro	2.430	up	1.174	up	0.020	0.034	
A_51_P145404	Tuba3a	2.528	up	1.498	up	0.040		
A_51_P316816	Uba7	2.507	up	1.780	up	0.007	0.020	
A_52_P214740	Ube2l6	2.301	up	1.879	up	0.048		
A_51_P426353	Ucp1	9.821	down	5.653	up	0.007		
A_51_P164219	Usp18	11.856	up	2.052	up	0.000	0.003	
A_52_P284652	Wrb	1.487	up	2.000	up	0.041		
A_51_P494403	Xaf1	7.908	up	2.536	up	0.001	0.004	
A_51_P184936	Zbp1	6.186	up	2.333	up	0.002	0.006	
A_51_P177744	Zc3hav1	2.382	up	1.417	up	0.011	0.031	
A_52_P231610	Zc3hav1	3.069	up	1.623	up	0.024		
A_51_P352216	Zfp365	6.018	up	2.091	up	0.001	0.004	
A_51_P144438	Znfx1	2.497	up	1.298	up	0.007	0.026	
A_51_P136181	none identified	2.771	up	1.215	up	0.015	0.029	
A_51_P225764	none identified	1.699	up	5.009	up	0.046		
A_52_P1100772	none identified	2.648	up	1.145	up	0.023	0.041	
A_52_P241032	none identified	1.534	up	2.928	up	0.048		
A_52_P321627	none identified	1.533	up	2.033	up	0.040		0.030
A_52_P325598	none identified	5.523	up				0.048	
A_52_P326187	none identified	7.162	up	1.782	up	0.001	0.002	
A_52_P36261	none identified	3.129	up	1.116	up	0.001	0.003	
A_52_P374983	none identified	4.822	up	1.847	up	0.013	0.026	

Agilent Probe Name	GeneSymbol	Fold Change (0 vs 3 hours)	Regulation (0 vs 3 hours)	Fold Change (0 vs 6 hours)	Regulation (0 vs 6 hours)	Corrected p value, One way anova (BHFD)	Corrected p value, Unpaired T-test (0 vs 3 hours) (BHFD)	Corrected p value, Unpaired T-test (0 vs 6 hours) (BHFD)
A_52_P510790	none identified	5.170	up	1.293	up	0.014	0.002	
A_52_P540690	none identified	1.590	down	1.333	up	0.047		
A_52_P612668	none identified	2.881	up				0.015	
A_52_P615247	none identified	2.591	up	1.291	up	0.008	0.027	
A_52_P648759	none identified	8.305	up	3.131	up	0.000	0.001	
A_52_P653054	none identified	6.748	up	2.314	up	0.000	0.002	
A_52_P670399	none identified	1.599	down	2.090	up	0.029		
A_52_P68235	none identified	5.743	up	2.566	up	0.001	0.003	
A_52_P787894	none identified	3.105	up	1.067	up	0.013	0.012	
A_52_P852190	none identified	5.319	up	1.639	up	0.001	0.002	
A_52_P915536	none identified	5.322	up	1.520	up	0.037	0.002	
A_52_P932813	none identified	1.326	up	2.354	up	0.040		
A_52_P973470	none identified	3.820	up	1.559	up	0.017	0.013	

## B. Thymic IFN $\alpha$ regulated genes absent from the Interferome

<b>Gene Symbol</b>	<b>Ensembl Gene ID</b>
1600014C10	ENSMUSG00000054676
1700003F17R	ENSMUSG00000086327
2310042D19	ENSMUSG00000078486
4930599N23	ENSMUSG00000073144
5430416O09	ENSMUSG00000028475
9330175E14R	ENSMUSG00000074153
9830107B12	ENSMUSG00000073386
9930111J21R	ENSMUSG00000069893
9930111J21R	ENSMUSG00000069892
A530040E14R	ENSMUSG00000072109
A530064D06	ENSMUSG00000043939
A930019D19	ENSMUSG00000085958
AC125149.6	ENSMUSG00000079800
AC133103.1	ENSMUSG00000079189
AC133103.4	ENSMUSG00000079193
Adamts4	ENSMUSG00000006403
Al607873	ENSMUSG00000073490
Apol7a	ENSMUSG00000010601
Armc3	ENSMUSG00000037683
Asb13	ENSMUSG00000033781
B430306N03	ENSMUSG00000043740
Batf2	ENSMUSG00000039699
Ccl12	ENSMUSG00000035352
Ccl22	ENSMUSG00000031779
Cd247	ENSMUSG00000005763
Chit1	ENSMUSG00000026450
Cidea	ENSMUSG00000024526
Ep400	ENSMUSG00000029505
Fabp3	ENSMUSG00000028773
Fabp3-ps1	ENSMUSG00000056366
Fat2	ENSMUSG00000055333
Fcgr1	ENSMUSG00000015947
Fcgr4	ENSMUSG00000059089
Gbp10	ENSMUSG00000054588
Gbp6	ENSMUSG00000079362
Gbp7	ENSMUSG00000040253
Gbp9	ENSMUSG00000029298
Gdf15	ENSMUSG00000038508
Gm10552	ENSMUSG00000073628
Gm10553	ENSMUSG00000073631
Gm11531	ENSMUSG00000075587

Gm12185	ENSMUSG00000048852
Gm12187	ENSMUSG00000083178
Gm12250	ENSMUSG00000082292
Gm12799	ENSMUSG00000082264
Gm14446	ENSMUSG00000079339
Gm16825	ENSMUSG00000085149
Gm4955	ENSMUSG00000037849
Gpr50	ENSMUSG00000056380
Gria3	ENSMUSG00000001986
Gzma	ENSMUSG00000023132
H2-T10	ENSMUSG00000079491
H2-T22	ENSMUSG00000056116
Hlf	ENSMUSG00000003949
Hoxc10	ENSMUSG00000022484
I830012O16R	ENSMUSG00000062488
Ica1	ENSMUSG00000062995
Kcnj9	ENSMUSG00000038026
Mitd1	ENSMUSG00000026088
Mlana	ENSMUSG00000024806
Mlkl	ENSMUSG00000012519
Mmp13	ENSMUSG00000050578
Ms4a4d	ENSMUSG00000024678
Ms4a6b	ENSMUSG00000024677
Ms4a6c	ENSMUSG00000079419
Mx1	ENSMUSG00000000386
Ncoa7	ENSMUSG00000039697
Nhs12	ENSMUSG00000079481
Nlrc5	ENSMUSG00000074151
Oas1b	ENSMUSG00000029605
Oas1f	ENSMUSG00000053765
Oasl2	ENSMUSG00000029561
Olf1198	ENSMUSG00000075117
Olf187	ENSMUSG00000043357
Olf266	ENSMUSG00000043529
Olf357	ENSMUSG00000055838
Olf741	ENSMUSG00000060108
Olf742	ENSMUSG00000068431
Olf765	ENSMUSG00000056853
Olf767	ENSMUSG00000059762
Otub2	ENSMUSG00000021203
Papd7	ENSMUSG00000034575
Parp14	ENSMUSG00000034422
Parp9	ENSMUSG00000022906
Per2	ENSMUSG00000055866

Pik3ap1	ENSMUSG00000025017
Plscr2	ENSMUSG00000032372
Pydc4	ENSMUSG00000073491
Rabepk	ENSMUSG00000070953
Rilpl1	ENSMUSG00000029392
Rnf213	ENSMUSG00000070327
Rnf43	ENSMUSG00000034177
Rpl17	ENSMUSG00000062328
Serpina3f	ENSMUSG00000066363
Slfn1	ENSMUSG00000078763
Slfn2	ENSMUSG00000072620
Slfn8	ENSMUSG00000035208
Slfn9	ENSMUSG00000069793
snoU13.18	ENSMUSG00000089232
Thsd1	ENSMUSG00000031480
Tmem171	ENSMUSG00000052485
Tor1aip1	ENSMUSG00000026466
Trim12a	ENSMUSG00000066258
Trim30a	ENSMUSG00000030921
Trim30d	ENSMUSG00000057596
Trim6	ENSMUSG00000072244
Tro	ENSMUSG00000025272
U29423	ENSMUSG00000076575
Ucp1	ENSMUSG00000031710
Wrb	ENSMUSG00000023147
Zfp365	ENSMUSG00000037855

**C. Probes basally different between *Socs1<sup>+/+</sup>Ifn $\gamma$ <sup>-/-</sup>* and *Socs1<sup>-/-</sup>Ifn $\gamma$ <sup>-/-</sup>* mice**

Agilent Probe Name	Gene Symbol	Fold Change ( <i>Socs1<sup>+/+</sup>Ifn<math>\gamma</math><sup>-/-</sup></i> vs <i>Socs1<sup>-/-</sup>Ifn<math>\gamma</math><sup>-/-</sup></i> )	Regulation ( <i>Socs1<sup>+/+</sup>Ifn<math>\gamma</math><sup>-/-</sup></i> vs <i>Socs1<sup>-/-</sup>Ifn<math>\gamma</math><sup>-/-</sup></i> )	Corrected p-value Unpaired T-test (BHFD)
A_52_P225888	1110018N20Rik	2.182	up	0.020
A_52_P649276	1110032A04Rik	2.206	down	0.018
A_52_P533780	1110037F02Rik	5.574	down	0.038
A_51_P433679	1600014C10Rik	3.728	down	0.041
A_52_P85893	1600021P15Rik	5.416	down	0.027
A_51_P142206	1600029O15Rik	14.032	down	0.014
A_52_P625270	1700024G13Rik	2.164	down	0.032
A_51_P160536	1700026D08Rik	2.567	down	0.026
A_52_P252996	1700047I17Rik1	3.470	down	0.019
A_52_P50417	1700084J12Rik	4.360	down	0.027
A_51_P139096	1700122O11Rik	2.748	down	0.020
A_52_P931190	1810013L24Rik	2.074	down	0.038
A_51_P334318	2010110P09Rik	2.014	down	0.016
A_52_P670654	2210409E12Rik	2.771	down	0.022
A_51_P360122	2610028H24Rik	2.041	down	0.027
A_52_P218792	3830406C13Rik	2.026	down	0.031
A_52_P1163494	4930480K23Rik	2.269	up	0.027
A_52_P1035451	4930518J21Rik	4.909	up	0.023
A_52_P247915	4930526F13Rik	2.381	down	0.037
A_51_P107039	4930555G01Rik	6.627	down	0.029
A_51_P155565	4930590J08Rik	2.320	up	0.020
A_52_P241640	4930599N23Rik	2.310	up	0.012

Agilent Probe Name	Gene Symbol	Fold Change ( <i>Socs1<sup>+/+</sup>lfnγ<sup>-/-</sup></i> vs <i>Socs1<sup>-/-</sup>lfnγ<sup>-/-</sup></i> )	Regulation ( <i>Socs1<sup>+/+</sup>lfnγ<sup>-/-</sup></i> vs <i>Socs1<sup>-/-</sup>lfnγ<sup>-/-</sup></i> )	Corrected p-value Unpaired T-test (BHFR)
A_52_P1051779	6330403A02Rik	2.622	up	0.039
A_52_P393589	9030425E11Rik	2.581	up	0.029
A_51_P206144	9030425E11Rik	2.635	up	0.017
A_51_P456114	9930013L23Rik	2.218	up	0.042
A_51_P496795	A330049M08Rik	2.031	up	0.013
A_51_P279616	A430089I19Rik	3.713	down	0.027
A_51_P443082	Abca3	2.648	down	0.038
A_51_P239236	Acacb	2.301	up	0.013
A_51_P463452	Acs11	2.035	up	0.032
A_52_P420504	Acta2	2.434	up	0.038
A_52_P210078	Acta2	2.089	up	0.027
A_51_P241269	Actg2	4.339	down	0.048
A_51_P110830	Adamts8	2.420	up	0.014
A_52_P509020	Adamts8	2.309	up	0.019
A_51_P505738	Adig	2.462	up	0.024
A_51_P458451	Adipoq	2.231	up	0.034
A_52_P458169	Adm2	3.021	up	0.027
A_52_P661412	Adora1	2.797	up	0.018
A_52_P172272	Adora1	2.185	up	0.018
A_52_P551743	Aff4	7.654	down	0.013
A_52_P199633	Al451617	2.102	up	0.028
A_52_P151393	Al646023	3.246	down	0.018
A_52_P346037	Akr1c12	2.004	up	0.011
A_51_P256170	Akr1c18	6.596	up	0.013

Agilent Probe Name	Gene Symbol	Fold Change ( <i>Socs1<sup>+/+</sup>lfnγ<sup>-/-</sup></i> vs <i>Socs1<sup>-/-</sup>lfnγ<sup>-/-</sup></i> )	Regulation ( <i>Socs1<sup>+/+</sup>lfnγ<sup>-/-</sup></i> vs <i>Socs1<sup>-/-</sup>lfnγ<sup>-/-</sup></i> )	Corrected p-value Unpaired T-test (BHFD)
A_51_P180213	Akr1c19	2.171	up	0.012
A_52_P58145	Aldh1a2	2.272	up	0.017
A_51_P219088	Alpk2	2.862	up	0.016
A_51_P404815	Apol6	3.266	up	0.044
A_52_P403405	Aqp7	2.056	up	0.025
A_51_P378063	Aqp7	2.195	up	0.018
A_52_P288456	Arhgap11a	4.835	down	0.012
A_51_P505372	Art2b	2.863	up	0.030
A_52_P227267	Atp1a2	2.205	up	0.010
A_52_P125485	AU042651	2.071	up	0.037
A_52_P54176	Axin2	7.645	down	0.024
A_52_P397814	B230340J04Rik	2.402	down	0.032
A_51_P295848	Bai1	2.275	down	0.042
A_51_P309293	BC046331	2.929	down	0.036
A_52_P460929	BC048507	5.691	down	0.028
A_52_P605319	BC051665	2.040	down	0.020
A_51_P279154	Bex1	2.874	down	0.026
A_51_P208793	C1s	2.336	up	0.023
A_52_P634218	C1s	2.109	up	0.026
A_52_P428699	C2	2.330	up	0.016
A_52_P583097	C2cd4a	2.516	up	0.024
A_51_P428708	C4b	3.234	up	0.018
A_52_P68175	C77080	11.103	down	0.043
A_51_P280384	Cacna1h	2.654	up	0.015

Agilent Probe Name	Gene Symbol	Fold Change ( <i>Socs1<sup>+/+</sup>Ifny<sup>-/-</sup></i> vs <i>Socs1<sup>-/-</sup>Ifny<sup>-/-</sup></i> )	Regulation ( <i>Socs1<sup>+/+</sup>Ifny<sup>-/-</sup></i> vs <i>Socs1<sup>-/-</sup>Ifny<sup>-/-</sup></i> )	Corrected p-value Unpaired T-test (BHFD)
A_51_P357573	Cald1	2.124	up	0.018
A_51_P167232	Cask	2.575	down	0.026
A_52_P229997	Cbx8	6.745	down	0.043
A_52_P249514	Ccl12	2.056	up	0.014
A_51_P114462	Ccl17	2.787	up	0.012
A_51_P509573	Ccl4	2.057	up	0.029
A_51_P231042	Cd163	4.805	down	0.039
A_52_P466268	Cd22	2.166	up	0.016
A_52_P483911	Cdc42bpa	2.668	down	0.025
A_52_P109403	Cebpz	2.573	down	0.025
A_51_P273979	Cenpa	2.553	down	0.047
A_52_P371666	Cep68	2.043	down	0.013
A_51_P375969	Ces3	2.259	up	0.037
A_51_P496905	Cfi	2.220	up	0.018
A_51_P112966	Ch25h	3.193	up	0.006
A_51_P299107	Chst5	6.876	up	0.013
A_51_P199168	Cidea	2.279	up	0.025
A_51_P490456	Cidec	2.199	up	0.026
A_51_P313294	Cir1	4.444	down	0.042
A_51_P196243	Ckap5	2.989	down	0.028
A_51_P469568	Cldn13	2.435	up	0.031
A_52_P558609	Clec16a	2.359	up	0.028
A_52_P447284	Clic6	2.967	down	0.013
A_52_P186937	Cmpk2	2.344	up	0.013

Agilent Probe Name	Gene Symbol	Fold Change ( <i>Socs1<sup>+/+</sup>lfn<sup>y-/-</sup></i> vs <i>Socs1<sup>-/-</sup>lfn<sup>y-/-</sup></i> )	Regulation ( <i>Socs1<sup>+/+</sup>lfn<sup>y-/-</sup></i> vs <i>Socs1<sup>-/-</sup>lfn<sup>y-/-</sup></i> )	Corrected p-value Unpaired T-test (BHFD)
A_51_P400190	Cmpk2	2.159	up	0.022
A_51_P505384	Cntn4	2.201	down	0.028
A_52_P658611	Col1a1	2.008	up	0.047
A_52_P282058	Col8a1	3.183	up	0.013
A_51_P148612	Cox7a1	2.468	up	0.018
A_52_P136153	Cox7c	5.833	down	0.026
A_51_P246001	Cpe	2.061	up	0.028
A_52_P78417	Cpe	2.107	up	0.026
A_51_P170562	Cpn2	4.471	up	0.020
A_51_P232913	Cpt1b	2.200	up	0.028
A_51_P139108	Cpxm1	2.337	up	0.021
A_51_P300618	Crb2	2.138	up	0.013
A_52_P460734	Crhbp	2.601	up	0.013
A_52_P420500	Cry1	3.354	down	0.013
A_52_P278064	Cspg4	2.081	up	0.018
A_51_P137419	Cst7	2.048	up	0.049
A_52_P38029	Cwf19l1	2.488	down	0.021
A_52_P99810	Cx3cr1	2.121	up	0.026
A_51_P294235	Cxcl17	2.612	down	0.014
A_52_P559975	Cxcr2	2.631	up	0.019
A_52_P95517	Cyp2a22	6.096	down	0.013
A_52_P481346	Cyp2g1	2.019	down	0.028
A_51_P252859	Cyr61	2.362	up	0.010
A_52_P380369	D14Ert668e	2.444	up	0.025

Agilent Probe Name	Gene Symbol	Fold Change ( <i>Socs1<sup>+/+</sup>lfnγ<sup>-/-</sup></i> vs <i>Socs1<sup>-/-</sup>lfnγ<sup>-/-</sup></i> )	Regulation ( <i>Socs1<sup>+/+</sup>lfnγ<sup>-/-</sup></i> vs <i>Socs1<sup>-/-</sup>lfnγ<sup>-/-</sup></i> )	Corrected p-value Unpaired T-test (BHFR)
A_52_P305579	D330041H03Rik	2.488	down	0.043
A_52_P204331	D630039A03Rik	2.379	up	0.013
A_52_P445346	Dapk1	6.678	down	0.012
A_52_P37826	Dapk1	2.877	down	0.007
A_51_P156144	Dbx1	2.896	down	0.045
A_51_P384936	Ddo	2.465	up	0.036
A_51_P393748	Ddx58	2.207	up	0.014
A_51_P197910	Ddx60	2.673	up	0.042
A_51_P512820	Dera	2.702	down	0.028
A_51_P256369	Dot1l	5.168	down	0.019
A_51_P115441	Dpysl3	2.034	up	0.010
A_51_P249848	Dsg2	2.208	up	0.014
A_52_P141715	Dtna	2.614	down	0.025
A_52_P108607	Dtna	2.322	down	0.016
A_51_P365744	Duoxa2	2.638	up	0.047
A_51_P242634	Dusp16	4.786	down	0.012
A_52_P127813	E030037K03Rik	3.871	up	0.018
A_51_P157524	E2f4	12.484	down	0.027
A_52_P349216	E2f6	3.297	down	0.026
A_52_P157726	Ear7	3.017	down	0.013
A_51_P266103	Edc4	3.281	down	0.047
A_51_P493364	Eif4a1	12.113	down	0.013
A_52_P613688	Elmo1	2.876	down	0.048
A_51_P422257	Emx1	3.102	down	0.041

Agilent Probe Name	Gene Symbol	Fold Change ( <i>Socs1<sup>+/+</sup>lfn<math>\gamma</math><sup>-/-</sup></i> vs <i>Socs1<sup>-/-</sup>lfn<math>\gamma</math><sup>-/-</sup></i> )	Regulation ( <i>Socs1<sup>+/+</sup>lfn<math>\gamma</math><sup>-/-</sup></i> vs <i>Socs1<sup>-/-</sup>lfn<math>\gamma</math><sup>-/-</sup></i> )	Corrected p-value Unpaired T-test (BHFR)
A_51_P332309	Eomes	6.211	up	0.013
A_52_P475229	Ep400	3.666	down	0.022
A_51_P209903	Erc2	2.448	up	0.044
A_52_P197965	Erdr1	2.170	down	0.018
A_51_P329043	Ets1	2.002	down	0.020
A_51_P174961	F10	2.009	up	0.042
A_51_P167535	Fabp3	3.365	up	0.031
A_51_P387764	Fabp5	5.094	down	0.026
A_51_P368285	Fam101a	2.526	down	0.033
A_52_P437850	Fam13c	2.214	down	0.032
A_52_P57317	Fam19a3	2.099	up	0.025
A_51_P237512	Fam33a	4.107	down	0.018
A_52_P375970	Fam38b	2.058	up	0.028
A_52_P362828	Fat3	2.757	up	0.010
A_51_P499020	Fbp2	2.487	up	0.033
A_51_P181517	Fcgr4	2.976	up	0.011
A_52_P416518	Fgd4	3.643	down	0.032
A_52_P326548	Fhod3	2.066	up	0.038
A_51_P286423	Foxd3	2.527	down	0.018
A_51_P344790	Foxl2	2.059	down	0.018
A_51_P401096	Foxp3	2.202	up	0.027
A_51_P481261	Foxq1	3.300	down	0.032
A_51_P312485	Fpr1	2.229	up	0.041
A_52_P89305	Frmf5	2.070	up	0.019

Agilent Probe Name	Gene Symbol	Fold Change ( <i>Socs1<sup>+/+</sup>lfnγ<sup>-/-</sup></i> vs <i>Socs1<sup>-/-</sup>lfnγ<sup>-/-</sup></i> )	Regulation ( <i>Socs1<sup>+/+</sup>lfnγ<sup>-/-</sup></i> vs <i>Socs1<sup>-/-</sup>lfnγ<sup>-/-</sup></i> )	Corrected p-value Unpaired T-test (BHFR)
A_51_P381821	Fst	3.371	up	0.005
A_52_P129428	Fzd2	2.661	up	0.027
A_51_P404077	Fzd2	3.166	up	0.023
A_51_P490997	Gas2l1	4.380	down	0.038
A_51_P213260	Gata5	3.406	up	0.039
A_52_P327664	Gbp5	2.148	up	0.028
A_51_P406913	Gdf7	2.914	down	0.029
A_51_P241426	Gfra4	2.234	up	0.027
A_51_P331431	Glit25d2	2.179	down	0.028
A_52_P602847	Glycam1	19.839	up	0.045
A_52_P657123	Gm10270	5.435	down	0.029
A_52_P219741	Gm10324	7.446	down	0.024
A_52_P481279	Gm1060	2.411	up	0.032
A_52_P164821	Gm12250	2.593	up	0.009
A_51_P514553	Gm12504	8.189	down	0.013
A_52_P302041	Gm12755	2.236	down	0.022
A_52_P108492	Gm12770	4.559	down	0.018
A_52_P106399	Gm13253	4.563	down	0.016
A_52_P347796	Gm14420	2.038	down	0.030
A_51_P500082	Gm14446	3.599	up	0.020
A_52_P294064	Gm14446	3.019	up	0.040
A_52_P234910	Gm15032	5.841	down	0.018
A_51_P286431	Gm15247	2.479	down	0.036
A_51_P286426	Gm15247	2.426	down	0.037

Agilent Probe Name	Gene Symbol	Fold Change ( <i>Socs1<sup>+/+</sup>lfnγ<sup>-/-</sup></i> vs <i>Socs1<sup>-/-</sup>lfnγ<sup>-/-</sup></i> )	Regulation ( <i>Socs1<sup>+/+</sup>lfnγ<sup>-/-</sup></i> vs <i>Socs1<sup>-/-</sup>lfnγ<sup>-/-</sup></i> )	Corrected p-value Unpaired T-test (BHFR)
A_51_P180176	Gm16223	5.141	down	0.018
A_52_P13216	Gm16381	7.022	down	0.014
A_52_P157880	Gm1947	3.513	down	0.029
A_52_P975691	Gm4371	3.761	down	0.044
A_52_P1082736	Gm4532	2.733	down	0.044
A_52_P639689	Gm4907	2.090	down	0.029
A_52_P219791	Gm4961	3.732	down	0.031
A_52_P151378	Gm5076	6.269	down	0.033
A_52_P195358	Gm5176	3.186	down	0.018
A_52_P136741	Gm5222	4.231	up	0.023
A_52_P648246	Gm5699	8.941	down	0.013
A_52_P150114	Gm5731	3.982	down	0.028
A_52_P638319	Gm5828	3.542	down	0.023
A_52_P401295	Gm5989	8.163	down	0.036
A_51_P494655	Gm6484	2.899	up	0.029
A_52_P740427	Gm6484	2.220	up	0.029
A_52_P759266	Gm6787	4.422	down	0.016
A_51_P163261	Gm6985	5.796	down	0.015
A_52_P629037	Gm6987	5.396	down	0.028
A_52_P602180	Gm7098	16.001	down	0.018
A_52_P341489	Gm7120	2.631	down	0.030
A_52_P113916	Gm7146	4.950	down	0.047
A_52_P403527	Gm8109	5.205	down	0.028
A_52_P337821	Gm8300	5.735	down	0.025

Agilent Probe Name	Gene Symbol	Fold Change ( <i>Socs1<sup>+/+</sup>lfnγ<sup>-/-</sup></i> vs <i>Socs1<sup>-/-</sup>lfnγ<sup>-/-</sup></i> )	Regulation ( <i>Socs1<sup>+/+</sup>lfnγ<sup>-/-</sup></i> vs <i>Socs1<sup>-/-</sup>lfnγ<sup>-/-</sup></i> )	Corrected p-value Unpaired T-test (BHFD)
A_52_P74637	Gm9292	5.366	down	0.025
A_52_P351686	Gm9558	3.919	down	0.010
A_52_P579252	Gm9644	3.488	down	0.042
A_51_P293853	Gpd1	2.552	up	0.018
A_52_P16419	Gpd1	2.494	up	0.018
A_51_P292008	Gpx3	2.770	up	0.011
A_52_P87997	Gsdmc2	2.245	up	0.013
A_51_P470475	Gsdmcl-ps	3.652	up	0.018
A_51_P322016	Gsx1	2.157	down	0.029
A_51_P382732	Gtf3c6	15.527	down	0.038
A_51_P195153	Gtse1	6.014	down	0.026
A_51_P333274	Gzmb	2.260	up	0.017
A_51_P138510	Gzmc	3.429	up	0.037
A_51_P142196	H19	2.575	up	0.046
A_52_P571350	H19	2.469	up	0.030
A_51_P230267	H2-Q10	2.258	up	0.033
A_52_P581082	H2-T24	2.118	up	0.036
A_52_P189812	H2-T24	2.050	up	0.021
A_51_P129127	H2-T3	2.323	down	0.014
A_51_P492456	Has1	2.635	up	0.013
A_51_P342897	Heatr5b	3.145	down	0.038
A_52_P36591	Hmmr	3.752	down	0.018
A_52_P14666	Hnrnpa112	7.484	down	0.013
A_51_P509263	Hoxa7	3.349	down	0.040

Agilent Probe Name	Gene Symbol	Fold Change ( <i>Socs1<sup>+/+</sup>Ifny<sup>-/-</sup></i> vs <i>Socs1<sup>-/-</sup>Ifny<sup>-/-</sup></i> )	Regulation ( <i>Socs1<sup>+/+</sup>Ifny<sup>-/-</sup></i> vs <i>Socs1<sup>-/-</sup>Ifny<sup>-/-</sup></i> )	Corrected p-value Unpaired T-test (BHFD)
A_51_P436342	Hoxb5	2.062	up	0.019
A_51_P235945	Hp	2.160	up	0.047
A_51_P388819	Hpcal4	4.433	up	0.013
A_51_P419007	Hspb3	2.485	down	0.032
A_51_P453142	Ibtk	2.589	down	0.032
A_52_P86693	Ifi2711	2.143	up	0.029
A_52_P90363	Ifi2712a	2.135	up	0.026
A_51_P358233	Ifi2712a	2.223	up	0.021
A_52_P90364	Ifi2712a	2.775	up	0.014
A_52_P541802	Ifitm1	2.585	up	0.012
A_51_P150710	Igj	2.051	up	0.036
A_52_P957659	Igkv1-117	2.193	up	0.048
A_51_P142703	Il19	2.025	up	0.013
A_51_P339793	Il1rl1	3.151	up	0.018
A_52_P484194	Il1rl1	3.136	up	0.029
A_52_P360280	Ints2	2.662	down	0.017
A_51_P421876	Irf7	2.758	up	0.026
A_52_P176013	Irf9	2.344	up	0.026
A_51_P127367	Irf9	2.540	up	0.020
A_52_P463936	Isg15	2.631	up	0.028
A_51_P292221	Kcnk3	2.197	up	0.022
A_52_P639402	Kcnk3	2.309	up	0.019
A_52_P665887	Kdm5a	2.666	down	0.028
A_52_P538490	Klk7	3.584	down	0.007

Agilent Probe Name	Gene Symbol	Fold Change ( <i>Socs1<sup>+/+</sup>lfnγ<sup>-/-</sup></i> vs <i>Socs1<sup>-/-</sup>lfnγ<sup>-/-</sup></i> )	Regulation ( <i>Socs1<sup>+/+</sup>lfnγ<sup>-/-</sup></i> vs <i>Socs1<sup>-/-</sup>lfnγ<sup>-/-</sup></i> )	Corrected p-value Unpaired T-test (BHFR)
A_51_P256983	Klrg1	2.419	up	0.013
A_51_P287691	Kremen2	2.383	up	0.025
A_52_P410685	Krt7	2.541	up	0.040
A_52_P666855	Ksr1	3.129	down	0.034
A_52_P142807	Lamp3	4.297	down	0.020
A_51_P125345	Lce1b	2.077	down	0.028
A_51_P298615	Lhx8	2.387	up	0.042
A_52_P229278	Limch1	2.050	down	0.049
A_51_P435366	Lipe	2.022	up	0.015
A_52_P426554	Lmnb2	3.794	down	0.039
A_51_P427964	Lmod3	2.970	down	0.012
A_52_P445474	Lmtk2	4.438	down	0.028
A_52_P246277	LOC633417	2.312	down	0.014
A_52_P671812	LOC641192	5.601	down	0.029
A_52_P186785	LOC675539	2.657	down	0.036
A_52_P565396	LOC676708	2.850	down	0.014
A_51_P288295	LOC677484	2.595	up	0.045
A_51_P304239	Loxl1	2.103	up	0.018
A_51_P229498	Lrfr2	2.565	up	0.018
A_52_P285470	Lrp2	2.467	up	0.036
A_51_P407780	Ly6h	2.140	up	0.013
A_51_P407786	Ly6h	2.574	up	0.023
A_52_P215597	Lztl1	5.554	down	0.035
A_51_P504214	Magix	2.102	up	0.043

Agilent Probe Name	Gene Symbol	Fold Change ( <i>Socs1<sup>+/+</sup>lfnγ<sup>-/-</sup></i> vs <i>Socs1<sup>-/-</sup>lfnγ<sup>-/-</sup></i> )	Regulation ( <i>Socs1<sup>+/+</sup>lfnγ<sup>-/-</sup></i> vs <i>Socs1<sup>-/-</sup>lfnγ<sup>-/-</sup></i> )	Corrected p-value Unpaired T-test (BHFD)
A_51_P480390	Meig1	2.178	down	0.014
A_51_P124535	Mest	2.272	up	0.017
A_51_P195244	Mfap4	2.330	up	0.013
A_51_P255699	Mmp3	2.750	up	0.032
A_51_P122071	Muc5b	2.060	down	0.043
A_51_P514085	Mx2	2.807	up	0.023
A_51_P455157	Mybpc2	2.975	up	0.042
A_51_P159367	Myo16	3.602	down	0.020
A_51_P431785	Myom2	2.764	up	0.020
A_52_P183138	Nab2	11.308	down	0.014
A_51_P500882	Ncr1	2.958	up	0.017
A_52_P1076033	Ndufs5	2.179	down	0.021
A_51_P283759	Nfkb1	3.753	down	0.016
A_52_P382107	Nlrc5	2.190	up	0.018
A_51_P187210	Nol11	2.764	down	0.030
A_52_P505501	Nsmce2	2.202	down	0.015
A_51_P305003	Ntrk1	2.517	up	0.013
A_52_P486360	Nubpl	2.952	down	0.010
A_51_P204121	Nudt6	2.889	down	0.017
A_52_P337357	Oas1a	3.635	up	0.028
A_52_P110877	Oas1b	2.039	up	0.013
A_51_P277994	Oas2	4.210	up	0.013
A_51_P472867	Oas3	2.181	up	0.039
A_51_P437309	Oasl1	3.484	up	0.016

Agilent Probe Name	Gene Symbol	Fold Change ( <i>Socs1<sup>+/+</sup>lfnγ<sup>-/-</sup></i> vs <i>Socs1<sup>-/-</sup>lfnγ<sup>-/-</sup></i> )	Regulation ( <i>Socs1<sup>+/+</sup>lfnγ<sup>-/-</sup></i> vs <i>Socs1<sup>-/-</sup>lfnγ<sup>-/-</sup></i> )	Corrected p-value Unpaired T-test (BHFD)
A_52_P377492	Olf1122	2.120	down	0.042
A_51_P436790	Olf144	2.049	down	0.027
A_51_P386280	Olf187	2.703	down	0.013
A_51_P219752	Olf382	2.015	down	0.047
A_52_P557059	Olf536	2.091	up	0.013
A_51_P319460	Osmr	2.084	up	0.016
A_52_P495729	Osmr	2.300	up	0.037
A_51_P486190	Pabpc2	4.503	down	0.018
A_51_P422540	Paqr8	2.326	down	0.010
A_52_P241129	Pcbp1	14.599	down	0.014
A_51_P184223	Pcdhb7	2.613	up	0.022
A_51_P483878	Pcdhb9	2.802	up	0.027
A_51_P137688	Pex1	2.367	down	0.033
A_51_P414927	Pigw	2.008	down	0.038
A_52_P99848	Pik3cd	2.809	down	0.050
A_52_P608312	Pitpnb	5.031	down	0.020
A_51_P225427	Pkp2	2.137	up	0.006
A_52_P94983	Pla2g5	2.473	up	0.018
A_51_P244497	Plin1	2.522	up	0.014
A_51_P495780	Plin4	2.811	up	0.016
A_51_P262757	Plin5	2.605	up	0.018
A_52_P372901	Plscr2	2.915	up	0.028
A_51_P251022	Plscr2	2.740	up	0.030
A_51_P202331	Plunc	3.477	down	0.019

Agilent Probe Name	Gene Symbol	Fold Change ( <i>Socs1<sup>+/+</sup>lfnγ<sup>-/-</sup></i> vs <i>Socs1<sup>-/-</sup>lfnγ<sup>-/-</sup></i> )	Regulation ( <i>Socs1<sup>+/+</sup>lfnγ<sup>-/-</sup></i> vs <i>Socs1<sup>-/-</sup>lfnγ<sup>-/-</sup></i> )	Corrected p-value Unpaired T-test (BHFR)
A_51_P490397	Pold3	3.491	down	0.037
A_51_P450924	Pole4	4.748	down	0.036
A_51_P293538	Ppp1r1a	2.270	up	0.022
A_51_P461779	Ppp2r2c	2.324	up	0.041
A_51_P307243	Ppp5c	6.034	down	0.024
A_51_P414072	Prom1	2.134	down	0.013
A_51_P127425	Prpf4b	4.132	down	0.047
A_51_P508959	Prr15	2.064	up	0.022
A_52_P137104	Prr15	2.120	up	0.025
A_51_P418644	Prr15l	2.376	down	0.041
A_52_P366790	Psmb11	3.857	down	0.024
A_51_P327874	Pth1r	2.176	up	0.025
A_52_P622042	Pth2	3.956	down	0.039
A_51_P129360	Pthlh	2.995	up	0.012
A_51_P129363	Pthlh	2.581	up	0.010
A_51_P264084	Rab36	2.106	down	0.014
A_51_P211471	Rab40b	2.244	up	0.042
A_52_P413805	Rad18	2.262	down	0.013
A_52_P39756	Rap1gap2	4.408	down	0.032
A_52_P466147	Rarres2	2.127	up	0.014
A_52_P496726	Rasd1	2.208	up	0.044
A_51_P105927	Rasl12	2.647	up	0.050
A_51_P503194	Rbm15b	2.479	down	0.049
A_51_P233597	Retn	2.072	up	0.032

Agilent Probe Name	Gene Symbol	Fold Change ( <i>Socs1<sup>+/+</sup>lfnγ<sup>-/-</sup></i> vs <i>Socs1<sup>-/-</sup>lfnγ<sup>-/-</sup></i> )	Regulation ( <i>Socs1<sup>+/+</sup>lfnγ<sup>-/-</sup></i> vs <i>Socs1<sup>-/-</sup>lfnγ<sup>-/-</sup></i> )	Corrected p-value Unpaired T-test (BHFR)
A_51_P257951	Retnla	2.751	up	0.020
A_52_P254817	Retnla	2.340	up	0.032
A_52_P298301	Rfwd2	2.824	down	0.031
A_52_P392229	Rnf152	2.286	up	0.028
A_52_P678800	Rps21	3.804	down	0.018
A_52_P740562	Rps21	2.940	down	0.046
A_51_P292357	Rps3a	2.564	down	0.042
A_52_P780667	Rps4x	3.895	down	0.014
A_52_P573727	Rrm2b	5.866	down	0.019
A_51_P505132	Rsad2	3.086	up	0.019
A_52_P670026	Rsad2	3.179	up	0.013
A_51_P505134	Rsad2	2.588	up	0.023
A_52_P312826	Rtf1	3.354	down	0.020
A_51_P304170	Rtp4	3.717	up	0.010
A_51_P478688	Samd10	2.144	down	0.036
A_52_P789023	Sarnp	2.232	down	0.017
A_52_P682382	Scd1	2.956	up	0.044
A_51_P184340	Scn3b	4.459	up	0.009
A_52_P228899	Scn3b	2.658	up	0.037
A_51_P184331	Scn3b	2.631	up	0.005
A_52_P127115	Sema5b	2.234	down	0.027
A_51_P231364	Sepsecs	2.876	down	0.032
A_52_P324042	Serpina1b	3.016	up	0.030
A_52_P598495	Serpina1c	2.148	up	0.027

Agilent Probe Name	Gene Symbol	Fold Change ( <i>Socs1<sup>+/+</sup>lfny<sup>-/-</sup></i> vs <i>Socs1<sup>-/-</sup>lfny<sup>-/-</sup></i> )	Regulation ( <i>Socs1<sup>+/+</sup>lfny<sup>-/-</sup></i> vs <i>Socs1<sup>-/-</sup>lfny<sup>-/-</sup></i> )	Corrected p-value Unpaired T-test (BHFD)
A_51_P236303	Serpina1d	2.978	up	0.032
A_51_P157112	Serpina3c	2.428	up	0.013
A_51_P326191	Serpina3g	2.062	up	0.020
A_51_P159453	Serpina3n	3.892	up	0.012
A_52_P430348	Serpib1b	2.782	down	0.013
A_51_P207763	Serpib3b	7.011	down	0.024
A_51_P406328	Serpib6c	2.630	down	0.010
A_52_P602669	Serpib6d	3.687	down	0.011
A_51_P376238	Serping1	2.193	up	0.013
A_51_P201747	Sez6l	2.221	up	0.045
A_52_P427377	Sez6l	2.356	up	0.031
A_52_P583728	Sfrs8	4.231	down	0.015
A_51_P359891	Siglec1	2.984	up	0.028
A_51_P352324	Slc16a2	2.051	up	0.025
A_52_P971776	Slc25a12	2.169	down	0.018
A_51_P514405	Slc2a5	2.216	up	0.042
A_51_P164400	Slc33a1	4.341	down	0.013
A_51_P221256	Slc34a2	3.161	up	0.005
A_51_P366672	Slc36a2	2.552	up	0.026
A_52_P503384	Slc4a1ap	2.086	down	0.012
A_52_P108502	Slc4a7	3.141	down	0.013
A_51_P268193	Slc7a10	2.183	up	0.027
A_52_P367829	Slc9a8	2.259	down	0.020
A_51_P403636	Smad7	2.151	down	0.031

Agilent Probe Name	Gene Symbol	Fold Change ( <i>Socs1<sup>+/+</sup>lfnγ<sup>-/-</sup></i> vs <i>Socs1<sup>-/-</sup>lfnγ<sup>-/-</sup></i> )	Regulation ( <i>Socs1<sup>+/+</sup>lfnγ<sup>-/-</sup></i> vs <i>Socs1<sup>-/-</sup>lfnγ<sup>-/-</sup></i> )	Corrected p-value Unpaired T-test (BHFR)
A_52_P478025	Smpd3	2.034	up	0.018
A_52_P395149	Smtnl2	2.376	up	0.018
A_51_P279606	Socs1	1204.233	down	0.010
A_51_P163639	Spaca4	2.589	down	0.018
A_51_P370552	Spink12	2.032	down	0.013
A_51_P497350	Spint2	4.181	down	0.030
A_52_P242321	Spon1	2.021	up	0.013
A_51_P225903	Sprr4	2.065	down	0.022
A_51_P119055	Ssb	4.447	down	0.041
A_52_P59006	St13	2.995	down	0.028
A_52_P290090	Stbd1	2.033	up	0.018
A_51_P471458	Sult5a1	2.212	up	0.014
A_52_P306162	Syne1	2.401	down	0.036
A_52_P62986	Synpo	4.564	down	0.050
A_52_P299292	Tardbp	2.244	down	0.031
A_51_P484329	Tcra	2.286	down	0.039
A_51_P338336	Tdg	2.395	down	0.024
A_51_P251402	Tgds	7.922	down	0.005
A_51_P212754	Tgfbi	2.252	up	0.018
A_52_P676510	Tgtp1	2.054	up	0.024
A_51_P478722	Tgtp1	2.195	up	0.005
A_51_P353221	Thbs4	3.520	up	0.016
A_52_P401504	Thbs4	3.690	up	0.013
A_51_P194099	Thrsp	2.343	up	0.044

Agilent Probe Name	Gene Symbol	Fold Change ( <i>Socs1<sup>+/+</sup>lfnγ<sup>-/-</sup></i> vs <i>Socs1<sup>-/-</sup>lfnγ<sup>-/-</sup></i> )	Regulation ( <i>Socs1<sup>+/+</sup>lfnγ<sup>-/-</sup></i> vs <i>Socs1<sup>-/-</sup>lfnγ<sup>-/-</sup></i> )	Corrected p-value Unpaired T-test (BHFD)
A_52_P229052	Tmeff2	2.048	up	0.029
A_51_P210611	Tmem30a	7.712	down	0.014
A_51_P368496	Tmem98	2.231	up	0.013
A_52_P217937	Tmlhe	3.931	down	0.028
A_52_P450780	Tmod3	4.968	down	0.028
A_51_P415775	Tmtc1	2.051	up	0.027
A_51_P484371	Tnfsf8	2.285	up	0.019
A_52_P418477	Tpm2	2.078	up	0.045
A_51_P466436	Tprg	2.025	down	0.033
A_52_P442567	Trim30	2.555	up	0.013
A_52_P401824	Tsg101	3.959	down	0.043
A_52_P203404	Ttc24	2.023	up	0.019
A_51_P480062	Ubap1	2.162	down	0.028
A_51_P426353	Ucp1	2.942	up	0.032
A_51_P164219	Usp18	2.149	up	0.032
A_52_P153265	Uvrag	2.298	down	0.042
A_52_P577533	Vat1l	2.853	up	0.042
A_51_P298107	Vit	2.619	up	0.013
A_51_P383629	Vps4a	2.123	down	0.039
A_51_P133260	Vsnl1	2.940	up	0.013
A_52_P515880	Vsnl1	2.278	up	0.020
A_52_P485450	Vta1	3.060	down	0.019
A_51_P390314	Wdfy1	2.949	down	0.013
A_52_P511821	Wdfy1	2.198	up	0.037

Agilent Probe Name	Gene Symbol	Fold Change ( <i>Socs1<sup>+/+</sup>lfnγ<sup>-/-</sup></i> vs <i>Socs1<sup>-/-</sup>lfnγ<sup>-/-</sup></i> )	Regulation ( <i>Socs1<sup>+/+</sup>lfnγ<sup>-/-</sup></i> vs <i>Socs1<sup>-/-</sup>lfnγ<sup>-/-</sup></i> )	Corrected p-value Unpaired T-test (BHFD)
A_52_P328825	Wdfy1	2.978	down	0.017
A_51_P288558	Wdr16	2.286	down	0.028
A_52_P292632	Wdr20b	4.351	down	0.018
A_52_P185568	Wdr76	2.520	down	0.024
A_51_P462708	Wfdc15b	2.086	down	0.023
A_51_P390804	Wisp2	2.235	up	0.013
A_51_P494403	Xaf1	2.678	up	0.013
A_51_P234956	Xcl1	2.138	up	0.013
A_51_P463607	Xpnpep3	2.003	down	0.025
A_51_P184936	Zbp1	2.179	up	0.025
A_52_P382040	Zcchc11	2.983	down	0.028
A_51_P377826	Zfand2a	2.218	down	0.023
A_52_P547251	Zfp560	2.379	down	0.013
A_52_P17112	Znrf1	2.065	down	0.043
A_52_P704340	none identified	4.326	down	0.028
A_52_P165315	none identified	13.999	down	0.018
A_52_P17306	none identified	5.293	down	0.018
A_52_P941407	none identified	10.742	down	0.023
A_52_P624998	none identified	4.311	down	0.019
A_52_P653054	none identified	2.010	up	0.037
A_52_P662562	none identified	2.093	up	0.018
A_52_P462540	none identified	11.180	down	0.016
A_52_P326187	none identified	3.042	up	0.023
A_52_P615247	none identified	2.064	up	0.032

Agilent Probe Name	Gene Symbol	Fold Change ( <i>Socs1<sup>+/+</sup>lfnγ<sup>-/-</sup></i> vs <i>Socs1<sup>-/-</sup>lfnγ<sup>-/-</sup></i> )	Regulation ( <i>Socs1<sup>+/+</sup>lfnγ<sup>-/-</sup></i> vs <i>Socs1<sup>-/-</sup>lfnγ<sup>-/-</sup></i> )	Corrected p-value Unpaired T-test (BHFD)
A_52_P439745	none identified	4.261	down	0.026
A_52_P739689	none identified	2.854	down	0.018
A_52_P20211	none identified	2.618	down	0.045
A_52_P764924	none identified	7.370	down	0.022
A_52_P398554	none identified	2.514	down	0.032
A_52_P242631	none identified	6.259	down	0.040
A_52_P250664	none identified	5.489	down	0.024
A_51_P133953	none identified	3.494	down	0.050
A_52_P583399	none identified	6.818	down	0.025
A_51_P225764	none identified	7.723	down	0.044
A_52_P1149594	none identified	2.185	down	0.010
A_52_P559189	none identified	2.190	down	0.049
A_52_P763262	none identified	4.192	down	0.043
A_52_P141077	none identified	7.878	down	0.013
A_51_P380350	none identified	4.492	down	0.014
A_52_P167500	none identified	3.022	down	0.027
A_52_P599964	none identified	2.948	up	0.013
A_52_P427759	none identified	4.184	down	0.029
A_52_P41506	none identified	7.113	down	0.042
A_51_P376454	none identified	11.410	down	0.016
A_52_P47121	none identified	2.280	down	0.027
A_52_P72186	none identified	8.529	down	0.025
A_52_P488011	none identified	2.181	down	0.018
A_52_P670399	none identified	3.432	up	0.028

Agilent Probe Name	Gene Symbol	Fold Change ( <i>Socs1<sup>+/+</sup>lfnγ<sup>-/-</sup></i> vs <i>Socs1<sup>-/-</sup>lfnγ<sup>-/-</sup></i> )	Regulation ( <i>Socs1<sup>+/+</sup>lfnγ<sup>-/-</sup></i> vs <i>Socs1<sup>-/-</sup>lfnγ<sup>-/-</sup></i> )	Corrected p-value Unpaired T-test (BHFR)
A_52_P322962	none identified	2.761	down	0.023
A_52_P238492	none identified	3.485	down	0.046
A_52_P4482	none identified	3.382	down	0.010
A_52_P74715	none identified	8.451	down	0.027
A_52_P399604	none identified	5.332	down	0.014
A_52_P299311	none identified	3.365	down	0.043
A_52_P594036	none identified	3.068	down	0.035
A_52_P476400	none identified	3.677	down	0.019
A_52_P430427	none identified	11.468	down	0.022
A_52_P612840	none identified	6.243	down	0.013
A_52_P163541	none identified	2.549	down	0.043
A_52_P725041	none identified	2.033	up	0.033
A_52_P535084	none identified	4.999	down	0.028
A_52_P549754	none identified	2.749	down	0.044
A_52_P132612	none identified	4.393	down	0.028
A_52_P756465	none identified	4.573	down	0.014
A_52_P398494	none identified	2.921	down	0.016
A_52_P612868	none identified	5.131	down	0.020
A_52_P542970	none identified	2.233	down	0.020
A_52_P171197	none identified	2.464	up	0.041
A_52_P87118	none identified	2.724	down	0.012
A_51_P264922	none identified	2.469	up	0.030
A_52_P241032	none identified	3.225	down	0.036
A_52_P948927	none identified	4.373	down	0.033

Agilent Probe Name	Gene Symbol	Fold Change ( <i>Socs1<sup>+/+</sup>lfnγ<sup>-/-</sup></i> vs <i>Socs1<sup>-/-</sup>lfnγ<sup>-/-</sup></i> )	Regulation ( <i>Socs1<sup>+/+</sup>lfnγ<sup>-/-</sup></i> vs <i>Socs1<sup>-/-</sup>lfnγ<sup>-/-</sup></i> )	Corrected p-value Unpaired T-test (BHFR)
A_52_P44534	none identified	4.353	down	0.028
A_51_P201445	none identified	5.578	down	0.026
A_51_P145232	none identified	2.789	down	0.027
A_52_P579279	none identified	2.271	down	0.036
A_52_P406195	none identified	4.072	down	0.040
A_51_P235835	none identified	2.293	up	0.042
A_52_P84234	none identified	3.626	down	0.017
A_52_P444260	none identified	3.136	up	0.049
A_51_P292332	none identified	2.307	down	0.014
A_52_P105890	none identified	2.503	down	0.031
A_52_P510790	none identified	2.184	up	0.016
A_51_P152725	none identified	3.283	down	0.028
A_52_P378084	none identified	7.707	down	0.049
A_52_P553820	none identified	9.054	down	0.015
A_51_P305239	none identified	2.632	up	0.025
A_52_P498702	none identified	3.628	down	0.026
A_52_P296632	none identified	5.572	down	0.023
A_52_P374983	none identified	2.163	up	0.027
A_51_P187579	none identified	4.520	down	0.028
A_52_P359071	none identified	2.048	up	0.005
A_52_P127513	none identified	2.746	down	0.042
A_51_P297993	none identified	4.606	down	0.017
A_52_P206322	none identified	3.915	up	0.037
A_52_P104444	none identified	4.173	down	0.012

Agilent Probe Name	Gene Symbol	Fold Change ( <i>Socs1<sup>+/+</sup>lfnγ<sup>-/-</sup></i> vs <i>Socs1<sup>-/-</sup>lfnγ<sup>-/-</sup></i> )	Regulation ( <i>Socs1<sup>+/+</sup>lfnγ<sup>-/-</sup></i> vs <i>Socs1<sup>-/-</sup>lfnγ<sup>-/-</sup></i> )	Corrected p-value Unpaired T-test (BHFD)
A_51_P279994	none identified	2.550	down	0.028
A_52_P272054	none identified	4.360	down	0.044
A_52_P475630	none identified	4.593	down	0.022
A_51_P264914	none identified	2.263	up	0.048
A_52_P223814	none identified	8.174	down	0.014
A_52_P81664	none identified	2.671	down	0.037
A_52_P460285	none identified	3.359	down	0.024
A_52_P295012	none identified	2.805	down	0.009
A_52_P1133703	none identified	3.314	down	0.016
A_52_P618417	none identified	3.396	down	0.038
A_51_P450394	none identified	6.335	down	0.020
A_52_P1076265	none identified	2.019	down	0.013
A_52_P594107	none identified	8.498	down	0.026
A_52_P477269	none identified	7.912	down	0.026
A_52_P511243	none identified	2.012	up	0.005
A_52_P322976	none identified	4.487	down	0.038
A_52_P561772	none identified	9.485	down	0.010
A_52_P467900	none identified	9.189	down	0.014
A_52_P417624	none identified	2.466	down	0.028
A_52_P217100	none identified	5.469	down	0.039
A_52_P356562	none identified	2.928	down	0.038
A_52_P224413	none identified	2.207	down	0.013
A_52_P287739	none identified	2.234	down	0.036
A_52_P288669	none identified	3.745	down	0.030

Agilent Probe Name	Gene Symbol	Fold Change ( <i>Socs1<sup>+/+</sup>lfnγ<sup>-/-</sup></i> vs <i>Socs1<sup>-/-</sup>lfnγ<sup>-/-</sup></i> )	Regulation ( <i>Socs1<sup>+/+</sup>lfnγ<sup>-/-</sup></i> vs <i>Socs1<sup>-/-</sup>lfnγ<sup>-/-</sup></i> )	Corrected p-value Unpaired T-test (BHFD)
A_51_P326922	none identified	2.107	down	0.021
A_52_P1028560	none identified	6.565	down	0.031
A_52_P443904	none identified	2.909	down	0.027
A_52_P107542	none identified	3.974	down	0.023
A_52_P1021832	none identified	6.987	down	0.027
A_52_P318023	none identified	2.929	down	0.038
A_52_P716675	none identified	5.219	down	0.028
A_52_P493509	none identified	5.953	down	0.013
A_51_P140829	none identified	26.110	up	0.011
A_51_P282279	none identified	4.667	down	0.020
A_52_P208213	none identified	2.308	down	0.017
A_52_P284203	none identified	7.774	down	0.013
A_52_P473813	none identified	2.283	down	0.042
A_52_P484000	none identified	3.191	down	0.027
A_52_P664965	none identified	2.459	down	0.043
A_52_P57557	none identified	7.648	down	0.017
A_52_P445135	none identified	5.070	down	0.025
A_52_P229167	none identified	3.633	down	0.033
A_52_P274624	none identified	2.536	down	0.010
A_52_P190059	none identified	3.146	down	0.035
A_52_P553749	none identified	6.232	down	0.025
A_52_P513153	none identified	2.435	up	0.005
A_51_P383950	none identified	4.781	down	0.013
A_51_P166849	none identified	2.046	down	0.049

<b>Agilent Probe Name</b>	<b>Gene Symbol</b>	<b>Fold Change (<i>Socs1<sup>+/+</sup>lfnγ<sup>-/-</sup></i> vs <i>Socs1<sup>-/-</sup></i>)</b>	<b>Regulation (<i>Socs1<sup>+/+</sup>lfnγ<sup>-/-</sup></i> vs <i>Socs1<sup>-/-</sup></i>)</b>	<b>Corrected p-value Unpaired T-test (BHFD)</b>
A_52_P190286	none identified	4.570	down	0.033
A_52_P107717	none identified	2.041	down	0.005
A_52_P227937	none identified	2.816	down	0.027

**D. IFN $\alpha$  regulated probes within the thymus of *Socs1*<sup>+/+</sup>*Ifny*<sup>-/-</sup> mice**

Agilent Probe Name	GeneSymbol	Fold Change (0 vs 3 hours)	Regulation (0 vs 3 hours)	Fold Change (0 vs 6 hours)	Regulation (0 vs 6 hours)	Corrected p value, One way anova (BHFDR)	Corrected p value, Unpaired T-test (0 vs 3 hours) (BHFDR)	p value, Unpaired T-test (0 vs 6 hours) (BHFDR)
A_52_P77093	1600014C10Rik	2.336	up				0.007	
A_51_P453616	1700003F17Rik	13.275	up				0.013	
A_51_P322473	2310042D19Rik	4.778	up				0.003	
A_52_P542502	2310042D19Rik	5.977	up				0.018	
A_51_P107039	4930555G01Rik			3.069	up			0.034
A_52_P241640	4930599N23Rik	4.935	up				0.010	
A_51_P249471	9530028C05	5.137	up				0.037	
A_52_P61697	9930111J21Rik2	2.677	up				0.008	
A_51_P158072	A230050P20Rik	3.200	up				0.008	
A_51_P158073	A230050P20Rik	3.137	up				0.009	
A_52_P564444	A530064D06Rik	4.535	up				0.010	
A_52_P30728	Abca17	2.433	up				0.031	
A_52_P183181	Adar	2.861	up				0.020	
A_51_P257134	Adar	3.564	up				0.039	
A_52_P199633	Al451617	9.252	up				0.010	
A_52_P360742	Apol7a	2.787	up				0.022	
A_52_P439874	Arfgap3			2.251	up			0.018
A_51_P134627	Asb13	4.308	up				0.047	
A_52_P537941	Asb13	3.084	up			0.047	0.006	
A_52_P549985	Asb13	2.753	up				0.020	
A_52_P233811	B430306N03Rik	2.763	up				0.004	

Agilent Probe Name	GeneSymbol	Fold Change (0 vs 3 hours)	Regulation (0 vs 3 hours)	Fold Change (0 vs 6 hours)	Regulation (0 vs 6 hours)	Corrected p value, One way anova (BHFDR)	Corrected p value, Unpaired T-test (0 vs 3 hours) (BHFDR)	p value, Unpaired T-test (0 vs 6 hours) (BHFDR)
A_52_P321358	BC006779	5.463	up				0.003	
A_51_P406604	BC006779	4.952	up			0.048	0.004	
A_52_P392638	Bin1			10.435	down			0.032
A_52_P508131	Capn11			3.964	up			0.025
A_52_P249514	Ccl12	5.464	up				0.008	
A_52_P208763	Ccl7	4.766	up				0.031	
A_51_P436652	Ccl7	4.598	up				0.029	
A_51_P253074	Chit1	4.278	up				0.015	
A_52_P265855	Clec4g			3.252	up			0.036
A_51_P514035	Cma1			2.083	down			0.011
A_51_P514029	Cma1			2.411	down			0.026
A_52_P186937	Cmpk2	25.142	up				0.003	
A_51_P400190	Cmpk2	22.974	up				0.003	
A_51_P177491	Ctrl	2.036	up				0.007	
A_51_P432641	Cxcl10	4.628	up			0.048	0.004	
A_51_P461665	Cxcl9	2.522	up				0.029	
A_52_P380369	D14Erttd668e	6.685	up				0.004	
A_51_P215143	D430006K04	7.253	up				0.022	
A_51_P393748	Ddx58	6.559	up				0.004	
A_52_P385536	Ddx58	7.117	up				0.022	
A_52_P523946	Ddx58	6.766	up			0.048	0.004	
A_52_P479001	Ddx58	6.284	up				0.006	
A_51_P234274	Ddx60	13.455	up				0.040	

Agilent Probe Name	GeneSymbol	Fold Change (0 vs 3 hours)	Regulation (0 vs 3 hours)	Fold Change (0 vs 6 hours)	Regulation (0 vs 6 hours)	Corrected p value, One way anova (BHFDR)	Corrected p value, Unpaired T-test (0 vs 3 hours) (BHFDR)	p value, Unpaired T-test (0 vs 6 hours) (BHFDR)
A_51_P197910	Ddx60	11.942	up				0.020	
A_52_P223809	Dhx58	8.297	up				0.013	
A_52_P127813	E030037K03Rik	7.728	up				0.028	
A_52_P559919	Eif2ak2	9.809	up				0.007	
A_52_P582374	Epsti1	3.760	up				0.022	
A_51_P376050	Epsti1	3.328	up				0.015	
A_51_P100852	Fam26f	2.343	up				0.025	
A_51_P181517	Fcgr4	3.414	up				0.012	
A_52_P309418	Ftsjd2	2.273	up				0.012	
A_51_P203955	Gbp2	4.333	up				0.011	
A_52_P327664	Gbp5	4.072	up				0.022	
A_51_P463846	Gbp6	7.494	up				0.047	
A_51_P323180	Gbp9	6.294	up				0.030	
A_52_P344949	Gbp9	4.561	up				0.014	
A_51_P385639	Gjb5			2.083	down			0.020
A_52_P164821	Gm12250	11.479	up				0.004	
A_51_P500082	Gm14446	13.196	up				0.013	
A_52_P294064	Gm14446	13.286	up				0.028	
A_52_P176865	Gm5431	4.841	up				0.034	
A_51_P162326	Gm5933	5.532	up				0.034	
A_51_P333274	Gzmb	2.478	up				0.029	
A_52_P581082	H2-T24	7.209	up				0.015	
A_52_P189812	H2-T24	6.158	up				0.004	

Agilent Probe Name	GeneSymbol	Fold Change (0 vs 3 hours)	Regulation (0 vs 3 hours)	Fold Change (0 vs 6 hours)	Regulation (0 vs 6 hours)	Corrected p value, One way anova (BHFDR)	Corrected p value, Unpaired T-test (0 vs 3 hours) (BHFDR)	p value, Unpaired T-test (0 vs 6 hours) (BHFDR)
A_51_P249313	Herc3	2.133	up				0.025	
A_52_P64514	Herc5	4.728	up				0.020	
A_52_P522427	Hsh2d	5.595	up				0.007	
A_52_P663686	I830012O16Rik	8.811	up				0.008	
A_51_P408343	Ifi204	7.135	up				0.047	
A_51_P487690	Ifi44	6.235	up				0.037	
A_51_P129229	Ifi47	5.252	up			0.037	0.002	
A_51_P387810	Ifih1	7.332	up				0.007	
A_52_P121468	Ifih1	9.669	up				0.013	
A_51_P327751	Ifit1	12.039	up				0.009	
A_52_P542388	Ifit2	4.788	up				0.037	
A_51_P359570	Ifit3	8.138	up				0.005	
A_51_P112355	Igtp	3.606	up				0.015	
A_51_P421876	Irf7	6.444	up				0.013	
A_52_P176013	Irf9	5.160	up				0.008	
A_51_P127367	Irf9	4.912	up				0.008	
A_51_P262171	Irgm1	7.461	up				0.006	
A_52_P126158	Irgm1	7.806	up				0.004	
A_51_P416295	Irgm2	5.234	up				0.005	
A_52_P463936	Isg15	13.336	up				0.008	
A_52_P614207	LOC100047222			3.433	down			0.049
A_51_P395899	LOC100047628			3.761	down			0.044
A_52_P165856	LOC639910	3.643	up				0.030	

Agilent Probe Name	GeneSymbol	Fold Change (0 vs 3 hours)	Regulation (0 vs 3 hours)	Fold Change (0 vs 6 hours)	Regulation (0 vs 6 hours)	Corrected p value, One way anova (BHFDR)	Corrected p value, Unpaired T-test (0 vs 3 hours) (BHFDR)	p value, Unpaired T-test (0 vs 6 hours) (BHFDR)
A_52_P203833	Mitd1	3.522	up				0.008	
A_52_P203837	Mitd1	3.719	up				0.010	
A_51_P303332	Mitd1	5.674	up				0.037	
A_51_P440535	Mikl	2.666	up				0.008	
A_51_P377620	Mnda	4.879	up				0.038	
A_51_P169495	Mov10	3.471	up				0.031	
A_52_P189772	Mpa2l	11.555	up				0.010	
A_52_P211956	Ms4a4d	4.900	up				0.027	
A_51_P422300	Ms4a6b	2.877	up				0.008	
A_51_P149714	Ms4a6d	2.207	up				0.037	
A_52_P446431	Mx1	11.986	up				0.018	
A_52_P614259	Mx1	12.153	up				0.013	
A_51_P514085	Mx2	26.969	up				0.004	
A_51_P248638	Myoz2			12.168	down			0.039
A_52_P311903	Ncoa7	4.742	up				0.030	
A_51_P435987	Ndst4			2.450	up			0.001
A_52_P382107	Nlrc5	3.456	up				0.002	
A_51_P125067	Nmi	2.160	up				0.004	
A_51_P182693	Npr1			2.246	down			0.048
A_52_P110877	Oas1b	8.867	up				0.004	
A_51_P428529	Oas1c	2.736	up				0.022	
A_51_P134030	Oas1e	2.156	up			0.048	0.015	
A_51_P154842	Oas1f	3.755	up				0.022	

Agilent Probe Name	GeneSymbol	Fold Change (0 vs 3 hours)	Regulation (0 vs 3 hours)	Fold Change (0 vs 6 hours)	Regulation (0 vs 6 hours)	Corrected p value, One way anova (BHFDR)	Corrected p value, Unpaired T-test (0 vs 3 hours) (BHFDR)	p value, Unpaired T-test (0 vs 6 hours) (BHFDR)
A_51_P277994	Oas2	13.835	up				0.008	
A_51_P472867	Oas3	11.923	up				0.004	
A_52_P516296	Oas3	6.733	up				0.004	
A_51_P437309	Oasl1	8.800	up				0.007	
A_51_P387123	Oasl2	2.623	up				0.043	
A_51_P276715	Olfr1350			2.155	down			0.038
A_51_P195598	Olfr259			2.540	down			0.034
A_52_P468639	Olfr450			2.342	down			0.002
A_51_P459908	Olfr56	3.335	up				0.046	
A_51_P129199	Parp10	2.922	up				0.047	
A_51_P452227	Parp11	2.001	up			0.037	0.004	
A_51_P214747	Parp12	6.176	up				0.004	
A_51_P341767	Parp14	6.537	up				0.006	
A_52_P97680	Parp14	6.361	up				0.006	
A_51_P514712	Parp14	5.864	up				0.003	
A_51_P218984	Parp9	6.862	up				0.003	
A_51_P122855	Pax5			2.484	down			0.010
A_51_P262515	Phf11	4.639	up				0.009	
A_51_P199199	Pik3ap1	2.037	up				0.036	
A_51_P282799	Pml	3.190	up				0.047	
A_52_P121087	Pml	3.453	up			0.048	0.024	
A_51_P363258	Prss22	2.110	up				0.028	
A_51_P505132	Rsad2	41.824	up				0.003	

Agilent Probe Name	GeneSymbol	Fold Change (0 vs 3 hours)	Regulation (0 vs 3 hours)	Fold Change (0 vs 6 hours)	Regulation (0 vs 6 hours)	Corrected p value, One way anova (BHFDR)	Corrected p value, Unpaired T-test (0 vs 3 hours) (BHFDR)	p value, Unpaired T-test (0 vs 6 hours) (BHFDR)
A_52_P670026	Rsad2	37.453	up				0.004	
A_51_P505134	Rsad2	42.211	up				0.003	
A_51_P304170	Rtp4	12.010	up				0.002	
A_52_P466090	Samhd1	2.452	up				0.004	
A_51_P245558	Scnn1g			2.148	down			0.047
A_52_P419678	Serpina3f	6.742	up				0.003	
A_52_P419679	Serpina3f	3.566	up				0.008	
A_51_P326191	Serpina3g	2.543	up				0.034	
A_51_P173678	Slc10a6	2.172	up				0.043	
A_51_P447329	Slc25a22	2.054	up				0.007	
A_51_P113403	Slc26a11	2.029	down				0.032	
A_52_P425890	Slfn1	4.595	up				0.005	
A_51_P504991	Slfn10	6.300	up				0.031	
A_51_P183812	Slfn4	11.017	up				0.048	
A_51_P364694	Slfn5	8.023	up				0.020	
A_52_P543489	Slfn8	12.700	up				0.025	
A_51_P504988	Slfn9	12.353	up				0.022	
A_52_P127720	Sp100	2.289	up				0.020	
A_51_P255016	Sp100	2.814	up				0.003	
A_51_P305583	Sp100	2.988	up				0.006	
A_51_P458638	Spink8			2.066	down			0.047
A_51_P119055	Ssb			3.217	up			0.044
A_52_P496503	Stat1	4.293	up				0.008	

Agilent Probe Name	GeneSymbol	Fold Change (0 vs 3 hours)	Regulation (0 vs 3 hours)	Fold Change (0 vs 6 hours)	Regulation (0 vs 6 hours)	Corrected p value, One way anova (BHFDR)	Corrected p value, Unpaired T-test (0 vs 3 hours) (BHFDR)	p value, Unpaired T-test (0 vs 6 hours) (BHFDR)
A_52_P70255	Stat1	4.829	up				0.003	
A_52_P505218	Stat1	4.112	up				0.003	
A_52_P70261	Stat1	4.750	up				0.007	
A_52_P542540	Stat1	7.306	up				0.032	
A_52_P280967	Stk36			2.317	down			0.021
A_51_P481777	Tcstv1	3.935	up				0.025	
A_51_P143200	Tcstv3	3.896	up				0.027	
A_51_P271835	Tdrd7	2.749	up			0.048	0.007	
A_52_P676510	Tgtp1	9.644	up				0.003	
A_51_P478722	Tgtp1	11.943	up				0.003	
A_51_P517525	Tmem169	2.212	up				0.013	
A_51_P448741	Tnfsf10	2.725	up				0.028	
A_52_P602018	Tor1aip1	2.241	up				0.023	
A_52_P52357	Tor3a	3.215	up				0.025	
A_52_P634829	Trim12	4.946	up				0.025	
A_52_P267391	Trim12	4.441	up				0.020	
A_52_P252348	Trim14	3.403	up			0.037	0.003	
A_52_P640484	Trim21	3.939	up				0.005	
A_52_P654161	Trim25	4.160	up			0.048	0.004	
A_51_P212854	Trim25	3.854	up			0.047	0.003	
A_52_P353038	Trim26	2.058	up				0.008	
A_52_P442567	Trim30	7.885	up				0.006	
A_51_P275454	Trim30	9.461	up				0.017	

Agilent Probe Name	GeneSymbol	Fold Change (0 vs 3 hours)	Regulation (0 vs 3 hours)	Fold Change (0 vs 6 hours)	Regulation (0 vs 6 hours)	Corrected p value, One way anova (BHFDR)	Corrected p value, Unpaired T-test (0 vs 3 hours) (BHFDR)	p value, Unpaired T-test (0 vs 6 hours) (BHFDR)
A_52_P278853	Trim34	6.224	up				0.022	
A_52_P367034	Trim34	5.517	up				0.015	
A_52_P157316	Trim34	3.928	up				0.005	
A_51_P244820	Trim56	2.250	up			0.037	0.003	
A_52_P199019	Trim6	2.964	up				0.028	
A_51_P165504	Twist2			2.098	down			0.027
A_51_P316816	Uba7	2.541	up				0.033	
A_51_P164219	Usp18	11.301	up			0.048	0.006	
A_52_P42834	Usp25	3.079	up				0.033	
A_51_P494403	Xaf1	7.658	up				0.004	
A_51_P184936	Zbp1	7.272	up				0.006	
A_51_P144438	Znfx1	2.262	up				0.046	
A_52_P648759	none identified	7.526	up			0.048	0.002	
A_52_P653054	none identified	8.258	up				0.004	
A_52_P326187	none identified	9.388	up				0.004	
A_52_P1187714	none identified			2.746	up			0.030
A_52_P1100772	none identified	2.880	up				0.032	
A_51_P379905	none identified	2.777	up				0.030	
A_52_P1092709	none identified	2.501	up				0.040	
A_52_P121942	none identified			2.725	down			0.048
A_52_P620240	none identified			2.063	down			0.027
A_52_P599964	none identified	9.564	up				0.007	
A_52_P973470	none identified	4.331	up				0.031	

Agilent Probe Name	GeneSymbol	Fold Change (0 vs 3 hours)	Regulation (0 vs 3 hours)	Fold Change (0 vs 6 hours)	Regulation (0 vs 6 hours)	Corrected p value, One way anova (BHFDR)	Corrected p value, Unpaired T-test (0 vs 3 hours) (BHFDR)	p value, Unpaired T-test (0 vs 6 hours) (BHFDR)
A_52_P68235	none identified	6.894	up				0.002	
A_51_P151888	none identified			4.690	down			0.010
A_52_P86965	none identified	6.128	up				0.046	
A_52_P36261	none identified	3.663	up			0.048	0.009	
A_52_P510790	none identified	6.542	up				0.005	
A_51_P301117	none identified	2.679	up				0.009	
A_51_P159503	none identified	7.230	up				0.002	
A_52_P374983	none identified	3.875	up				0.035	
A_52_P359071	none identified	5.093	up				0.005	
A_51_P181785	none identified	2.310	up				0.013	
A_52_P852190	none identified	4.963	up				0.032	
A_52_P1173559	none identified	6.696	up				0.035	
A_51_P188527	none identified	2.957	up	2.113	down		0.048	0.014
A_52_P612668	none identified	3.074	up				0.022	
A_52_P577992	none identified	3.723	up				0.022	
A_51_P325281	none identified	3.260	up				0.008	

**E. IFN $\alpha$  regulated probes within the thymus of *Socs1*<sup>-/-</sup>*Ifny*<sup>-/-</sup> mice**

Agilent Probe Name	GeneSymbol	Fold Change (0 vs 3 hours)	Regulation (0 vs 3 hours)	Fold Change (0 vs 6 hours)	Regulation (0 vs 6 hours)	Corrected p value, One way anova (BHFD R)	Corrected p value, Unpaired T-test (0 vs 3 hours) (BHFD R)	Corrected p value, Unpaired T-test (0 vs 6 hours) (BHFD R)
A_52_P77093	1600014C10Rik	2.889	up	1.491	up	0.024	0.050	
A_51_P453616	1700003F17Rik	10.749	up	3.761	up	0.006	0.022	0.028
A_51_P326555	1700093K21Rik	2.616	up	1.005	up	0.029		
A_51_P105380	2010005H15Rik	2.238	up	1.756	up	0.021	0.040	
A_51_P322473	2310042D19Rik	3.746	up	1.384	up	0.009	0.032	
A_52_P542502	2310042D19Rik	7.562	up	2.646	up	0.008	0.023	
A_52_P986608	2610301H18Rik	2.719	up	1.710	up	0.031	0.039	
A_52_P241640	4930599N23Rik	3.173	up	2.790	up	0.005	0.022	0.015
A_52_P311976	9330175E14Rik	2.026	up	1.659	up	0.004	0.020	
A_52_P417945	9330175E14Rik	2.970	up	2.081	up	0.007	0.024	
A_52_P250268	9430034N14Rik	2.260	up	1.835	up	0.032		
A_51_P249471	9530028C05	3.389	up	2.115	up	0.021	0.038	
A_52_P61697	9930111J21Rik2	2.252	up	1.549	up	0.031	0.033	
A_51_P158072	A230050P20Rik	2.722	up	2.079	up	0.013	0.030	0.028
A_51_P158073	A230050P20Rik	2.668	up	1.884	up	0.020	0.035	
A_52_P649038	A230050P20Rik	3.861	up	2.480	up	0.004	0.018	0.039
A_52_P638457	A430084P05Rik	2.051	up	1.483	up	0.021	0.037	
A_51_P274803	A530023O14Rik	5.791	up	2.837	up	0.049		
A_52_P499640	A530032D15Rik	2.012	up	1.370	up	0.038	0.044	
A_52_P564444	A530064D06Rik	8.643	up	3.356	up	0.011	0.026	
A_52_P30728	Abca17	5.359	up	2.293	up	0.025	0.037	

Agilent Probe Name	GeneSymbol	Fold Change (0 vs 3 hours)	Regulation (0 vs 3 hours)	Fold Change (0 vs 6 hours)	Regulation (0 vs 6 hours)	Corrected p value, One way anova (BHFD)	Corrected p value, Unpaired T-test (0 vs 3 hours) (BHFD)	Corrected p value, Unpaired T-test (0 vs 6 hours) (BHFD)
A_52_P213932	Adamts1	2.692	up	1.257	up	0.048	0.041	
A_52_P489295	Adamts1	2.174	up	1.153	up	0.049		
A_51_P234944	Adamts4	3.435	up	1.105	down	0.027	0.037	
A_51_P257134	Adar	2.444	up	1.954	up	0.020	0.046	
A_51_P238563	Agpat2						0.037	
A_52_P199633	Al451617	5.238	up	2.856	up	0.004	0.018	0.030
A_52_P371494	Al451617	5.645	up	3.142	up	0.023	0.033	
A_52_P375312	Amica1	2.081	up	1.444	up	0.048	0.030	
A_52_P368690	Amica1	2.247	up	1.614	up	0.020	0.033	
A_52_P803082	Apol9a	3.843	up	2.203	up	0.008	0.030	0.031
A_52_P549166	Arsj	2.257	up	1.053	up	0.021	0.020	
A_51_P134627	Asb13	3.662	up	1.684	up	0.050	0.030	
A_52_P537941	Asb13	2.641	up	1.728	up	0.032		
A_52_P549985	Asb13	2.586	up	1.925	up	0.019	0.034	
A_52_P452689	Atf3	2.169	up	1.318	up	0.041		
A_51_P190639	Atp8b4	2.364	up	1.503	up	0.034		
A_52_P233811	B430306N03Rik	3.122	up	1.397	up	0.004	0.018	
A_51_P324535	B4galt5						0.040	
A_51_P165182	Batf2	3.793	up	1.455	up	0.008	0.020	
A_52_P321358	BC006779	3.788	up	2.155	up	0.003	0.018	0.015
A_51_P406604	BC006779	3.690	up	2.329	up	0.018	0.034	0.039
A_51_P494597	BC013712	2.000	up	1.310	up	0.012	0.022	
A_52_P480044	BC023105	11.934	up	5.728	up	0.033		

Agilent Probe Name	GeneSymbol	Fold Change (0 vs 3 hours)	Regulation (0 vs 3 hours)	Fold Change (0 vs 6 hours)	Regulation (0 vs 6 hours)	Corrected p value, One way anova (BHFDR)	Corrected p value, Unpaired T-test (0 vs 3 hours) (BHFDR)	Corrected p value, Unpaired T-test (0 vs 6 hours) (BHFDR)
A_52_P452599	Bco2	2.454	up	1.246	up	0.030		
A_51_P169693	Bst2	2.451	up	2.416	up	0.020	0.040	
A_52_P249514	Ccl12	3.715	up	1.878	up	0.003	0.018	
A_51_P286737	Ccl2	5.099	up	2.183	up	0.004	0.020	0.032
A_52_P208763	Ccl7	6.055	up	2.770	up	0.003	0.018	0.019
A_51_P436652	Ccl7	5.700	up	2.823	up	0.003	0.018	0.015
A_52_P561716	Ccny1	2.596	up	1.846	up	0.035	0.047	
A_51_P232682	Ccr1	3.024	up	1.278	up	0.020	0.044	
A_52_P334593	Ccr1	3.205	up	1.445	up	0.036		
A_52_P573255	Cdc42ep1	2.166	down	1.271	down	0.019	0.032	
A_52_P360112	Clip2	2.181	down	1.755	down	0.018	0.036	
A_52_P186937	Cmpk2	13.341	up	4.793	up	0.003	0.018	0.008
A_51_P400190	Cmpk2	14.685	up	5.056	up	0.004	0.018	0.019
A_51_P300618	Crb2	3.496	down	1.331	down	0.007	0.018	
A_52_P267564	Creb5	2.046	up	1.188	up	0.037		
A_52_P917015	Csprs						0.022	
A_51_P432641	Cxcl10	6.570	up	1.370	up	0.011	0.033	
A_52_P380369	D14Ert668e	4.632	up	3.076	up	0.006	0.023	0.039
A_51_P215143	D430006K04	4.896	up	2.563	up	0.011	0.026	
A_52_P110052	Darc	2.301	up	1.129	up	0.032	0.045	
A_51_P223569	Ddx4	6.869	up	5.381	up	0.015	0.035	
A_51_P393748	Ddx58	3.731	up	2.274	up	0.008	0.024	0.041
A_52_P385536	Ddx58	5.912	up	2.104	up	0.041	0.034	

Agilent Probe Name	GeneSymbol	Fold Change (0 vs 3 hours)	Regulation (0 vs 3 hours)	Fold Change (0 vs 6 hours)	Regulation (0 vs 6 hours)	Corrected p value, One way anova (BHFDR)	Corrected p value, Unpaired T-test (0 vs 3 hours) (BHFDR)	Corrected p value, Unpaired T-test (0 vs 6 hours) (BHFDR)
A_52_P523946	Ddx58	4.792	up	2.462	up	0.005	0.020	0.016
A_52_P479001	Ddx58	4.265	up	2.150	up	0.003	0.018	0.015
A_51_P197910	Ddx60	6.803	up	4.282	up	0.018	0.040	
A_52_P223809	Dhx58	5.741	up	3.782	up	0.005	0.022	0.019
A_51_P306017	Dll1	2.082	up	1.301	up	0.005	0.023	
A_52_P483799	E030037K03Rik	9.292	up	5.804	up	0.038	0.046	
A_52_P127813	E030037K03Rik	5.915	up	3.977	up	0.004	0.018	0.017
A_52_P559919	Eif2ak2	5.900	up	2.340	up	0.005	0.018	
A_52_P379277	Enpp3	2.111	up	1.549	up	0.024	0.048	
A_52_P582374	Epsti1			2.011	down		0.041	
A_51_P376050	Epsti1	2.229	up	2.011	up	0.012	0.035	0.021
A_51_P100852	Fam26f						0.041	
A_51_P492047	Fam3b	2.343	up	1.450	up	0.015	0.028	
A_51_P426008	Fbxo39	8.576	up	5.144	up	0.008	0.026	
A_52_P47846	Fcgr1	2.608	up	3.005	up	0.012	0.024	
A_51_P296755	Fcgr1	2.449	up	2.659	up	0.017	0.022	
A_51_P181517	Fcgr4	3.039	up	3.342	up	0.003	0.018	0.019
A_52_P551974	Ffar1	2.022	up	1.320	up	0.024	0.047	
A_51_P344790	Foxl2			2.392	down			0.031
A_51_P288138	Fpr2	3.787	up	2.398	up	0.021	0.037	
A_52_P109378	Fpr2	4.485	up	2.513	up	0.005	0.018	
A_52_P309418	Ftsjd2	2.060	up	1.515	up	0.012	0.019	
A_51_P203955	Gbp2	3.886	up	2.592	up	0.018	0.040	0.016

Agilent Probe Name	GeneSymbol	Fold Change (0 vs 3 hours)	Regulation (0 vs 3 hours)	Fold Change (0 vs 6 hours)	Regulation (0 vs 6 hours)	Corrected p value, One way anova (BHFDR)	Corrected p value, Unpaired T-test (0 vs 3 hours) (BHFDR)	Corrected p value, Unpaired T-test (0 vs 6 hours) (BHFDR)
A_51_P463562	Gbp4	2.684	up	1.389	up	0.025	0.041	
A_52_P327664	Gbp5	3.794	up	1.813	up	0.020	0.039	
A_51_P463846	Gbp6	4.429	up	1.802	up	0.020	0.038	
A_51_P323180	Gbp9	3.718	up	2.347	up	0.033	0.045	
A_52_P344949	Gbp9	4.036	up	2.735	up	0.021	0.040	
A_51_P267587	Gdap10	3.534	up	1.967	up	0.020	0.041	
A_52_P525317	Gja5	2.175	down	1.170	down	0.050	0.049	
A_52_P494730	Gm12185	8.013	up	3.284	up	0.004	0.020	
A_52_P164821	Gm12250	8.086	up	3.229	up	0.004	0.019	0.015
A_51_P500082	Gm14446	8.279	up	4.581	up	0.009	0.029	0.030
A_52_P294064	Gm14446	8.980	up	4.831	up	0.010	0.029	0.032
A_52_P116184	Gm2795	2.192	up	1.083	up	0.037		
A_52_P315423	Gm3224			3.386	up		0.050	
A_52_P947847	Gm4951	9.550	up	3.241	up	0.028	0.034	
A_52_P176865	Gm5431	5.347	up	2.201	up	0.004	0.018	
A_51_P162326	Gm5933	3.555	up	2.168	up	0.018	0.034	
A_51_P333274	Gzmb	2.648	up	2.369	up	0.030		0.045
A_52_P581082	H2-T24	4.410	up	3.505	up	0.004	0.020	0.019
A_52_P189812	H2-T24	3.945	up	2.726	up	0.004	0.018	0.038
A_51_P147850	Hand2	3.392	up	2.007	up	0.048		
A_51_P492456	Has1	4.692	up	1.346	down	0.008	0.040	
A_52_P64514	Herc5	4.214	up	2.658	up	0.021	0.040	
A_52_P679860	Herc5	5.508	up	3.189	up	0.028	0.038	

Agilent Probe Name	GeneSymbol	Fold Change (0 vs 3 hours)	Regulation (0 vs 3 hours)	Fold Change (0 vs 6 hours)	Regulation (0 vs 6 hours)	Corrected p value, One way anova (BHFDR)	Corrected p value, Unpaired T-test (0 vs 3 hours) (BHFDR)	Corrected p value, Unpaired T-test (0 vs 6 hours) (BHFDR)
A_51_P436342	Hoxb5	2.205	up	1.397	down	0.008	0.046	
A_52_P522427	Hsh2d	3.799	up	2.374	up	0.006	0.020	0.035
A_51_P130332	Hspa12b	2.196	down	1.178	down	0.023	0.039	
A_52_P663686	I830012O16Rik	9.308	up	4.808	up	0.018	0.032	
A_51_P286488	Ier3	2.041	up	1.167	up	0.038		
A_52_P811745	Ifi203	4.180	up	1.961	up	0.043	0.049	
A_51_P408346	Ifi204	4.276	up	3.008	up	0.022	0.047	
A_51_P408343	Ifi204	4.161	up	2.556	up	0.026	0.047	
A_51_P414889	Ifi35	2.447	up	1.660	up	0.018	0.033	
A_52_P550858	Ifi44	10.936	up	4.990	up	0.018	0.036	
A_51_P487690	Ifi44	6.427	up	2.916	up	0.041	0.034	
A_51_P129229	Ifi47	3.750	up	2.039	up	0.006	0.024	0.019
A_51_P387810	Ifih1	5.737	up	2.922	up	0.009	0.028	
A_52_P121468	Ifih1	7.384	up	3.510	up	0.018	0.034	
A_51_P327751	Ifit1	9.103	up	4.018	up	0.007	0.020	
A_52_P542388	Ifit2	4.791	up	2.202	up	0.015	0.034	
A_51_P161021	Ifit2	4.998	up	2.216	up	0.028	0.046	
A_51_P359570	Ifit3	6.663	up	4.509	up	0.006	0.023	0.017
A_51_P112355	Igtp	2.486	up	1.209	up	0.041	0.035	
A_51_P387239	Iigp1	8.303	up	4.039	up	0.017	0.036	
A_52_P18746	Ikzf3	2.079	down	1.128	down	0.020	0.035	
A_51_P430766	Il10	2.645	up	1.485	up	0.022	0.032	
A_52_P15461	Il15	2.118	up	1.177	up	0.009	0.032	

Agilent Probe Name	GeneSymbol	Fold Change (0 vs 3 hours)	Regulation (0 vs 3 hours)	Fold Change (0 vs 6 hours)	Regulation (0 vs 6 hours)	Corrected p value, One way anova (BHFDR)	Corrected p value, Unpaired T-test (0 vs 3 hours) (BHFDR)	Corrected p value, Unpaired T-test (0 vs 6 hours) (BHFDR)
A_51_P217218	Il6	7.137	up	1.527	up	0.022	0.040	
A_51_P421876	Irf7	3.449	up	3.064	up	0.009	0.027	0.041
A_52_P176013	Irf9	2.079	up	1.934	up	0.026	0.048	
A_51_P123625	Irg1	3.609	up	1.515	up	0.046		
A_51_P262171	Irgm1	4.352	up	2.482	up	0.003	0.018	0.005
A_52_P126158	Irgm1	4.831	up	2.500	up	0.003	0.018	0.015
A_51_P416295	Irgm2	3.194	up	1.760	up	0.004	0.018	
A_52_P463936	Isg15	6.476	up	3.424	up	0.004	0.018	0.047
A_52_P546175	LOC100045156	2.365	up	1.941	up	0.030		
A_52_P315421	LOC544818	3.402	up	2.757	up	0.020	0.044	
A_52_P203833	Mitd1	2.621	up	1.825	up	0.004	0.018	
A_52_P203837	Mitd1	3.015	up	1.594	up	0.019	0.023	
A_51_P303332	Mitd1	3.907	up	2.115	up	0.018	0.036	
A_51_P440535	Miikl	2.599	up	2.001	up	0.011	0.030	0.022
A_51_P184484	Mmp13	11.238	up	9.406	up	0.006	0.024	0.017
A_51_P377620	Mnda	3.296	up	1.878	up	0.041		
A_52_P189772	Mpa2l	5.743	up	3.200	up	0.007	0.022	
A_52_P393488	Ms4a4c	4.418	up	3.642	up	0.027		0.047
A_52_P211956	Ms4a4d	3.479	up	2.930	up	0.010	0.034	0.039
A_51_P294505	Ms4a4d	3.814	up	2.685	up	0.022		
A_51_P422300	Ms4a6b	2.219	up	1.872	up	0.011	0.034	
A_51_P149714	Ms4a6d	2.130	up	1.799	up	0.007	0.026	
A_52_P446431	Mx1	12.610	up	4.425	up	0.006	0.023	0.033

Agilent Probe Name	GeneSymbol	Fold Change (0 vs 3 hours)	Regulation (0 vs 3 hours)	Fold Change (0 vs 6 hours)	Regulation (0 vs 6 hours)	Corrected p value, One way anova (BHFD R)	Corrected p value, Unpaired T-test (0 vs 3 hours) (BHFD R)	Corrected p value, Unpaired T-test (0 vs 6 hours) (BHFD R)
A_52_P614259	Mx1	12.662	up	4.604	up	0.006	0.023	0.028
A_51_P514085	Mx2	12.368	up	4.468	up	0.003	0.018	0.023
A_52_P6328	Nampt	2.332	up	1.639	up	0.023	0.049	
A_51_P387235	Nampt	2.294	up	1.490	up	0.031		
A_52_P476950	Ncoa7	3.215	up	1.669	up	0.040		
A_52_P311903	Ncoa7	3.141	up				0.035	
A_52_P382107	Nlrc5	2.499	up	1.644	up	0.035		
A_52_P337357	Oas1a	3.355	up	3.303	up	0.021		
A_52_P110877	Oas1b	4.785	up	2.625	up	0.003	0.018	0.015
A_51_P428529	Oas1c	2.342	up	1.773	up	0.009	0.027	
A_52_P587071	Oas2	12.617	up	7.013	up	0.009	0.033	
A_51_P277994	Oas2	6.947	up	4.313	up	0.004	0.019	0.015
A_51_P472867	Oas3	8.314	up	4.852	up	0.008	0.026	0.030
A_52_P516296	Oas3	6.174	up	6.487	up	0.050		
A_51_P437309	Oasl1	5.167	up	2.555	up	0.006	0.020	
A_51_P387123	Oasl2	2.909	up	2.399	up	0.028		0.019
A_51_P459908	Olfir56	5.889	up	2.331	up	0.010	0.022	
A_51_P120738	P2ry14	2.171	up	1.763	up	0.009	0.032	
A_51_P129199	Parp10	2.501	up	1.622	up	0.033	0.040	
A_51_P452227	Parp11	2.065	up	1.194	up	0.015	0.039	
A_51_P214747	Parp12	4.384	up	3.054	up	0.015	0.040	0.016
A_51_P341767	Parp14	4.214	up	1.742	up	0.009	0.019	
A_52_P97680	Parp14	4.217	up	2.186	up	0.003	0.018	0.024

Agilent Probe Name	GeneSymbol	Fold Change (0 vs 3 hours)	Regulation (0 vs 3 hours)	Fold Change (0 vs 6 hours)	Regulation (0 vs 6 hours)	Corrected p value, One way anova (BHFD R)	Corrected p value, Unpaired T-test (0 vs 3 hours) (BHFD R)	Corrected p value, Unpaired T-test (0 vs 6 hours) (BHFD R)
A_51_P514712	Parp14	3.769	up	2.175	up	0.004	0.018	0.015
A_51_P218984	Parp9	4.497	up	2.392	up	0.006	0.023	
A_51_P262515	Phf11	4.820	up	4.365	up	0.019	0.048	0.015
A_52_P642239	Pik3ap1	3.266	up	2.156	up	0.045		
A_51_P270339	Pik3ap1	2.107	up	1.590	up	0.049	0.046	
A_51_P199199	Pik3ap1	2.307	up	1.406	up	0.028	0.024	
A_52_P372901	Plscr2	2.770	up	1.763	up	0.020	0.040	
A_51_P251022	Plscr2	2.897	up	1.591	up	0.022	0.038	
A_51_P282799	Pml	2.639	up	1.431	up	0.044		
A_52_P121087	Pml	3.068	up	1.677	up	0.021	0.033	
A_52_P229271	Pnpt1	3.141	up	1.719	up	0.041		
A_51_P363729	Prg3	1.584	down	2.211	down	0.022		
A_51_P363258	Prss22	2.078	up				0.047	
A_51_P374726	Ptx3	12.046	up	1.375	up	0.003	0.014	
A_52_P26161	Ptx3	13.980	up	1.368	up	0.004	0.018	
A_52_P193657	Pyhin1	4.179	up	2.113	up	0.050		
A_52_P563280	Pyhin1						0.042	
A_51_P340699	Rasl11a	2.108	up	1.150	up	0.038		
A_52_P425839	Retnlg	2.697	up				0.026	
A_51_P177819	Rnf114	2.094	up	1.739	up	0.041		
A_51_P505132	Rsad2	20.654	up	7.440	up	0.003	0.018	0.019
A_52_P670026	Rsad2	17.280	up	6.263	up	0.003	0.018	0.009
A_51_P505134	Rsad2	21.025	up	7.965	up	0.003	0.018	0.015

Agilent Probe Name	GeneSymbol	Fold Change (0 vs 3 hours)	Regulation (0 vs 3 hours)	Fold Change (0 vs 6 hours)	Regulation (0 vs 6 hours)	Corrected p value, One way anova (BHFD)	Corrected p value, Unpaired T-test (0 vs 3 hours) (BHFD)	Corrected p value, Unpaired T-test (0 vs 6 hours) (BHFD)
A_51_P304170	Rtp4	3.704	up	3.055	up	0.003	0.018	0.016
A_52_P466090	Samhd1	2.844	up	1.796	up	0.018	0.040	
A_52_P136316	Samhd1	4.216	up	1.560	up	0.020	0.034	
A_52_P419678	Serpina3f	9.056	up	3.046	up	0.007	0.023	0.028
A_52_P419679	Serpina3f	6.118	up	3.254	up	0.041		
A_51_P326191	Serpina3g	2.569	up	1.688	up	0.047	0.035	
A_51_P173678	Slc10a6	4.269	up	1.106	up	0.047		
A_51_P277373	Slc8a1			2.103	down			0.027
A_52_P425890	Slfn1	3.980	up	2.951	up	0.008	0.026	0.016
A_51_P504991	Slfn10	3.906	up	2.074	up	0.018	0.035	
A_51_P228768	Slfn3	2.209	up	1.605	up	0.042		
A_51_P183812	Slfn4	22.093	up	10.757	up	0.017	0.039	
A_51_P413359	Slfn5	6.032	up	2.568	up	0.007	0.022	
A_51_P364694	Slfn5	5.613	up	2.434	up	0.010	0.026	
A_52_P543489	Slfn8	6.320	up	2.753	up	0.008	0.022	
A_51_P504988	Slfn9	5.597	up	2.556	up	0.012	0.022	
A_51_P255016	Sp100	2.546	up	1.702	up	0.020	0.033	
A_51_P305583	Sp100	2.573	up	1.808	up	0.037	0.034	
A_52_P496503	Stat1	2.939	up	1.977	up	0.006	0.024	
A_52_P70255	Stat1	3.058	up	1.917	up	0.004	0.018	
A_52_P505218	Stat1	2.820	up	1.998	up	0.013	0.023	
A_52_P70261	Stat1	3.229	up	2.119	up	0.004	0.018	0.017
A_52_P542540	Stat1	4.272	up	2.908	up	0.004	0.018	0.032

Agilent Probe Name	GeneSymbol	Fold Change (0 vs 3 hours)	Regulation (0 vs 3 hours)	Fold Change (0 vs 6 hours)	Regulation (0 vs 6 hours)	Corrected p value, One way anova (BHFDR)	Corrected p value, Unpaired T-test (0 vs 3 hours) (BHFDR)	Corrected p value, Unpaired T-test (0 vs 6 hours) (BHFDR)
A_51_P225808	Stat2	2.132	up	1.499	up	0.020	0.037	
A_51_P474278	Sun5						0.049	
A_51_P508580	Tcf15	2.437	down	1.089	up	0.049		
A_51_P143200	Tcstv3	3.191	up	2.407	up	0.008	0.027	0.028
A_51_P271835	Tdrd7	2.542	up	1.509	up	0.008	0.027	
A_52_P676510	Tgtp1	5.933	up	3.402	up	0.005	0.022	0.028
A_51_P478722	Tgtp1	7.970	up	3.540	up	0.003	0.018	0.007
A_52_P337092	Thbs1	3.767	up	1.219	down	0.018	0.035	
A_52_P363951	Thbs1	4.657	up	1.663	up	0.018	0.032	
A_52_P85174	Tlr3	4.840	up				0.040	
A_51_P291906	Tlr3	4.164	up	1.872	up	0.039		
A_51_P371710	Tlr7	2.563	up	2.139	up	0.041		
A_52_P261086	Tmem140	2.160	up	1.382	up	0.006	0.023	
A_52_P799815	Tmem171	5.821	up	1.983	up	0.008	0.018	
A_51_P448741	Tnfsf10	2.308	up	1.600	up	0.031		
A_52_P253167	Tor1aip2	2.274	up	1.514	up	0.019	0.025	
A_51_P198179	Tor3a	3.057	up	1.672	up	0.021	0.041	
A_52_P52357	Tor3a	3.239	up	2.171	up	0.023	0.049	0.019
A_52_P634829	Trim12	3.584	up	2.343	up	0.009	0.023	
A_52_P267391	Trim12	3.015	up	2.116	up	0.020	0.034	
A_52_P252348	Trim14	2.902	up	1.677	up	0.004	0.019	
A_52_P640484	Trim21	2.867	up	1.689	up	0.004	0.018	
A_52_P654161	Trim25	3.005	up	1.745	up	0.015	0.034	

Agilent Probe Name	GeneSymbol	Fold Change (0 vs 3 hours)	Regulation (0 vs 3 hours)	Fold Change (0 vs 6 hours)	Regulation (0 vs 6 hours)	Corrected p value, One way anova (BHFD R)	Corrected p value, Unpaired T-test (0 vs 3 hours) (BHFD R)	Corrected p value, Unpaired T-test (0 vs 6 hours) (BHFD R)
A_51_P212854	Trim25	2.413	up	1.695	up	0.003	0.018	
A_52_P353038	Trim26	2.008	up	1.454	up	0.024	0.034	
A_52_P442567	Trim30	4.578	up	2.204	up	0.004	0.018	
A_51_P275454	Trim30						0.022	
A_52_P278853	Trim34	3.642	up	2.347	up	0.005	0.022	0.042
A_52_P367034	Trim34	3.249	up	1.908	up	0.003	0.018	
A_52_P157316	Trim34	2.751	up	2.051	up	0.004	0.020	0.027
A_52_P199019	Trim6	2.753	up	1.508	up	0.041		
A_52_P654703	Trim69	2.595	up	1.455	up	0.046	0.044	
A_51_P316816	Uba7	2.180	up	2.118	up	0.018	0.050	0.015
A_51_P164219	Usp18	6.425	up	2.836	up	0.004	0.019	0.021
A_52_P42834	Usp25	2.488	up	1.330	up	0.020	0.034	
A_52_P251703	Vcan	2.884	up	1.965	up	0.038		
A_51_P494403	Xaf1	4.543	up	3.047	up	0.004	0.020	0.015
A_51_P312121	Xdh	2.128	up	1.900	up	0.048		
A_51_P184936	Zbp1	4.194	up	2.468	up	0.018	0.034	
A_52_P373961	Zcchc2	2.362	up	1.571	up	0.021	0.039	
A_51_P352216	Zfp365	3.552	up	2.034	up	0.004	0.018	0.015
A_51_P144438	Znfx1	2.311	up	1.601	up	0.044	0.049	
A_52_P178002	none identified	2.479	up				0.018	
A_52_P648759	none identified	5.218	up	3.756	up	0.008	0.026	0.020
A_52_P653054	none identified	7.453	up	4.925	up	0.009	0.024	0.049
A_52_P326187	none identified	5.934	up	3.222	up	0.006	0.023	

Agilent Probe Name	GeneSymbol	Fold Change (0 vs 3 hours)	Regulation (0 vs 3 hours)	Fold Change (0 vs 6 hours)	Regulation (0 vs 6 hours)	Corrected p value, One way anova (BHFD R)	Corrected p value, Unpaired T-test (0 vs 3 hours) (BHFD R)	Corrected p value, Unpaired T-test (0 vs 6 hours) (BHFD R)
A_52_P615247	none identified	2.993	up	1.825	up	0.020	0.040	
A_52_P1100772	none identified	2.417	up	1.288	up	0.032	0.020	
A_52_P599964	none identified	5.735	up	3.045	up	0.004	0.018	0.036
A_52_P973470	none identified	2.696	up	2.133	up	0.004	0.018	0.021
A_52_P68235	none identified	4.832	up	3.644	up	0.006	0.024	0.025
A_52_P423810	none identified	4.601	up	1.042	up	0.041		
A_52_P325598	none identified	5.364	up	2.908	up	0.035	0.034	
A_52_P787894	none identified	4.452	up	2.951	up	0.012	0.031	
A_52_P86965	none identified	4.223	up	2.633	up	0.038	0.024	
A_52_P36261	none identified	2.487	up	1.451	up	0.009	0.023	
A_52_P448829	none identified	5.133	up	3.270	up	0.028		
A_52_P510790	none identified	3.914	up	2.265	up	0.008	0.025	0.041
A_52_P1116491	none identified	2.234	up	1.617	up	0.008	0.023	
A_51_P250049	none identified						0.044	
A_52_P52653	none identified						0.047	
A_51_P159503	none identified	4.779	up	3.377	up	0.004	0.020	0.005
A_52_P374983	none identified	3.621	up	1.727	up	0.020	0.020	
A_52_P359071	none identified	3.740	up	2.257	up	0.004	0.019	0.019
A_52_P1132687	none identified	4.282	up	3.422	up	0.024	0.040	
A_52_P852190	none identified	2.473	up	1.640	up	0.017	0.022	
A_51_P136181	none identified	2.506	up	1.382	up	0.006	0.014	
A_52_P612668	none identified	2.639	up	2.052	up	0.003	0.014	0.019
A_51_P293401	none identified	3.455	up	1.367	up	0.006	0.024	

Agilent Probe Name	GeneSymbol	Fold Change (0 vs 3 hours)	Regulation (0 vs 3 hours)	Fold Change (0 vs 6 hours)	Regulation (0 vs 6 hours)	Corrected p value, One way anova (BHFDR)	Corrected p value, Unpaired T-test (0 vs 3 hours) (BHFDR)	Corrected p value, Unpaired T-test (0 vs 6 hours) (BHFDR)
A_52_P577992	none identified	5.322	up	2.609	up	0.013	0.020	
A_51_P167097	none identified							0.027
A_52_P218894	none identified	4.288	up	3.139	up	0.020	0.035	
A_52_P353081	none identified						0.033	
A_51_P325281	none identified	3.126	up	1.545	up	0.003	0.018	
A_51_P300986	none identified	4.111	up	4.647	up	0.023	0.043	
A_52_P915536	none identified	4.208	up	2.732	up	0.018	0.020	